



United States Nuclear Regulatory Commission

Protecting People and the Environment

NUREG/CR-7153, Vol. 3
ORNL/TM-2013/532

Expanded Materials Degradation Assessment (EMDA)

Volume 3: Aging of Reactor Pressure Vessels



Office of Nuclear Regulatory Research

AVAILABILITY OF REFERENCE MATERIALS IN NRC PUBLICATIONS

NRC Reference Material

As of November 1999, you may electronically access NUREG-series publications and other NRC records at NRC's Public Electronic Reading Room at <http://www.nrc.gov/reading-rm.html>. Publicly released records include, to name a few, NUREG-series publications; *Federal Register* notices; applicant, licensee, and vendor documents and correspondence; NRC correspondence and internal memoranda; bulletins and information notices; inspection and investigative reports; licensee event reports; and Commission papers and their attachments.

NRC publications in the NUREG series, NRC regulations, and Title 10, "Energy," in the *Code of Federal Regulations* may also be purchased from one of these two sources.

1. The Superintendent of Documents
U.S. Government Printing Office
Mail Stop SSOP
Washington, DC 20402-0001
Internet: bookstore.gpo.gov
Telephone: 202-512-1800
Fax: 202-512-2250
2. The National Technical Information Service
Springfield, VA 22161-0002
www.ntis.gov
1-800-553-6847 or, locally, 703-605-6000

A single copy of each NRC draft report for comment is available free, to the extent of supply, upon written request as follows:

Address: U.S. Nuclear Regulatory Commission
Office of Administration
Publications Branch
Washington, DC 20555-0001

E-mail: DISTRIBUTION.RESOURCE@NRC.GOV
Facsimile: 301-415-2289

Some publications in the NUREG series that are posted at NRC's Web site address <http://www.nrc.gov/reading-rm/doc-collections/nuregs> are updated periodically and may differ from the last printed version. Although references to material found on a Web site bear the date the material was accessed, the material available on the date cited may subsequently be removed from the site.

Non-NRC Reference Material

Documents available from public and special technical libraries include all open literature items, such as books, journal articles, transactions, *Federal Register* notices, Federal and State legislation, and congressional reports. Such documents as theses, dissertations, foreign reports and translations, and non-NRC conference proceedings may be purchased from their sponsoring organization.

Copies of industry codes and standards used in a substantive manner in the NRC regulatory process are maintained at—

The NRC Technical Library
Two White Flint North
11545 Rockville Pike
Rockville, MD 20852-2738

These standards are available in the library for reference use by the public. Codes and standards are usually copyrighted and may be purchased from the originating organization or, if they are American National Standards, from—

American National Standards Institute
11 West 42nd Street
New York, NY 10036-8002
www.ansi.org
212-642-4900

Legally binding regulatory requirements are stated only in laws; NRC regulations; licenses, including technical specifications; or orders, not in NUREG-series publications. The views expressed in contractor-prepared publications in this series are not necessarily those of the NRC.

The NUREG series comprises (1) technical and administrative reports and books prepared by the staff (NUREG-XXXX) or agency contractors (NUREG/CR-XXXX), (2) proceedings of conferences (NUREG/CP-XXXX), (3) reports resulting from international agreements (NUREG/IA-XXXX), (4) brochures (NUREG/BR-XXXX), and (5) compilations of legal decisions and orders of the Commission and Atomic and Safety Licensing Boards and of Directors' decisions under Section 2.206 of NRC's regulations (NUREG-0750).

DISCLAIMER: This report was prepared as an account of work sponsored by an agency of the U.S. Government. Neither the U.S. Government nor any agency thereof, nor any employee, makes any warranty, expressed or implied, or assumes any legal liability or responsibility for any third party's use, or the results of such use, of any information, apparatus, product, or process disclosed in this publication, or represents that its use by such third party would not infringe privately owned rights.



United States Nuclear Regulatory Commission

Protecting People and the Environment

NUREG/CR-7153, Vol. 3
ORNL/TM-2013/532

Expanded Materials Degradation Assessment (EMDA)

Volume 3: Aging of Reactor Pressure Vessels

Manuscript Completed: October 2013

Date Published: October 2014

Prepared by Expert Panel

Oak Ridge National Laboratory: Randy K. Nanstad,
Thomas M. Rosseel, and Mikhail A. Sokolov

ATI Consulting: William L. Server

Japan Central Research Institute of Electric Power Industry:
Taku Arai and Naoki Soneda

Electric Power Research Institute: Robin Dyle

The University of California, Santa Barbara: G. Robert Odette

U.S. Nuclear Regulatory Commission: Mark T. Kirk

Westinghouse: Brian N. Burgos and J. Brian Hall

On behalf of

Oak Ridge National Laboratory

Managed by UT-Battelle, LLC

J. T. Busby, DOE-NE LWRS EMDA Lead

P. G. Oberson and C. E. Carpenter, NRC Project Managers

M. Srinivasan, NRC Technical Monitor

Office of Nuclear Regulatory Research

ABSTRACT

In NUREG/CR-6923, “Expert Panel Report on Proactive Materials Degradation Assessment,” referred to as the PMDA report, NRC conducted a comprehensive evaluation of potential aging-related degradation modes for core internal components, as well as primary, secondary, and some tertiary piping systems, considering operation up to 40 years. This document has been a very valuable resource, supporting NRC staff evaluations of licensees’ aging management programs and allowing for prioritization of research needs.

This report describes an expanded materials degradation assessment (EMDA), which significantly broadens the scope of the PMDA report. The analytical timeframe is expanded to 80 years to encompass a potential second 20-year license-renewal operating-period, beyond the initial 40-year licensing term and a first 20-year license renewal. Further, a broader range of structures, systems, and components (SSCs) was evaluated, including core internals, piping systems, the reactor pressure vessel (RPV), electrical cables, and concrete and civil structures. The EMDA uses the approach of the phenomena identification and ranking table (PIRT), wherein an expert panel is convened to rank potential degradation scenarios according to their judgment of susceptibility and current state of knowledge. The PIRT approach used in the PMDA and EMDA has provided the following benefits:

- Captured the status of current knowledge base and updated PMDA information,
- Identified gaps in knowledge for a SSC or material that need future research,
- Identified potential new forms of degradation, and
- Identified and prioritized research needs.

As part of the EMDA activity, four separate expert panels were assembled to assess four main component groups, each of which is the subject of a volume of this report.

- Core internals and piping systems (i.e., materials examined in the PMDA report) – Volume 2
- Reactor pressure vessel steels (RPV) – Volume 3
- Concrete civil structures – Volume 4
- Electrical power and instrumentation and control (I&C) cabling and insulation – Volume 5

The present volume summarizes the results of the expert panel convened to evaluate aging-related degradation of the RPV. The conceptual starting point for the evaluation of the RPV was found in the Materials Degradation Matrix (MDM) and the Issue Management Tables (IMTs) recently developed by the Electric Power Research Institute (EPRI). For EPRI, the MDM and IMT serve a similar role as the PMDA does for NRC, in that potential degradation scenarios are identified and evaluated to highlight knowledge gaps and prioritize research needs. Starting from the MDM and IMT, the EMDA panel independently determined whether degradation mechanisms for consideration should be added, removed, or modified. A consensus of the issues to be assessed was obtained through discussions among the members of the panel.

The technical issues evaluated by the panel for the RPV are summarized in the technical background assessments found in Chapters 2-6 of this report. These include

- Environmental effects on fracture resistance
- Thermal embrittlement of RPV steels
- Long-term integrity of dissimilar metal welds
- Fatigue mechanism/mode
- Neutron embrittlement

The section on neutron embrittlement includes subsections assessing rate effects, effect of high fluence on alloys with high nickel content, attenuation, master curve fracture toughness, and thermal annealing, embrittlement beyond the beltline. Chapter 7 of this report summarizes the PIRT scoring for the RPV, and conclusions and recommendations are captured in Chapter 8.

The report concludes that although remarkable progress has been made in developing a mechanistic understanding of irradiation embrittlement, including the development of physically based and statistically calibrated models of Charpy V-notch-indexed transition-temperature shifts, important technical issues still need to be addressed to reduce the uncertainties in RPV material behavior. These include the effects of high fluence, prolonged irradiation exposure, and flux on the RPV material behavior evaluation process.

FOREWORD

According to the provisions of Title 10 of the *Code of Federal Regulations* (CFR), Part 54, “Requirements for Renewal of Operating Licenses for Nuclear Power Plants,” licensees may apply for twenty-year renewals of their operating license following the initial forty-year operating period. The majority of plants in the United States have received the first license renewal to operate from forty to sixty years and a number of plants have already entered the period of extended operation. Therefore, licensees are now assessing the economic and technical viability of a second license renewal to operate safely from sixty to eighty years. The requirements of 10 CFR, Part 54 include the identification of passive, long-lived structures, systems, and components which may be subject to aging-related degradation, and the development of aging management programs (AMPs) to ensure that their safety function is maintained consistent with the licensing basis during the extended operating period. NRC guidance on the scope of AMPs is found in NUREG-1800 “Standard Review Plan for Review of License Renewal Applications for Nuclear Power Plants” (SRP-LR) and NUREG-1801, “Generic Aging Lessons Learned (GALL) Report.”

In anticipation to review applications for reactor operation from sixty to eighty years, the Office of Nuclear Reactor Regulation (NRR) requested the Office of Nuclear Regulatory Research (RES) to conduct research and identify aging-related degradation scenarios that could be important in this timeframe, and to identify issues for which enhanced aging management guidance may be warranted and allowing for prioritization of research needs. As part of this effort, RES agreed to a Memorandum of Understanding with the U.S. Department of Energy (DOE) to jointly develop an Expanded Materials Degradation Assessment (EMDA) at Oak Ridge National Laboratory (ORNL). The EMDA builds upon work previously done by RES in NUREG/CR-6923, “Expert Panel Report on Proactive Materials Degradation Assessment.” Potential degradation scenarios for operation up to forty years were identified using an expert panel to develop a phenomena identification and ranking table (PIRT). NUREG/CR-6923 mainly addressed primary system and some secondary system components. The EMDA covers a broader range of components, including piping systems and core internals, reactor pressure vessel, electrical cables, and concrete structures. To conduct the PIRT and to prepare the EMDA report, an expert panel for each of the four component groups was assembled. The panels included from 6 to 10 members including representatives from NRC, DOE national laboratories, industry, independent consultants, and international organizations. Each panel was responsible for preparing a technical background volume and a PIRT scoring assessment. The technical background chapters in each volume summarizes the current state of knowledge concerning degradation of the component group and highlights technical issues deemed to be the most important for subsequent license renewal.

Detailed background discussions, PIRT findings, assessments, and comprehensive analysis for each of these component groups are presented in the following chapters.

CONTENTS

	Page
ABSTRACT.....	iii
FOREWORD	v
FIGURES.....	ix
TABLES.....	xi
ACKNOWLEDGMENTS.....	xiii
ABBREVIATED TERMS	xv
1. INTRODUCTION	1
1.1 TECHNICAL APPROACH.....	3
1.2 DESCRIPTION OF THE EMDA PROCESS	8
1.3 REFERENCES	11
2. ENVIRONMENTAL EFFECTS ON FRACTURE RESISTANCE	13
2.1 REFERENCES	15
3. THERMAL EMBRITTLEMENT OF RPV STEELS	17
3.1 ATOMIC ENERGY RESEARCH ESTABLISHMENT HARWELL RESULTS.....	17
3.2 OAK RIDGE NATIONAL LABORATORY RESULTS.....	17
3.3 BABCOCK AND WILCOX AGING RESULTS	18
3.4 FRENCH RSE-M RESULT	18
3.5 RPV COMPONENTS POTENTIALLY AFFECTED BY THERMAL EMBRITTLEMENT.....	18
3.6 SUMMARY AND RECOMMENDED RESEARCH.....	19
3.7 REFERENCES	20
4. LONG-TERM INTEGRITY OF DISSIMILAR METAL WELDS	23
4.1 INTRODUCTION	23
4.1.1 Current Status of R&D and Gaps	24
4.1.2 Residual Stress and Crack Growth Evaluation	25
4.2 SUMMARY OF ACTIONS NECESSARY TO EXTEND REACTOR OPERATION TO 80 YEARS.....	26
4.3 REFERENCES	26
5. ENVIRONMENTALLY ASSISTED FATIGUE	29
5.1 REFERENCES	31
6. NEUTRON EMBRITTLEMENT	33
6.1 INTRODUCTION TO MAJOR EMBRITTLEMENT ISSUES	33
6.2 FLUX EFFECTS AT HIGH-NEUTRON FLUENCE	36
6.2.1 Motivation.....	36
6.2.2 Flux Effects	36

6.2.3	Slowly Developing or Late Onset Embrittlement Mechanisms	42
6.2.4	Near- and Intermediate-Term Research	43
6.2.5	Longer-Term Research Needs	44
6.3	HIGH-NICKEL EFFECTS AND OTHER POTENTIAL HIGH-FLUENCE EMBRITTELEMENT MECHANISMS	44
6.4	THERMAL ANNEALING AND REIRRADIATION	47
6.5	ATTENUATION OF EMBRITTELEMENT	51
6.5.1	Experimental Validation	56
6.5.2	Summary of Recommendations	56
6.6	MASTER CURVE FRACTURE TOUGHNESS	57
6.7	EMBRITTELEMENT BEYOND THE BELTLINE	63
6.8	REFERENCES	65
7.	DISCUSSION OF PIRT EVALUATIONS AND SUMMARY RECOMMENDATIONS	79
7.1	REFERENCES	84
8.	RECOMMENDATIONS AND CONCLUSIONS	85
8.1	ENVIRONMENTAL EFFECTS ON FRACTURE RESISTANCE	85
8.2	THERMAL EMBRITTELEMENT OF RPV STEELS	85
8.3	LONG-TERM INTEGRITY OF DISSIMILAR METAL WELDS	86
8.4	ENVIRONMENTAL ASSISTED FATIGUE	86
8.5	NEUTRON EMBRITTELEMENT	87
APPENDIX A. BWR VESSEL BREAKDOWN FROM IMTs		A-1
APPENDIX B. PWR VESSEL BREAKDOWN FROM IMTs		B-1
APPENDIX C. DISPLACEMENTS PER ATOM AND PHYSICAL DEFECTS		C-1
APPENDIX D. PIRT TABLES BY MATERIAL, PHENOMENA, AND MECHANISM		D-1

FIGURES

Figure 2.1	Charpy impact toughness of A533B steel, hydrogen charged up to 1.6 ppm [9].	14
Figure 2.2	Charpy impact toughness of A542 steel, hydrogen charged up to 2.2 ppm [9].	14
Figure 2.3	The effect of hydrogen on the ductile fracture toughness of VVER RPV steel [10].	15
Figure 4.1	Summary of SCC issues for RPV.	23
Figure 6.1	Predicted minus measured ΔT for the EONY model applied to surveillance data and high-flux test reactor data, showing increasing nonconservatism with increasing fluence [5]. The two solid lines are $\pm 2\sigma$.	35
Figure 6.2	Yield stress increases in the ORNL 73W steel as a function of fluence for different flux range bins [12].	39
Figure 6.3	(a) Raw IVAR and BR2 RADAMO TTS data for HSSI Weld 73W; (b) TTS data adjusted to a common high-flux condition using the calibrated three-feature model; (c) TTS data adjusted to a common low-flux condition using the calibrated three-feature model; (d) TTS at high and low flux. [6]	40
Figure 6.4	Example showing similar hardening trends in high- and low-flux irradiations [16].	41
Figure 6.5	(a) Illustrative model predictions of the dose dependence of hardening in a high-Cu, medium-Ni steel due to CRP hardening and in high-Ni, low-Cu steel due to LBP hardening. (b) Atom probe tomography maps of Ni and Mn distributions and an enlargement (inset) of an Mn-Ni LBP precipitate in a Cu-free 1.6 wt % Ni, 1.6 wt % Mn model alloy irradiated to 1.8×10^{19} n/cm ² at high flux and 290 °C (554 °F). (c) $\Delta\sigma_y$ as a function of the square root of the volume fraction of precipitates in low-Cu steels and model alloys. [21]	45
Figure 6.6	Correlation between ΔRT_{NDT} and $(V_f r)^{1/2}$, where V_f is the volume fraction and r is the average Guinier radius of solute atom clusters determined by atom probe tomography [21].	47
Figure 6.7	Effects of thermal annealing at 343 °C and 454 °C (650 °F and 850 °F) on the Charpy impact energy of the high-copper Midland Unit 1 RPV beltline weld [6].	49
Figure 6.8	Effect of thermal annealing for 168 h at 454 °C (850 °F) on the fracture toughness of the high-copper Midland Unit 1 RPV beltline weld [6].	49
Figure 6.9	Variations of fluence on the inner diameter of the Ocone 1 vessel. (a) Azimuthal variation at the axial location of the peak fluence and (b) axial variation at the azimuthal location of peak fluence [1].	52
Figure 6.10	Attenuation of exposure parameter ratio for a typical PWR spectrum, with respect to neutron fluence, $E > 0.1$ MeV and $E > 1.0$ MeV, dpa, and the exponential formula from RG 1.99-2 [5] for a typical PWR. [4]	54

Figure 6.11	Comparison of Master Curve [20] from Materials Properties Council PCVN test program with the results from 1TC(T) tests from ORNL [13, 14]. All tests were conducted with HSSI Weld 72W and indicate a PCVN bias of $-21\text{ }^{\circ}\text{C}$.	58
Figure 6.12	Median K_{Jc} values for temper embrittled A302B (Mod) steel after normalization to 1T equivalence compared to the Master Curve based on data at the three lowest test temperatures, showing unstable brittle fracture $150\text{ }^{\circ}\text{C}$ ($270\text{ }^{\circ}\text{F}$) above T_0 [28].	60
Figure 6.13	Variation in Master Curve slope (the Master Curve “C” value is 0.019) reported by Leax [32].	61
Figure 6.14	Variation in the value of 30 ft-lb (41 J) TTS (ΔT_{30}) associated with the definition of the word “beltline” [2].	63
Figure 7.1	PIRT process schematic illustrating the combinations of “damage susceptibility” and “knowledge” scores suggesting various life-management responses [4]. Key to scores: 1, low; 2, medium; 3, high.	80
Figure 7.2	Rainbow chart showing sensitivity, high knowledge, and high confidence for PWRs and BWRs.	81
Figure 7.3	Rainbow chart showing low sensitivity, low knowledge, and low confidence for PWRs.	83

TABLES

Table 1.1	PWR primary pressure boundary [3]	4
Table 1.2	BWR primary pressure boundary [3]	5
Table 1.3	EMDA degradation modes relative to all RPVs* [1–3]	6
Table 1.4	Gaps as identified in EPRI IMTs [4, 5]	7
Table 3.1	Thermal embrittlement comparison	20
Table 7.1	PWR: High sensitivity, high knowledge, and high confidence	81
Table 7.2	BWR: High sensitivity, high knowledge, and high confidence	82
Table 7.3	PWR: Low sensitivity, low knowledge, and low confidence.....	83

ACKNOWLEDGMENTS

This work was performed jointly under contract with the U.S. Nuclear Regulatory Commission (NRC) Office of Nuclear Regulatory Research (RES) and under the U.S. DOE Office of Nuclear Energy Light Water Reactor Sustainability Program. The authors thank R. Reister, the DOE-NE LWRS Program Manager; K. McCarthy, the DOE-NE LWRS Technical Integration Office Lead, and J. Busby, the DOE-NE LWRS Technical Manager; P. G. Oberson and C. E. Carpenter, the NRC Project Managers; M. Srinivasan, the NRC Technical Monitor; and J. Stringfield, the Oak Ridge National Laboratory (ORNL) NRC Program Manager for support and guidance. J. Busby, T. Rosseel, and D. Williams at ORNL provided helpful suggestions that were essential in the execution of the panel discussion and incorporation of the results into the report. Many valuable review comments were received from NRC staff members of RES and the Division of Engineering. The authors also wish to thank W. Koncinski, A. Harkey, K. Jones, and S. Thomas at ORNL for assistance in formatting and preparing the final document. G. West at ORNL deserves special attention and thanks for his assistance in developing a database to compile, sort, and format the extensive data generated in the PIRT process.

ABBREVIATED TERMS

%	percent	ASTM	American Society for Testing and Materials
°C	degrees Celsius	at %	atomic percent
°F	degrees Fahrenheit	ATI	ATI Consulting
γ	gamma	ATR	Advanced Test Reactor
γ'	gamma prime	B&W	Babcox and Wilcox
Δ	delta; denotes change	BAC	boric acid corrosion
$\Delta\sigma_y$	change in yield strength	BR3	Belgian reactor 3
σ	sigma; denotes variability	BWR	boiling water reactor
τ	UMD recovery time	C	carbon
ϕ	flux	C&LAS	carbon and low alloy steels
ϕt	fluence	CASS	cast austenitic stainless steel
$\langle T_{dam} \rangle$	total average damage energy per atom	CFR	<i>Code of Federal Regulations</i>
0.5T	½T compact tension specimen	Cl⁻	chloride ion
1TC(T)	1T compact tension specimen	cm	centimeter
3/4-t	three-quarters of the way through the vessel	Cr	chromium
3DAP	three-dimensional atom probe	CR	cold rolled
41J	41 joules (absorbed energy level in which Charpy v-notch specimen reaches the ductile-to-brittle transition temperature)	CRD	control rod drive
AAR	alkali-aggregate reaction	CRDM	control rod drive mechanism
ADP	annealing demonstration project	CREEP	thermal creep
AERE	Atomic Energy Research Establishment (UK)	CREV	crevice corrosion
AFCEN	French Society for Design and Construction and In-Service Inspection Rules for Nuclear Islands	CRIEPI	Central Research Institute of Electric Power Industry (Japan)
AMP	aging management program	CRP	Cu-rich precipitates
AMR	aging management review	Cu	copper
ANO-1	Arkansas Nuclear One Unit 1	CUF	cumulative fatigue usage factor
APT	atom probe tomography	CVCS	chemical and volume control system
ASME	American Society of Mechanical Engineers	CVN	Charpy V-notch
		CW	cold-worked
		DBTT	ductile-to-brittle transition temperature
		DEBOND	debonding
		DH	dissolved hydrogen
		DOE	U.S. Department of Energy
		dpa	displacements per atom

E, neutron spectrum flux
EBSD, electron backscatter diffraction
EC, erosion–corrosion
ECCS, emergency core cooling system
ECP, electric chemical potential
E_d, displacement threshold energy
EDF, Electricite de France
EDS, energy-dispersive X-ray spectroscopy
EK, Erickson Kirk
Emb., Embrittlement
EMDA, Extended Materials Degradation Assessment
Env., environmental
EONY, Eason, Odette, Nanstad, and Yamamoto
EPMDA, Extended Proactive Materials Degradation Assessment
EPR, electrochemical potentiokinetic reactivation
EPRI, Electric Power Research Institute
eV, electron volt
FAC, flow-accelerated corrosion
FAT, corrosion fatigue
Fe, iron
f_p, volume fraction
FR, fracture resistance
GALL, generic aging lessons learned
GALV, galvanic corrosion
GC, general corrosion
h, hour
HAZ, heat-affected zone
HC, high cycle
HSSI, Heavy-Section Steel Irradiation
HSST, Heavy Section Steel Technology
HWC, hydrogen water chemistry
HWR, heavy water reactor
I&C, instrumentation and controls
IA, irradiation assisted
IAEA, International Atomic Energy Agency
IASCC, irradiation-assisted stress corrosion cracking
IC, irradiation creep
IG, intergranular
IGC, intergranular corrosion
IGF, intergranular fracture
IGSCC, intergranular stress corrosion cracking
IMP, Implementation
IMT, Issue Management Table
in., inch
INL, Idaho National Laboratory
IPA, integrated plant assessment
IVAR, irradiation variables
JAEA, Japan Atomic Energy Agency
JAERI, Japan Atomic Energy Research Institute
JMTR, Japan Materials Testing Reactor
JNES, Japan Nuclear Safety Organization
JPDR, Japan Power Demonstration Reactor
K, stress intensity
keV, thousand electron volt
K_{Ia}, crack-arrest toughness
K_{Ic}, fracture toughness
K_{Jc}, elastic-plastic fracture toughness at onset of cleavage fracture
LAS, low alloy steel
LBP, late-blooming phase
LC, low cycle
LMC, lattice Monte Carlo
LRO, long-range ordering
LTCP, low-temperature crack propagation
LTO, long-term operation

LWR, light water reactor

LWRS, Light-Water Reactor Sustainability

LWRSP, Light Water Reactor Sustainability Program

MA, mill-anneal

MDM, materials degradation matrix

MeV, million electron volts

MIC, microbially induced corrosion

MF, matrix feature

MIG, metal inert gas (welding)

Mn, manganese

MO, Mader and Odette

Mo, molybdenum

MOU, memorandum of understanding

MOY, Mader, Odette, and Yamamoto

MPa \sqrt{m} , stress intensity factor; fracture toughness in units of megapascal square root meter

MPC, Materials Properties Council

n/cm², fluence

n/cm²·s, flux

NE, DOE Office of Nuclear Energy

NEI, Nuclear Energy Institute

Ni, nickel

NMCA, noble metal chemical addition

NOSY, Nanstad, Odette, Stoller, and Yamamoto

NPP, nuclear power plant

NRC, U.S. Nuclear Regulatory Commission

NWC, normal water chemistry

ORNL, Oak Ridge National Laboratory

P, phosphorous

PA, proton annihilation

PIA, postirradiation annealing

PIRT, phenomenon identification and ranking technique

PIT, pitting

PLIM, Nuclear Power Plant Integrity Management

PMDA, Proactive Materials Degradation Assessment

PMMD, proactive management of materials degradation

PNNL, Pacific Northwest National Laboratory

PRA, primary recoil atom

PRE, Prediction of Radiation Embrittlement

PREDB, Power Reactor Engineering Database

PSF, Poolside Facility

PT, penetration test

PTS, pressurized thermal shock

PWHT, post-weld heat treatment

PWR, pressurized water reactor

PWROG, Pressurized Water Reactor Owners Group

PWSCC, primary water stress corrosion cracking

R&D, research and development

RADAMO, SCK-CEN TR model and corresponding TR database

RCS, reactor coolant system

RES, NRC Office of Nuclear Research

RHRS, residual heat removal system

RIS, radiation-induced segregation

RPV, reactor pressure vessel

RSE-M, Rules for In-Service Inspection of Nuclear Power Plant Components (France)

RT, reference temperature

SA, solution anneal

SANS, small-angle neutron scattering

SCC, stress corrosion cracking

SCK-CEN, Studiecentrum voor Kernenergie—Centre d'Etude de l'Énergie Nucléaire (Belgian Nuclear Research Centre)

SE(B), single-edge, notched bend

SEM, scanning electron microscopy

SG, steam generator

SIA, self-interstitial atom

SIS, safety injection system

SM, Stationary Medium Power

SMF, stable matrix feature

SR, stress relaxation

SS, stainless steel

SSC, system, structure, and component

SSRT, slow strain rate test

SW, swelling

T₀, fracture toughness reference temperature

T_{41J}, ductile-to-brittle transition temperature measured at 41 joules of Charpy impact energy

TEM, transmission electron microscopy

TG, transgranular

Th, thermal

T_i, irradiation temperature

TIG, tungsten inert gas (welding)

TiN, titanium nitride

TLAA, time-limited aging analysis

TMS, The Minerals, Metals and Materials Society

TR, test reactor

TT, reference transition temperature; thermal treatment

TTS, transition temperature shift

UCSB, University of California, Santa Barbara

UK, United Kingdom

UMD, unstable matrix defect

UNS, Unified Numbering System

U.S., United States

USE, upper-shelf energy

UT, ultrasonic test

VS, void swelling

VVER, Voda-Vodyanoi Energetichesky Reaktor (Water-Water Energetic Reactor)

WEAR, fretting/wear

Wstg., wastage

wt %, weight percent

Zn, zinc

1. INTRODUCTION

A Proactive Materials Degradation Analysis (PMDA) is a comprehensive evaluation of potential aging-related degradation modes for light-water reactor (LWR) materials and components, based on existing technical and operating experience knowledge levels, expected severity of degradation, and the likelihood of occurrence. The degradation of reactor core internals and primary piping for nuclear reactor applications was evaluated in considerable detail in the original NRC-led PMDA (*Expert Panel Report on Proactive Materials Degradation Assessment*, NUREG/CR-6923, BNL-NUREG-77111-2006) [1].

The development of an expanded materials degradation analysis (EMDA) of degradation mechanisms that could impact passive long-lived systems, structures and components (SSCs) was determined to be valuable in supporting renewal of license to safely operate beyond the first license renewal (period of extended operation, PEO) to beyond the 60 years. Thus, the objective is to expand the original PMDA to consider technical issues for longer time frames (i.e., to at least 80 years of operation) and include components beyond the primary piping and core internals reviewed in the original NUREG/CR-6923 report, namely concrete, cables, reactor pressure vessel.

A PMDA-approach to extended service has the following benefits:

- Captures the current knowledge base
- Identifies gaps in knowledge for an SSC or material
- May help identify new forms of degradation
- Provides information helpful for the identification and prioritization of future research needs

This volume summarizes the results of an expert-panel assessment of the aging and degradation of reactor pressure vessels of light water nuclear power reactors.

The PMDA performed during 2004–2007 focused mainly on nuclear reactor piping systems for which stress corrosion cracking and fatigue are the primary mechanisms of aging and degradation affecting component integrity and safe reactor operation. The overall objective of the PMDA was to lay a technical foundation for any research that may be needed to provide technical information to ensure that future material degradation at extended operation would not diminish the integrity of key components or the safety of the operating light water reactors (LWRs). Any degradation mechanisms that may involve phenomena not yet experienced in the operating fleet, and any laboratory data and/or mechanistic understanding pertinent to future reactor operations, were to be identified. The insights from the PMDA have been applied to the “Generic Aging Lessons Learned (GALL) Report,” NUREG-1801, Revision 2 [2]. Moreover, these technical gaps and insights have also been integrated into industry research planning and activities through the development of the Materials Degradation Matrix (MDM) [3] and the Issue Management Tables (IMTs) [4, 5]. Those documents help determine the priorities for most ongoing research planning. However, the reactor pressure vessel (RPV) was not directly evaluated in the PMDA. This extended PMDA (EMDA) was conducted to address issues that may arise if the licenses are extended beyond 60 years (also known as subsequent license renewal, SLR).

NRC regulations require that RPV steels maintain conservative margin for fracture toughness so that postulated flaws do not threaten the integrity of a RPV during either normal operation and maintenance cycles or under accident transients such as pressurized thermal shock (PTS). Neutron irradiation degrades fracture toughness, in some cases severely. Thermal aging, although not generally considered a significant issue for 40 or 60 years of operation, must be an additional consideration for extended operating life to 80 or more years. Regulations in Title 10, Code of Federal Regulations, Part 50 (10 CFR 50), "Domestic Licensing of Production and Utilization of Facilities," [6]; and implementation guidance found in Section XI, Appendix G, *Boiler and Pressure Vessel Code (BPVC)*, American Society of Mechanical Engineers, "Rules for Inservice Inspection of Nuclear Power Plant Components," [7]; and Regulatory Guide 1.99 Rev 2, "Radiation Embrittlement of Reactor Vessel Materials," [8] recognize that embrittlement has a potential for reducing toughness below acceptable levels.

The last few decades have seen remarkable progress in developing a mechanistic understanding of irradiation embrittlement, including the development of physically based and statistically calibrated models of Charpy V-notch (CVN)-indexed transition-temperature shifts. Those semiempirical models account for key embrittlement variables and their interactions, including the effects of copper (Cu), nickel (Ni), phosphorous (P), fluence (ϕt), flux (ϕ), and irradiation temperature (T_i). Models of the evolution of nanoscale precipitates, rich in Cu, manganese (Mn), and Ni, are quantitatively consistent with experimental observations of the complex interplay between those elements and other embrittlement variables. The models have provided early warnings of potential technical challenges, such as the contribution of Mn and Ni in high-Ni steels to embrittlement by so-called "late blooming" phases, and have enabled the assessment of outliers in the Transition Temperature Shift Database as well as other contradictory observations. However, these models and the present understanding of radiation damage are not fully quantitative and do not take into consideration the potential contribution of all potentially significant variables and aging technical issues.

Over the past three decades, advances in fracture mechanics have led to a number of consensus standards and codes for determining the fracture-toughness parameters needed for development of databases that are useful for statistical analysis and establishment of uncertainties. The CVN toughness, however, is a qualitative measure that must be correlated with the fracture toughness (K_{Ic}) and crack-arrest toughness properties (K_{Ia}) necessary for structural integrity evaluations. Where practical, direct measurements of fracture-toughness properties are desirable to reduce the uncertainties associated with correlations. Moreover, sufficient fracture-toughness data have been obtained to permit probabilistic determinations. However, specimen-size-effect issues must be resolved to enable the use of typical surveillance specimens for reliable determinations of fracture toughness, applicable at the component level.

Such progress notwithstanding, significant technical issues still need to be addressed to reduce the uncertainties in RPV material behavior. The issues regarding irradiation effects are the most significant issues for RPVs [9]. Of the many significant issues discussed, the following are those deemed to have the most impact on the current RPV material behavior evaluation process:

- High fluence, prolonged irradiation duration, and flux effects
- Material variability
- Alloys with high-ni content
- The fracture toughness master curve

- The bias in reference toughness derived from precracked charpy specimens
- Neutron attenuation or through-thickness irradiation effect
- Modeling and microstructural analysis
- Thermal annealing and reirradiation
- Thermal aging

1.1 TECHNICAL APPROACH

The MDM and IMTs, which were updated to cover 80 years of operating life (Revision 2), were used as a starting point to organize possible degradation mechanisms and develop the form of the PIRT tables to be used in this EMDA for boiling water reactor (BWR) and pressurized water reactor (PWR) vessels. From this starting point, the panelists independently determined whether degradation mechanisms for consideration should be added, removed, or modified. For example, Tables 1.1 and 1.2, which are derived from the MDM, identify the overall array of degradation mechanisms for the entire pressure boundary, including the RPV, pressurizer, steam generator channel head, tubesheet surfaces exposed to primary water, divider plate, and primary piping system. Because we are only interested in the RPV, Tables 1.1 and 1.2 can be reduced in size by eliminating any materials not in the RPV and any mechanisms that are not pertinent to the RPV. The only material that clearly can be eliminated is cast stainless steel (CASS). The degradation mechanisms that can be eliminated are irradiation creep/stress relaxation, void swelling, corrosion, and wear. Thus Tables 1.1 and 1.2 can be reduced to Table 1.3 by combining the BWR and PWR issues into one table and by simplifying the stress corrosion cracking (SCC) and fatigue into single degradation modes. By integrating the knowledge gaps identified in the IMTs, Table 1.4 links with Table 1.3 to describe the key elements of concern for the RPVs. Each of the degradation modes can be broken down into subsets as shown for neutron embrittlement. Moreover, the IMTs provide detailed information related to RPV subcomponents. Those details have been extracted from the IMTs, rearranged, and summarized in Appendixes A (BWR) and B (PWR). The specifics of the subcomponents provide a detailed resource for the reader to determine a specific location where a mechanism may be important, but generally will not be covered in the individual discussions of the degradation mechanisms.

Each of the individual mechanisms/modes are described and discussed in numerical order of the gaps noted in Table 1.4.

Table 1.1. PWR primary pressure boundary [3]

MATERIAL	DEGRADATION MODE													
	SCC		Corrosion				Wear	Fatigue		Reduction in Fract Properties		Irradiation Effects		
	IG/ITG	IA	Wstg.	Pitting	FAC	Foul	Wear	HC	LC-Env.	Th.	Env.	Emb.	VS	IC/SR
<u>C&LAS</u>	γLTO p1-1a	N	N	N	N	N	N	N	γLTO p1-9a	γLTO p1-10a	γLTO p1-11a	γLTO p1-12a	N	N
<u>C&LAS: Welds</u>	γLTO p1-1b	N	N	N	N	N	N	N	γLTO p1-9b	γLTO p1-10b	γLTO p1-11b	γLTO p1-12b	N	N
<u>SS: Base Metal</u>	γLTO p1-1c	N	N	Y p1-4c	N	N	N	γIMP p1-8c	γLTO p1-9c	N	?	N	N	N
<u>SS: Welds & Clad</u>	γLTO p1-1d	N	N	Y p1-4d	N	N	N	γIMP p1-8d	γLTO p1-9d	Y p1-10d	Y p1-11d	Y p1-12d	N	N
<u>CASS</u>	γLTO p1-1e	N	N	N	N	N	N	γIMP p1-8e	γLTO p1-9e	γIMP p1-10e	Y p1-11e	N	N	N
<u>Ni-Alloy: Base Metal (A600)</u>	γIMP p1-1f	N	N	N	N	N	N	N	γLTO p1-9f	N	Y p1-11f	N	N	N
<u>Ni-Alloy: Base Metal (A690)</u>	γLTO p1-1g	N	N	N	N	N	N	N	γLTO p1-9g	γIMP p1-10g	Y p1-11g	N	N	N
<u>Ni-Alloy: Welds & Clad (A82/182)</u>	γIMP p1-1h	N	N	N	N	N	N	N	γLTO p1-9h	N	Y p1-11h	N	N	N
<u>Ni-Alloy: Welds & Clad (A52/152)</u>	γLTO p1-1i	N	N	N	N	N	N	N	γLTO p1-9i	γIMP p1-10i	Y p1-11i	N	N	N

Abbreviations

Emb. Embrittlement
 Env. Environmental
 FAC Flow-accelerated corrosion
 HC High cycle
 IA Irradiation assisted
 IC Irradiation creep
 IG Intergranular

IMP

LC Low cycle
 LTO Long-term operation
 SR Stress relaxation
 TG Transgranular
 Th Thermal
 VS Void swelling
 Wstg. Wastage

Implementation

Key to Colors

Green = existing programs adequate, no more research needed.
 Yellow = research underway is believed to be such that gaps will be better understood or closed (green).
 Orange = not enough being done to resolve the gap.
 Blue = insufficient knowledge on issue to rank.

Table 1.2. BWR primary pressure boundary [3]

DEGRADATION MODE														
MATERIAL	SCC		Corrosion			Wear	Fatigue		Reduction in Fract Properties		Irradiation Effects			
	IG/ITG	IA	Wstg.	Pitting	FAC		Foul	HC	LC-Env.	Th.	Env.	Emb.	VS	IC/SR
<u>C&LAS</u>	γ LTO b1-1a	γ LTO b1-2a	N	N	γ IMP b1-5a	N	N	γ IMP b1-8a	γ LTO b1-9a	N	γ LTO b1-11a	γ LTO b1-12a	N/A	N
<u>C&LAS:</u> <u>Welds</u>	γ LTO b1-1b	γ LTO b1-2b	N	N	γ IMP b1-5b	N	N	γ IMP b1-8b	γ LTO b1-9b	N	γ LTO b1-11b	γ LTO b1-12b	N/A	N
<u>SS:</u> <u>Wrought / Forged</u> <u>& HAZ</u>	γ LTO b1-1c	N	N	N	N	N	N	γ IMP b1-8c	γ LTO b1-9c	N	Y b1-11c	N	N/A	N
<u>SS:</u> <u>Welds & Clad</u>	γ LTO b1-1d	N	N	N	N	N	N	γ IMP b1-8d	γ LTO b1-9d	Y b1-10d	? b1-11d	Y b1-12d	N/A	N
<u>CASS</u>	γ LTO b1-1e	N	N	N	N	N	N	N	γ LTO b1-9e	γ IMP b1-10e	? b1-11e	N	N/A	N
<u>Ni-Alloy:</u> <u>Wrought (A600)</u>	γ LTO b1-1f	N	N	N	N	N	N	N	γ LTO b1-9f	N	Y b1-11f	N	N/A	N
<u>Ni-Alloy:</u> <u>Welds & Clad (A82 / 182)</u>	γ LTO b1-1g	N	N	N	N	N	N	N	γ LTO b1-9g	N	Y b1-11g	N	N/A	N

Abbreviations

Emb. Embrittlement
 Env. Environmental
 FAC Flow-accelerated corrosion
 HC High cycle
 IA Irradiation assisted
 IC Irradiation creep
 IG Intergranular

Key to Colors

Green = existing programs adequate, no more research needed.
 Yellow = research underway is believed to be such that gaps will be better understood or closed (green).
 Orange = not enough being done to resolve the gap.
 Blue = insufficient knowledge on issue to rank.

Implementation

Low cycle
 Long-term operation
 Stress relaxation
 Transgranular
 Thermal
 Void swelling
 Wastage

IMP

LC
 LTO
 SR
 TG
 Th
 VS
 Wstg.

Table 1.3. EMDA degradation modes relative to all RPVs* [1–3]

Material	Degradation Mode			
	SCC	Fatigue	Reduction in Fracture Properties	Irradiation Embrittlement
C&LAS	3	4	1	5
C&LAS welds	3	4	1	5
SS: base metal	3	4	1	
SS: welds and clad	3	4	1, 2	5
Ni alloy: base metal (A600)	3	4		
Ni alloy: base metal (A690)	3	4		
Ni alloy: welds and clad (A82/A182)	3	4	1	
Ni alloy: welds and clad (A52/A152)	3	4	1	

* The numbers in the boxes cross reference the line items in Table 1.4.



 Not applicable to PWR or BWRs
 Not applicable to BWRs

Table 1.4. Gaps as identified in EPRI IMTs [4, 5]

Section in This Report	Title/Description	EPRI- Identified Gap Numbers	Table 1.3 Identifier	Limitations/comments
2	Environmental Effects on Fracture Resistance	P-DM-09, B-DM-06	1	Probably a hydrogen effect if it is proven to be a problem
3	Thermal Embrittlement of RPV Steels	P-DM-10	2	MDM did not suggest a problem for BWRs
4	Long-Term Integrity of Dissimilar Metal Welds	P-DM-13, B-DM-09	3	More of an issue for A600 and A82/182 for BWRs
5	Environmentally Assisted Fatigue	P-AS-02, B-AS-07	4	All materials
6	Neutron Embrittlement	P-AS-04, B-AS-05	5	PWR high fluence BWR flux effects
6.1	Introduction to Major Embrittlement Issues	P-AS-04		
6.2	Flux Effects at High Neutron Fluence	P-AS-04, B-AS-05		
6.3	High-Nickel Effects and Other Potential High-Fluence Embrittlement Mechanisms	P-AS-04, B-AS-05		
6.4	Thermal Annealing and Reirradiation	P-AS-04		
6.5	Attenuation of Embrittlement	P-AS-04		
6.6	Master Curve Fracture Toughness	P-AS-04		
6.7	Embrittlement beyond the Beltline	P-AS-04		

1.2 DESCRIPTION OF THE EMDA PROCESS

As noted above, an expanded PMDA activity benefits all stakeholders in providing a comprehensive analysis of degradation modes and identifying potential gaps, which may need to be addressed by further research to provide data and information for assurance of safe and efficient extended reactor operation. Expansion of the PMDA to longer time frames and additional systems is a challenging assignment, involving experts from more disciplines and consideration of more experimental and operational experience information. The addition of new and distinct material and component systems such as RPVs and concrete to the existing scope of NUREG/CR-6923 [1] was deemed too difficult to encompass in a single document or process given the divergence in materials systems, degradation modes, and respective, cognizant technical community. Thus, separate and distinct expert panels were assembled to address key material issues for piping and core internals, reactor pressure vessel steels, concrete, and cabling for reactor long term operation. While each panel addressed very different materials and degradation modes, the methodology used for assessment was the same for each panel.

The expert elicitation process conducted for each panel is based on the Phenomena Identification and Ranking Table (PIRT) process. This process has been used in many industries for ranking and prioritizing any number of issues. This methodology is commonly used by NRC, including the original NUREG/CR-6923, which is the basis for this activity. The PIRT process provides a systematic means of obtaining information from experts and involves generating lists (tables) of phenomena where “phenomena” can refer to a particular reactor condition, a physical or engineering approximation, a reactor component or parameter, or anything else that might influence some relevant figure-of-merit, which is related to reactor safety. The process usually involves ranking of these phenomena using a series of scoring criteria. The results of the scoring can be assembled to lead to a quantitative ranking of issues or needs. This list can then be used by stakeholders to prioritize research or other decision-making needs.

Each PIRT application has been unique in some respect and the current project is unique in its application. The current PIRT can be described in terms of several key steps. These are described for the generic process below, although each panel made minor adjustments, based on the needs of that material system, and such adjustments will also be described below.

For NUREG/CR-6923, eight experts were utilized for conducting PIRT. For the current activity, 8-10 experts were selected for each of the key panels. To ensure a diverse set of background and expertise, each panel was assembled to include

- At least one member from the NRC
- At least two members representing industry (EPRI, vendors, etc.)
- At least one member from the DOE national laboratories
- At least one member from academia
- At least two members from outside the United States
- Members from non-nuclear may also be beneficial (for example, civil engineering experience may be very valuable in the concrete assessment)

Selection and assembly of panel experts was performed with NRC and DOE input and approval.

Initial white paper assessments of key degradation modes were then developed to be used as a starting foundation for broader discussion, evaluation, and ranking. For the RPV, concrete, and cable assessments, this was captured by the critical reviews written by the panelists. For the piping and core internal assessment, this was captured by the existing NUREG/CR-6923 and additional discussion on the potential changes that might be experienced during subsequent operating periods. Each white paper assessment was peer reviewed within the panel and revisions were made accordingly. These assessments are listed as the opening chapters of each volume in this activity.

Based on the initial assessment, each panel then developed a PIRT scoring matrix. Typically, this involved identifying key material systems, components, or subcomponents (e.g., nozzles, liners, or polymer types, depending on the panel). For each material, system, component, or subcomponent, the environmental conditions (such as temperature, humidity, water chemistry, or irradiation conditions) were then listed and catalogued. Finally, for each relevant material, system, component, and environment combination, the potential degradation modes, based on laboratory and operational data, were identified and listed. The entire list of material, environment, and degradation mode combinations were then reviewed and revised for consistency.

With a matrix of material, environment, and degradation modes thus developed, scoring was the next task. For each degradation mode, each panelist was asked to provide three scores: Susceptibility, Confidence, and Knowledge. Each panelist ranked these three factors over a range of 0 or 1 to 3. The definition of each factor and meaning of each ranking score is described below.

The **Susceptibility** score gives the panelist's opinion on whether significant material degradation can develop under plausible conditions. Susceptibility was scored 0, 1, 2, or 3, with the following definitions.

0 = not considered to be an issue

1 = conceptual basis for concern from data, or potential problems under unusual operating conditions, etc.

2 = reasonable basis for concern or some plant experience

3 = demonstrated, compelling problem or multiple plant observations

Confidence is a measure of the experts' *personal* confidence in his or her judgment of susceptibility. Confidence was scored as 1, 2, or 3, with the following definitions.

1 = low confidence

2 = moderate confidence

3 = high confidence

Note, a score of "3" is assumed if the Susceptibility Factor is 0.

Finally, **Knowledge** is the experts' current belief of the sufficiency of how the relevant dependencies have been quantified either through laboratory studies, operating experience, or both. As above, knowledge was scored as 0, 1, 2, or 3, with the following definitions.

- 1 = poor understanding, little and/or low-confidence data
- 2 = some reasonable basis to know dependencies qualitatively or semi-quantitatively from data or extrapolation in similar “systems”
- 3 = extensive, consistent data covering all dependencies relevant to the component, perhaps with models—should provide clear insights into mitigation or management of problem.

Subsequent to the completion of panelists scoring, all scores were compiled and the average of Susceptibility and Knowledge were calculated. As Confidence is a measure of personal confidence, the average it is not explicitly factored in the phenomena ranking. Once compiled, any Susceptibility or Knowledge score with a set amount beyond the average was flagged as an “outlier.” This set amount is somewhat arbitrary, but a value of 0.7 was typically used. It is also important to note that the term “outlier” should not be interpreted as incorrect or of questionable value. Indeed, this identification of “outliers” was only performed to spur discussion on scoring amongst the panelists.

After completion of scoring and identification of “outliers,” the panels were reassembled for discussion of the scoring. In most panels, this was done as a face-to-face meeting, but this was not required in all cases. During this discussion, each degradation mode and related scoring was discussed with the “outliers” being of highest priority. In these discussions, the scoring panelist presented rationale for any scores that differed from the average. The objective was not to develop a consensus score or force conformity among the panelists. The primary goal of this discussion was to foster debate and exchange differing points of view. In some cases, the “outlier” was changed based on the debate. In others cases, the other “average” scores were changed as new points of view were presented. This debate and discussion among panelists was an important part of the process to ensure all points of view were considered, including consideration of any new information on the subject area which was not previously considered, and accounted for in the final scoring.

After compiling any changes in scoring following this debate, the PIRT scoring was tabulated to determine relative needs and priorities (Appendix D and Chapter 7). In this process, the average susceptibility and average knowledge scores can be plotted versus each other on a simple plot. Several key categories stand out in such metrics.

- Low knowledge, high susceptibility degradation modes are those that could be detrimental to service with high susceptibility (>2) scores and low Knowledge scores (<2). These scores indicate gaps in understanding and are areas of requiring research into mechanisms and underlying causes to predict occurrence.
- High knowledge, high susceptibility degradation modes are those that could be detrimental to service with high Susceptibility (>2) scores and high Knowledge scores (>2). These modes of degradation are well understood and have likely been observed in service. While there may be mechanistic understanding of the underlying causes, reconfirmation for extended service and research into mitigation or detection technologies may be warranted.
- High knowledge, low susceptibility degradation modes are those that are relatively well understood and of low consequent to service with high Susceptibility (>2) scores and high Knowledge scores (>2). These modes of degradation are well understood and may have been observed in service. Mitigation and maintenance can readily manage this form of

degradation. No research is likely required for these modes of degradation under extended service conditions.

Other combinations of Knowledge and Susceptibility are of course possible and fit between the cases listed above in terms of priority.

Finally, the results of the PIRT scoring were compared to the background chapters to ensure all of the important modes of degradation and points were captured. Revisions were then made to the supporting chapters and analysis to ensure adequate discussion of key topics, outcomes, and underlying causes. Thus, the technical basis information for conducting PIRT and the results of the PIRT were reiterated to ensure that coverage and consistency is maintained in the various PIRT subject areas.

1.3 REFERENCES*

1. NRC, *Expert Panel Report on Proactive Materials Degradation Assessment*, NUREG/CR-6923, U.S. Nuclear Regulatory Commission, February 2007.
2. NRC, *Generic Aging Lessons Learned (GALL) Report*, NUREG-1801, Revision 2, U.S. Nuclear Regulatory Commission, December 2010.
3. EPRI, *Primary System Corrosion Research Program: EPRI Materials Degradation Matrix, Revision 2*, Technical Report 1020987, Electric Power Research Institute, 2010.
4. EPRI, *BWR Vessel and Internals Project: Boiling Water Reactor Issue Management Tables*, BWRVIP-167NP, Revision 2, Technical Report 1020995, Electric Power Research Institute, 2010.
5. EPRI, *Materials Reliability Program: Pressurized Water Reactor Issue Management Tables, Revision 2*, MRP-205, Technical Report 1021024, Electric Power Research Institute, 2010.
6. *U.S. Code of Federal Regulations*, Part 50, Title 10, "Energy," 2013.
7. ASME, "Rules for Inservice Inspection of Nuclear Power Plant Components," Section XI, Appendix G, *Boiler and Pressure Vessel Code (BPVC)*, American Society of Mechanical Engineers, 1995.
8. NRC, *Radiation Embrittlement of Reactor Vessel Materials*, Regulatory Guide 1.99, Revision 2, U.S. Nuclear Regulatory Commission, 1988.
9. R. K. Nanstad, and G. R. Odette, "Reactor Pressure Vessel Issues for the Light-Water Reactor Sustainability Program," *Proc. 14th Int. Conf. on Environmental Degradation of Materials in Nuclear Power Systems*, Virginia Beach, Virginia, August 23–27, 2009.

* Inclusion of references in this report does not necessarily constitute NRC approval or agreement with the referenced information.

2. ENVIRONMENTAL EFFECTS ON FRACTURE RESISTANCE

This chapter addresses only the effects of hydrogen on RPVs. Environmental effects on fracture resistance are identified in the MDM as gap No. P-DM-09 and B-DM-06 [1]. Although the inner surface of LWR RPVs is generally lined with austenitic stainless steel to prevent corrosion, in the event of cracks developing in the austenitic cladding, the base metal of the pressure vessel, a ferritic low-alloy steel (LAS), could absorb the hydrogen produced by corrosion and other reactions [2, 3] because of direct contact with the high-temperature coolant water. The principal sources of hydrogen in PWR systems under normal operating conditions are (a) dissociations of the hydrogen present in the water at the steel-water interface; (b) corrosion reactions at the steel-water interface; and (c) radiolytic decomposition of the water. Harries and Broomfield [3] have critically examined all three scenarios and concluded that only the corrosion reaction at the steel-water interface could be a significant source of hydrogen in RPV materials. By assuming pessimistic and unacceptable corrosion rates, they concluded that the hydrogen concentration in the steel would not exceed 1 to 2 ppm.

It is known that the adverse effects due to hydrogen become most acute in high-strength steels, where instances of loss of ductility [4] and delayed failure have been attributed to the presence of hydrogen at the 1 ppm or lower levels. Further, aqueous environments [5] have been shown to generate sufficient hydrogen at the metal-water interface to embrittle high-strength steel. For lower-strength or mild steels, higher hydrogen concentrations are required to effect a decrease in ductility similar to that of high-strength steels at equivalent hydrogen concentrations [6].

There are very limited data on the effect of hydrogen on fracture resistance of RPV steels, and only a few studies have considered hydrogen effects on irradiated RPV steels. In all these studies, hydrogen was cathodically charged into preirradiated or unirradiated steel prior to testing. For example, Brinkman and Beeston [7] studied the effects of postirradiation hydrogen charging on the ductility of A302 Grade B, A542 Class 2, and HY-80 (A543) steels. It was shown that the ductility of A302B steel after irradiation to fluences of nearly 3×10^{20} n/cm² ($E > 1$ MeV) was not significantly affected by the presence of up to 2 ppm hydrogen. However, as hydrogen concentration increased above 2 ppm, a marked decrease in ductility was observed with essentially a nil ductility condition reached at the 5 to 6 ppm level. These conditions are relevant primarily to a PWR. Lower fluences will be experienced in BWRs although higher hydrogen concentrations may be found in the coolant. HY-80 and A542 steel in the normal quenched and tempered condition were much more responsive to the presence of 1 to 2 ppm hydrogen. Subsequent to irradiation to 2×10^{20} n/cm² ($E > 1$ MeV), A542 steel showed essentially nil ductility at the 2 to 3 ppm level, and HY-80 displayed nil ductility at 1 to 2 ppm. Heat treatment or cold working, which increased the tensile strength (like irradiation), resulted in a condition that was more sensitive to hydrogen-induced ductility reduction, particularly after a strength level of approximately 1,240 MPa (180 ksi) had been attained.

Cho and Kim [8] studied the effects of hydrogen on tensile properties of SA508 Cl.3 RPV steel at room temperature and at 288 °C (550 °F). Additionally, tensile properties of SA508 Cl.3 steel were investigated at room temperature and at 288 °C (550 °F) before and after electrolysis hydrogen charging. At room temperature, the charged hydrogen-induced distinct hardening and ductility loss occurred where quasi-cleavage features were observed around inclusions. The results may be due to interactions between the dissolved hydrogen and dislocations and an increase of hydrogen concentration near the inclusions. On the other hand, at 288 °C (550 °F), the charged hydrogen induced some softening, which was explained in terms of the hydrogen shielding effect and of strain localization by dynamic strain aging. Further, at 288 °C (550 °F),

the fracture surfaces of the hydrogen-charged specimens showed brittle regions where the hydrogen might have been trapped in microvoids, leading to internal pressurization.

Takaku and Kayano [9] examined the effects of hydrogen absorption on mechanical properties of A533B and A542 steels. Their observations on loss of ductility as a result of hydrogen charging were similar to the previous results. However, in addition to tensile tests, they studied Charpy impact toughness with and without hydrogen. Their results demonstrated that hydrogen does not have any effect on the ductile-to-brittle transition temperature (DBTT), but it causes noticeable reduction in the upper-shelf energy (USE), as shown in Figures 2.1 and 2.2.

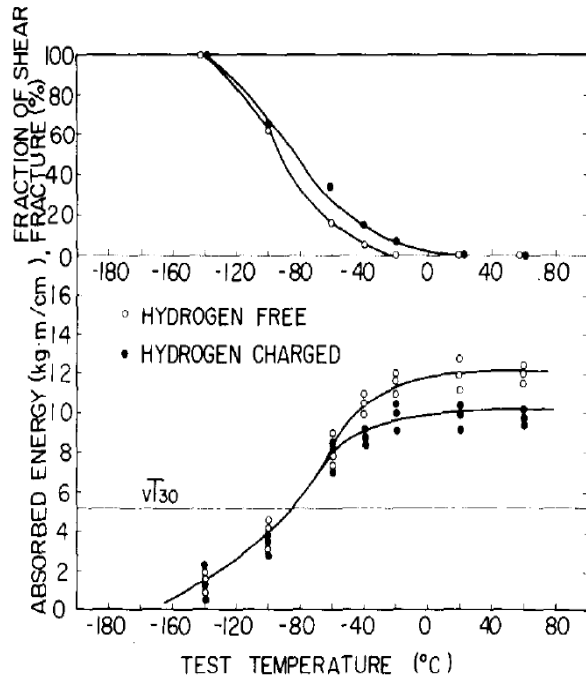


Figure 2.1. Charpy impact toughness of A533B steel, hydrogen charged up to 1.6 ppm [9]. Reprinted from H. Takaku and H. Kayano, "Hydrogen Embrittlement of Unirradiated Steels for Nuclear Reactor Pressure Vessels," *Journal of Nuclear Materials* 78, 299–308 (1978), with permission from Elsevier.

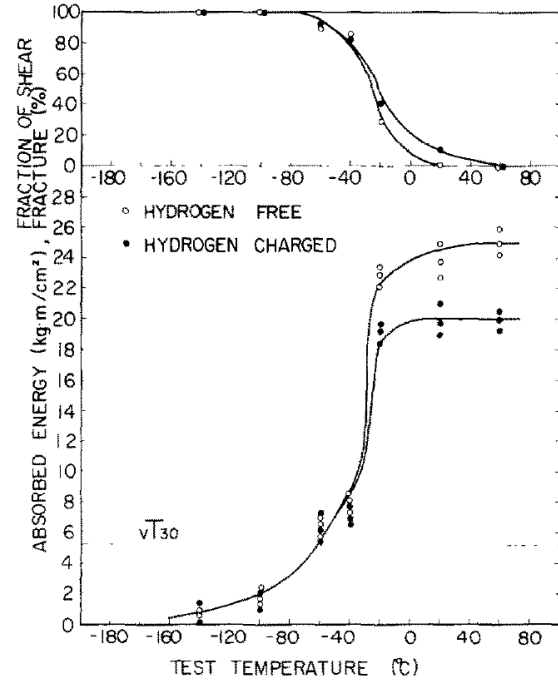


Figure 2.2. Charpy impact toughness of A542 steel, hydrogen charged up to 2.2 ppm [9]. Reprinted from H. Takaku and H. Kayano, "Hydrogen Embrittlement of Unirradiated Steels for Nuclear Reactor Pressure Vessels," *Journal of Nuclear Materials* 78, 299–308 (1978), with permission from Elsevier.

Splichal et al. [10] studied the effect of hydrogen on irradiated fracture toughness of Voda-Vodyanoi Energetichesky Reaktor (VVER) RPV steel. Although the chromium (Cr) content in steels used for VVER RPV is higher compared to LWR RPV steels, the effect of hydrogen on fracture toughness of VVER steel appears to be similar to the results shown in Figures 2.1 and 2.2. At hydrogen levels below 3 ppm, no effects were observed from hydrogen on transition fracture toughness temperature. However, hydrogen reduced the ductile initiation fracture toughness for both unirradiated and irradiated VVER steel as shown in Figure 2.3.

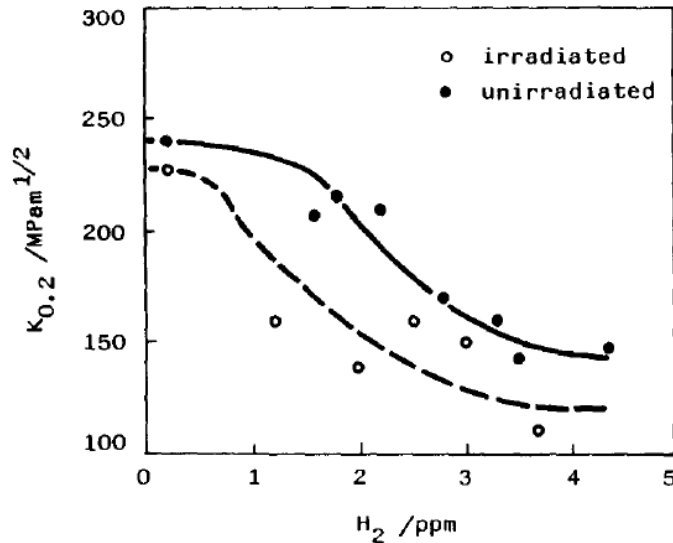


Figure 2.3. The effect of hydrogen on the ductile fracture toughness of VVER RPV steel [10].

Reprinted from K. Spichal, M. Ruscak, and J. Zdarek, "Combination of Radiation and Hydrogen Damage of Reactor Pressure Vessel Materials," *International Journal of Pressure Vessels and Piping* 55, 361–373 (1993), with permission from Elsevier.

Thus, hydrogen embrittlement is a potential degradation mechanism of fracture resistance of RPV materials. It appears, based on very limited data for hydrogen not exceeding 2 ppm [3], that this mechanism should not present a concern for LWRs under normal operating conditions. However, if future relevant test data and extended operating experience indicate that 60 year operation of RPVs could cause hydrogen buildup, then an assessment of hydrogen buildup and the development of subsequent mitigation procedure for 80 year operation may be needed. Based on the data available, a hydrogen level of 4 ppm and higher in the RPV material could become a contributor to the overall degradation in fracture resistance of the RPV.

2.1 REFERENCES*

1. EPRI, *Primary System Corrosion Research Program: EPRI Materials Degradation Matrix*, Revision 2, Technical Report 1020987, Electric Power Research Institute, 2010.
2. G. H. Broomfield, "Hydrogen Effects in an Irradiated 1Cr and ½ Mo PWR Pressure Vessel Steel," *Journal of Nuclear Materials* 16, 249–259 (1965).
3. D. R. Harries and G. H. Broomfield, "Hydrogen Embrittlement of Steel Pressure Vessels in Pressurized Water Reactor Systems," *Journal of Nuclear Materials* 9, 327–338 (1963).
4. K. Farrell and A. G. Quarrell, "Hydrogen Embrittlement of Ultra-High-Tensile Steel," *Journal of the Iron & Steel Institute* 202(12), 1002–1011 (December 1964).
5. E. E. Fletcher and A. R. Elsea, "Problems of Hydrogen in High-Strength Steels," *Battelle Technical Review* 16(12), 10–15 (December 1967).

* Inclusion of references in this report does not necessarily constitute NRC approval or agreement with the referenced information.

6. W. H. Munse, "Brittle Fracture in Weldments," p. 371 in *Fracture, an Advanced Treatise, Vol. 4: Engineering Fracture Design*, H. Liebowitz (ed.), Academic Press, Waltham, Massachusetts, 1969.
7. C. R. Brinkman and J. M. Beeston, *The Effects of Hydrogen on the Ductile Properties of Irradiated Pressure Vessel Steels*, IN-1359, Idaho Nuclear Corporation, February 1970.
8. H. Cho and I. S. Kim, "Effects of Hydrogen on Tensile Properties of SA508 Cl.3 Reactor Pressure Vessel Steel at High Temperature," *Materials Science Forum* **475–479**, 4121–4124 (2005).
9. H. Takaku and H. Kayano, "Hydrogen Embrittlement of Unirradiated Steels for Nuclear Reactor Pressure Vessels," *Journal of Nuclear Materials* **78**, 299–308 (1978).
10. K. Splichal, M. Ruscak, and J. Zdarek, "Combination of Radiation and Hydrogen Damage of Reactor Pressure Vessel Materials," *International Journal of Pressure Vessels & Piping* **55**, 361–373 (1993).

3. THERMAL EMBRITTLEMENT OF RPV STEELS

The state of the knowledge of thermal embrittlement of RPV LASs was summarized in 2003 [1]. This is reflected in the EPRI MDM as gap No. P-DM-10. Those results with a description of potentially affected components are highlighted in this section and are followed by a brief description of recommended research. The ferritic primary pressure boundary LASs that operate at higher temperatures are prone to thermal aging embrittlement. The pressurizer experiences the highest operating temperature at around 343 °C (650 °F). The LAS components, such as the RPV flange, nozzle shell ring, and outlet nozzles, experience temperatures of up to [315 °C (~600 °F)].

3.1 ATOMIC ENERGY RESEARCH ESTABLISHMENT HARWELL RESULTS

Extensive thermal aging studies were performed on commercially produced PWR pressure vessel steels, welds, and heat-affected zones (HAZs) by Druce et al. at the Atomic Energy Research Establishment (AERE), Harwell (UK Atomic Energy Authority), during the 1970s and 1980s in support of the Sizewell Reactor Projects [2]. The materials tested included SA-533, Grade B plate; SA-508, Class 3 forgings; and weld metal. The studies covered the temperature range from 300 °C (572 °F) to 600 °C (1112 °F) for durations of up to 20,000 h.

Various microstructures were created, including coarse-grained, fine-grained, refined-grained, and coarse-grained inter-critical simulated HAZ materials. Aging at 300 °C (572 °F) produced no detectable changes in mechanical or Charpy impact properties in either the coarse- or fine-grained HAZ material that was aged for up to 20,000 h. Aging at 400 °C (752 °F) for 20,000 h caused the DBTT shift of the coarse-grained HAZ material to increase by 175 °C (315 °F) with no indication of saturation, but with little changes in the USE and mechanical properties. The fine-grained HAZ material showed an increase in the DBTT as well when aged at 400 °C (752 °F) for 20,000 h, but DBTT was significantly less than for the coarse-grained HAZ material. The simulated, refined-grained HAZ material exhibited considerable variability in initial DBTT and an entirely transgranular-cleavage, low-temperature fracture appearance. Aging at 300 °C (572 °F) and 400 °C (752 °F) produced no detectable changes in the refined-grained HAZ material, indicative of a microstructure resistant to thermal aging effects. The unaged simulated intercritical HAZ microstructures had DBTT values similar to those of the unaged coarse- and fine-grained HAZ material. Aging at 450 °C (842 °F) produced an increase of 35 °C to 45 °C (63 °F to 81 °F) in DBTT, indicating a microstructure that could be considered more resistant to thermal aging embrittlement than coarse-grained HAZ material.

3.2 OAK RIDGE NATIONAL LABORATORY RESULTS

Nanstad et al., at Oak Ridge National Laboratory (ORNL), reported short-term, thermal-aging results for typical RPV steels [3], such as SA-302, Grade B; SA-533, Grade B; and SA-508, Class 2. The steels were heat-treated to simulate a coarse-grained HAZ from a typical weld pass and were annealed at 399 °C, 450 °C, and 482 °C (750 °F, 842 °F, and 900 °F) for 168 h to simulate an RPV annealing procedure. Aging at 399 °C (750 °F) for 168 h resulted in no changes in the DBTT of all four materials tested. However, aging at 450 °C and 482 °C (842 °F and 900 °F) caused a noticeable increase in DBTT in the coarse-grained HAZ material. Nanstad et al. suggested 399 °C (750 °F) as a lower-bound aging temperature for temper embrittlement in coarse-grained regions of the HAZ in RPV steels. However, an aging duration of 168 h is

considered to be too short to establish the lower-bound embrittlement temperature for operation up to 80 years.

3.3 BABCOCK AND WILCOX AGING RESULTS

Blocks of RPV steel consisting of an SA-508 Class 2 forging, a Linde 80 Mn-Mo-Ni submerged-arc weld, and an SA-533, Grade B, Class 1 correlation monitor material were thermally aged on top of a Babcock and Wilcox (B&W) designed plant RPV head [4]. The materials were exposed to a thermal environment of about 260 °C (500 °F) for 200,000 h, which is below the range [minimum of 370 °C (698 °F)] where the effects of long-term thermal aging are typically considered directly relevant and below the RPV down comer (cold leg) temperatures of PWRs and BWRs. Charpy impact, Master Curve transition temperature, upper-shelf fracture toughness, and tensile testing were conducted to evaluate the long-term thermal aging changes in material properties. Small changes in the mechanical properties were observed for all the materials, but they were generally not statistically significant. The materials were also tested to 100,000 h. They have continued to age on a replacement RPV head since the fall of 2005. The replacement head has better insulation, so the current aging temperature is higher and now closer to the RPV temperature.

3.4 FRENCH RSE-M RESULT

The French nuclear code, Rules for In-Service Inspection of Nuclear Power Plant Components (RSE-M), provides guidance for estimating the thermal-aging-embrittlement shift as a function of temperature and phosphorous (P) for two temperature ranges after 40 years of operation: <300 °C and 300 °C to 325 °C (<572 °F and 572 °F to 617 °F) [5]. Phosphorous is a significant cause of grain boundary embrittlement (temper embrittlement). Predictions are given for base metal, welds, and underclad HAZs. An estimate has also been proposed for a higher temperature range, 325 °C to 350 °C (617 °F to 662 °F). Using the RSE-M-proposed estimation for a high-P forging (0.020, taken from the U.S. RPV database as a typical high-P forging [6]), the proposed HAZ DBTT shift is 108 °C (195 °F) at the pressurizer temperature, potentially exceeding the RPV embrittlement shift. Using the RSE-M code estimation at the hot leg temperature for a high-P forging, the predicted HAZ DBTT shift is 46 °C (84 °F).

3.5 RPV COMPONENTS POTENTIALLY AFFECTED BY THERMAL EMBRITTLEMENT

The HAZs of higher-temperature LAS components are potentially prone to thermal aging. Of the LAS components in the primary loop, the pressurizer experiences the highest temperature. It typically operates at a temperature around 343 °C (650 °F) and could undergo a significant shift in HAZ DBTT (rivaling the RPV irradiation embrittlement shift).

Some pressurizers were constructed from carbon steel, which are not prone to thermal aging. Pressurizers typically experience less extreme faulted transient stresses than those in the RPV. However, due to thermal stratification in both components, normal heatup/cooldown transient stresses in the pressurizer could be as high as those in the RPV. Therefore, the pressurizer, if fabricated from LAS, and portions of the RPV that operate at high temperature could be prone to thermal aging and have significant stresses. Corrosion, stress corrosion, and other related degradation modes for low-alloy and carbon steels are discussed in considerably more detail in Volume 3, Chapter 5 of this Expanded Materials Degradation Assessment.

The RPV components that reach higher temperatures [315 °C (~600 °F)] would consist of the RPV flange, the nozzle shell ring, and the outlet nozzles of all plants as well as the vessel heads of some reactors, which have head temperatures near the hot leg temperature of about 315 °C (~600 °F). Many of the RPV heads of the U.S. plants, including the heads in all hot head plants, have been replaced. Thus the aging clock has been reset. The nozzle shell ring and outlet nozzles receive a low neutron dose rate exposure, which could synergistically combine with thermal aging, potentially creating greater-than-expected embrittlement. That region, known as the extended beltline, is undergoing pressure-temperature curve evaluation by the Pressurized Water Reactor Owners Group (PWROG); however, thermal aging shift in DBTT is not being considered in the PWROG evaluation, because the postulated nozzle flaws do not intersect with an HAZ.

3.6 SUMMARY AND RECOMMENDED RESEARCH

Combustion Engineering pressurizers were fabricated with materials similar to RPV materials and operate at about 343 °C (650 °F). Because the pressurizer is the reactor coolant system (RCS) pressure boundary component that reaches the highest temperature, any thermal-aging embrittlement seen would be a leading indicator for the rest of the RCS. Pressurizers have been retired at Saint Lucie 1 (Fall 2005), Millstone 2 (Fall 2006), and Fort Calhoun (Fall 2006); they may be available for material examination. Selection should be based on availability of baseline properties or material, owner acceptance, and material suitability. Finding baseline unaged material properties could be difficult; however, even without baseline properties, relatively high DBTT, evidence of grain boundary P segregation, and intergranular fracture indicating thermal aging can be determined using the retired pressurizer material. Examination of LAS pressurizer HAZs will provide information on the extent of the long-term embrittlement of a component which has experienced reactor operation. This information (along with information cited above) can be used to determine if there is a need to address thermal aging embrittlement for LTO.

A number of steam generators have been replaced. The bottom head of Westinghouse designed steam generators was fabricated from SA-508 forgings, the same type as the RPV. The same bottom head bowl forging has a cold leg and a hot leg nozzle welded to it. Therefore, retired SG bottom bowl nozzle HAZs could be examined. The properties and microstructure of the cold leg side (where no thermal ageing is expected) could be compared to the hot leg side (where thermal aging is possible). The HAZ of the same material could be evaluated for evidence of long-term thermal aging.

In the PWROG/EPRI research program, thermal aging continues for the B&W origin materials cited above on the RPV head of Arkansas Nuclear One Unit 1 (ANO-1). A 300,000 h exposure is projected to be reached in 2017. The aging temperature since the specimens were placed on the new ANO-1 head at about 200,000 h is higher than the previous aging temperature (due to better head insulation). Although the aging temperature is relatively low, the material has an exceptionally long aging time and the mechanical properties and microstructure have been well documented, making it a unique candidate for evaluation. It is recommended that some of the material be tested after 300,000 h aging to assess any changes in the transition temperature, HAZ microhardness, and microstructure.

Table 3.1 displays the measured shift in coarse grain HAZ thermal embrittlement (green), RSE-M code guidance (blue), LAS components in the RCS (peach), and potential sources of test materials (white) sorted by aging temperature. This table shows clearly the time and temperature of the operating components relative to the data and potential available test material. The data need and potential available test material can be deduced from this table.

Table 3.1. Thermal embrittlement comparison

Study/Component	Coarse Grain HAZ Thermal Embrittlement Summary			
	Time (1,000 h)	Temperature (°C)/(°F)	Embrittlement Shift (°C /°F)	Comments
B&W	200	260 / (500)	None	Measured data
B&W future	300	260 & 280 / (500 & 536)		
Cold leg/RPV beltline	630	<294 / (< 561)		80 years
RSE-M	300	<300 / < 572	16 / (8.9)	Code guidance
AERE (Atomic Energy Research Establishment)	20	300 / (572)	None	Measured data
Retired SG bowl forging	~230	315 / (599)		
Hot leg/upper RPV	630	315 / (599)		80 years
RSE-M	300	300 to 325 / (599 to 617)	46 / (25.6)	Code guidance
Retired pressurizer	~230	340 / (644)		No baseline data
Pressurizer	630	340 / (644)		80 years
RSE-M	300	325 to 350 / (617 to 662)	108 / (60)	Code guidance
AERA	20	400 / (752)	175	Measured data
ORNL	0.17	400 / (752)	No	Measured data
ORNL	0.17	450 / 752	Yes	Measured data

Key: , coarse grain HAZ thermal embrittlement; , potential sources of test materials; , LAS components in the RCS; , RSE-M code guidance.

3.7 REFERENCES*

1. EPRI, *Materials Reliability Program: A Review of Thermal Aging Embrittlement in Pressurized Water Reactors (MRP-80)*, Technical Report 1003523, Electric Power Research Institute, 2003.
2. S. G. Druce, G. Gage, and G. R. Jordan, The Effect of Long Term Thermal Aging on the Mechanical Properties of ASTM A533B and A508 Steels in the Quenched and Tempered and Simulated Heat Affected Zone Conditions, AERE-R11459, U.K. Atomic Energy Authority, Harwell, April 1985.
3. R. K. Nanstad, D. E. McCabe, M. A. Sokolov, C. A. English, and S. R. Ortner, "Investigation of Temper Embrittlement in Reactor Pressure Vessel Steels Following Thermal Aging, Irradiation, and Thermal Annealing," *Effects of Radiation on Materials, 20th Int. Symp.*, ASTM STP 1405, ASTM International, 2001.

* Inclusion of references in this report does not necessarily constitute NRC approval or agreement with the referenced information.

4. H. P. Gunawardane, J. B. Hall, and S. T. Rosinski, "Mechanical Property Changes in Reactor Vessel Materials Thermally Aged for 209 000 Hours at 260 °C," *Effects of Radiation on Materials: 22nd Int. Symp.*, ASTM JAI 9006, ASTM International, 2002.
5. RSE-M, "In-Service Inspection Rules for Mechanical Components of PWR Nuclear Islands," Appendix 5.6, Materials Characteristics, French Society for Design, Construction and In-service Inspection Rules for Nuclear Islands (AFCEN).
6. Reactor Vessel Integrity Database Version 2.0.1, U.S. Nuclear Regulatory Commission, July 2000.

4. LONG-TERM INTEGRITY OF DISSIMILAR METAL WELDS

4.1 INTRODUCTION

Ni alloy weld metal has been used for dissimilar metal weld joints at RPV penetrations in both BWRs and PWRs. SCC of Alloy 600 series weld metals, such as Alloy 182 and 132, has occurred at several locations, including the top head control rod drive mechanism (CRDM) nozzles, main coolant outlet nozzles, and steam generator (SG) inlet nozzles in PWRs and control rod drive (CRD) nozzles and shroud supports in BWRs. The cracks initiated at the inner surfaces of the RPVs, but no crack extension into the LASs at those locations has been identified, even though the cracks went through the Ni alloy weld metals to reach the interface (fusion line) between the weld metals and LASs. Laboratory experiments showed that Ni alloy weld metals are susceptible to SCC under the water conditions of both PWRs and BWRs. LASs are susceptible to SCC under the oxygenated conditions of BWRs. Efforts to address those situations have been devoted to identifying the mechanism of SCC growth, developing advanced methods of residual stress evaluation, improving the SCC resistance of materials, and mitigating SCC susceptibility via water chemistry control and stress improvement (see Figure 4.1). These aspects are also addressed rather extensively in Volume 2, which contains the PIRT for piping and internals.

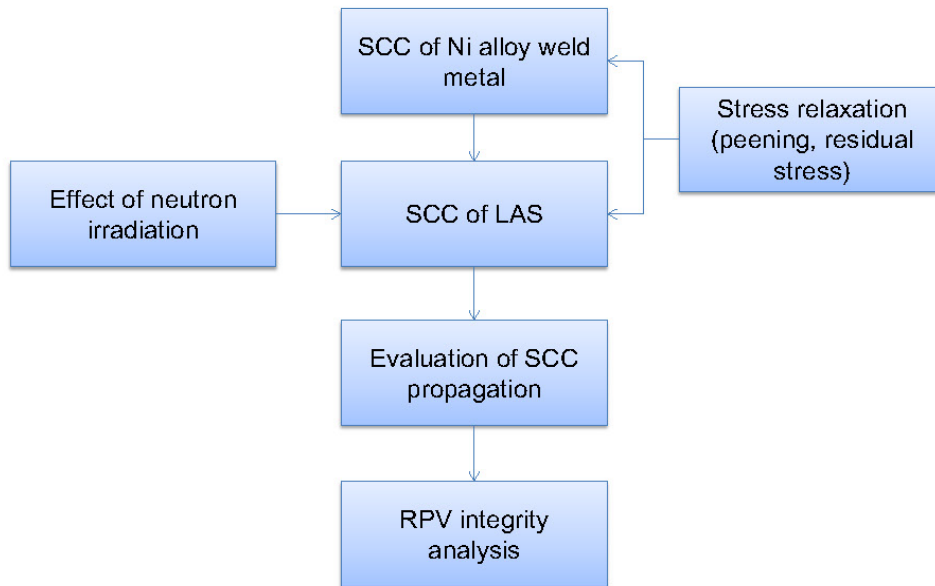


Figure 4.1. Summary of SCC issues for RPV.

If SCC in the Ni alloy weld metal of dissimilar metal weld joints were to propagate into the RPV steel, a concern would arise about the structural integrity of the RPV. Particularly, because frequent nondestructive inspection is difficult at the bottom head of a BWR reactor vessel and because LAS is susceptible to SCC under the normal water chemistry (NWC) conditions, the presence of SCC at the dissimilar metal weld joints could be a significant issue in ensuring the long-term structural integrity of the RPVs in the plants where the hydrogen water chemistry (HWC) operation has not been adopted. It should be noted that there are no domestic BWRs operating under normal water chemistry. They are using HWC or noble metal chemical application (NMCA), with all planning to move to NMCA over the next few years. In the PWR

primary system environment, on the other hand, weld metals such as Alloy 182, 82, and 132 have SCC susceptibility, and thus the SCC that initiates in a weld metal is likely to reach a LAS base metal. However, the likelihood that SCC will propagate into the LAS base metal will be very low because the ECP in the PWR primary system is lower than that in the BWR HWC or NMCA environment. Long-term integrity of dissimilar metal welds has also been addressed in MDM Gap Nos. P-DM-13 and B-DM-09.

4.1.1 Current Status of R&D and Gaps

4.1.1.1 SCC susceptibility of Ni weld metal

SCC in Alloy 182 weld metals under a BWR environment has been well characterized, and the SCC growth disposition curve has been developed [1]. On the other hand, the crack growth disposition curve of the SCC growth rate in Alloy 82 weld metals has not been specified because of the very low SCC susceptibility of Alloy 82 weld metals compared with that of Alloy 182 weld metals [2]. However, Alloy 82 weld metals are widely used in many of the relatively new plants, and thus the characterization of the SCC in Alloy 82 weld metals and the standardization of the evaluation method of SCC in Alloy 82 weld metals are required to improve the integrity assessment of such nuclear power plants that use Alloy 82 weld metals. It should be noted that there are no reported cases of cracking to date of Alloy 82.

The effect of long-term thermal aging (i.e., 80 years of operation at operating temperatures) on the SCC susceptibility of Alloy 82 weld metals is not yet understood. It is well accepted that the surface oxide film plays a very important role in the initiation of SCC, and some evidence has been reported to show the effects of machining, stress, and neutron irradiation on surface oxide film [3]. However, no information is currently available about the status of the surface oxide layer exposed to the reactor water environment for a period of 80 years. For such a case, the possibility of delayed occurrence of SCC cannot be denied.

In the PWR environment, primary water stress corrosion cracking (PWSCC) in Ni Alloy 600 series weld metals such as Alloy 182 and 132 has also been well characterized, and the SCC growth disposition curve has been developed [4], but initiation behavior after long term exposure is not understood. As discussed in Volume 2, Aging of Core Internals and Piping Systems, the information on the SCC growth rate in Alloy 690 series weld metals such as Alloy 152 and 52, both of which are known to show high SCC resistance, is not necessarily sufficient, and research is still under way [5, 6]. The SCC initiation behavior in these weld metals has not been well understood; the SCC initiation after long-term operation needs to be fully investigated.

For 60 to 80 years of reactor operation, in addition to a possible change in the property of the surface layer due to long-term exposure to the reactor water environment such as that found in BWRs, the formation of long-range ordering (LRO) of intermetallic compounds of the Ni_2M type, such as Ni_2Cr , needs to be considered in both BWRs and PWRs. For example, in Alloy 690, because γ' intermetallic compounds of the Ni_2M type (mainly consisting of Ni and Cr) are more thermally stable at temperatures near 572 °F (300 °C) than the austenitic γ -phase, ordering precipitates of the Ni_2M type intermetallic compounds may occur after long-term operation [7]. Because LRO of the precipitates of intermetallic compounds can affect the hardness and toughness of alloys, their effect on on SCC susceptibility for LTO may need further research.

4.1.1.2 SCC susceptibility of LAS

For the BWR environment, LASs show SCC susceptibility under oxygenated conditions, and the work by Seifert has identified several variables that affect the SCC characteristics in LAS [8]. The SCC disposition curves in EPRI VIP-60 and VIP-233 were determined using the results of multiple investigators including Seifert's results [9].

It is well known that the SCC growth rate depends on the concentration of chloride ions (Cl^-) and particularly that SCC growth rate is significantly increased when the concentration of Cl^- exceeds 5 ppb [8]. However, the effect of Cl^- at a concentration lower than that of EPRI *BWR Water Chemistry Guidelines*, BWRVIP-79 [10] action level 1 ($\text{Cl}^- = 5$ ppb) is not well understood.

The validity of the crack growth rate obtained for LASs is another issue that must be considered. Much of the crack growth data were obtained from small specimens that do not meet the requirement of American Society for Testing and Materials (ASTM)-E399, "Standard Test Method for Linear-Elastic Plane-Strain Fracture Toughness K_{Ic} of Metallic Materials," for the plain-strain condition [8]. The reliability in estimating the growth rates of the cracks in RPVs from crack data obtained from small samples needs further research and confirmation. In the absence of more reliable disposition curves, this issue needs to be addressed with appropriate conservatism.

The crack extension behavior at the fusion line between Ni alloy weld metals and LASs is very important because it is not certain that the cracks initiated in the Ni-based weld metals propagate into the vessel. Two occurrences have been reported in Japan. At Tsuruga Unit 1, no SCC propagation into the vessel steel was identified [11], whereas at the Japan Power Demonstration Reactor (JPDR) of the Japan Atomic Energy Agency (JAEA) [the former Japan Atomic Energy Research Institute (JAERI)], the SCC that occurred in the stainless cladding propagated into the vessel steel, and a corrosion pit was formed in the LAS vessel [12]. This was studied by Kumagai et al. [13, 14]; however, additional investigations are necessary to understand crack extension behavior for long-term operation (beyond 60 years).

The SCC propagation properties of LASs depend on hardness (i.e., hardening enhances the crack growth rate) [8]. Therefore, the hardening of LASs due to neutron irradiation may enhance the crack propagation rate. Thus, the effect of neutron irradiation on SCC susceptibility should be a new issue to be considered. Although there is a report stating that no effect of neutron irradiation on SCC susceptibility was identified at the neutron fluence of 1.7×10^{22} n/cm², $E > 1$ MeV [15], the information is very limited, and further research is required.

The susceptibility of LAS to SCC in a PWR environment is very low because of its low ECP [16], and it is not likely that SCC would occur in PWR RPV steels. However, as in BWRs, it is still an open question whether neutron irradiation in PWRs has an effect on the susceptibility of LAS to SCC.

4.1.2 Residual Stress and Crack Growth Evaluation

Residual stress evaluation is another important aspect of the assessment of SCC in RPVs. The compressive part of residual stress is expected to act to suppress SCC propagation. However, the possibility of the relaxation of residual stress under long-term thermal aging at reactor operating temperatures cannot be excluded. Relaxation of residual stress would result in the reduction of tension stress near the surface, which might reduce the chance of crack initiation but might also reduce the compression stress that could stop the crack propagation.

Stress improvement techniques such as IHSI (Induction Heat Stress Improvement), mechanical stress improvement, and optimized WOL (weld overlay) have been widely applied on RPV nozzles. Techniques such as shot peening, water jet peening, and laser peening have been widely accepted outside of the United States, and implemented in both BWRs and PWRs as measures to improve residual stress conditions near the surface (to shift the residual stress from a tension state to a compression state) [17, 18]. At the same time, mitigation via water chemistry control has also been investigated. In BWRs, HWC and noble metal chemical addition (NMCA) have been used to reduce the electric chemical potential (ECP) of the coolant water [19]. In PWRs, to reduce the occurrence of PWSCC, zinc (Zn) addition and dissolved hydrogen (DH) optimization have been considered [20, 21]. However, these methods have not been endorsed by the NRC. Stress improvement techniques mentioned in this section have been found to be a very effective action to prevent the occurrence of SCC but are not currently used in the United States. However, the relaxation of stress after long-term thermal aging at the operating temperatures and its effect on SCC mitigation are not well understood and need to be addressed in the evaluation of extending reactor operating time to 80 years.

4.2 SUMMARY OF ACTIONS NECESSARY TO EXTEND REACTOR OPERATION TO 80 YEARS

Unless experiences from the initial 40 year operation and the first license renewal operating period (40 to 60 years) indicate that the following factors are insignificant, they must be considered in the evaluation of whether the operating time for BWRs and PWRs can be extended from 60 to 80 years:

- Effect of long-term thermal aging on the susceptibility of Alloy 82 weld metals to SCC
- Effect of long-term operation on the susceptibility of Alloy 152 and 52 weld metals to SCC
- Effect of alloying elements and their compounds formed during heat treatment on the susceptibility of lass to SCC under BWR conditions
- Validity of the crack growth data for LAS and in the SCC disposition curves
- Crack behavior at the fusion weld line between Ni alloy weld metal and LAS
- Effect of neutron irradiation on the susceptibility of lass to SCC

4.3 REFERENCES*

1. R. Pathania and R. G. Carter, "Nickel Alloy Crack Growth Correlations in BWR Environment and Application to Core Support Structure Welds Evaluation," *Proc. of 2008 ASME Pressure Vessels and Piping Division Conference*, PVP2008-61299, American Society of Mechanical Engineers, 2008.
2. M. Ozawa, Y. Yamamoto, K. Nakata, M. Itow, N. Tanaka, M. Kikuchi, M. Koshiishi, and J. Kuniya, "Evaluation of SCC Crack Growth Rate in Alloy 600 and Its Weld Metals in Simulated BWR Environments," *12th Int. Conf. on Environmental Degradation of Materials in Nuclear Systems—Water Reactors*, The Minerals, Metals & Materials Society, 2005.

* Inclusion of references in this report does not necessarily constitute NRC approval or agreement with the referenced information.

3. Y. Takeda, T. Sato, D. Yamauchi, T. Shoji, A. Ohji, "Non-Linear Dynamics of the Morphology at the Oxide/Metal Interface of Austenitic Steels in Simulated Light Water Reactor Environments and Its Implications for SCC Initiation," *Proc. 15th Int. Conf. on Environmental Degradation of Materials in Nuclear Power Systems—Water Reactors*, August 7–11, 2011, The Minerals, Metals and Materials Society, 2011.
4. G. A. White, N. S. Nordmann, J. Hickling, and C. D. Harrington, "Development of Crack Growth Rate Disposition Curves for Primary Water Stress Corrosion Cracking (PWSCC) of Alloy 82, 182, And 132 Weldments," *Proc. 12th Int. Conf. on Environmental Degradation of Materials in Nuclear Power System—Water Reactors*, The Minerals, Metals & Materials Society, 2005.
5. B. Alexandreanu, Y. Yang, Y. Chen, and W. J. Shack, "The Stress Corrosion Cracking Behavior of Alloys 690 and 152 Weld in a PWR Environment," *Proc. 14th Int. Conf. on Environmental Degradation of Materials in Nuclear Power Systems, Virginia Beach, Virginia*, August 23–27, 2009, American Nuclear Society, 2009.
6. M. B. Toloczko and S. M. Brummer, "Crack Growth Response of Alloy 152 And 52 Weld Metals in Simulated PWR Primary Water," *Proc. 14th Int. Conf. on Environmental Degradation of Materials in Nuclear Power Systems, Virginia Beach, Virginia*, August 23–27, 2009, American Nuclear Society, 2009.
7. F. Delabrouille, D. Renaud, F. Vaillant and J. Massoud, "Long Range Ordering of Alloy 690," *14th Int. Conf. on Environmental Degradation of Materials in Nuclear Power Systems, Virginia Beach, Virginia*, August 23–27, 2009, American Nuclear Society, 2009.
8. H. P. Seifert and S. Ritter, "Stress Corrosion Cracking of Low-Alloy Reactor Pressure Vessel Steels under Boiling Water Reactor Conditions," *Journal of Nuclear Materials* **372**, 114–131 (2008).
9. EPRI, *Evaluation of Stress Corrosion Crack growth in Low Alloy Steel Vessel Materials in the BWR Environment*, BWRVIP-60-A, Electric Power Research Institute, 2003.
10. EPRI, BWR Vessel and Internals Project, *BWR Water Chemistry Guidelines – 2000 Revision*, Electric Power Research Institute, 2000.
11. T. Aoki, S. Hattori, H. Anzai, and H. Sumimoto, "Stress Corrosion Cracking in Ni-Base Alloy Used for a Long Time in a BWR," *Maintenology* **4**(1), 34–40 (2005).
12. T. Kondo, H. Nakajima, R. Nagasaki, "Metallographic Investigation on the Cladding Failure in the Pressure Vessel of a BWR," *Nuclear Engineering & Design* **16**, 205–222, 1971.
13. K. Kumagai, M. Morra, P. Andresen, G. Catlin, L. Nelson, S. Suzuki Y. Takagi, and R. Horn, "Effects of K and Anion Impurity Concentration on Crack Growth Kinetics Near Alloy 182/A533B Weld Overlay Boundaries in BWRs," *14th Int. Conf. on Environmental Degradation of Materials in Nuclear Power Systems, Virginia Beach, Virginia*, August 23–27, 2009, American Nuclear Society, 2009.
14. T. Kubo, M. Itow, N. Tanaka, and T. Saito, "SCC Retardation and Propagation Behavior in Dissimilar Weldment of Alloy 182 and Low Alloy Steel," *14th Int. Conf. on Environmental Degradation of Materials in Nuclear Power Systems, Virginia Beach, Virginia*, August 23–27, 2009, American Nuclear Society, 2009.
15. G. Brümmer, H. Hoffmann, F. Hüttner, U. Ilg, O. Wachter, M. Widera, A. Brozova, J. Burda, O. Erben, M. Ernestova, J. Kysela, M. Postler, and R. Vsolak, "Investigation on Environmentally Assisted Cracking Behavior of a Ferritic Reactor Pressure Vessel Steel under the Simultaneous Influence of Simulated BWR Coolant and Irradiation," *Proc. 11th*

- Int. Conf. Environmental Degradation of Materials in Nuclear Systems, Stevenson, Washington, August 10–14, 2003, American Nuclear Society, 2003.*
16. P. Hurst, P. Banks, G. Remberton and A. S. Raffel, "Stress Corrosion Behavior of A533B and A508-III Steels and Weldments in High Temperature Water Environments," *Proc. 2nd Int. Symp. on Environmental Degradation of Materials in Nuclear Systems—Water Reactors*, Monterey, 1985, American Nuclear Society, 1986.
 17. T. Uehara and M. Yoda, "Laser Peening Systems for Preventive Maintenance Against Stress Corrosion Cracking in Nuclear Power Reactors," *Proc. 16th Int. Conf. on Nuclear Engineering*, ICONE16-48202, Orlando, Florida, May 11–15, 2008, American Society of Mechanical Engineers, 2008.
 18. K. Okimura, T. Konno M. Narita, T. Ohta, M. Toyoda, "Reliability of Water Jet Peening as Residual Stress Improvement Method for Alloy 600 PWSCC Mitigation," *Proc. 16th Int. Conf. on Nuclear Engineering*, ICONE16-48375, Orlando, Florida, May 11–15, 2008, American Society of Mechanical Engineers, 2008.
 19. R. Jones, "Mitigating Corrosion Problems in LWRs via Chemistry Changes," *Proc. Int. Conf. on Water Chemistry of Nuclear Reactors Systems*, San Francisco, October 2004, Electric Power Research Institute, 2004.
 20. D. Akutagawa, N. Nagata, K. Dozaki, H. Takiguchi, K. Norring, A. Jenssen, and A. Molander, "Environmental Mitigation of PWSCC Initiation- Low DH Chemistry for PWR Primary System," *14th Int. Conf. on Environmental Degradation of Materials in Nuclear Power Systems, Virginia Beach, Virginia*, August 23–27, 2009, American Nuclear Society, 2009.
 21. P. L. Andresen, R. Reid, and J. Wilson, "SCC Mitigation OF Ni Alloys and Weld Metals by Optimizing Dissolved H₂," *14th Int. Conf. on Environmental Degradation of Materials in Nuclear Power Systems, Virginia Beach, Virginia*, August 23–27, 2009, American Nuclear Society, 2009.

5. ENVIRONMENTALLY ASSISTED FATIGUE

For the RPV, fatigue is generally not considered to be a significant issue except for the replaceable closure flange studs and potentially in the nozzle regions where safety injection water is introduced into the RPV. As discussed in MDM Gap No. P-AS-02; B-AS-07 [1], fatigue can be separated into two categories: low-cycle fatigue and high-cycle fatigue.

High-cycle fatigue is not considered to be an issue unless an attachment to the vessel is moving relative to the RPV, creating oscillating stresses (often the case with main coolant pumps). Another possibility is when thermal stresses are constantly changing due to mixing, as has been experienced in BWR feedwater nozzles. Also, thermal striping, again near the nozzles at the BWR safe ends, can result in potential high cycle fatigue. Similar events have occurred in PWR feedwater nozzles attached to the steam generators (not the RPV), but both issues have been alleviated by changes in operating strategies. Thus, high cycle fatigue is not considered to be an issue for extended operation.

Low-cycle fatigue may occur at high-stress-intensity locations of the vessel nozzle region due to the general operating transients of the plant. Thus, vessel nozzles are a region where fatigue can be a significant issue. Older BWR vessels may have a region or regions near feedwater nozzles where the protective stainless steel has been removed, resulting in the potential for crack initiation and growth in the ferritic LAS. Service-induced flaws that have been observed are cracks at feedwater nozzles associated with mixing of lower-temperature water with hot water in a BWR vessel [2]. Feedwater nozzle inner radius cracking has not been detected since the plants changed operation of the low flow feedwater controller. Similar issues have been documented for PWRs [3], and significant inspections and repairs were required in the late 1970s and early 1980s to address these problems. As mentioned for high cycle fatigue, the redesign of safe end/thermal sleeve configurations and feedwater spargers, coupled with changes in operating procedures, has been effective to date; no further occurrences of nozzle fatigue cracking have been reported for PWRs or BWRs.

Should BWR reactor water come in contact with the LAS, the water chemistry (e.g., Cl⁻ content) could be important based upon data suggesting that increased crack growth occurs at Cl⁻ concentrations below the EPRI *BWR Water Chemistry Guidelines* level of 5 ppb [4]. Since the inside of the ferritic vessel is clad with stainless steel, any potential fatigue crack initiation and growth, with possible acceleration due to the water environment, could only be expected to initiate in the stainless steel clad and then to potentially propagate into the ferritic LAS. There are a number of locations in PWRs [3] where the clad is missing, and service experience over 20 years or more in PWRs has shown no issues. However, reactor operational experience beyond this period needs to be examined to support these conclusions.

Some cracks have developed in the cladding of BWR reactor vessel heads. In some cases, the cracks have penetrated short distances into the LAS base material. The cracking has required inspection and analysis to confirm the continued safe condition of the affected components. In a few cases, it was suggested that the cladding cracks may have penetrated into the base material as the result of service, which would include fatigue, but it appears more likely that such penetration occurred during fabrication. If these cracks have penetrated into the LAS, there may be further concern for continued crack growth in the water environment.

The relationship between laboratory environmental fatigue testing and actual operating conditions is the topic of an important and ongoing debate. Environmental fatigue effects

measured in the laboratory have demonstrated that fatigue resistance in a water environment is lower than that in air [5, 6]. However, the effect of an enhanced environmental fatigue component has not been demonstrated for large components such as a vessel in actual operation. The relatively simple methods currently available for application of laboratory environmental effects appear to be overly conservative and do not address the complex, three-dimensional geometries that occur in actual plant components and nonlinear, time-dependent stress loadings. Current license renewal guidance requires the assessment of environmental fatigue effects generally for a small set of RPV locations except for connections to the RPV at nozzles [7]. Sample sets of RPV locations to be assessed are recommended in [7] as provided in NUREG/CR-6260, "Application of NUREG/CR-5999, "Interim Fatigue Curves to Selected Nuclear Power Plant Components." [8]. Plants currently address most environmental fatigue issues through stress-based monitoring and cycle counting, which can involve detailed reassessment of the cyclic loadings and associated stresses that are occurring at the nozzle connections. In other cases, refined stress analyses that more accurately reflect the actual stresses at the areas of concern have been performed. In most cases, fatigue issues can be resolved by using these approaches for current extended (60 year) operating life as well as for an additional 20 years of operation.

Some multiple component locations could potentially exceed a calculated cumulative fatigue usage factor (CUF) of 1.0 when environmental effects are included [9, 10]. Thus, there is a need to develop an improved understanding of environmental fatigue effects, especially through modeling and testing of real components under realistic strain-rate loadings and in the proper plant chemistry ranges. The effects of water environment on fatigue crack growth rates are being established for materials of concern in service, and the application of these generally enhanced growth rates may present situations where additional inspections will be required to ensure that flaw tolerance evaluations are adequate for continued service.

The terminology used for fatigue issues can often be confusing. Corrosion fatigue can be viewed as an extension of SCC and strain-induced cracking in the overall scheme of "environmentally assisted cracking" modes. Whatever the environmental component of crack advance is, it generally may be assumed to be superimposed on the crack advance due to mechanical fatigue occurring in a dry environment. For carbon and LAS, the interactions between the various system parameters that could have an effect on the extent of corrosion fatigue can generally be predicted from mechanistic understanding [11]. By contrast to the deleterious effect of oxygenated BWR water chemistry on the fatigue life of carbon and LAS, significant reductions in the fatigue lives of stainless steels have been observed in simulated hydrogenated PWR environments (i.e., at low corrosion potential). However, in contrast to the situation for carbon steel and LAS, there is currently no adequate mechanistic interpretation of the phenomenon in stainless steel.

In summary, real fatigue issues for the RPV generally are insignificant and seldom as important as for the associated piping that can be connected to the RPV. Fatigue in water environments at regions where CUF values are significant up to 80 years of operation may require monitoring or assessment to provide better quantification. Development of the relationship between laboratory test data, real operating stresses, and loading sequences is essential to assure that environmental fatigue never becomes a significant factor for long-term operation. Finally, it should be noted that environmentally assisted fatigue is also addressed for C&LAS in Volume 2, Core Internals and Primary and Secondary Piping.

5.1 REFERENCES*

1. EPRI, *Primary System Corrosion Research Program: EPRI Materials Degradation Matrix, Revision 2*, Technical Report 1020987, Electric Power Research Institute, 2010.
2. R. Snaider, *BWR Feedwater Nozzle and Control Rod Drive Return Line Nozzle Cracking: Resolution of Generic Technical Activity A-10 (Technical Report)*, NUREG-0619-Rev-1, U.S. Nuclear Regulatory Commission, November 1980.
3. W. Bamford and K. R. Hsu, "Reactor Vessel Cladding Damage Analysis," ICONE 8, Baltimore, 2000, American Society of Mechanical Engineers, 2000.
4. EPRI, BWR Vessel and Internals Project, *BWR Water Chemistry Guidelines-2000 Revision*, Electric Power Research Institute, 2000.
5. O. K. Chopra and W. J. Shack, *Effects of LWR Coolant Environments on Fatigue Design Curves for Carbon and Low-Alloy Steels*, NUREG/CR-6583, U.S. Nuclear Regulatory Commission, March 1998.
6. O. K. Chopra, *Effects of LWR Coolant Environments on Fatigue Design Curves for Austenitic Stainless Steels*, NUREG/CR-5704, U.S. Nuclear Regulatory Commission, April 1999.
7. NRC, *Generic Aging Lessons Learned (GALL) Report*, NUREG-1801, Revision 2, U.S. Nuclear Regulatory Commission, December 2010.
8. A. G. Ware, D. K. Morton, and M. E. Nitzel, *Application of NUREG/CR-5999 Interim Fatigue Curves to Selected Nuclear Power Plant Components*, NUREG/CR-6260, INEL-95/0045, Idaho National Engineering Laboratory, February 1995.
9. O. K. Chopra and W. J. Shack, *Effects of LWR Coolant Environments on the Fatigue Life of Reactor Materials*, NUREG/CR-6909, U.S. Nuclear Regulatory Commission, February 2007.
10. NRC, *Guidelines for Evaluating Fatigue Analyses Incorporating the Life Reduction of Metal Components Due to the Effects of The Light-Water Reactor Environment for New Reactors*, Regulatory Guide 1.207, U.S. Nuclear Regulatory Commission, March 2007.
11. F. P. Ford, H. D. Solomon, L. M. Young, P. L. Andresen, D. Weinstein, A. Unruh, E. Tolksdorf, and R. Pathania, "Prediction of Corrosion Fatigue Crack Initiation in Low Alloy Pressure Vessel Steels," pp. 315–325 in *Proc. Int. Symp. on Plant Aging and Life Predictions of Corrodible Structures*, Sapporo, Japan, May 1995, Japan Society of Corrosion Engineering and NACE International, 1997.

* Inclusion of references in this report does not necessarily constitute NRC approval or agreement with the referenced information.

6. NEUTRON EMBRITTLEMENT

6.1 INTRODUCTION TO MAJOR EMBRITTLEMENT ISSUES

Neutron irradiation can cause embrittlement in RPV steels [1–4], with its magnitude depending on the composition (Cu, Ni, Mn, P) of the steel, its product form (plate, weld, forging), and the conditions (fluence, flux, temperature) under which it is exposed. This technical area corresponds to MDM Gap No. P-AS-04. Although specific in application, the topic of RPV embrittlement covers a diverse range of activities, from fundamental multiscale (multiphysics) modeling and nanofeature characterization studies to fracture mechanics assessments of vessel integrity, which are too broad to cover in this brief review. Regulations, guides, and standard practices currently characterize embrittlement in terms of elevation of the temperature regime of brittle cleavage fracture, characterized by transition temperature shifts determined with the CVN impact test at 41 J (ΔT_{NDT}) and decreases in the upper-shelf energy (ΔUSE). Much of the information in this chapter is contained in [5] and [6]. Note that we have used ΔT_{NDT} and ΔT interchangeably in this chapter to refer to the CVN 41 J (30 ft-lb) temperature shift.

Since 1988, the Regulatory Guide 1.99, Revision 2 (RG 1.99-2) has provided the basis used in the United States to evaluate ΔT in terms of the Cu and Ni contents in RPV steels and welds subjected to fast neutron fluence ($E > 1 \text{ MeV}$) [7]. The model equations for RG 1.99-2 were statistically fit to a small surveillance database (177 data points) on steels irradiated in surveillance capsules at flux levels somewhat higher (1 to slightly over 5 times) than at the vessel wall itself. The RG 1.99-2 model was developed prior to 1985; it reflected the then emerging, but far from complete, physical understanding of embrittlement mechanisms [8]. Test reactor data obtained at high fluxes were not used to define the coefficients in the RG 1.99-2 ΔT equation [9] but were used to check the fit in regions where surveillance data were lacking (Cu < 0.10 wt%). Over the last 25 years, advances in understanding of embrittlement mechanisms and improved physically motivated ΔT models, such as described in [1, 2, 10], now provide the basis for statistical fits to a much larger U.S. power reactor (surveillance) embrittlement database. The model in [1, 2] has been incorporated in 10 CFR 50.61a [11]. Further, test reactor data have been obtained through many national and international efforts. Some recent test reactor investigations include the following:

- The Irradiation Variables (IVAR) program [12] was a large, systematic effort to characterize embrittlement mechanisms by developing high-resolution maps of the effects of embrittlement variables and variable combinations, with special emphasis on flux effects. While the IVAR data were not used to define the fit coefficients for the ΔT equation in [1, 2], it did provide *a priori* physical insights concerning the form of the fitting equation and variable interdependencies to look for in the surveillance database. The IVAR data also indicated *a posteriori* application in [1, 2] as one of several checks performed on the ΔT model.
- RADAMO [13] was specifically oriented to measure the irradiation effects on the tensile properties of RPV materials. Fourteen RPV materials (plates, forgings, and welds) with various chemical compositions (Cu, Ni, and P) were irradiated in the Belgian Reactor No. 2 (BR2) materials test reactor under well-controlled conditions at two temperatures, 300 °C and 265 °C (572 °F and 509 °F), in a large neutron fluence range, from low

(1×10^{19} n/cm², E > 1 MeV) to high (>math>1 \times 10^{20}</math> n/cm², E > 1 MeV), and various flux levels (0.2 to 8 × 10¹³ n/cm²-s, E > 1 MeV).

- Two major projects on high-fluence irradiations were performed in Japan in the recent past [14]. To study the transition temperature shifts in several RPV steels irradiated in the Japan Materials Testing Reactor (JMTR), the Japan Power Engineering and Inspection Corporation conducted the Pressurized Thermal Shock (PTS) project in the late 1980s. The results of the PTS project were used to develop a Japanese embrittlement correlation equation, Japan Electric Association Code JEAC4201-1991 [15]. The Japan Nuclear Energy Safety Organization (JNES) conducted the Nuclear Power Plant Integrity Management (PLIM) project in the early 2000s to obtain the data to develop an embrittlement correlation equation for the Charpy USE changes; additionally, the full curves of Charpy impact tests were obtained. Subsequently, JNES started a new project in 2005, named Prediction of Radiation Embrittlement (PRE) for a High Fluence Range project, in which the materials irradiated in the PTS and PLIM projects were used to study the mechanism of embrittlement in RPVs irradiated to high fluences. Extensive microstructural analyses utilizing three-dimensional atom probe (3DAP) tomography, positron annihilation (PA) spectroscopy, and transmission electron microscopy (TEM) were performed, and the results were utilized to confirm the basis of a new embrittlement correlation referred to as “JEAC4201-2007.”

Since the development of RG 1.99-2, research has continued to develop improved ΔT models, including one that has already been used in regulatory assessments of PTS [1, 2]. In the following sections we briefly review the status of the recent ΔT models, with emphasis on the major outstanding issues to be resolved for extended operation to 80 years.

- The current technical understanding suggests that ΔT depends on, to varying magnitudes, the *combined effects* of neutron flux (ϕ), flux spectrum, fluence (ϕt), irradiation temperature (T_i), alloy composition (Cu, Ni, Mn, P) and start-of-life microstructure, or product form [1–3, 16]. Due to scatter and clumped and confounded distributions of variables, however, the U.S. surveillance database lacks the resolution to accurately resolve causal effects that are small relative to the scatter in the database. Supplementing the database with high-resolution test reactor data, such as that obtained in the IVAR program, may help to improve the reliability of future ΔT models.
- Existing ΔT models based only on surveillance may become inaccurate when extrapolated to the high fluence levels (≈ 5 to 10×10^{19} n/cm²) pertinent to extended operating conditions for some PWRs because the data are sparse in the high-fluence regime. High-fluence data from other surveillance programs and test reactor irradiations could be used to develop improved ΔT models for extended life. Figure 6.1 shows predicted minus measured residuals for the Eason, Odette, Nanstad, Yamamoto (EONY) ΔT model fit only to surveillance data [1, 2] and applied to a large independent body of higher-flux test reactor data and high-fluence surveillance data compiled by Kirk [17].* The large negative residuals that increase with fluence show that the model systematically and significantly underpredicts ΔT for this data set. Thus, reliably modeling high-fluence embrittlement is a critical issue.

* Dr. M. Kirk provided a test reactor database to the authors in the form of an Excel spreadsheet. Kirk also derived a number of ΔT models based on systematic fits to the PREDB and selected subsets of the test reactor database, as described in detail in draft NRC report *Technical Basis for Revision of Regulatory Guide 1.99: NRC Guidance on Methods to Estimate the Effects of Radiation Embrittlement on the Charpy V-Notch Impact Toughness of Reactor Vessel Materials*. A summary of that work is presented in [17].

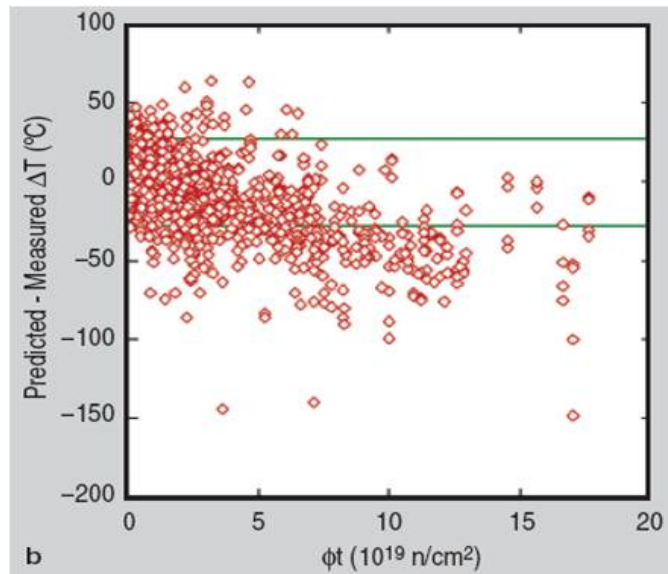


Figure 6.1. Predicted minus measured ΔT for the EONY model applied to surveillance data and high-flux test reactor data, showing increasing nonconservatism with increasing fluence [5]. The two solid lines are $\pm 2\sigma$.

With kind permission from Springer Science+Business Media: G. R. Odette and R. K. Nanstad, "Predictive Reactor Pressure Vessel Steel Irradiation Embrittlement Models: Issues and Opportunities," *Journal of Metals* 61(7), 19–25 (2009).

- Models have long predicted that Mn-Ni-Si late blooming phases (LBPs) could form in low Cu steels after a significant incubation fluence (hence, the term "late blooming"), resulting in severe unanticipated ΔT [3, 12, 18–21]. Current regulatory ΔT models do not reflect potential LBP contributions to ΔT . However, recent research has demonstrated the existence of LBPs for a wide range of alloys and irradiation conditions [21–24]. Moreover, Mn-Ni-Si precipitates have recently been observed in low Cu welds from the surveillance program of a commercial PWR having a high nickel and low copper content [25].

The following specific issues are discussed separately in Sections 6.2 to 6.7 of this report:

- Flux effects at high neutron fluence
- High-nickel effects and other potential high-fluence embrittlement mechanisms
- Thermal annealing and reirradiation
- Attenuation of embrittlement
- Master Curve fracture toughness
- Embrittlement beyond the beltline

6.2 FLUX EFFECTS AT HIGH-NEUTRON FLUENCE

6.2.1 Motivation

Extended life of the current U.S. fleet of PWR reactor vessels^{*} will require accurate transition temperature shift (TTS) predictions up to fluences[†] of $\approx 10^{20}$ n/cm² (see MDM gap numbers P-AS-04 and B-AS-05). The regulatory TTS model in Regulatory Guide 1.99-2 [1] is solely based on the low-flux and low-fluence U.S. surveillance database of the early 1980s, assembled in the Power Reactor Embrittlement Database (PREDB) [2]. Non-U.S. surveillance data or test reactor data have not been included in the database used for developing U.S. regulatory TTS models, but test reactor data have been used to inform the process [3–5]. Subsequently, an ASTM Committee E10 activity resulted in an updated TTS analysis database in 2004. This TTS analysis database was developed from the PREDB and later surveillance reports as described in Sects. 4.3 and 4.4 of a report published by Eason, Odette, Nanstad, and Yamamoto (EONY) [4]. That report presented an extensive study of the TTS database in late 2007. At that time, the frozen TTS database contained a total of 885 TTS data. Only nine data points were at fluence $> 5 \times 10^{19}$ n/cm², and six data points were at $> 6 \times 10^{19}$ n/cm² at that time, representing roughly 1% and 0.6% of the overall surveillance database, respectively. Since then, more high-fluence surveillance data have become available, and more data will become available in the future.[‡] Thus, high-fluence surveillance data may provide a sufficient basis for timely informed decisions regarding extended life for PWRs expected to reach very high fluences. However, developing a significant database on high-fluence effects from test reactor (TR) data would provide a useful complement to the surveillance TTS data. The use of accelerated higher-flux TR data ultimately requires understanding and modeling flux effects [4–6].

In the discussion that follows, two different perspectives on flux effects are described. The first argues that high-flux irradiation may result in artifacts in TTS that would not be encountered in low-flux (e.g., power reactor) irradiations. The second gives one of several examples where TTS curves as a function of fluence appear to be insensitive to flux. The fact that there are contradictory views, and indeed contradictory data sets, underscores the importance of performing research to explain and quantify the effect of neutron flux on TTS at intermediate and high fluence.

6.2.2 Flux Effects

The EONY TTS two-feature correlation model was motivated by mechanistic considerations, including hardening contributions from both Cu-rich precipitates (CRPs) and stable matrix features (SMFs) (see Chap. 2 in [4, 5]); the latter form in Cu-bearing steels having either low or higher concentrations of copper. The final fitted EONY TTS model excluded terms that were not statistically justified by the TTS database. The statistical analysis used in the EONY model development documented in [4, 5] included analysis of residuals and data subsets with large

^{*} The corresponding end of extended life fluences for BWRs are much lower than for PWRs. There are some relatively high BWR fluence data in the database obtained at higher surveillance lead factors (i.e., higher flux levels than typical). Some proposed U.S. regulatory TTS models based on the U.S. surveillance database include flux effects; others have been proposed that do not. Thus this issue remains unresolved.

[†] Here, flux and fluence values are in units of n/cm²-s and n/cm², respectively, for neutrons with energies > 1 MeV.

[‡] Twenty-eight data points above 5×10^{19} n/cm², and 18 above 6×10^{19} n/cm², are now available. (Information provided by Brian Hall, 3 January 2011.)

differences between potentially important variables, particularly flux in the case of PWR versus lower-flux BWR TTS data. The EONY model treats the effect of flux in terms of an effective fluence. The EONY model also initially contained some terms that were statistically indicated but that were not fully mechanistically understood. For those reasons, some of these terms were excluded in the final model adopted in 10 CFR 50.61a.

The EONY model provides an excellent fit to the USA TTS database, including the limited TTS at high fluence. The average predicted TTS minus measured residual TTS for the nine data points at fluence $>5 \times 10^{19}$ n/cm² and the six data points at fluence $>6 \times 10^{19}$ n/cm² are 4.3 °C and 5.0 °C (7.7 °F and 9.0 °F), respectively. The EONY model was also shown to be in excellent overall agreement with a very large (and largely independent) IVAR database (see Chap. 6 in [4, 5]). The IVAR irradiation program was specifically designed to generate a high-accuracy, high-resolution empirical map on the effects of embrittlement (hardening) variables and variable combinations by carrying out precisely controlled irradiations of a large matrix of alloys with different but controlled chemical compositions (≈ 100) in three ranges of flux over overlapping ranges of fluence. IVAR irradiations were also carried out at three irradiation temperatures: 270 °C, 290 °C, and 310 °C (518 °F, 554 °F, and 590 °F).

The IVAR database shows a very strong, systematic, and statistically significant flux effect on the CRP contribution to irradiation hardening, consistent with solute-enhanced recombination, reducing the efficiency of radiation-enhanced diffusion at higher dose rates. The IVAR database also shows a flux effect on the SMF contribution to irradiation hardening. However the SMF hardening is generally much less than that from CRPs; thus, the magnitude of the flux effect is also smaller for SMF. However, analysis of individual low-Cu IVAR alloys shows a strong, systematic, and statistically significant flux effect. The effect of flux depends on the irradiation temperature and alloy composition. Broadly similar flux effects are observed in the EONY analysis of the TTS database. The IVAR and EONY analyses both show that the effect of flux can be treated in terms of a physically based effective fluence [4, 5].

EricksonKirk (EK) developed a large database that combined the USA TTS database, the IVAR database, and a wide range of TR data as well as surveillance data collected outside the USA [7]. EK also derived a TTS model from these data and compared its predictions to data from other sources. EK argued that the TTS model is superior to the EONY model in terms of its traceability. The EK TTS model is generally similar to the one previously derived by EONY (see below). EK also found that slightly better fits could be obtained by including a flux effect in the CRP contribution to TTS but ascribed a lower statistical significance to that result than in the EONY analysis. As in the case of EONY, EK showed that his model is also generally consistent with the IVAR database. The major limitation of the low-flux TTS database models is that they are empirically limited to fluence of less than $\approx 4 \times 10^{19}$ n/cm².

Notably, EK also found that his model underpredicts the TTS measured in TR irradiations at higher fluence. As illustrated in Figure 6.1, the trend of increasing TTS underpredictions with increasing fluence for the EK model and (largely) the TR database is also true for the EONY model. *The under predictions by the low-flux TTS models is a significant factor motivating continuing research regarding flux effects.*

EK suggested that the TTS underpredictions at higher fluence could be remedied by transitioning from a lower-flux PREDB model to a TR-based model at high fluence such as was derived from a set of data for irradiations in the Belgian Nuclear Research Centre (SCK-CEN) BR2 TR at flux levels that were generally higher to much higher than in the TTS database and

IVAR. The TR model and corresponding TR database are called RADAMO. EK presented data that were interpreted to suggest that flux effects were small enough to be ignored.

Nanstad, Odette, Stoller, and Yamamoto (NOSY) analyzed the EK model and composite TTS prediction procedure [8]. They concluded the EONY and EK low-flux TTS database models were generally similar. However, they rejected the use of the composite TTS procedure for a variety of reasons as detailed in their report.

Kirk subsequently developed an updated trend curve [9] that is based on embrittlement data expressed in terms of ΔT_{41J} and yield strength increases ($\Delta\sigma_y$) from a wide variety of data sources, including the U.S. surveillance program, non-U.S. surveillance programs, and test reactor irradiation programs. The database developed by Kirk from these sources includes over 2,500 data. The resulting trend curve based on analysis of the whole database, as well as significant data subsets, was denoted a “wide range” embrittlement trend curve, WR-C(5) [9]. Of particular note is the following, taken directly from that reference:

Of particular importance, the WR-C(5) model indicates the existence of trends in high fluence data ($\Phi > 2-3 \times 10^{19}$ n/cm², $E > 1$ MeV) that are not as apparent in the U.S. surveillance data due to the limited quantity of ΔT_{30} data measured at high fluence in this dataset. Additionally, WR-C(5) models well the trends in both test and power reactor data despite the fact it has no term to account for flux.

Kirk further notes that the combined use of data from such a variety of sources to develop a trend curve is being debated by the technical community. Nevertheless, efforts in 2012 and 2013 within ASTM Subcommittee E10.02 to recommend a new TTS model for ASTM Standard E900, “Standard Guide for Prediction Radiation-Induced Transition Temperature Shift in Reactor Vessel Materials, E706 (IIF),” are using just such a combined database.

The NOSY report pointed out that the TR underpredictions could be rationalized by a three-feature model that adds an unstable matrix defect (UMD) to CRP and matrix feature (MF) hardening contributions. The UMDs form and anneal under irradiation at sufficiently long times that scale with the UMD recovery time, τ . The UMDs build up over an interval of fluence that scales with flux and time such that, at sufficiently high fluence, the UMDs reach a steady-state concentration that varies in proportion to the flux. Thus, UMDs are only important at high flux. The three-feature model derives from earlier work by Mader and Odette (MO) [10]. The MO model was largely based on UMD recovery kinetics determined from low-temperature postirradiation annealing (PIA) hardness recovery measurements at 290 °C and 350 °C (554 °F and 662 °F) that resulted in annealing of the UMDs, while leaving the CRPs and SMFs largely unaffected. The original MO model was derived from relatively low fluence data.

The MO model posits that the UMDs: (1) contribute to hardening and (2) act as defect sinks to delay CRP and SMF hardening. Thus, higher flux can lead to increases, decreases, or no changes in the TTS, depending on the combination of all the metallurgical and irradiation variables. Odette and Yamamoto updated and slightly revised the MO model [11]. The NOSY report showed that the resulting three-feature Mader, Odette, and Yamamoto (MOY) model can rationalize the hardening/TTS behavior in higher-flux TR data, lower-flux IVAR data, and surveillance data. These results suggest that the high-fluence underprediction of TR TTS data is at least partly a result of the high TR flux associated with a significant population of UMDs. The MOY model also shows that the overall hardening at low and high flux may be similar over a considerable range of fluence but that the net hardening results from different balances of nanometer-scale features contributed by CRPs, SMFs, and UMDs.

Figure 6.2 shows an example of the flux effect for the Heavy Section Steel Irradiation (HSSI) weld 73W irradiated in both the IVAR (low-flux) and BR2 RADAMO (high-flux) irradiations [12]. In Figure 6.2, the data are binned into flux groups (in units of $n/cm^2\cdot s$) that are bound by 3.3×10^n , where n varies from 11 to 14. For example, the 10^{11} group is for flux less than 3.3×10^{11} , and the 10^{12} group is between 3.3×10^{11} and 3.3×10^{12} . The higher flux BR2 300 °C (572 °F) data have been slightly adjusted to an irradiation temperature of 290 °C (554 °F) using the temperature-dependent factor contained in the RADAMO model [12]. At low fluence, in the pre-plateau CRP regime, equivalent hardening is shifted up by well over an order of magnitude in fluence between the flux groups of $\approx 10^{11}$ and 10^{14} $n/cm^2\cdot s$, indicating that peak hardening occurs at progressively lower fluence as flux is reduced. The highest flux-fluence BR2 hardening appears to cross over the lower flux, saturating trend at $\approx 3 \times 10^{19}$ n/cm^2 . However, more higher-fluence lower-flux data are needed to confirm this trend. Figure 6.3 shows application of the three-feature MOY model to the 73W data. Figure 6.3(a) shows the raw RADAMO and IVAR data. Figure 6.3(b) shows all the data adjusted to a high reference flux, and Figure 6.3(c) shows the data adjusted to a low reference flux, reasonably collapsing the data in both cases. The dashed line shows that the predicted UMD hardening contribution is large at high flux and negligible at low flux. Figure 6.3(d) shows the crossover between low and high reference flux cases.

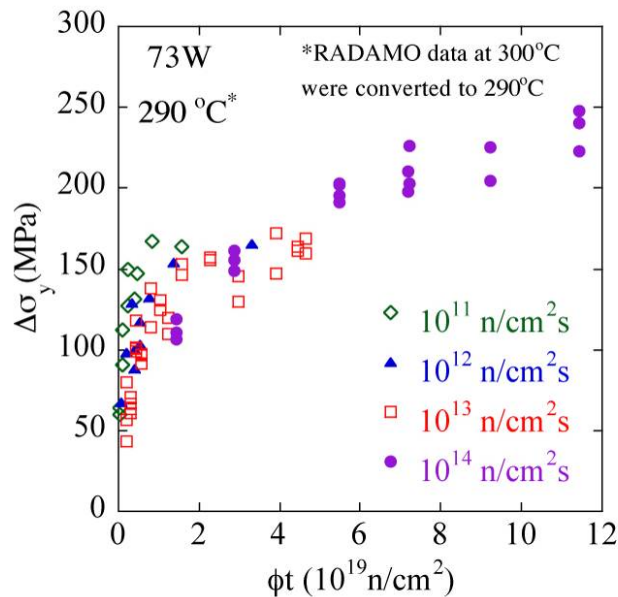


Figure 6.2. Yield stress increases in the ORNL 73W steel as a function of fluence for different flux range bins [12].

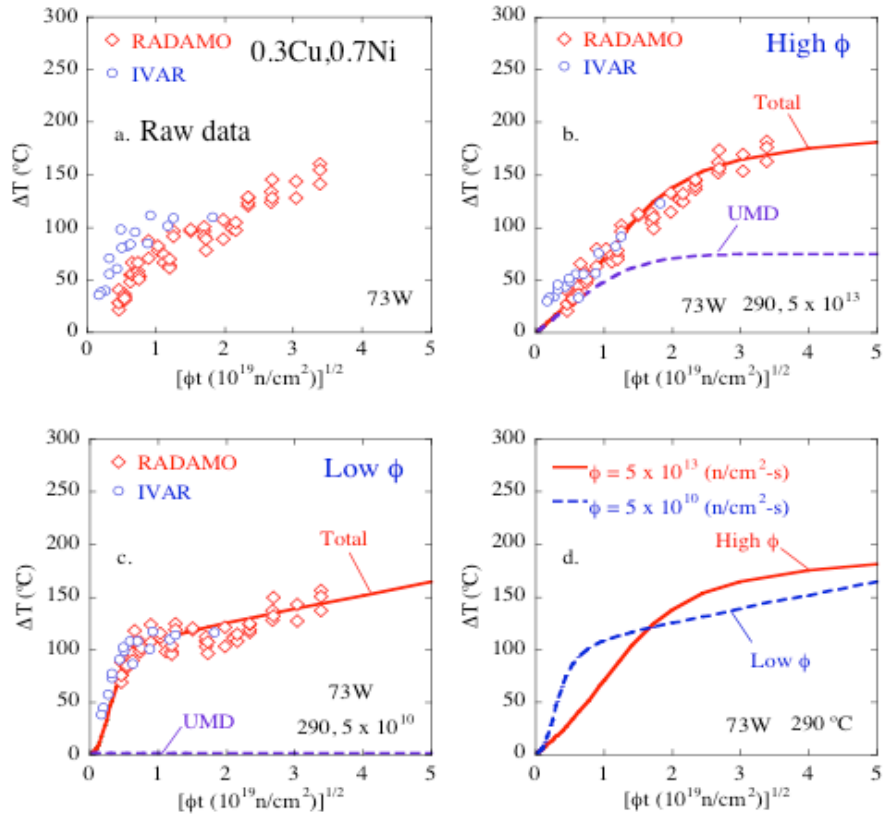


Figure 6.3. (a) Raw IVAR and BR2 RADAMO TTS data for HSSI Weld 73W; (b) TTS data adjusted to a common high-flux condition using the calibrated three-feature model; (c) TTS data adjusted to a common low-flux condition using the calibrated three-feature model; (d) TTS at high and low flux. [6]

With kind permission from Springer Science+Business Media: G. R. Odette and R. K. Nanstad, “Predictive Reactor Pressure Vessel Steel Irradiation Embrittlement Models: Issues and Opportunities,” *Journal of Metals* 61(7), 19–25 (2009).

Recent studies by Odette and co-workers support the three-feature model [8]. Those studies compared the same alloys irradiated in the IVAR program at low flux ($<10^{12}$ n/cm²-s) and in the BR2 reactor at high flux ($\approx 10^{14}$ n/cm²-s). The comparisons include the high versus low flux CRP microstructures and the as-irradiated versus low-temperature, short-time [350 °C (662 °F), 5 h] PIA hardening at higher and lower flux. The Belgian Reactor 3 (BR3) data extend up to a fluence $\approx 1.2 \times 10^{20}$ n/cm². In the range of similar fluence, the high-flux BR2 hardening recovers more than for IVAR irradiations at lower flux. The high-flux as-irradiated hardening is also higher than for low-flux irradiations at high fluence, especially in the low-Cu steel. However, the residual hardening after the 350 °C (662 °F), 5 h PIA is lower than for low-flux irradiations, consistent with delayed CRP + SMF contributions in high-flux irradiations.

The hardening trends in both the as-irradiated and PIA conditions are highly consistent with small-angle neutron scattering (SANS) microstructural characterization studies of CRP evolution in the IVAR versus BR2 irradiations [13]. Indeed, more generally, there is near universal agreement in a wide range of microstructural studies that are based on a variety of techniques that higher flux delays the formation of a given volume fraction of CRPs and that the CRPs are smaller and generally more numerous than for low-flux irradiations. The PIA data are also

consistent with a body of previous research showing that there is significantly more recovery for high-flux irradiation conditions than for low-flux irradiation conditions for PIA below ≈ 375 °C to 400 °C (707 °F to 752 °F) [14]. The PIA models derived in this previous work are contained in the NRC regulatory guidelines for RPV annealing [15].

However, Odette and co-workers have also found some of their data are contradictory to predictions by the three-feature model, including the observation of more low-temperature PIA recovery for some lower-flux irradiations than expected and less recovery for some high-flux irradiation conditions than predicted by the three-feature model. Further, Chaouadi and co-workers and a number of other researchers have reported a number of datasets comparing low- and high-flux irradiations that show similar trends, with one example shown in Figure 6.4 [16]. More significantly, Chaouadi found that low-temperature PIA after the high flux irradiation results in little or no recovery, in stark contradiction to the observations summarized above. Relative to the incorporation of flux as a parameter in predictive embrittlement models, Eason et al. [4, 5], Williams et al. [17], and Soneda et al. [18] are among those whose models include flux. Examples of models that do not include flux are those of Kirk [19] and Todeschini [20].

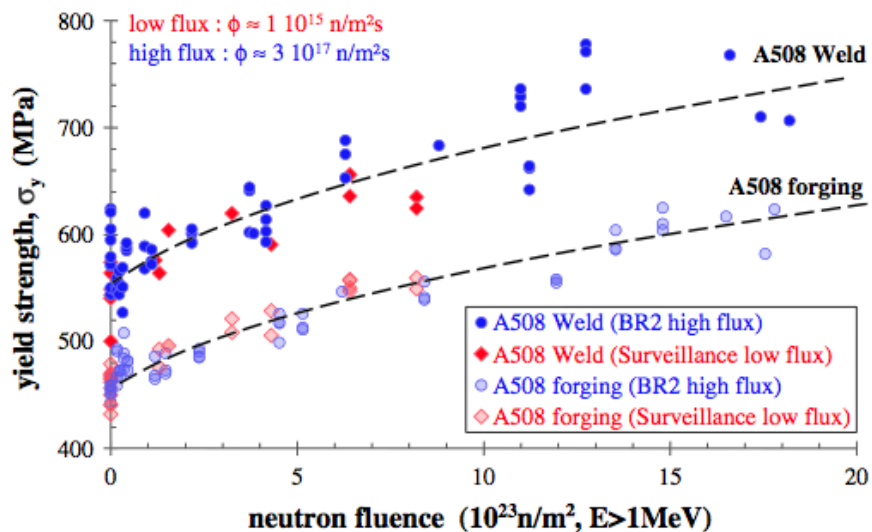


Figure 6.4. Example showing similar hardening trends in high- and low-flux irradiations [16]. Reprinted from Chaouadi and R. Gérard, “Neutron Flux and Annealing Effects on Irradiation Hardening of RPV Materials,” *Journal of Nuclear Materials* 418, 137–142 (2011), with permission from Elsevier.

The following observations can be made to summarize the current findings regarding the status of the TTS model research:

- There is general agreement that there are significant flux effects on preplateau CRP hardening, although there are differences in opinion regarding the corresponding statistical significance of the effects of flux in the TTS database.
- There are also differences of opinion on the effects of flux on the low-Cu steel SMF hardening contributions.
- There are little or, at the highest relevant fluence, no low-flux data in the U.S. TTS database characteristic of extended RPV life at fluence $\approx 10^{20}$ n/cm²-s.

- The low-flux TTS database models systematically underpredict other TTS data at high fluence. The other TTS data are mostly from TR irradiations at higher flux.
- Physical considerations and three-feature models can rationalize at least part of the TTS underpredictions as being due to artifacts associated with the higher flux in TR irradiations. This is due to competing effects of significant populations of UMDs and high flux on increased hardening and decreasing the amount of radiation-enhanced diffusion at a specified fluence, thus delaying CRP and SMF contributions. A significant and growing body of independent data supports the three-feature model hypothesis, but the model remains to be fully validated.
- A considerable body of data shows similar trends between surveillance and test reactor TTS. There are also data that are contradictory to the three-feature model [7]. Thus, additional research is recommended to resolve the issue of using higher flux test reactor data to predict TTS for high-fluence, low-flux conditions.

6.2.3 Slowly Developing or Late Onset Embrittlement Mechanisms

The issue of high fluence embrittlement mechanisms is discussed in more detail in Sect. 6.3, but is briefly discussed here to emphasize the importance of flux effects relative to the various slowly developing or late onset embrittlement mechanisms. As cited in the EONY and NOSY reports, Odette and co-workers have long predicted the existence of Mn-Ni-Si-rich phases that could form in low-Cu steels at high fluence [21–23]. Small amounts of Cu would help catalyze the formation of these precipitates, which were dubbed “late blooming phases” (LBPs). Thus, delayed or slow development of Mn-Ni-Si-rich cluster hardening could also rationalize the underprediction of TTS data at high fluence for steels having low copper content. The existence of an LBP was shown in the IVAR program for some alloys and irradiation conditions [6]. Moreover, in recent years observation of Mn-Ni-Si clusters has been reported in several studies, in part due to enhanced ability to detect small solute clusters, including observations from a PWR surveillance program for a low copper/high nickel steel [24]. Thus, there is evidence for Mn-Ni-Si-rich cluster formation; but it remains to be determined the conditions under which such cluster formation can be expected. For example, it has been shown that those solutes play an important role in what has been ascribed to SMF at relatively small volume fractions. The conditions under which the solute clusters evolve to larger volume fractions of well-formed Mn-Ni-Si precipitates that can cause a significant increase in hardening and TTS remain to be determined. The latter potential low-flux, high-fluence Mn-Ni-Si precipitation-hardening mechanisms are not included in current TTS regulatory models. Another important issue is the potential for Mn-Ni-Si precipitates to form and accelerate hardening at high fluence in Cu-bearing steels after the hardening plateau from Cu-Ni-Mn phases is reached due to Cu depletion from the matrix.

Other potential high-fluence embrittlement mechanisms include hardening due to dislocation loops and the emergence of nonhardening embrittlement mechanisms such as irradiation-assisted P segregation to grain boundaries and possible long-term coarsening of grain boundary carbides.

Physical considerations suggest that there will be significant flux effects on the slowly developing or late-onset embrittlement mechanisms as well. Because the Mn-Ni-Si precipitates grow by radiation-enhanced solute diffusion, higher flux would be expected to shift their contributions to higher fluence. In contrast, higher flux may promote the formation of dislocation loops.

Additional research is recommended on these potential low-flux, high-fluence phenomena that are not accounted for in current regulatory models.

6.2.4 Near- and Intermediate-Term Research

There are a number of ongoing activities related to the challenge of robust TTS predictions for low-flux, high-fluence extended life conditions. They include but are not limited to the following U.S. efforts.

1. The U.S. Department of Energy (DOE) sponsored Light-Water Reactor Sustainability (LWRS) Program is focused on a number of materials issues related to extended vessel service. One activity is focused on obtaining surveillance specimens from very high fluence irradiations (e.g., the Palisades vessel at a relatively high lead factor, and high-Ni weld specimens from Swedish power reactors) [25].
2. A significant experimental effort to develop a basis for low-flux, high-fluence TTS predictions is sponsored by the DOE LWRS Program and led by the University of California, Santa Barbara (UCSB) in cooperation with ORNL. One significant activity is to continue to characterize the effect of flux on irradiation hardening and microstructure, both before and after low temperature PIA for low-flux IVAR and high-flux BR2 irradiations. The UCSB is also leading a large National Scientific Users Facility experiment at the Idaho National Laboratory (INL) Advanced Test Reactor (ATR) [26]. The peak target flux and fluence in the ATR-2 Experiment are $\approx 3.8 \times 10^{12}$ n/cm²-s and $\approx 9 \times 10^{19}$ n/cm², respectively. The corresponding irradiation temperatures are 250 °C, 279 °C, 290 °C (base condition) and 310 °C (482 °F, 534 °F, 554 °F, and 590 °F). ATR-2 includes 180 alloy conditions in the form of 1650 specimens of various types. The majority of the specimens are multipurpose disc and tensile coupons, while fracture toughness tests of three alloys will be performed. Many of the alloys have been previously irradiated over a wide range of flux, including in IVAR, BR2, and even some power reactor surveillance programs. A new set of alloys is also included that will expand the composition range of the hardening database, especially in terms of the alloy Mn and Ni contents. The ATR-2 irradiation is unique not only in its scope, but also in providing high-fluence hardening data at an intermediate flux that is only about four times higher than the highest flux in IVAR. Thus, it is expected that any effects of flux will be more modest than more highly accelerated irradiations that have previously reached high fluence. The lowest fluence will overlap the IVAR and PREDB conditions and thus will provide for a direct tie to previous flux effects studies. The effects of UMDs in these irradiations are expected to be modest to minimal, with estimated maximum hardening contributions of 10 MPa (high Cu) to 15 MPa (low Cu). Low-temperature PIA will be used to remove any UMD hardening if present. Extensive characterization studies using a large toolkit of techniques will be used to evaluate the baseline and evolved nanoscale and mesoscale microstructures. The effect of flux on the effective fluence and associated delay in CRP and SMF hardening contributions will be evaluated experimentally and in the framework of both solute-enhanced and UMD sink recombination models. The expanded composition space will be particularly useful for mapping the conditions for the formation of Mn-Ni-Si clusters and precipitates (LBP) in low- and higher-Cu-bearing steels.
3. An NRC-funded project at ORNL is developing a comprehensive database that includes U.S. power reactor surveillance data, similar available data from non-U.S. power reactors, and relevant data from TR research programs [27]. The database will be web-based and available in the public domain but will allow for a level of confidentiality to enable broad

participation. The storage and upkeep of the database will be sustained to ensure readability of data in perpetuity [27].

6.2.5 Longer-Term Research Needs

One aspect not included in the ATR-2 experiment is the capability for more typical engineering-scale specimens generally used to determine irradiation-induced embrittlement (e.g., CVN impact specimens and fracture toughness specimens), with the exception of the fracture toughness tests of three alloys in the ATR-2 experiment.).

Thus, initial plans by the LWRS Program for irradiation experiments following ATR-2 includes design of an experiment using somewhat larger specimens of selected materials that are included in ATR-2. The planning for such an experiment is under way to define the specific materials, the irradiation facility, and the irradiation vehicle. However, it is clear that the experiment would be performed at a lower flux in a facility of larger volume to enable inclusion of larger mechanical property specimens (e.g., CVN), including fracture toughness (e.g., 0.5 T compact specimens). There are limited available facilities in the United States for such an irradiation experiment, and there are some outside of the United States. The current capabilities for such experiments are under evaluation.

6.3 HIGH-NICKEL EFFECTS AND OTHER POTENTIAL HIGH-FLUENCE EMBRITTLEMENT MECHANISMS

The strong effect of Ni on embrittlement has long been recognized, and the underlying mechanism was first modeled more than a decade ago [1–4] (see MDM Gap Nos. P-AS-04 and B-AS-05). Thermodynamic models and microanalytical characterization studies have shown that strong Ni-Mn bonds and low Ni/Mn-Fe interface energies result in the coenrichment of Ni and Mn in nanoscale CRPs [1–18], which results in larger precipitate volumes ($\text{Cu} + \text{Ni} + \text{Mn} > \text{Cu}$) and correspondingly increased hardening. Lattice Monte Carlo (LMC) simulations predicted precipitate structures with Cu-rich cores surrounded by Mn-Ni-rich shells [13], which are observed in atom probe tomography (APT) studies [6, 16]. The typical range of Mn is modest (Mn is typically lower in forgings); Ni contents vary from about 0.1% to 1.3% in U.S. RPVs. Although the Ni effect has often been viewed in isolation, it derives from Ni-Mn synergisms. Similarly, Si-Ni and Si-Mn interactions also result in Si enrichment in CRPs.

Thermodynamic-kinetic models also predicted the formation of Mn-Ni phases, even in the absence of Cu, but at low nucleation rates compared with that for CRPs, resulting in relatively high incubation fluences [1–4]. However, as schematically illustrated in Figure 6.5(a), once nucleated, such Mn-Ni-Si LBPs rapidly grow to large volume fractions, causing severe embrittlement. The models also show that small concentrations of Cu may act as a catalyst for LBP nucleation. Notably, current TTS models do not reflect the potential contributions to embrittlement by LBP, probably in part because they may require critical combinations of higher Ni and fluence and lower temperature and flux than have yet to be extensively encountered in the TTS database.

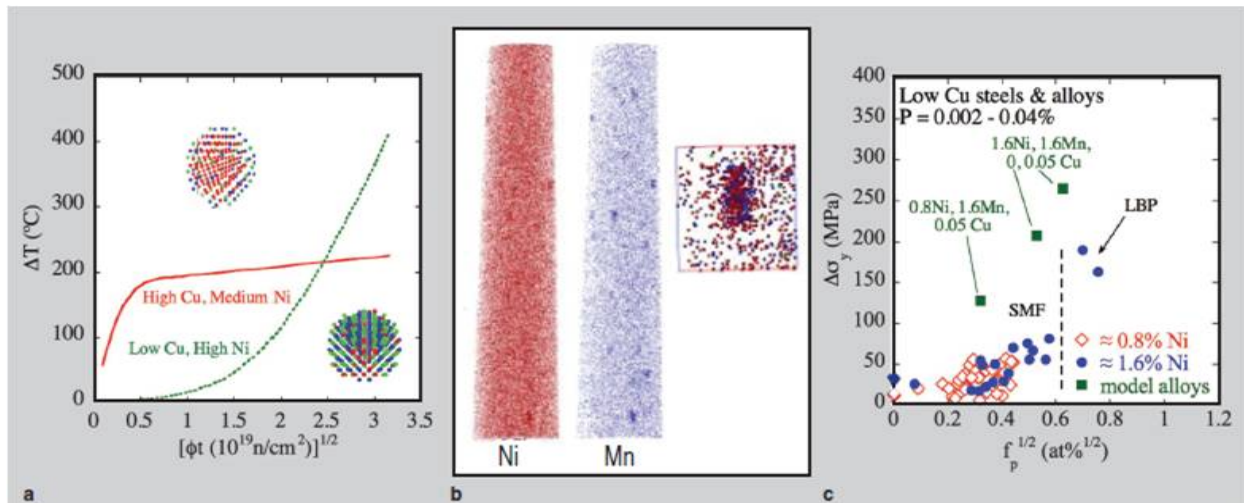


Figure 6.5. (a) Illustrative model predictions of the dose dependence of hardening in a high-Cu, medium-Ni steel due to CRP hardening and in high-Ni, low-Cu steel due to LBP hardening. (b) Atom probe tomography maps of Ni and Mn distributions and an enlargement (inset) of an Mn-Ni LBP precipitate in a Cu-free 1.6 wt % Ni, 1.6 wt % Mn model alloy irradiated to 1.8×10^{19} n/cm² at high flux and 290 °C (554 °F). (c) $\Delta\sigma_y$ as a function of the square root of the volume fraction of precipitates in low-Cu steels and model alloys. [21]
 With kind permission from Springer Science+Business Media: G. R. Odette and R. K. Nanstad, "Predictive Reactor Pressure Vessel Steel Irradiation Embrittlement Models: Issues and Opportunities," *Journal of Metals* 61(7), 19–25 (2009).

The previously described IVAR (see Chapter 6 in [19, 20]) irradiations contained both complex steels and simple ferritic model alloys that were specially designed to search for LBPs and to map their formation regimes. The search has clearly demonstrated the existence of LBPs, as illustrated in Figure 6.5(b), which shows an APT map of Mn and Ni atom positions, and an enlarged view of an Mn-Ni precipitate in a Cu-free, 1.6Ni-1.6Mn wt % model alloy. Similar observations have been reported by other researchers around the world [6–8]. Figure 6.5(c) shows yield strength increase for low-Cu steels and model ferritic alloys as a function of Mn-Ni(-Si) precipitates, measured by the resistivity-Seebeck coefficient technique [17, 18]. The green arrows highlight two Cu-free Ni-Mn steels with different P concentrations, irradiated to 1.6×10^{19} n/cm² at 270 °C (518 °F) and intermediate flux. The large precipitate volume fractions (f_p) and high $\Delta\sigma_y$ indicate that the alloy composition-irradiation conditions have clearly crossed the LBP boundary. Figure 6.5(c) also shows the results for steels with lower Ni concentrations and/or higher irradiation temperatures and fluxes. Although such hardening is generally attributed to SMFs, the results suggest that LBPs are actually part of a continuum of chemically complex SMF-LBP features that form in low-Cu alloys. Thus, the SMFs may be precursors to well-defined LBPs that subsequently develop at higher fluence. LBPs and significant positive $\Delta\sigma_y$ are also found in IVAR in Mn-Ni-low Cu (≤ 0.05 wt %) model alloys irradiated at 290 °C (554 °F) and high flux to 1.8×10^{19} [21]. Higher Ni and trace Cu result in larger $\Delta\sigma_y$ in the model alloys, but 0.8% Ni, 1.6% Mn and 0.05% Cu are sufficient to produce significant LBP precipitation and hardening.

Soneda et al. [22] performed an extensive microstructural characterization of RPV materials that were irradiated in a test reactor at high fluxes (5×10^{12} n/cm²-s or 1×10^{13} n/cm²-s) to very high fluences (3 to 13×10^{19} n/cm²) and at 290 °C \pm 10 °C (554 °F \pm 18 °F). In one example of a plate with very low Cu content (0.06 wt %) and high Ni content (1.78 wt %), the transition temperature shift (ΔRT_{NDT}) was three times greater than that for a similar plate but with Ni

content of 0.58 wt %, 180 °C and 60 °C (356 °F and 140 °F), respectively. The authors noted that Ni alone could cause embrittlement in addition to the synergetic effect of Cu. Moreover, they stated: “These results suggest that an increase in Ni content enhances the nucleation of solute atom clusters.” Figure 6.6 (from [22]) shows an excellent correlation between the ΔRT_{NDT} and the square root of the volume fraction multiplied by the average Guinier radius of solute atom clusters detected by atom probe tomography (APT). The low-Cu, high-Ni material (P4B) is the data point with the highest ΔRT_{NDT} in the figure and is compared with the low-Cu, medium-Ni material (P3B) shown in the lower left portion of the figure, demonstrating the significant effect of high Ni content in a low-Cu steel.

Relative to commercial surveillance conditions, the Ringhals Units 3 and 4 reactors are PWRs designed and supplied by Westinghouse Electric Company, with commercial operation that commenced in 1981 and 1983, respectively. The RPVs for both reactors were fabricated by the Uddcomb Company with ring forgings of SA 508 class 2 material made by Klöckner Werke. Surveillance blocks for both units were also supplied by Uddcomb using the same weld wire heat, welding procedures, and base metals used for the RPVs. As discussed by Efsing et al. [23], these weld metals are very high in Ni content, with 1.58 and 1.66 wt % for Unit 3 and Unit 4, respectively, and with relatively low Cu contents of 0.08 and 0.05 wt %, respectively. For reference, the highest nickel content in the NRC Regulatory Guide 1.99, Rev. 2 is 1.20 wt % [24]. Both weld metals have exhibited very high irradiation-induced Charpy 41-J transition temperature shifts in surveillance testing. Efsing et al. [23] reported CVN 41 J shifts of 192 °C (345 °F) at 5.0×10^{19} n/cm² (>1 MeV) for Unit 3, and 162 °C (292 °F) at 6.0×10^{19} n/cm² (>1 MeV) for Unit 4. Microstructural examinations are under way with those surveillance materials to identify the dominant features that caused such extensive embrittlement, and APT has revealed relatively large irradiation-induced precipitates containing Ni, Mn, and Si, with phosphorus evident in some of the precipitates. This particular surveillance specimen had been irradiated at 284 °C (543 °F), at a flux of 1.32×10^{11} n/cm²-s to a fluence of 4.34×10^{19} n/cm². Perhaps not surprisingly, the precipitate elemental concentrations are dominated by Ni and Mn atoms, with only a relatively few number of Cu atoms contained within the precipitates [25, 26].

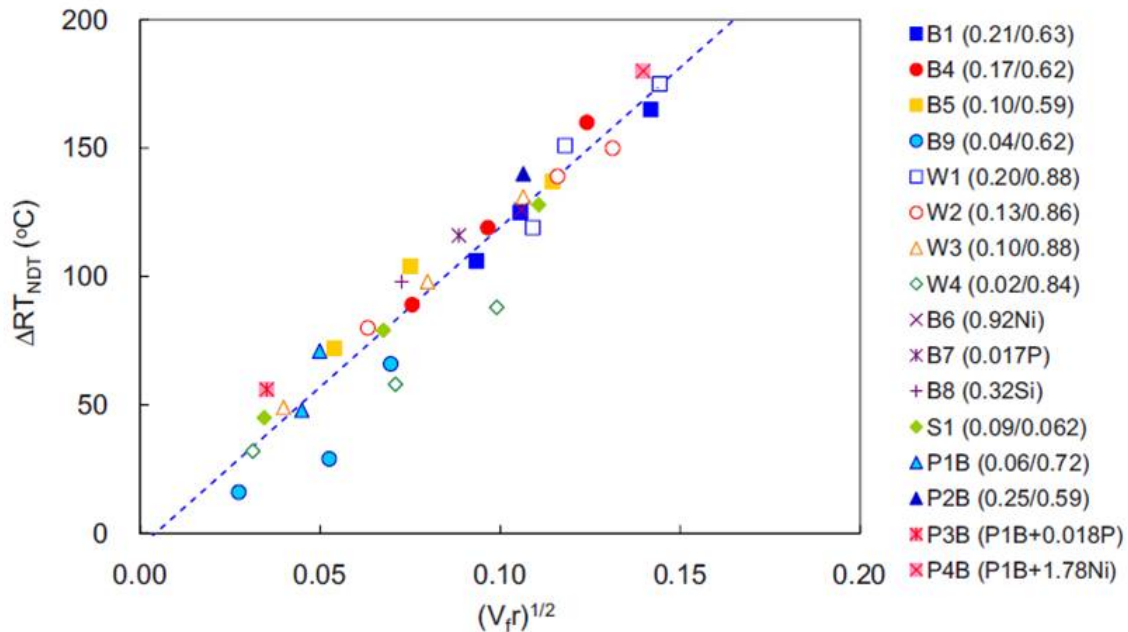


Figure 6.6. Correlation between ΔRT_{NDT} and $(V_f r)^{1/2}$, where V_f is the volume fraction and r is the average Guinier radius of solute atom clusters determined by atom probe tomography [21].

With kind permission from Springer Science+Business Media: G. R. Odette and R. K. Nanstad, "Predictive Reactor Pressure Vessel Steel Irradiation Embrittlement Models: Issues and Opportunities," *Journal of Metals* 61(7), 19–25 (2009).

Thus, LBPs may result in significantly increased embrittlement not predicted by current embrittlement models, which are currently based on the available surveillance data. However, additional research is recommended to determine (1) the conditions leading to the formation of LBP and (2) the severity of the corresponding embrittlement. We also note that other hardening features, especially self-interstitial atom cluster dislocation loops, may be important at high fluence.

6.4 THERMAL ANNEALING AND REIRRADIATION

As noted in previous sections, there are a number of degradation modes that will influence the RPV aging. Irradiation effects are among the most limiting to performance and have been examined extensively for the initial licensing period (i.e., 40 years). However, there are a number of potential options available to mitigate the effects of irradiation embrittlement on the RPV (noted in MDM Gap No. P-AS-04), including thermal annealing. These include:

- Using fuel management schemes to reduce the neutron flux, which reduces the fluence and, therefore, embrittlement
- Shielding critical areas (e.g., with stainless steel) to reduce flux
- Heating the emergency core cooling system (ECCS) water to reduce the thermal shock effects during a PTS event

- Using various analytical methods, such as the alternative PTS rule in 10 CFR 50.61a [1], to justify the safety of continued operation with RT_{PTS} values above the 10 CFR 50.61 screening criteria
- Mechanically prestressing the RPV by compressive loading with structural bands to increase strength of the beltline region of the RPV [2]
- Replacing welds with material that is more resistant to embrittlement if it is in the critical area for embrittlement [3]
- Thermally annealing the RPV to recover fracture toughness
- Replacing the RPV

In addition to the option of thermal annealing, many of the embrittlement mitigation options listed above are discussed by Planman, Pelli, and Torronen [4]. Post-irradiation annealing to recover material toughness is of international interest, especially given the potential doubling or more of neutron exposure with life extensions to 80 years. Thermal annealing involves heating the RPV beltline region to temperatures $\sim 50\text{ }^{\circ}\text{C}$ to $200\text{ }^{\circ}\text{C}$ ($122\text{ }^{\circ}\text{F}$ to $392\text{ }^{\circ}\text{F}$) above the normal operating temperature for about one week to reverse the irradiation embrittlement (recovery); the amount of recovery increases with increasing annealing temperature. Two different procedures can be used to perform the thermal anneal, a wet anneal or a dry anneal. A wet anneal is performed with cooling water remaining in the RPV and cannot be performed above the RPV design temperature of $343\text{ }^{\circ}\text{C}$ ($650\text{ }^{\circ}\text{F}$). A dry anneal requires removal of the cooling water and internal components and would normally be performed at temperatures in the range of $430\text{ }^{\circ}\text{C}$ to $500\text{ }^{\circ}\text{C}$ ($806\text{ }^{\circ}\text{F}$ to $932\text{ }^{\circ}\text{F}$). If thermal annealing is considered, then evaluation of the post-annealing reirradiation response of the steel is recommended. The regulation 10 CFR 50 [1] specifies thermal annealing as a method for recovering the fracture toughness and refers to Regulatory Guide 1.162 (RG 1.162), "*Format and Content of Report for Thermal Annealing of Reactor Pressure Vessels*," [5], which provides guidance for determining the amount of recovery, the reembrittlement trend (assumed to occur at the same rate as in the irradiated case), and establishing post-anneal material properties.

There are many examples of thermal annealing results on U.S. PWR steels. One example, for a high-Cu weld from the Midland Unit 1 reactor, is shown in Figures 6.7 and 6.8 [6]. Although the reactor did not operate, material was removed from the RPV and was evaluated for various fracture mechanics and irradiation effects studies under the HSSI Program [7, 8]. Figure 6.7 shows the beneficial effect of a 1 week high-temperature annealing at $454\text{ }^{\circ}\text{C}$ ($850\text{ }^{\circ}\text{F}$) compared with that for a one-week anneal at $343\text{ }^{\circ}\text{C}$ ($650\text{ }^{\circ}\text{F}$). The higher-temperature anneal resulted in a Charpy 41-J transition temperature recovery of about 80%; the lower-temperature anneal resulted in about a 50% recovery. For the experiments, the materials were irradiated in a test reactor at a flux of about $8 \times 10^{11}\text{ n/cm}^2\text{-s}$ ($>1\text{ MeV}$). Figure 6.8 shows that the high-temperature anneal provided a fracture toughness recovery of more than 90%, somewhat greater than the 80% recovery of the Charpy impact results.

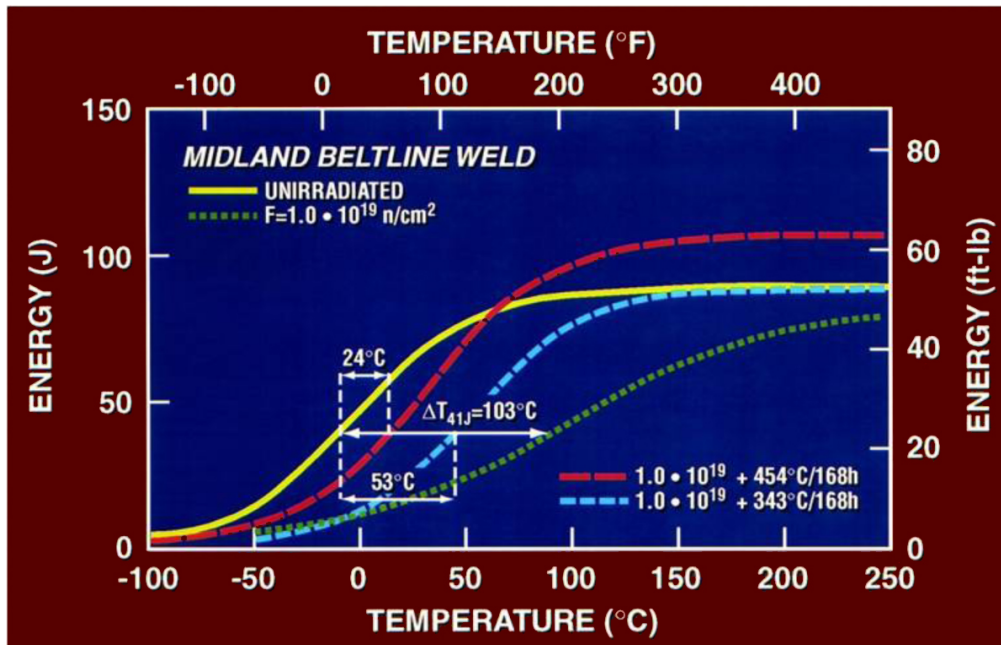


Figure 6.7. Effects of thermal annealing at 343 °C and 454 °C (650 °F and 850 °F) on the Charpy impact energy of the high-copper Midland Unit 1 RPV beltline weld [6]. Reprinted with permission from ASTM STP 1270, copyright ASTM International, 100 Barr Harbor Drive, West Conshocken, PA 19428.

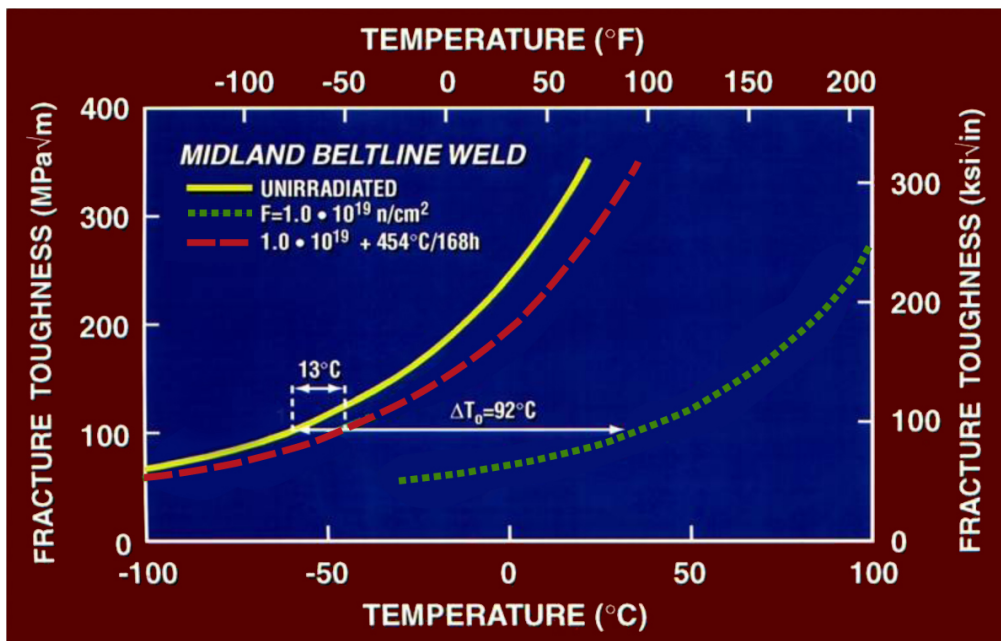


Figure 6.8. Effect of thermal annealing for 168 h at 454 °C (850 °F) on the fracture toughness of the high-copper Midland Unit 1 RPV beltline weld [6]. Reprinted with permission from ASTM STP 1270, copyright ASTM International, 100 Barr Harbor Drive, West Conshocken, PA 19428.

A fair amount of data exists for annealing of U.S. RPV steels, but not for reirradiation. Moreover, the time-temperature response and the dependence of that response to metallurgical and

irradiation variables have only scarcely been mapped, and the microstructural processes involved in damage recovery are not well understood. Additionally, the effects of the annealed microstructure on the reirradiation response and the effects of metallurgical and irradiation variables on the reembrittlement of RPV steels have only had cursory examination to date. The issue of intergranular fracture is also considered to be relevant to RPV steels that have been irradiated and then thermally annealed. Although no observations of significant intergranular fracture (IGF) of irradiated RPV base metals or weld metals from surveillance programs have been reported, observations of IGF have been reported by research programs for some irradiated, thermally annealed, and reirradiated RPV steels [9, 10].

Thermal annealing of operating nuclear reactors has been performed at least 16 times, once in the United States, once in Belgium, and 14 times at Russian-designed VVER-440 plants. The first annealing operation was performed by the U.S. Army under the Army Nuclear Power Program on the Stationary Medium Power (SM)-1A nuclear reactor (1A indicates the first field plant of that type), in Fort Greely, Alaska, in August 1967 [11, 12]. In 1984, BR3 was the first commercial power reactor to be annealed; primary pump heat was used for a wet anneal [13]. Following the annealing of the BR3 reactor, many thermal annealing treatments were performed on VVER-440 reactors [13]. Thus, there is experience with annealing and re-operation of nuclear plants to give credence to application of the technology [14]. The Annealing Demonstration Project (ADP) funded jointly by the DOE and the U.S. nuclear industry was performed at the never completed Marble Hill nuclear plant in Indiana in 1996 and 1997. An independent evaluation concluded that "Successful completion of the ADP has demonstrated that functional requirements for in-place annealing of a U.S. RPV can be met using existing equipment and procedures" [15]. The method was a dry annealing procedure by which an indirect gas-fired heat source supplied heat through a heat exchanger. The RPV was instrumented with strain gages and thermocouples to assess strain levels and temperatures over the entire RPV, including nozzles, during and after the annealing operation. Overall, the results were successful in showing that annealing could be performed with reasonable assurance of low thermally induced strains in the RPV and with an adequately uniform temperature distribution [16].

Additionally, RG 1.162 describes the format and content of an acceptable thermal annealing report. RG 1.162 refers to NUREG/CR-6327 [17], which provides a predictive model for estimating recovery of fracture toughness following annealing. The ASTM Standard Guide E509, "*Standard Guide for In-Service Annealing of Light-Water Moderated Nuclear Reactor Vessels*," also provides expanded guidance on thermal annealing and associated supplemental material surveillance programs [18]. An ASME Code Case, N-557-1, "In-Place Dry Annealing of a PWR Nuclear Reactor Vessel (Section XI, Division 1)" [19] provides guidance for ensuring design conformance after performing a thermal anneal heat treatment, and the technical basis was published by EPRI in TR-106967, "*White Paper: Technical Basis for ASME Code Case N-557, In-Place Dry Annealing of a PWR Nuclear Reactor Vessel*." [20].

Although annealing of LWR RPVs is technically viable based on international experience and there are standard procedures and codes in place that provide rules acceptable to regulatory bodies, they were not developed with the material conditions that may occur at very high fluence. Thus, additional efforts are warranted to gain acceptance within the domestic nuclear power industry relative to extended operation. A number of issues have been identified regarding the use of thermal annealing to recover the fracture toughness of U.S. RPVs that may experience sufficient irradiation-induced embrittlement that could potentially threaten the structural integrity.

1. Although there is a reasonable amount of annealing data for U.S. RPV steels applicable to 40 years of operation, as evidenced by the existence of RG 1.162 [5], there are no applicable annealing data for irradiation effects at the high dose levels that RPVs will experience during 80 years of operation (i.e., a fluence of $\sim 1 \times 10^{20}$ n/cm²).
2. Significantly, because a crucial aspect of an annealing operation is the behavior of the RPV during reirradiation, the amount of post-annealing reirradiation data is sparse for the 40 year scenario and nonexistent for 80 years of operation. Thus, the uncertainties associated with the reirradiation response are high. Moreover, new or improved models for the reirradiation condition are desired, and fracture toughness data are preferable to Charpy impact data to determine reembrittlement.
3. The microstructural processes involved in damage recovery are reasonably understood, but those for the reirradiation response are not as well understood and have had only cursory examination to date. Understanding the underlying physical mechanisms involved in PIA and, especially, reirradiation embrittlement will be key to reducing uncertainties regarding fracture toughness recovery and reembrittlement.
4. Based on NRC regulations and guidance (e.g., RG 1.162 [5]), there is evidence of a flux effect (dose rate effect) on annealing recovery at low annealing temperatures [less than 427 °C (801 °F)]. If consideration is given by the U.S. nuclear industry to thermal annealing in that temperature range, substantial additional information will be required to characterize such effects on the annealing recovery as well as the reirradiation rate. This is also noted in ASTM E509 [18].
5. Although significant IGF has not yet been reported in surveillance programs for irradiated U.S. RPV steels, the steels have been demonstrated to be sensitive to temper embrittlement under certain circumstances, and IGF has been observed in the HAZ of some steels in the postannealed condition after irradiation to a fluence about 1×10^{19} n/cm², raising concern regarding behavior after irradiation to even higher fluences [10].
6. Engineering considerations for thermal annealing may be the least problematic aspect of the technology, given that many previous procedures have been applied to commercial reactors. Although those annealing operations were performed in other countries, the United States has the benefit of the ADP. Nonetheless, various engineering considerations should be addressed (e.g., the potential degrading effects of the high-temperature exposure on other parts of the structure), and those issues will likely differ with different reactor designs. Based on guidance in ASTM E509 [18] and ASME Code Case N-557-1, an annealing operation must be performed to minimize thermally induced stresses in the nozzle region. Therefore, the maximum temperature of annealing would probably be limited to 505 °C (941 °F).
7. In addition to the research actions discussed above, the development of a surveillance program for the post-annealed operation is also recommended. This issue could be quite challenging as the availability of materials could be very limited or even nonexistent.

6.5 ATTENUATION OF EMBRITTLEMENT

Attenuation is an issue with regard to the RPV because the properties of the RPV need to be determined through the vessel thickness (see MDM Gap No. P-AS-04). For example, the

properties at three-quarters of the way through the vessel (3/4-t) are required for analysis during heat-up and cooldown conditions. Because most reactor cores are not configured as a circle, the neutron flux is not the same around the circumference of the RPV. Also, because the core does not occupy the entire height of the RPV, the flux also changes axially along the inner surface of the RPV. Figure 6.9 (a) and (b) provide examples of variation in neutron fluence (>1 MeV) on the inner diameter of a typical PWR [1]. Because of such variations, applications of neutron flux and fluence projections from surveillance locations to the RPV are more complicated. Moreover, because steel has a relatively high scattering cross section for fast neutrons, the fast neutron fluence is attenuated through the RPV thickness. That effect should be incorporated for a reasonable projection of the neutron exposure at the location of interest in the vessel wall.

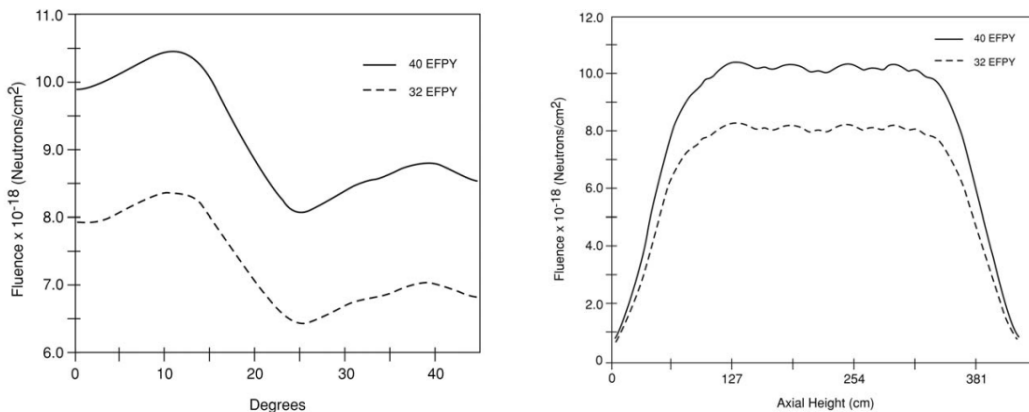


Figure 6.9. Variations of fluence on the inner diameter of the Oconee 1 vessel. (a) Azimuthal variation at the axial location of the peak fluence and (b) axial variation at the azimuthal location of peak fluence [1].

An excellent general discussion of attenuation procedures and issues can be found in [2]. Two circumstances suggest a systematic and physically justifiable approach to attenuation predictions based on the use of TTS correlation models. First, the only physically justified damage dose unit is displacements per atom (dpa), which is a directly calculated measure of the atomic kinetic energy dose deposited in a steel by neutron irradiation (see Appendix C). Second, the dose unit in U.S. TTS models is fluence for neutron energies greater than 1 MeV. Thus, dpa adjusted effective fluence values (>1 MeV) should be used in the models to predict TTS attenuation. That approach involves approximations that add to the uncertainties in the model-based TTS predictions. Quantitative estimates of these uncertainties are not available, but could be determined in future research. What follows is an attempt to systematically describe the approach to attenuation predictions and to list some outstanding issues. It is assumed that the accurate neutronic models of neutron fluxes and spectra are available, either on a plant-specific basis or as the foundation for generic approaches.

Current practice is to base TTS models on flux and fluence for neutrons with energies >1 MeV. Here flux (>1 MeV) and fluence (>1 MeV) are neutron exposure measures, or dose rates and dose, respectively. The $E > 1 \text{ MeV}$ is not a physical unit of dose. Any physical unit of dose must take into account the neutron spectrum flux (E) over the entire range of energies capable of producing atomic displacements, typically measured in a dose unit of dpa. The dpa can be computed for any neutron spectrum based on a standard displacement cross section for iron (Fe) [$\sigma_{\text{dpa}}(E)$] such as tabulated in ASTM E-693, "Standard Practice for Characterizing Neutron

Exposure in Iron and Low Alloy Steels in Terms of Displacements Per Atom (DPA), E 706(ID),” [3] as

$$\text{dpa} = \int f(E,t) \sigma_{\text{dpa}}(E) dE_{\text{dt}} \quad (1)$$

In the case of RPVs, most dpa are produced by neutrons with $E > 0.1$ MeV. However, in special cases, generally not pertinent to RPV embrittlement, dpa from thermal neutrons, and even γ -rays, should be included.

The unit “dpa” is a true unit of radiation damage dose because it is directly proportional to the total kinetic energy deposited per atom for recoil energies greater than a low threshold value (typically 40 eV). The dpa is equal to the total deposited kinetic energy divided by the threshold energy. In this sense dpa is analogous to the dose unit for ionizing radiation such as a gray. Proposals to improve the dose unit by using model-based energy-dependent weighting factors to relate the recoil spectrum to physical production of defects, such as for surviving vacancies and self-interstitials and freely migrating defects and defect clusters, might be marginally better than dpa. However, such units are not generally unique and would be very difficult or impossible to identify and apply in practice (see Appendix C).

The TTS correlations based on fluence >1 MeV or any other fluence or dose unit are acceptable if the flux (E) is assumed to be the same or very similar in all the irradiation locations. That is an unavoidable approximation but generally an acceptable and practical assumption for TTS models. It adds to the uncertainty in TTS correlations and in predicting embrittlement in a different neutron spectrum. Thus, to use current models to predict TTS in different neutron spectra, it is necessary to establish an equivalent dpa dose for neutron fluence (>1 MeV) for the surveillance irradiations. The nominal conversion factor is ≈ 0.015 dpa/ 10^{19} n/cm² (>1 MeV).

It is necessary to predict TTS in the vessel at various locations where the flux and fluence have decreased in magnitude and shifted in spectrum from the conditions at the inside vessel wall. In this case, attenuating the flux and fluence based on the fluences >1 MeV is not physically justified and may be nonconservative. Neutrons with energies <1 MeV also cause dpa and further, neutron spectrum changes along with the flux and fluence in a way that increases the fraction of neutrons <1 MeV. Thus, as shown in Figure 6.10, dpa attenuates more slowly than fluence (>1 MeV) [4]. A more conservative neutron dose unit is fluence (>0.1 MeV), which, as shown in Figure 6.9, attenuates even more slowly than dpa. This is due to efficient inelastic neutron scattering of neutrons with energies >1 MeV to the energy range from ≈ 0.1 to 1 MeV. The inelastic scattering results in a slight peak in fluence (>0.1 MeV) in the region just below the vessel surface. However, use of the $E > 0.1$ dose unit is not useful in practice because the ratio of fluence (>1 MeV)/fluence (>0.1 MeV) in the surveillance locations probably varies more than the corresponding ratio of fluence (>1 MeV)/dpa. Further, fluence (>0.1 MeV) is not an actual damage dose unit.

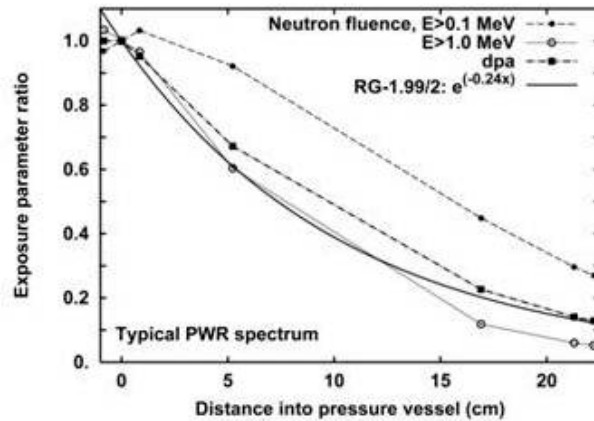


Figure 6.10. Attenuation of exposure parameter ratio for a typical PWR spectrum, with respect to neutron fluence, $E > 0.1$ MeV and $E > 1.0$ MeV, dpa, and the exponential formula from RG 1.99-2 [5] for a typical PWR. [4] Reprinted with permission from ASTM STP 1405, copyright ASTM International, 100 Barr Harbor Drive, West Conshocken, PA 19428.

The use of dpa in TTS models is very straightforward and can be based on a dpa-adjusted effective fluence:

1. By multiplying fluence (>1 MeV) by a factor for the dpa at 10^{19} n/cm² (>1 MeV) at the actual through-thickness location (x), where x is distance from the vessel inside surface, divided by the reference 0.015. For example, if the dpa at the actual location is 0.030 at 10^{19} n/cm² (>1 MeV), then the adjustment factor would be 2. This method requires either a vessel-specific neutron-spectrum-based calculation of dpa attenuation or the use of some type of generic attenuation equation.
2. The dpa-adjusted fluence is then used in the correlation models to predict TTS at a specified location in the vessel. The EONY correlation model [6, 7] accounts for the metallurgical variables in terms of composition and product form, and field variables in terms of dose rate (or effective dpa-adjusted flux), and dose (or effective dpa adjusted fluence and irradiation temperature).

The current published TTS model in RG1.99-2 [5] uses a generic expression to attenuate an effective fluence based on Eq. (2), where x is the distance from the inner surface of the vessel:

$$A(x) = \exp(-0.24x) . \quad (2)$$

The effective dpa adjusted fluence is then given by

$$\text{fluence}(x) = \text{fluence}(0) \cdot A(x) . \quad (3)$$

The -0.24 attenuation coefficient was derived by averaging the calculated dpa to fluence (>1 MeV) ratio at a depth of ≈ 20 cm (8 in.) for six PWR vessels [8]. However, as shown in Figure 6.10, the generic exponential attenuation overpredicts the attenuation of dpa at depths less than ≈ 12 cm (4.7 in.), thus underpredicting the dpa. Further, any PWR-based attenuation function

may not be appropriate for thinner BWR vessel walls, because these produce less neutron backscattering.

Based on extensive detailed neutronic calculations, Remec also observed that the RG 1.99-2 dpa adjusted effective fluence attenuates faster than the actual dpa. He states that, "...for a PV wall thickness of ~24 cm, the calculated ratio of the dpa rate at $\frac{1}{4}$ and $\frac{3}{4}$ of the PV wall thickness to the dpa value on the inner PV surface is ~14% and 19% higher, respectively, than predicted by the RG 1.99-2 formula" [9]. The results are dependent on many factors, including thermal shield thickness, water gap, RPV thickness, and azimuthal location. Other than to note that the use of one generic attenuation formula for all cases increases the uncertainties in the results, a discussion of the details is beyond the scope of this report. However, if generic approaches are to be used, they can be improved relative to that used in R.G. 1.99-2. R.G. 1.99-2 was published in 1988 and is based on even older calculations of dpa attenuation through the wall. Since then the cross sections for neutron transport calculations have been updated several times, in particular the cross sections for iron. New calculations show slower dpa attenuation through the vessel; this results in part from the changes in cross sections and in part from the changes in certain approximations that can better describe the anisotropic scattering. For these reasons, deriving a new exponent for the attenuation formula based on state-of-the-art calculations would be an improvement over the R.G. 1.99-2 formula. Further, assessment of the uncertainties in predicted TTS associated with generic methods is recommended. The issues raised regarding the use of a generic attenuation procedure argue for use of plant-specific approaches to attenuation. Vessel-specific approaches based on computed dpa and dpa rates converted to effective fluence and flux for use in TTS models would not be difficult to implement because the required neutronic calculations are generally available.

Other issues related to TTS attenuation predictions may be more important than some of the details related to damage dose discussed in this section. For example, it is not the TTSs that are of interest *per se*, but rather the reference transition temperatures themselves. Because the reference temperature of the unirradiated steel varies with depth in the vessel wall, it is difficult to accurately predict the irradiated transition temperature at specific locations in the vessel with the concomitant need for substantial uncertainties regarding transition temperature predictions for the irradiated material. Literature studies, time-temperature transformation (TTT) curves, thermal cooling rate models, and additional experimental characterization might be used to develop generic unirradiated transition temperature curves for various vessel thicknesses and heat treatments.

The main impact of high fluence on attenuation in the reactor beltline region is expected to reduce the through-wall TTS gradients because the rate of increase in the TTS with fluence is generally lower at high fluence, at least if high-fluence-threshold embrittlement effects are neglected. As a hypothetical example, if the dpa/effective fluence variation through the vessel lies entirely in the regime where the TTS is on a plateau, then there would be no gradient in TTS, as is the case in R.G. 1.99-2. However, reduced TTS gradients may not occur if late-onset mechanisms develop, leading to the acceleration of embrittlement at high fluence. In principle, robust TTS models can account for the effects of high-fluence attenuation in a direct and accurate way.

Another important effect of high fluence may be to expand the region of concern about TTS to outside the reactor beltline. One significant implication of an expanded embrittlement zone is that it could involve other steel compositions and product forms. This "expanded beltline" issue is discussed in Sect. 6.7.

6.5.1 Experimental Validation

Over the years there have been a number of experimental studies on TTS profile through either actual vessel walls that were sampled after service or in-vessel mockup irradiations. Reference [2] describes a number of such studies conducted up to approximately the year 2000. The following studies are of note:

- Poolside Facility (PSF) experiments performed at ORNL [10, 11]
- German Gundremmingen Reactor Vessel experiments [12]
- French Chooz A reactor vessel experiments [13]
- Japan Power Demonstration Reactor experiments [14]

A number of such experiments have been ongoing since 2000 in terms of data acquisition and analysis; others are proposed. For example, some test results have been reported from a recent attenuation experiment sponsored by the International Atomic Energy Agency (IAEA) to simulate a 180 mm (7.09 in.) thick RPV wall through the use of layers of mechanical test specimens, including CVN impact, tensile, and fracture toughness specimens, with each layer including all three types of specimens [15]. The irradiation experiment was performed at the Dimitrovgrad Reactor at an incident flux of 7×10^{12} n/cm²-s to a fluence of 6×10^{19} n/cm² (>1 MeV) and at an irradiation temperature of 286 ± 6 °C (547 ± 11 °F). Measurements of the CVN impact and fracture toughness specimens through the thickness showed that the through-wall change of the Master Curve reference fracture toughness, T_0 , is greater than that of the CVN 41-J transition temperature [15]. Full discussion of these attenuation experiments is beyond the scope of this brief report. However, assembling a catalogue of experimental studies pertinent to the issue of attenuation, and compiling a corresponding database that can be systematically analyzed using the outlined procedures is recommended as a high priority.

6.5.2 Summary of Recommendations

1. If generic approaches to attenuation are to be used, it is recommended they be improved relative to the approach used in RG 1.99-2. Derivation of a new exponent for the attenuation formula based on state-of-the-art calculations, cross sections, etc., would provide an improvement over the R.G. 1.99-2 formula. Further, assessment of the uncertainties in predicted TTS associated with generic methods is recommended.
2. The issues raised regarding the use of a generic attenuation procedure argue for use of plant-specific approaches to attenuation. Vessel-specific approaches based on computed dpa and dpa rates converted to effective fluence and flux for use in TTS models would not be difficult to implement because the required neutronic calculations are generally available.
3. Assembling a catalog of experimental studies pertinent to the issue of attenuation, and compiling a corresponding database that can be systematically analyzed using the outlined procedures is recommended as a very high priority.

6.6 MASTER CURVE FRACTURE TOUGHNESS

The issues regarding irradiation effects are those identified by a cross section of researchers in the international community [1–11], and the fracture toughness Master Curve was identified by almost every source as a recommended subject for continued research (see MDM Gap No. P-AS 04). The issues most identified were:

- Specimen size, especially regarding the pre-cracked Charpy specimen
- Shape of the Master Curve at high levels of embrittlement
- Dynamic loading (including crack-arrest)
- Effects of intergranular fracture
- Technical basis for the universal shape of the curve

The Charpy-sized single-edge, notched bend [SE(B)] specimen and smaller specimens are identified as a separate issue because of the important link to RPV surveillance programs. Various test programs have identified a difference in the fracture toughness reference temperature (T_0) that is estimated with the Charpy-sized SE(B) specimens. The difference ranges from a few degrees to as much as 45 °C (81 °F), when compared to T_0 values measured using larger specimens [12]. Figure 6.11 shows one example for a Materials Properties Council (MPC) round robin experimental study [13, 14]. Nine laboratories from four countries participated in testing more than 250 Charpy-sized SE(B) specimens of HSSI Weld 72W, with the reference temperature T_0 compared with that from 36 1T compact [1TC(T)] specimens, the specimen type and size generally used as the reference specimen. As shown in Figure 6.11, the T_0 from the Charpy-sized SE(B) specimens (fracture toughness is K_{Jc} adjusted to 1T size, (where $K_{Jc} = \sqrt{EJ_c}$, J_c is the value of J at onset of cleavage fracture, and E is Young's modulus) is 21 °C (38 °F) lower than that from the 1TC(T) specimens, meaning a difference in T_0 estimated by the Charpy-sized SE(B) specimen of –21 °C (–38 °F). Other results have shown a Charpy-sized SE(B) difference of –12 °C (–22 °F) for a heat of A533 Grade B Class 1 steel designated JRQ [12], and a Charpy-sized SE(B) bias of –37 °C (–67 °F) for another heat of the same grade of steel designated Heavy Section Steel Technology (HSST) Plate 13B [15, 16].

Although there are many potential reasons for these observed differences in T_0 , the primary focus is generally on different levels of mechanical constraint for the different specimen types. Differences in constraint for quasi-static loading rates are related to specimen geometry, specimen size, and the relationship of crack length to specimen width. A discussion of constraint issues is beyond the scope of this report, but it is noted that one major focus of many studies is the elastic crack tip T-stress, discussed in more detail in [17–18] and with additional references in the following paragraphs.

For the Plate 13B steel, two different constraint correction procedures, the Wasiluk, Petti, Dodds procedure [19] and the Scibetta procedure [20], reduced the difference to –13 °C (–24 °F) and –11 °C (–22 °F), respectively; the Scibetta procedure was based on a finite element analysis. Thus, even for different heats of the same steel specification, the difference in T_0 estimated using Charpy-sized SE(B) specimens and larger specimens can be significant. Further evaluation of specimen size effects is needed to enable reliable use of Charpy-sized SE(B) specimens as part of nuclear RPV surveillance programs.

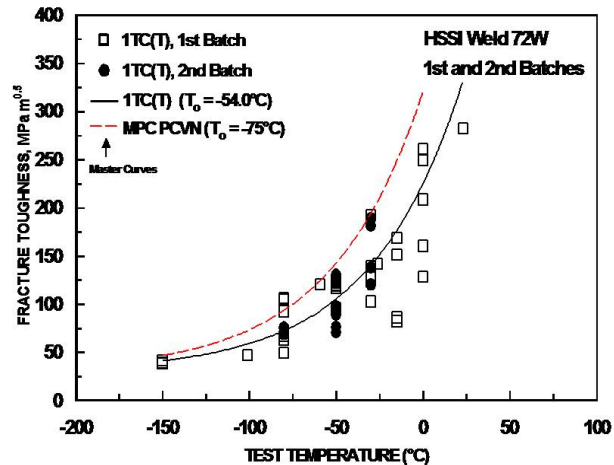


Figure 6.11. Comparison of Master Curve [20] from Materials Properties Council PCVN test program with the results from 1TC(T) tests from ORNL [13, 14]. All tests were conducted with HSSI Weld 72W and indicate a PCVN bias of $-21\text{ }^{\circ}\text{C}$.

In 2005, the IAEA conducted two coordinated research projects in which many different laboratories produced a considerable amount of fracture toughness data from tests of Charpy-sized SE(B) specimens. Results of the studies led to the development of guidelines for the application of Charpy-sized SE(B) fracture toughness data to RPV structural-integrity evaluations [12, 21].

Although the above discussion highlights significant differences in T_0 measurements that are thought to be attributable to specimen size, there is a very wide range within light-water RPV materials. For example, HSST Plate 02, a 305 mm (12 in.) thick plate of A533 grade B class 1 steel, exhibits essentially no difference between T_0 values estimated using Charpy-sized SE(B) specimens and 1TC(T) specimens [22]. Wallin has published numerous papers on small specimen fracture toughness, including [23], which presents test results for many different RPV materials, with three-point bend specimens of 5×5 mm (0.2×0.2 in.) in cross section reported in some cases. Wallin concludes that the miniature SE(B) specimens can be used to estimate T_0 , although he used the Charpy-sized SE(B) specimen as the reference geometry for the miniature specimen results. Further analysis in the same paper reported an average difference of $8\text{ }^{\circ}\text{C}$ ($14\text{ }^{\circ}\text{F}$) between three-point bend specimens and compact specimens [both of various sizes from 3 to 203 mm (0.12 to 8 in.) thick] with the bend specimen providing the lower T_0 , a value similar to that reported by Nanstad as the difference between 1TSE(B) and 1TC(T) specimens in [15, 16]. Wallin attributes the difference to different T-stresses of the specimens (T-stress is an elastic stress that is directly proportional to the load applied to the cracked geometry and affects the constraint at the crack tip.) Unfortunately, as discussed above, constraint correction procedures are not always successful in reconciling the differences in T_0 values estimated using different types of specimens and testing procedures; thus, this issue is not adequately resolved to enable the use of Charpy-sized SE(B) and smaller specimens in RPV surveillance programs with reliability and confidence.

As explicitly stated in E1921, "Determination of Reference Temperature, T_0 , for Ferritic Steels in the Transition Range, E1921-02," [24], the Master Curve development was based on fracture

toughness results from transgranular cleavage fracture. Some metallurgical phenomena, such as temper embrittlement, can lead to diffusion of solutes to or out of grain boundaries such that the boundaries are weakened. This fracture mode is typically associated with temper embrittlement [25], a phenomenon that can lead to intergranular rather than transgranular fracture, including mixed-mode fracture. While a number of LASs have been identified as being susceptible to that particular type of embrittlement mechanism, RPV steels tend to be relatively insensitive to temper embrittlement in the unirradiated condition [26]. Nevertheless, if the prior austenite grain diameter is nominally 65 μm (2.56 mils) (ASTM E112, grain size 5 or larger), sensitivity to temper embrittlement occurs after long-term exposure within the critical temper embrittlement temperature range, which is about 400 $^{\circ}\text{C}$ to 600 $^{\circ}\text{C}$ (752 $^{\circ}\text{F}$ to 1,112 $^{\circ}\text{F}$) [25]. This temperature range is well above the operating range for current LWRs, except in the case of post-irradiation thermal annealing. This condition has been the subject of study in a few experiments. The results by McElroy et al. [27] showed that thermal annealing for a temper-embrittled steel recovered the irradiation-hardening but resulted in an increase in the DBTT due to intergranular fracture. The heat treatment described in [27] was used on five heats of commercial RPV steels followed by thermal aging, which demonstrated the susceptibility of those RPV steels to temper embrittlement under the applied conditions [28]. Figure 6.12 shows results from testing of a relatively large number of compact specimens (the number at each temperature indicated in parenthesis). The specimens tested at -25 $^{\circ}\text{C}$ and 0 $^{\circ}\text{C}$ (-13 $^{\circ}\text{F}$ and 32 $^{\circ}\text{F}$) showed so-called ductile intergranular fracture but failed in an unstable manner. The transition range for the temper-embrittled material, defined in this case as the temperature range over which unstable fracture occurs, extends from below -100 $^{\circ}\text{C}$ to above 50 $^{\circ}\text{C}$ (-148 $^{\circ}\text{F}$ to above 122 $^{\circ}\text{F}$), significantly exceeding that for materials with conventional transition-range cleavage mechanisms [\sim 75 to 80 $^{\circ}\text{C}$ (\sim 135 $^{\circ}\text{F}$ to 144 $^{\circ}\text{F}$)]. The occurrence of predominantly intergranular fracture extended the transition temperature range between lower bound and upper-shelf behavior by a factor of at least 2 with respect to that for a typical cleavage-transition range. A similar observation has been made by Kantidis, Marini, and Pineau for temper embrittled A533 grade B class steel [29]. Yahya et al. [30] demonstrated full intergranular fracture in an A508 class3 forging as well, although they did not apply the Master Curve to their data.

Further investigations by Nanstad et al. with one of the five steels [31] showed that, although the steel in the as-received condition exhibited no intergranular fracture following irradiation, the simulated HAZ exhibited 10% to 20% intergranular fracture following irradiation. Moreover, following post-irradiation thermal annealing at 460 $^{\circ}\text{C}$ (860 $^{\circ}\text{F}$) for 168 h, the material exhibited predominantly (75%) intergranular fracture. This result is particularly applicable to irradiated coarse-grain HAZs following irradiation and thermal annealing at 450 $^{\circ}\text{C}$ (842 $^{\circ}\text{F}$) for 168 h.

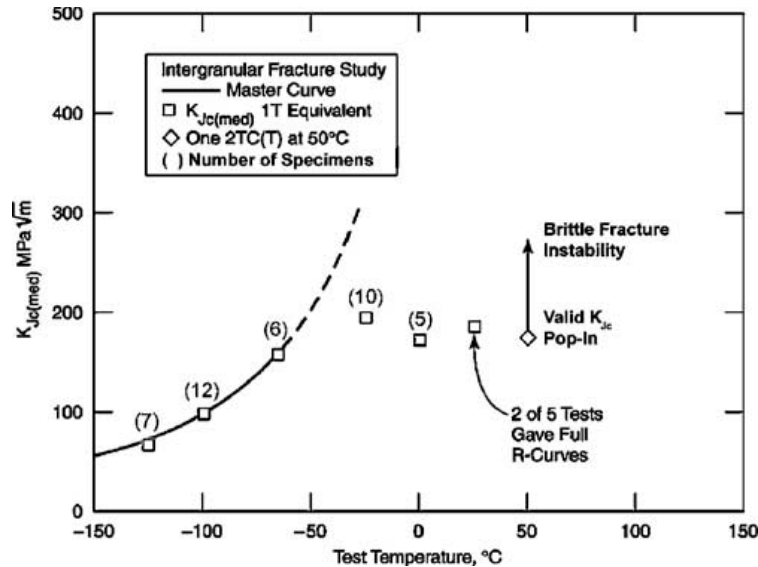


Figure 6.12. Median K_{Jc} values for temper embrittled A302B (Mod) steel after normalization to 1T equivalence compared to the Master Curve based on data at the three lowest test temperatures, showing unstable brittle fracture 150 °C (270 °F) above T_0 [28].

Reprinted with permission from ASTM STP 1405, copyright ASTM International, 100 Barr Harbor Drive, West Conshocken, PA 19428.

The shape of the Master Curve has been generally assumed to be unchanged as a result of irradiation, e.g., [21], although results have been typically presented at embrittlement levels of ΔT_0 to about 100 °C (180 °F). Kaun and Koehring [32] tested 4T size specimens and determined linear-elastic K_{Ic} values at different neutron fluences with fracture toughness transition temperature shifts, ΔK_{Ic} at 100 MPa \sqrt{m} , to about 170 °C (306 °F). The slopes (i.e., as reflected by the variable in the exponential term of the equation) of the curve fits to their K_{Ic} data decreased significantly at the higher fluences (to 2.5×10^{19} n/cm²), although they did not provide the actual K_{Ic} data, so a Master Curve-type statistical analysis is not possible to determine T_0 and ΔT_0 values. Other results by Sokolov and Nanstad [31, 33] have indicated lower slopes for highly embrittled materials, although the case with a T_0 of 160 °C (320 °F) was confounded by the appearance of 20% intergranular fracture in the irradiated specimens. Lee et al. [34] reported test results for an A508 class 3 forging with a ΔT_0 of 134 °C (241 °F) and showed generally good representation of the irradiated Charpy-sized SE(B) data by the Master Curve, although they concluded that the ΔT_0 was larger than the ΔT_{41J} from Charpy impact tests, that there are size effects issues with small specimens giving non-conservative results, and that lower test temperatures result in lower T_0 values. This test temperature effect has also been reported elsewhere [12, 15]. Leax assessed the effect of embrittlement level, as quantified by T_0 , on the Master Curve shape [35]. Figure 6.13 shows a slight dependence of the Master Curve “C” parameter (standard Master Curve value is 0.019) on T_0 , albeit with considerable scatter.

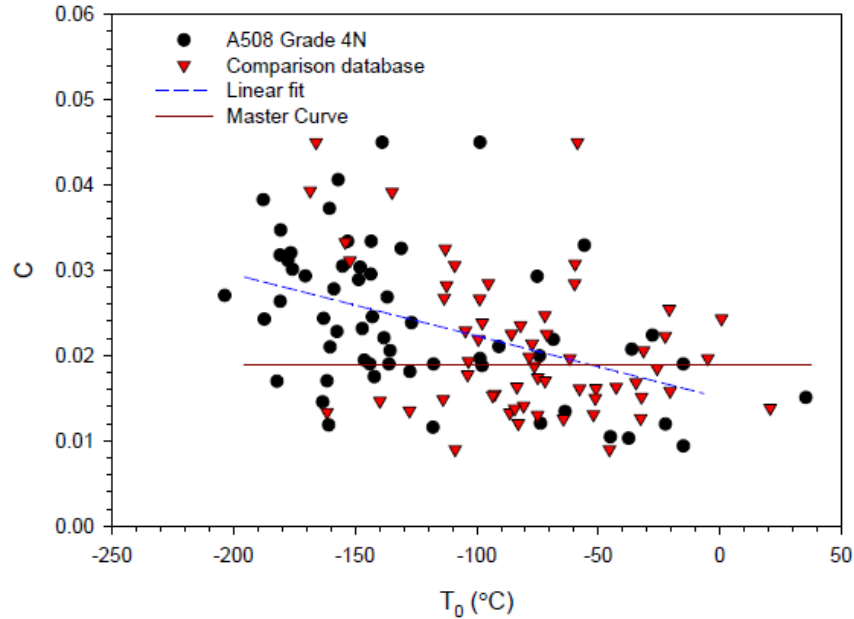


Figure 6.13. Variation in Master Curve slope (the Master Curve “C” value is 0.019) reported by Leax [32]. Reprinted with permission from ASTM STP 909, copyright ASTM International, 100 Barr Harbor Drive, West Conshocken, PA 19428.

The curve shape is also related to the issue of the technical underpinning of the Master Curve. The Master Curve description of cleavage initiation fracture toughness is empirical, and various attempts have been made to model the increase in fracture toughness with increasing test temperature. This is the case with both K_{Ic} and K_{Jc} . Reference [36] provides a review of much of the work, some of which is based on a dislocation mechanics model that also incorporates a microcrack propagation model to account for the temperature dependence of crack propagation across grain boundaries. A somewhat different approach was undertaken by Ortner [37], in which a statistical model of cleavage fracture was used to examine the effects of various material parameters on the transition region fracture toughness. She concluded that it is possible for irradiation-hardening to cause a temperature shift in the toughness without greatly affecting the slope of the curve fit. She also concluded that this is not the case for intergranular fracture or warm prestressing conditions. Odette and He demonstrated a relationship between the Master Curve shape and a temperature-dependent critical stress over a critical volume of material model [38].

The issue of dynamic fracture toughness, including crack arrest toughness, relative to the Master curve is discussed by Kirk and Mitchell [39] in a paper regarding regulatory application of the Master Curve. Reference is made to work by Wallin [40] and Joyce [41] demonstrating the applicability of the Master Curve to characterization of the transition temperature behavior of high-strain-rate fracture toughness data. Regarding crack arrest data, Wallin [42] compared initiation and crack-arrest data for 53 different datasets of RPV steels and found that the Master Curve provides a reasonable representation of crack-arrest data, but with a rather large uncertainty (1σ) on $T_{K_{Ia}}$ (at $100 \text{ MPa}\sqrt{\text{m}}$) of $18 \text{ }^\circ\text{C}$ ($32 \text{ }^\circ\text{F}$). Iskander et al. [43, 44] showed unirradiated and irradiated crack-arrest data that were reasonably represented by the Master Curve. The issue of a fixed temperature separation between the K_{Ic} and K_{Ia} curves in the ASME Boiler and Pressure Vessel Code is also briefly discussed in [39] as being physically inappropriate; such evidence to that effect is shown in [45] for HSSI Welds 72W and 73W [with

a ΔT_0 of 100 °C (180 °F)], for which the temperature differences between the two curves are 41 and 18 °C (74 °F and 32 °F) for the unirradiated and irradiated conditions, respectively. Both Wallin [40, 42] and Kirk [46] have developed formulas that use T_0 to estimate the transition fracture behavior (transition temperature, temperature dependence, and scatter) of K_{Jc} data as well as of crack arrest (K_{Ia}) data under dynamic loading conditions. Those models, as well as models that estimate upper-shelf behavior based on T_0 [47–49], have been used by the NRC as part of the probabilistic fracture mechanics analyses used to support the alternative rule for pressurized thermal shock [50–52].

In summary, the most significant issue impeding more comprehensive use of the Master Curve in RPV embrittlement monitoring and structural integrity analysis is the effect of specimen size on T_0 . In particular, it is important to establish how T_0 values measured using Charpy-sized SE(B) specimens can be used to reliably predict the transition behavior of much larger structures. This issue is recommended, therefore, as a high priority. The importance of the other issues discussed here is summarized below:

- *Intergranular fracture.* As discussed in this section, intergranular fracture can occur in RPV steels but only under conditions that are unlikely to occur in RPV service, with the possible exception being RPVs that have been thermally annealed at a high temperature [i.e., ~450 °C (842 °F)]. Other than the case for thermal annealing, additional work in this area is therefore expected to produce minimal benefit in improving the accuracy of RPV structural integrity models.
- *Universal transition temperature curve shape.* As stated by Leax, “the Master Curve, while not an exact description of the toughness behavior, provides a simple and accurate means to estimate toughness as a function of the temperatures of interest.” [32]. Nevertheless, evidence exists, as summarized herein, that at especially high levels of embrittlement there may be some change to the universal transition curve shape adopted by the Master Curve. Additional work focused on collecting together available data and using this information to perform a comprehensive assessment is recommended. Such a study may point to the need for further experimental investigations to fill gaps in the current empirical knowledge.
- *Applicability of the Master Curve to the characterization of dynamic loading.* Engineering models exist that predict available data with reasonable accuracy. Further, even postulated accident events (e.g. PTS) for RPVs do not occur at elevated loading rates. A better physical understanding of the transition behavior of ferritic steels under dynamic loading will be beneficial from a scientific viewpoint; however, the practical benefit of such knowledge to RPV structural integrity analyses is expected to be minimal.
- *Applicability of the Master Curve to the characterization of crack arrest.* Engineering models exist that predict available data with reasonable accuracy, and these models have been used in the United States to support the development of regulations. Further, at this time only the United States considers crack arrest data as part of RPV integrity assessment. While a better physical understanding and more accurate models of the crack arrest behavior of ferritic steels under dynamic loading will be beneficial, there may be little incremental benefit relative to currently available models.

6.7 EMBRITTLEMENT BEYOND THE BELTLINE

To assess the operating safety of a nuclear RPV, it is important to quantify the effects of neutron irradiation damage and to account for the effects when establishing operating envelopes and limits, such as the pressure and temperature operating limits (also see EPRI MDM Gap No. P-AS-04). Traditionally, the effects of neutron irradiation have been addressed only for materials in the “beltline” of the RPV. The definition of “beltline” from 10 CFR Part 50, Appendix G [1] is as follows:

Beltline or Beltline region of reactor vessel means the region of the reactor vessel (shell material including welds, heat affected zones, and plates or forgings) that directly surrounds the effective height of the active core and adjacent regions of the reactor vessel that are predicted to experience sufficient neutron radiation damage to be considered in the selection of the most limiting material with regard to radiation damage.

From this definition, the terms “effective height,” “adjacent regions,” and “sufficient neutron damage” are ambiguous and, therefore, require judgment to be applied. Such judgments have evolved over time. As illustrated in Figure 6.14, the originally proposed definition [2] excluded from the beltline any region of the RPV that did not exhibit at least 55.6 °C (100 °F) of predicted TTS over the anticipated lifetime of the vessel. That value was reduced to 28 °C (50 °F) in the early versions of 10 CFR 50, Appendix G, used through 1983 [3, 4].

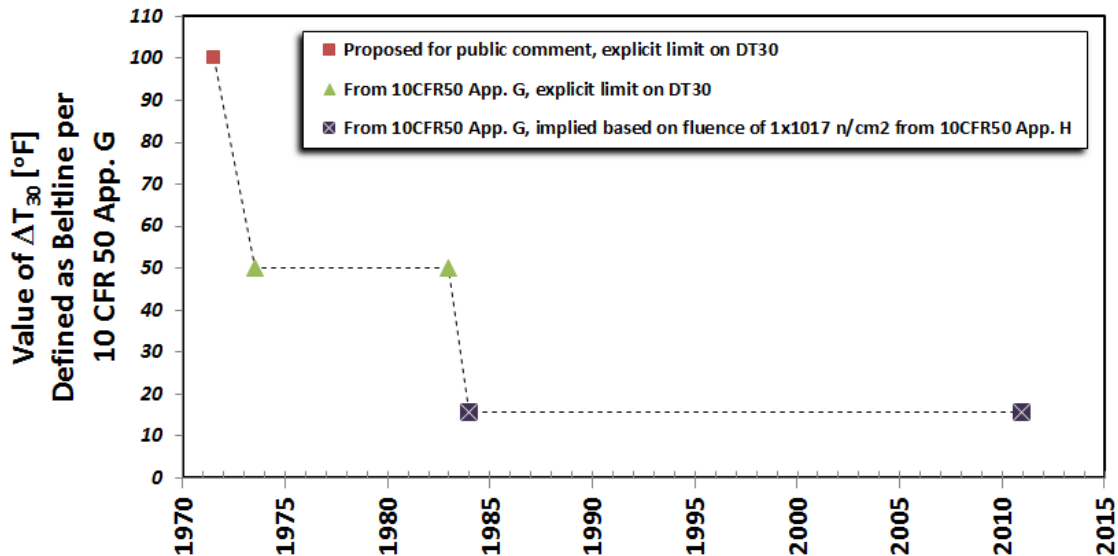


Figure 6.14. Variation in the value of 30 ft-lb (41 J) TTS (ΔT_{30}) associated with the definition of the word “beltline” [2].

Reprinted with permission from *Annual Book of ASTM Standards*, Vol. 12.0, copyright ASTM International, 100 Barr Harbor Drive, West Conshocken, PA 19428.

Since 1984, the current, commonly accepted definition of the beltline, which implies a fluence of at least 1×10^{17} n/cm² ($E > 1$ MeV), has expanded the beltline. The current definition is not specifically stated in any one document but, rather, is implied in the following quotations.

10 CFR 50, Appendix H [5], Section III.A:

No material surveillance program is required for reactor vessels for which it can be conservatively demonstrated by analytical methods applied to experimental data and tests performed on comparable vessels, making appropriate allowances for all uncertainties in the measurements, that the peak neutron fluence at the end of the design life of the vessel will not exceed 10^{17} n/cm² (E > 1 MeV).

ASTM Designation E 185 – 02, “Standard Practice for Design of Surveillance Programs for Light-Water Moderated Nuclear Power Reactor Vessels,” [2], Paragraph 1.2 addresses this issue for initial EOL as follows:

This practice was developed for all light-water moderated nuclear power reactor vessels for which the predicted maximum fast neutron fluence (E > 1 MeV) at the end of the design lifetime (EOL) exceeds 1×10^{17} n/cm² (1×10^{21} n/m²) at the inside surface of the reactor vessel.

Assuming that the current definition of beltline based on a fluence limit continues to be accepted, the physical extent of the “beltline” implied by this fluence limit has expanded beyond the shell course region to include regions of the RPV where there are nozzle penetrations and shell thickness transitions, as most plants in the United States will be operated for at least one, and possibly multiple, 20 year license renewal periods. Such long term reactor operation needs firmer technical basis and may require the following additional research:

- Evaluate the extended beltline materials that exceed the 1×10^{17} n/cm² fluence. However, the material property information (i.e., unirradiated transition temperatures, material compositions) is lacking for the materials of such components. Development of a better understanding of the properties of these relatively under-characterized materials is needed. This can be done by gathering information from available records and archive samples and developing generic properties for material classes. Development of a method for extracting small samples from the nozzles or welds for chemical composition measurements and/or small mechanical tests for assessment of embrittlement should also be considered.
- Ensure surveillance programs contain representative material of the extended beltline. This would include forging and plate material irradiated at a relatively low flux and fluence. The welds used in the extended beltline were typically the same as those used in the beltline. The BWR surveillance data would be a candidate because they represent generally lower flux/lower fluence conditions and most of the BWR RPVs were also fabricated by Babcock & Wilcox and Combustion Engineering.
- Justify more refined methods [e.g., use of smaller flaws, stress intensity factor (SIF) correlations] for use in structural integrity calculations of the nozzle region to show that materials in the “extended beltline” regions do not produce more restrictive limits (on, for example, pressure-temperature limit curves) than are imposed by the more highly irradiated materials closer to the active core.
- Assess thermal embrittlement in the hot leg nozzle HAZs; it could be a concern, especially if there is a synergistic effect with low flux irradiation (see thermal aging in Chapter 3). This would likely include physical measurements on a nozzle from a decommissioned RPV.

- Assess the following issue caused by the albedo effect (albedo refers to reflectivity of a surface), in which neutrons that pass through the RPV wall reflect off the concrete and stream up through the cavity to the nozzle area. As a result of such streaming, the fluence on the outside of the nozzles and RPV can be as high or higher than the fluence on the inside of the RPV in that nozzle region: For reactor operation within the 40 year license period, the concern with such neutron streaming and the albedo effect is associated with the potential for damage to equipment and cables located above the vessel and for limitations in personnel accessibility to such equipment. With higher fluence associated with extended operation and the increased potential for significant embrittlement, the ability to accurately model fluence in the various areas around the nozzles/extended beltline becomes more important, requiring accurate source terms, cross-section data, an albedo collision model, etc. [6, 7].

6.8 REFERENCES*

Sect. 6.1

1. E. D. Eason, G. R. Odette, R. K. Nanstad, and T. Yamamoto, "A physically-based correlation of irradiation-induced transition temperature shifts for RPV steels," *Journal of Nuclear Materials* **433**(1-3), 240–254 (2013).
2. E. D. Eason, G. R. Odette, R. K. Nanstad, and T. Yamamoto, *A Physically Based Correlation of Irradiation-Induced Transition Temperature Shifts for RPV Steels*, ORNL/TM-2006/530, Oak Ridge National Laboratory, February 2007.
3. G. R. Odette and G. E. Lucas, "Embrittlement of Nuclear Reactor Pressure Vessels," *J. Metals* **53**(7), 18–22 (2001).
4. R. K. Nanstad, M. A. Sokolov, and D. E. McCabe, "Applicability of the Fracture Toughness Master Curve to Irradiated Highly Embrittled Steel and Intergranular Fracture," *J. ASTM Int.* **5**(3), Paper ID JA1101346 (2008). Available online at www.astm.org.
5. G. R. Odette and R. K. Nanstad, "Predictive Reactor Pressure Vessel Steel Irradiation Embrittlement Models: Issues and Opportunities," *J. Metals* **61**(7), 19–25 (2009).
6. R. K. Nanstad and G. Robert Odette, "Reactor Pressure Vessel Issues for the Light-Water Reactor Sustainability Program," pp. 1667–1676 in *Proc. 14th Int. Conf. on Environmental Degradation of Materials in Nuclear Power Systems Water Reactors*, American Nuclear Society, 2010.
7. NRC, *Radiation Embrittlement of Reactor Vessel Materials*, Regulatory Guide 1.99, Revision 2, U.S. Nuclear Regulatory Commission, 1988.
8. G. R. Odette, "On the Controlling Mechanism of Radiation Embrittlement of Reactor Pressure Vessel Steels," *Scripta Metallurgica* **17**, 1183 (1983).
9. P. N. Randall, "Basis for Revision 2 of the U.S. Nuclear Regulatory Commission's Regulatory Guide 1.99," pp. 149–162 in *Radiation Embrittlement of Nuclear Reactor Pressure Vessel Steels: An International Review (Second Volume)*, ASTM STP 909, L. E. Steele (ed.), American Society for Testing and Materials, 1986.

* Inclusion of references in this report does not necessarily constitute NRC approval or agreement with the referenced information.

10. ASTM, "Standard Guide for Predicting Radiation-Induced Transition Temperature Shift in Reactor Vessel Materials," *Annual Book of ASTM Standards*, Vol. 12.01, ASTM International, 2012.
11. *U.S. Code of Federal Regulations*, "Fracture Toughness Requirements for Protection Against Pressurized Thermal Shock Events," Part 50.61a, Title 10, "Energy," Standard E900-02(2007), adopted on February 3, 2010, <http://www.nrc.gov/reading-rm/doc-collections/cfr/part050/part050-0061a.html>. (See also *Federal Register* **1**, 13-29, January 4, 2010).
12. G. R. Odette, T. Yamamoto, R. D. Klingensmith, D. Gragg, and G. E. Lucas, *The Irradiation Variables (IVAR) Program Database on Irradiation Induced Yield and Ultimate Tensile Stress Changes in Reactor Pressure Vessel Steels*, UCSB MRPG PV1-2009, The University of California, Santa Barbara, 2009.
13. R. Chaouadi, *RADAMO—An Experimental Databank for Investigating Irradiation Strengthening of RPV Materials*, Report R-3858, SCK•CEN, Belgium, 2004.
14. Naoki Soneda, Kenji Dohi, Akiyoshi Nomoto, Kenji Nishida, and Shiori Ishino, "Embrittlement Correlation Method for the Japanese Reactor Pressure Vessel Materials," *Journal of ASTM International* **7**(3), Paper ID JAI102127 (2010). Available online at www.astm.org.
15. Japan Electric Association, *Method of Surveillance Tests for Structural Materials of Nuclear Reactors*, JEAC 4201-1991, 1992, Chiyoda-ku, Tokyo, Japan.
16. G. R. Odette and G. E. Lucas, "Recent Progress in Understanding Reactor Pressure Vessel Steel Embrittlement," *Radiation Effects and Defects in Solids* **144**, 189 (1998).
17. M. T. Kirk, *Further Evaluation of High Fluence Data—Calculation Notes*, U.S. Nuclear Regulatory Commission, ADAMS ML081120600, January 2008.
18. G. R. Odette, "Microstructural Evolution During Irradiation," p. 137 in *MRS Symp. Proc.* **373**, Materials Research Society, 1995.
19. G. R. Odette, *Irradiation Effects on Pressure Vessel Steels*, IAEA IRRWG-LMNPP-98-3, International Atomic Energy Agency, 1998, p. 438.
20. G. R. Odette and B.D. Wirth, "A computational microscopy study of nanostructural evolution in irradiated pressure vessel steels," *Journal of Nuclear Materials* **251**, 157 (1998).
21. G. R. Odette, T. Yamamoto, and B. D. Wirth, "Late Blooming Phases and Dose Rate Effects in RPV Steels: Integrated Experiments and Models," p. 105 in *Proc. 2nd Int. Conf. on Multiscale Modeling*, University of California Los Angeles, 2004.
22. M. K. Miller and K. F. Russell, "Embrittlement of RPV Steels: An Atom Probe Tomography Perspective," *Journal of Nuclear Materials* **37**(1-3), 145 (2007).
23. M. K. Miller, A. A. Chernobaeva, Y. I. Shtrombakh, et al., "Evolution of the nanostructure of VVER-1000 RPV materials under neutron irradiation and post irradiation annealing," *Journal of Nuclear Materials* **385**, 615 (2009).
24. J. M. Hyde, D. Ellis, C. A. English and T. J. Williams, "Microstructural Evolution in High Nickel Submerged Arc Welds," p. 262 in *20th ASTM Int. Symp. on Effects of Radiation on Nuclear Materials*, ASTM STP 1405, ASTM International, 2001.
25. M. K. Miller, K. A. Powers, R. K. Nanstad, and P. Efsing, "Atom probe tomography characterizations of high nickel, low copper surveillance RPV welds irradiated to high fluences," *Journal of Nuclear Materials* **437**(1-3), 107-115 (2013).

Sect. 6.2

1. NRC, *Radiation Embrittlement of Reactor Vessel Materials*, Regulatory Guide 1.99, Revision 2, U.S. Nuclear Regulatory Commission, 1988.
2. J. J. Wang and R. Subramani, *PR-EDB: Power Reactor Embrittlement Database Version 3*, ORNL/TM-2006/605, Oak Ridge National Laboratory, August 2007.
3. P. N. Randall, "Basis for Revision 2 of the U.S. Nuclear Regulatory Commission's Regulatory Guide 1.99," pp. 149–162 in *Radiation Embrittlement of Nuclear Reactor Pressure Vessel Steels: An International Review* (Second Volume), ASTM STP 909, L. E. Steele (ed.), American Society for Testing and Materials, 1986.
4. E. D. Eason, G. R. Odette, R. K. Nanstad, and T. Yamamoto, "A physically-based correlation of irradiation-induced transition temperature shifts for RPV steels," *Journal of Nuclear Materials* **433**(1-3), 240–254 (2013).
5. E. D. Eason, G. R. Odette, R. K. Nanstad, and T. Yamamoto, *A Physically Based Correlation of Irradiation-Induced Transition Temperature Shifts for RPV Steels*, ORNL/TM-2006/530, Oak Ridge National Laboratory, 2007.
6. G. R. Odette and R. K. Nanstad, "Predictive Reactor Pressure Vessel Steel Irradiation Embrittlement Models: Issues and Opportunities," *Journal of Metals* **61** (7), 19–25 (2009).
7. M. T. EricksonKirk, *Technical Basis for Revision of Regulatory Guide 1.99: NRC Guidance on Methods to Estimate the Effects of Radiation Embrittlement on the Charpy V-Notch Impact Toughness of Reactor Vessel Materials*, Draft NUREG-XXXX, U.S. Nuclear Regulatory Commission, October 2007.
8. R. K. Nanstad, G. R. Odette, R. E. Stoller, and T. Yamamoto, *Review of Draft NUREG Report on Technical Basis for Revision of Regulatory Guide 1.99*, ORNL/NRC/LTR-08/03, Oak Ridge National Laboratory, 2008.
9. Mark T. Kirk, "A Wide-Range Trend Embrittlement Trend Curve for Western RPV Steels," Paper A-106/T1 in *Proc. of Fontevraud 7*, September 2010, Avignon, France.
10. E. V. Mader, "Kinetics of Irradiation Embrittlement and the Post-Irradiation Annealing of Nuclear Reactor Pressure Vessel Steels," PhD Thesis, University of California, Santa Barbara, 1995.
11. G. R. Odette, T. Yamamoto, and R. D. Klingensmith, "On the effect of dose rate on irradiation hardening of RPV steels," *Philosophical Magazine* **85**, 779 (2005).
12. R. Chaouadi, *RADAMO—An Experimental Databank for Investigating Irradiation Strengthening of RPV Materials*, Report R-3858, SCK•CEN, Belgium, 2004.
13. G. R. Odette, T. Yamamoto, and D. Klingensmith, "When the Turtle Can't Get There and the Rabbit Gets Lost: Predicting Low Flux-High Fluence RPV Embrittlement," *Symp. on the Mechanical Performance for Current and Next Generation Nuclear Reactors: Ensuring Lifetime and Reliability*, Seattle, Washington, February 14–18, TMS, 2010.
14. E. D. Eason et al., *Models for Embrittlement Recovery Due to Annealing of Reactor Pressure Vessel Steels*, NUREG/CR-6327, MCS 950302, U.S. Nuclear Regulatory Commission, May 1995.
15. U.S. Nuclear Regulatory Commission, *Format and Content of Report for Thermal Annealing of Reactor Pressure Vessels*, Regulatory Guide 1.162, U.S. Nuclear Regulatory Commission, February 1996.

16. R. Chaouadi and R. Gérard, "Neutron Flux and Annealing Effects on Irradiation Hardening of RPV Materials," *Journal of Nuclear Materials* **418**, 137–142 (2011).
17. T. J. Williams, D. Ellis, C. A. English, and J. Hyde, "A Model of Irradiation Damage in High Nickel Submerged Arc Welds," *International Journal of Pressure Vessels and Piping* **79**, 649–660 (2002).
18. Naoki Soneda, Kenji Dohi, Akiyoshi Nomoto, Kenji Nishida, and Shiori Ishino et al., "Embrittlement Correlation Method for the Japanese Reactor Pressure Vessel Materials," *Journal of ASTM International* **7**(3), Paper ID JAI102127 (February 2010).
19. M. Kirk, "A Wide-Range Embrittlement Trend Curve for Western RPV Steels," *ASTM Symposium on Effects of Radiation on Nuclear Materials*, vol. 25, ASTM STP-1547, T. Yamamoto, M. Sokolov, and B. Hanson (eds.), ASTM International, 2013.
20. P. Todeschini, Y. Lefebvre, H. Churier-Bossennec, N. Rupa, G. Chas, and C. Benhamou, "Revision of the irradiation embrittlement correlation used for the EDF RPV fleet," Paper A084-T01 in *Proc. of Fontevraud 7*, September 2010, Avignon, France.
21. G. R. Odette and G. E. Lucas, "Recent Progress in Understanding Reactor Pressure Vessel Steel Embrittlement," *Radiation Effects and Defects in Solids* **144**, 189 (1998).
22. G. R. Odette and B. D. Wirth, "A Computational Microscopy Study of Nanostructural Evolution in Irradiated Pressure Vessel Steels," *Journal of Nuclear Materials* **251**, 157 (1998).
23. G. R. Odette, B. D. Wirth, D. J. Bacon, and N. M. Ghoniem, "Multiscale-Multiphysics Modeling of Radiation Damaged Materials: Embrittlement of Pressure Vessel Steels," *Materials Research Society Bulletin* **176** (March 2000).
24. M. K. Miller, K. A. Powers, R. K. Nanstad, and P. Efsing, "Atom probe tomography characterizations of high nickel, low copper surveillance RPV welds irradiated to high fluences," *Journal of Nuclear Materials* **437**(1-3), 107–115 (2013).
25. R. K. Nanstad, and G. R. Odette, "Reactor Pressure Vessel Issues for the Light-Water reactor Sustainability Program", pp. 1667–1676 in *Proc. 14th Int. Conf. on Environmental Degradation of Materials in Nuclear Power Systems Water Reactors*, American Nuclear Society, 2010.
26. R. K. Nanstad, G. R. Odette, and M. A. Sokolov, "Ensuring the Performance of Nuclear Reactor Pressure Vessels for Long-Time Service," *Proc. of ASME PVP Conference*, PVP2010, July 2010.
27. H. B. Klasky et al., "Radiation Embrittlement Archive Project," *Trans. 22nd Conf. on Structural Mechanics in Reactor Technology, SMiRT-22*, San Francisco, California, August 18–23, 2013.

Sect. 6.3

1. G. R. Odette and G. E. Lucas, "Recent progress in understanding reactor pressure vessel steel embrittlement" *Radiation Effects and Defects in Solids* **144**, 189 (1998).
2. G. R. Odette, "Microstructural Evolution During Irradiation," p. 137 in *MRS Symp. Proc.* **373**, Materials Research Society, 1995.
3. G. R. Odette, *Neutron Irradiation Effects in Pressure Vessel Steels*, IAEA IRRWG-LMNPP-98-3, International Atomic Energy Agency, 1998, p. 438.

4. G. R. Odette and B.D. Wirth, "A computational microscopy study of nanostructural evolution in irradiated pressure vessel steels," *Journal of Nuclear Materials* **251**, 157 (1998).
5. G. R. Odette, T. Yamamoto, and B. D. Wirth, p. 105 in *Proc. 2nd Int. Conf. on Multiscale Modeling*, University of California Los Angeles, 2004.
7. M. K. Miller, A. A. Chernobaeva, Y. I. Shtrombakh, et al., "Evolution of the nanostructure of VVER-1000 RPV materials under neutron irradiation and post irradiation annealing," *Journal of Nuclear Materials* **385**, 615 (2009).
8. J. M. Hyde, D. Ellis, C. A. English, and T. J. Williams, "Microstructural Evolution in High Nickel Submerged Arc Welds," p. 262 in *20th ASTM Int. Symp. on Effects of Radiation on Nuclear Materials*, ASTM STP 1405, ASTM International, 2001.
9. C. L. Liu, G. R. Odette, B. D. Wirth and G. E. Lucas, "A lattice Monte Carlo simulation of nanophase compositions and structures in irradiated pressure vessel Fe-Cu-Ni-Mn-Si steels" *Materials Science and Engineering: A* **238**, 202 (1998).
10. W. J. Phythian and C. A. English, "Microstructural evolution in reactor pressure vessel steels," *Journal of Nuclear Materials* **205**, 162 (1993).
11. J. T. Buswell, W. J. Phythian, R. J. McElroy, et al., "Reactor irradiation-induced microstructural changes, and hardening mechanisms, in model PWR pressure vessel steels," *Journal of Nuclear Materials* **225**, 196 (1995).
12. G. R. Odette, "Microstructure Evolution During Irradiation," p. 457 in *MRS Symp. Proc.* **439**, Materials Research Society, 1998.
13. B. D. Wirth, G. R. Odette, W. Pavinich, G. E. Lucas, and S. Spoone, "Small Angle Neutron Scattering Study of Linde 80 RPV Welds," p. 102 in *18th Int. Symp. on the Effects of Radiation on Materials*, ASTM STP-1325, American Society for Testing and Materials, 1999.
14. R. G. Carter, N. Soneda, K. Dohi, et al., "Microstructural characterization of irradiation-induced Cu-enriched clusters in reactor pressure vessel steels," *Journal of Nuclear Materials* **298**, 211 (2001).
15. S. C. Glade, B. D. Wirth, G. R. Odette and P. Asoka-Kumar, "Positron annihilation spectroscopy and small angle neutron scattering characterization of nanostructural features in high-nickel model reactor pressure vessel steels," *Journal of Nuclear Materials* **351**, 27 (2006).
16. M. K. Miller, K. F. Russell, M. A. Sokolov, et al., "APT characterization of irradiated high nickel RPV steels," *Journal of Nuclear Materials* **361**(2-3), 248 (2007).
17. G. R. Odette, and C. Cowan, "Use of Combined Electrical Resistivity and Seebeck Coefficient Measurements to Characterize Solute Redistribution Under Irradiation and Thermal Aging," *CD Proc. 10th Int. Symp. on Environmental Degradation of Materials in Light Water Reactors*, National Association of Corrosion Engineers, 2001.
18. J. S. Smith, "Characterization of Irradiation and Thermal Aging Induced Solute Redistributions in Reactor Pressure Vessel Steels Using Combined Electrical Resistivity and Seebeck Coefficients," MS Thesis, University of California Santa Barbara, 2006.
19. Eason, E. D., G. R. Odette, R. K. Nanstad, and T. Yamamoto, "A physically-based correlation of irradiation-induced transition temperature shifts for RPV steels," *Journal of Nuclear Materials* **433**(1-3), 240-254 (2013).

20. E. D. Eason, G. R. Odette, R. K. Nanstad, and T. Yamamoto, *A Physically Based Correlation of Irradiation-Induced Transition Temperature Shifts for RPV Steels*, ORNL/TM-2006/530, Oak Ridge National Laboratory, 2007.
21. G. R. Odette and R. K. Nanstad, "Predictive Reactor Pressure Vessel Steel Irradiation Embrittlement Models: Issues and Opportunities," *Journal of Metals* **61**(7), 19–25 (2009).
22. N. Soneda et al., "Microstructural Characterization of RPV Materials Irradiated to High Fluences at High Flux," *Journal of ASTM International* **6**(7), Paper ID JAI102128 (2009).
23. P. Efsing et al., "Analysis of the Ductile-to-Brittle Transition Temperature Shift in a Commercial Power Plant with High Nickel Containing Weld Material," *Journal of ASTM International* **4**(7), Paper ID JAI100719 (2007). Available at www.astm.org.
24. NRC, *Radiation Embrittlement of Reactor Vessel Materials*, Regulatory Guide 1.99, Revision 2, U.S. Nuclear Regulatory Commission, 1988.
25. M. K. Miller, K. A. Powers, R. K. Nanstad, and P. Efsing, "Atom probe tomography characterizations of high nickel, low copper surveillance RPV welds irradiated to high fluences," *Journal of Nuclear Materials* **437**(1-3), 107–115 (2013).
26. R. K. Nanstad, M. K. Miller, and W. D. Lewis, *Results of Examinations of Surveillance Specimens from Commercial Reactors*, ORNL/TM-2012/447, Oak Ridge National Laboratory, September 2012.

Sect. 6.4

1. *U.S. Code of Federal Regulations*, "Fracture Toughness Requirements for Protection Against Pressurized Thermal Shock Events," Part 50.61a, Title 10, "Energy," adopted on February 3, 2010, <http://www.nrc.gov/reading-rm/doc-collections/cfr/part050/part050-0061a.html>. Also see *Federal Register* **75**(1), 13–29 (Jan. 4, 2010).
2. D. J. Ayres and B. M. Barishpolsky, "Vessel Prestress: A New Solution for Pressurized Thermal Shock," pp. 357–362 in *Trans. 12th Int. Conf. on Structural Mechanics in Reactor Technology (SMiRT)*, Vol. G, Stuttgart, Germany, 1993.
3. W. L. Server, T. J. Griesbach, E. L. Kennedy, and C. S. Venkatakrishnan, "Reactor Pressure Vessel Life Assurance Decisions," pp. 89–94 in PVP Vol. 261, *Service Experience and Life Management: Nuclear, Fossil, and Petrochemical Plants*, ASME, 1993.
4. T. Planman, R. Pelli, and K. Torronen, *State of the Art Review on Thermal Annealing*, AMES Report No. 2, EUR 16278 EN, European Commission, December 1994.
5. NRC, *Format and Content of Report for Thermal Annealing of Reactor Pressure Vessels*, Regulatory Guide 1.162, U.S. Nuclear Regulatory Commission, February 1996.
6. M. A. Sokolov, R. K. Nanstad, and S. K. Iskander, "Effects of Thermal Annealing on Fracture Toughness of Low Upper-Shelf Welds," pp. 690–705 in *Effects of Radiation on Materials: 17th Int. Symp.*, ASTM STP 1270, D. S. Gelles, R. K. Nanstad, A. S. Kumar, and E. A. Little (eds.), American Society for Testing and Materials, 1996.
7. R. K. Nanstad, D. E. McCabe, and R. L. Swain, "Evaluation of Variability in Material Properties and Chemical Composition for Midland Reactor Weld WF-70," pp. 125–156 in *Effects of Radiation on Materials: 18th Int. Symp.*, ASTM STP 1325, R. K. Nanstad, M. L. Hamilton, F. A. Garner, and A. S. Kumar (eds.), American Society for Testing and Materials, 1999.

8. R. K. Nanstad, B. R. Bass, J. G. Merkle, C. E. Pugh, T. M. Rosseel, and M. A. Sokolov, "Heavy-section Steel Technology and Irradiation Programs-Retrospective and Prospective Views," *Journal of Pressure Vessel Technology* **132**, 064001-1 (December 2010).
9. R. K. Nanstad, M. A. Sokolov, and D. E. McCabe, "Applicability of the Fracture Toughness Master Curve to Irradiated Highly Embrittled Steel and Intergranular Fracture," *Journal of ASTM International* **5**(3), Paper JAI101346 (2008). Available online at www.astm.org.
10. R. K. Nanstad, D. E. McCabe, M. A. Sokolov, C. A. English, and S. R. Ortner, "Investigation of Temper Embrittlement in Reactor Pressure Vessel Steels Following Thermal Aging, Irradiation, and Thermal Annealing," pp. 356–382 in *Effects of Radiation on Materials: 20th Int. Symp.*, ASTM STP 1405, S. T. Rosinski, M. L. Grossbeck, T. R. Allen, and A. S. Kumar (eds.), ASTM International, 2001.
11. U. Potapovs, J. R. Hawthorne, and C. Z. Serpan, Jr., "Notch Ductility Properties of SM-1A Reactor Pressure Vessel Following the In-Place Annealing Operation," *Nuclear Application* **5** (December 1968).
12. U. Potapovs, G. W. Knighton, and A. S. Denton, "Critique of In-Place Annealing of SM-1A Nuclear Reactor Vessel," *Nuclear Engineering and Design* **8**, 39–57 (1968).
13. M. Brumovsky et al., "Annealing and Re-Embrittlement of RPV Materials," *State of the Art Report ATHENA WP-4, AMES Report N. 19, Ageing Materials European Strategy*, European Commission, Joint Research Institute, JRC46534, EUR 23449 EN, ISSN 1018-5593, European Communities, 2008.
14. N. M. Cole and T. Friderichs, *Report on Annealing of the Novovoronezh Unit 3 Reactor Vessel in the USSR*, NUREG/CR-5760, MPR-1230, MPR Associates, Inc., 1991.
15. C. B. Oland, B. R. Bass, J. W. Bryson, L. J. Ott, and J. A. Crabtree, *Marble Hill Annealing Demonstration Evaluation*, NUREG/CR-6552 (ORNL/TM-13446), Oak Ridge National Laboratory, February 1998.
16. EPRI, *Marble Hill Demonstration Report*, EPRI TR-104934, Electric Power Research Institute, 1998.
17. E. D. Eason, J. Wright, E. Nelson, G. R. Odette, and E. Mader, *Models for Embrittlement Recovery Due to Annealing of Reactor Pressure Vessel Steels*, NUREG/CR-6327, U.S. Nuclear Regulatory Commission, 1995
18. ASTM, *Standard Guide for In-Service Annealing of Light-Water Moderated Nuclear Reactor Vessels*, Vol. 12.02, ASTM Standard E509-03 (Reapproved 2008), ASTM International, 2011.
19. ASME, "In-Place Dry Annealing of a PWR Nuclear Reactor Vessel," Section XI, Division 1, Code Cases: Nuclear Components, ASME Code Case N-557-1, *2010 ASME Boiler and Pressure Vessel Code*, American Society for Mechanical Engineers, 2010.
20. EPRI, *White Paper: Technical Basis for ASME Code Case N-557, In-Place Dry Annealing of a PWR Nuclear Reactor Vessel*, TR-106967, Electric Power Research Institute, December 1996.

Sect. 6.5

1. M. EricksonKirk et al., *Probabilistic Fracture Mechanics—Models, Parameters, and Uncertainty Treatment Used in FAVOR Version 04.1*, NUREG-1807, U.S. Nuclear Regulatory Commission, June 2007.

2. C. A. English, W. L. Server, and S. T. Rosinski, *Materials Reliability Program (MRP): Attenuation in U.S. RPV Steels (MRP-56)*, Technical Report 1006584, Electric Power Research Institute, 2002.
3. ASTM, "Standard Practice for Characterizing Neutron Exposure in Iron and Low Alloy Steels in Terms of Displacements Per Atom (DPA), E 706(ID)," ASTM Standard E693-01 (Reapproved 2007) *Annual Book of ASTM Standards*, Vol. 12.02, ASTM International, 2007.
4. R. E. Stoller and L.R. Greenwood, "An Evaluation of Through-Thickness Changes in Primary Damage Production in Commercial Reactor Pressure Vessels," in *Effects of Radiation on Materials: 20th Int. Symp.*, ASTM STP 1405, ed. S.T. Rosinski, M.L. Grossbeck, T.R. Allen, and A.S. Kumar, ASTM International, 2001.
5. NRC, *Radiation Embrittlement of Reactor Vessel Materials*, Regulatory Guide 1.99, Revision 2, U.S. Nuclear Regulatory Commission, May 1988.
6. E. D. Eason, G. R. Odette, R. K. Nanstad, and T. Yamamoto, "A physically-based correlation of irradiation-induced transition temperature shifts for RPV steels," *Journal of Nuclear Materials* **433** (1-3), 240–254 (2013).
7. E. D. Eason, G. R. Odette, R. K. Nanstad, and T. Yamamoto, *A Physically Based Correlation of Irradiation-Induced Transition Temperature Shifts for RPV Steels*, ORNL/TM-2006/530, Oak Ridge National Laboratory, 2007.
8. P. N. Randall, "Basis for Revision 2 of the U.S. Nuclear Regulatory Commission's Regulatory Guide 1.99," pp. 149–62 in *Radiation Embrittlement of Nuclear Reactor Pressure Vessel Steels: An International Review (Second Volume)*, ASTM STP 909, L. E. Steele (ed.), American Society for Testing and Materials, 1986.
9. I. Remec, *Study of the Neutron Flux and Dpa Attenuation in the Reactor Pressure-Vessel Wall*, ORNL/NRC/LTR-99/5, Oak Ridge National Laboratory, June 1999.
10. R. Gold and W.N. McElroy, "Radiation-Induced Embrittlement in Light Water Reactor Pressure Vessels," *Nuclear Engineering and Design* **104**, 155–174 (1987).
11. W. N. McElroy (ed.), *LWR Pressure Vessel Surveillance Dosimetry Improvement Program: PSF Experiments Summary and Blind Test Results*, NUREG/CR-3320, Vol. 1 (HEDL-TME 86-8), U.S. Nuclear Regulatory Commission, July 1986.
12. J. R. Hawthorne, *Gundremmingen RPV Materials Characterization, Annual Report for 1986*, NUREG/CR 3228, Vol. 2, Nuclear Regulatory Commission, July 1987.
13. C. Brillaud, Y. Grandjean, and S. Sallet, "Vessel Investigation Program of 'Chooz A' PWR Reactor After Shutdown," in *Effects of Radiation on Materials: 20th Int. Symp.*, ASTM STP 1405, ASTM International, 2001.
14. S. K. Iskander et al., *Preliminary Results from Charpy Impact Testing of Irradiated JPDR Weld Metal and Commissioning of a Facility for Machining of Irradiated Materials*, ORNL/NRC/LTR-99/23, Oak Ridge National Laboratory, September 1999.
15. W. L. Server et al., "Attenuation of Neutron Radiation Damage Through a Simulated RPV Wall," *Journal of ASTM International* **5**(1), (2008).

Sect. 6.6

1. G. R. Odette and G. E. Lucas, "Reactor Pressure Vessel Embrittlement: The Road Ahead," pp. 169–185 in *Proc. 27th Water Reactor Safety Information Meeting (October 25–27, 1999)*, NUREG/CP-0169, U.S. Nuclear Regulatory Commission, March 2000.

2. R. K. Nanstad et al., "Overview of Irradiation Effects on Fracture Toughness and Crack-Arrest Toughness of RPV Steels," pp. 187–208 in *Proc. 27th Water Reactor Safety Information Meeting (October 25–27, 1999)*, NUREG/CP-0169, U.S. Nuclear Regulatory Commission, March 2000.
3. Antonio Ballesteros, Wim Voorbraak, and Luigi Debarberis, "Dosimetry and Irradiation Programmes of AMES European Network," AMES Report No. 12, European Commission, DG-JRC, Joint Research Centre, Madrid, December 1997.
4. ORNL, *Proc. of the Research Assistance Task Force on Radiation Materials Science Applied to Reactor Pressure Vessel Embrittlement, September 20–22, 1999*, M99-105308, Oak Ridge National Laboratory.
5. L. M. Davies, W. L. Server, V. Lyssakov, and S. T. Rosinski, "Review of Current Recommendations from the Recent IAEA Specialists Meeting on Irradiation Effects on Reactor Pressure Vessel Steels and its Mitigation," pp. 3–7 in *Effects of Radiation on Materials: 20th Int. Symp.*, S. T. Rosinski, M. L. Grossbeck, T. R. Allen, and A. S. Kumar (eds.), ASTM STP 1405, ASTM International, 2001.
6. A. Ballesteros et al., *Proc. of the AMES Workshop on Reactor Pressure Vessel Life Predictions*, AMES Report No. 15, EUR 19638 EN, 2000.
7. Pierre Petrequin, *A Review of Formulas for Predicting Irradiation Embrittlement of Reactors Vessels Materials*, AMES Report No. 6, EUR 16455 EN, November 1996.
8. Takeo Onchi, "Japan's Regulatory R&D Activities on Life Time Management of Commercial Nuclear Power Reactors," *IGRDM-9 Workshop on Life Time of Nuclear Power Plants*, September 22, 2000.
9. Robert Gerard, "Belgian Approach to RPV Life Management—Research vs Legislation," *IGRDM-9 Workshop on Life Time of Nuclear Power Plants*, September 22, 2000.
10. Georges Bezdikian, "PWR Vessel Integrity Assessment & Life Management in French Nuclear Plants," *IGRDM-9 Workshop on Life Time of Nuclear Power Plants*, September 22, 2000.
11. R. D. Nicholson and R. H. Priest, "UK Regulatory and Utility Perspectives," *IGRDM-9 Workshop on Life Time of Nuclear Power Plants*, September 22, 2000.
12. IAEA, *Application of Surveillance Program Results to Reactor Pressure Vessel Assessment*, IAEA-TECDOC-1435, International Atomic Energy Agency, April 2005.
13. W. A. Van Der Sluys, J. G. Merkle, B. Young, and R. K. Nanstad, *Indexing Fracture Toughness Data, Part 1: Results from the MPC Cooperative Test Program on the Use of Pre-cracked Charpy Specimens for T_0 Determination*, WRC Bulletin 486, Welding Research Council, November 2003.
14. R. K. Nanstad, *Fracture Toughness Reference Temperature T_0 for HSSI Weld 72W*, ORNL/NRC/LTR-04/08, Oak Ridge National Laboratory, 2004.
15. R. K. Nanstad, D. E. McCabe, M. A. Sokolov, and J. G. Merkle, "Experimental Evaluation of Deformation and Constraint Characteristics in Pre-cracked Charpy and Other Three-point Bend Specimens," *Proc. of the ASME PVP2007 Conference*, Paper PVP200726651, American Society of Mechanical Engineers, July 2007.
16. R. K. Nanstad et al., "IAEA Coordinated Research Project on Master Curve Approach to Monitor Fracture Toughness of RPV Steels: Final Results of the Experimental Exercise to Support Constraint Effects," Paper PVP2009-78022, *Proc. of PVP 2009, ASME Pressure*

Vessel and Piping Division Conference, American Society of Mechanical Engineers, July 2009.

17. J. A. Joyce and R. L. Tregoning, "Determination of Constraint Limits for Cleavage Initiated Toughness Data," *Engineering Fracture Mechanics* **72**, 1559–1579 (2005).
18. H. J. Rathbun, G. R. Odette, T. Yamamoto, and G. E. Lucas, "Influence of statistical and constraint loss size effects on cleavage fracture toughness in the transition – a single variable experiment and database," *Engineering Fracture Mechanics* **73**, 134–158 (2006).
19. B. Wasiluk, J. Petti, and R. H. Dodds, Jr., "Constraint Differences Between C(T) and SE(B) for the Euro-material," presentation at ASTM E08.08.03 Meeting in Salt Lake City, Utah, May 2004.
20. Scibetta et al., "IAEA Coordinated Research Project on Master Curve Approach to Monitor Fracture Toughness of RPV Steels: Final Results of an Analytical Round Robin Exercise to Support Constraint Effects," Paper PVP2009-77722, *Proc. of PVP2009, July 26–30*, Prague, Czech Republic, American Society of Mechanical Engineers, 2009.
21. IAEA, *Guidelines for Application of the Master Curve Approach to Reactor Pressure Vessel Integrity*, Technical Reports Series No. 429, International Atomic Energy Agency, 2005.
22. M. A. Sokolov, D. E. McCabe, Y. A. Davidov, and R. K. Nanstad, "Use of Precracked Charpy and Smaller Specimens to Establish the Master Curve," pp. 238–252 in *Small Specimen Test Techniques*, ASTM STP 1329, W. R. Corwin and E. vanWalle (eds.), American Society for Testing and Materials, 1998.
23. K. Wallin, T. Planman, M. Valo, and R. Rintamaa, "Applicability of Miniature Size Bend Specimens to Determine the Master Curve Reference Temperature T_0 ," *Engineering Fracture Mechanics* **68**, 1265–1296 (2001).
24. ASTM, "Determination of Reference Temperature, T_0 , for Ferritic Steels in the Transition Range, E1921–02," *Annual Book of ASTM Standards*, Vol. 03.01, ASTM Standard E1921–13, ASTM International, 2013.
25. C. J. McMahon, Jr., V. Vitek, and J. Kameda, "Mechanics and Mechanisms of Intergranular Fracture," Chap. 4 in *Developments in Fracture Mechanics—2*, G. G. Chell (ed.), Applied Science Publishers, Englewood, N.J., 1981.
26. D. E. McCabe, *Initial Evaluation of the Heat-Affected Zone, Local Embrittlement Phenomenon as It Applies to Nuclear Reactors*, ORNL/NRC/LTR-99/10, Oak Ridge National Laboratory, September 1999.
27. R. J. McElroy, A. J. E. Foreman, G. Gage, W. J. Phythian, P. H. N. Ray, and I. A. Vatter, "Optimization of Reactor Pressure Vessel Surveillance Programmes and their Analysis," contribution to IAEA CRP 3 Research Program, AEA-RS-2426, December 1993.
28. R. K. Nanstad, D. E. McCabe, M. A. Sokolov, C. A. English, and S. R. Ortner, "Investigation of Temper Embrittlement in Reactor Pressure Vessel Steels Following Thermal Aging, Irradiation, and Thermal Annealing," *Effects of Radiation on Materials: 20th Int. Symp.*, ASTM STP 1405, S. T. Rosinski, M. L. Grossbeck, T. R. Allen, and A. S. Kumar (eds.), ASTM International, 2001.
29. E. Kantidis, B. Marini, and A. Pineau, "A Criterion for Intergranular Brittle Fracture of a Low Alloy Steel," *Fatigue and Fracture of Engineering Materials and Structures* **17** (6), 619–633 (1994).

30. O. M. L. Yahya et al., "Statistical Modelling of Intergranular Brittle Fracture in a Low Alloy Steel," *Fatigue and Fracture of Engineering Materials and Structures* **21**(12), 1485–1502 (1998).
31. R. K. Nanstad, M. A. Sokolov, and D. E. McCabe, "Applicability of the Fracture Toughness Master Curve to Irradiated Highly Embrittled Steel and Intergranular Fracture," *Journal of ASTM International* **5**(3), Paper JAI101346, 2008.
32. U. E. Kaun, and F. K. A. Koehring, "Investigation and Measures to Guarantee the Safety of a Pressurized Water Reactor's Pressure Vessel Against Brittle Fracture," pp. 127–148 in *Radiation Embrittlement of Nuclear Reactor Pressure Vessel Steels: An International Review* (Second Volume), ASTM STP 909, L. E. Steele (ed.), American Society for Testing and Materials, 1986.
33. M. A. Sokolov, R. K. Nanstad, and M. K. Miller, "Fracture Toughness Characterization of a Highly Embrittled RPV Weld," *Effects of Radiation on Material: 21st Int. Symp.*, ASTM STP 1447, M. L. Grossbeck (ed.), ASTM International, 2004.
34. B. S. Lee et al., "Master Curve Characterization of the Fracture Toughness in Unirradiated and Irradiated RPV Steels using Full- and 1/3-Size Pre-Cracked Charpy Specimens," *International Journal of Pressure Vessels and Piping* **77**, 599–604 (2000).
35. T. R. Leax, "Temperature Dependence and Variability of Fracture Toughness in the Transition Regime for A508 Grade 4N Pressure Vessel Steel," *Journal of ASTM International* (September 2005).
36. M. EricksonKirk, M. Wagenhofer, P. T. Williams, and S. Yin, "Accounting for Crack Propagation in a Model to Predict Fracture Toughness in Ferritic Steels," *Proc. of ASME 2009 Pressure Vessels and Piping Division Conf.*, PVP2009, Prague, Czech Republic, July 2009.
37. S. Ortner, "Factors Affecting the Shape of the Ductile-to-Brittle Transition," *International Journal of Pressure Vessels and Piping* **79**, 693–700 (2002).
38. G. R. Odette, and M. Y. He, "Micromechanical modeling of Master Curve temperature shifts due to constraint loss," *Journal of Nuclear Materials* **307-311**, 1624–1628 (2002).
39. M. Kirk and M. Mitchell, "Potential Roles for the Master Curve in Regulatory Application," *International Journal of Pressure Vessels and Piping* **78**, 111–123 (2001).
40. K. Wallin, "Loading Rate Effect on the Master Curve T_0 ," Paper IIW-X-1403-97, VTT Manufacturing Technology, Espoo, Finland, August 1997.
41. J. A. Joyce, "On the Utilization of High-Rate Pre-Cracked Charpy Test Results and the Master Curve to Obtain Accurate Lower Bound Toughness Predictions in the Ductile-To-Brittle Transition." *Small Specimen Test Techniques*, ASTM STP 1329, W. Corwin, S. Rosinski, and E. VanWalle (eds.), American Society for Testing and Materials, 1997.
42. K. Wallin, and R. Rintamaa, "Master Curve Based Correlation Between Static Initiation Toughness K_{Ic} and Crack Arrest Toughness K_{Ia} ," *Proc. of 24th MPA Seminar, Stuttgart, October 8–9, 1998*.
43. S. K. Iskander, W. R. Corwin, and R. K. Nanstad, "Effects of Irradiation on Crack-Arrest Toughness of Two High-Copper Welds," pp. 251–269 in *Effects of Radiation on Materials: 15th Int. Symp.*, ASTM STP 1125, R. E. Stoller, A. S. Kumar, and D. S. Gelles (eds.), American Society for Testing and Materials, 1992.

44. S. K. Iskander, W. R. Corwin, and R. K. Nanstad, *Crack-Arrest Tests on Two Irradiated High-Copper Welds, Phase II: Results of Duplex-Type Experiments*, NUREG/CR-6139 (ORNL/TM-12513), Oak Ridge National Laboratory, 1994.
45. Randy K. Nanstad, B. Richard Bass, John G. Merkle, Claud E. Pugh, Thomas M. Rosseel, and Mikhail A. Sokolov, "Heavy-Section Steel Technology and Irradiation Programs-Retrospective and Prospective Views," *Journal of Pressure Vessel Technology* **132** (December 2010), 064001-1 to 064001-20.
46. M. T. Kirk, M. E. Natishan, and M. Wagenhofer, "A Physics-Based Model for the Crack Arrest Toughness of Ferritic Steels," *Fatigue and Fracture Mechanics, 33rd Volume*, ASTM STP-1417, W. G. Reuter and R. S. Piascik (eds.), ASTM International, 2002.
47. M. EricksonKirk and M. EricksonKirk, "An Upper-Shelf Fracture Toughness Master Curve for Ferritic Steels," *International Journal of Pressure Vessels and Piping* **83** (8), 571–583 (2006).
48. M. EricksonKirk and M. EricksonKirk, "The Relationship Between the Transition and Upper Shelf Fracture Toughness of Ferritic Steels," *Fatigue and Fracture of Engineering Materials and Structures* **29**, 627–687 (2006).
49. M. T. EricksonKirk and M. A. EricksonKirk, "Use of a Unified Model for the Fracture Toughness of Ferritic Steels in the Transition and on the Upper Shelf in Fitness-For-Service Assessment and in the Design of Fracture Toughness Experiments," *Proc. of PVP2006-ICPVT-11: 2006 ASME Pressure Vessels and Piping Division Conference, July 23–27, 2006, Vancouver BC, Canada*, PVP2006-ICPVT11-93652, American Society of Mechanical Engineers.
50. M. T. EricksonKirk et al., *Technical Basis for Revision of the Pressurized Thermal Shock (PTS) Screening Limits in the PTS Rule (10 CFR 50.61): Summary Report*, NUREG-1806, U.S. Nuclear Regulatory Commission, August 2007, <http://www.nrc.gov/reading-rm/doc-collections/nuregs/staff/sr1806/>.
51. M. EricksonKirk, B. R. Bass, T. Dickson, C. Pugh, T. Santos, and P. Williams, *Probabilistic Fracture Mechanics—Models, Parameters, Uncertainty Treatment Used in FAVOR Version 04.1*, NUREG-1807, U.S. Nuclear Regulatory Commission, June 2007, <http://www.nrc.gov/reading-rm/doc-collections/nuregs/staff/sr1807/>.
52. *U.S. Code of Federal Regulations*, "Fracture Toughness Requirements for Protection Against Pressurized Thermal Shock Events," Part 50.61a, Title 10, "Energy," adopted on February 3, 2010, <http://www.nrc.gov/reading-rm/doc-collections/cfr/part050/part050-0061a.html>. Also see *Federal Register* **75** (1), 13–29 (Jan. 4, 2010).

Sect. 6.7

1. *U.S. Code of Federal Regulations*, "Appendix G, Fracture Toughness," Part 50, Title 10, "Energy," January 2011.
2. ASTM, "Standard Practice for Design of Surveillance Programs for Light-Water Moderated Nuclear Power Reactor Vessels," ASTM Designation E-185-02, *Annual Book of ASTM Standards*, Vol. 12.01, ASTM International, approved June 10, 2002.
3. *Federal Register* **36**(129), 12697–127003 (July 1971).
4. *Federal Register* **38**(136), 19012–1901617 (July 1973).
5. *U.S. Code of Federal Regulations*, "Appendix H, Reactor Vessel Material Surveillance Program Requirements," Part 50, Title 10, "Energy," January 2011.

6. K. Cho and C. Kang, "Radiation Streaming in KNU-1 Reactor Cavity," *Journal of the Korean Nuclear Society* **18**(1) (March 1986).
7. F. J. Rahn et al., "Standards for Dosimetry Beyond the Core," pp. 137–145 in *Neutron Standards and Applications, Proc. Int. Specialists Symp. on Neutron Standards and Applications, March 28–31, 1977*, C. D. Bowman, A. D. Carlson, H. O. Liskien, and L. Stewart (eds.), Gaithersburg, Maryland.

7. DISCUSSION OF PIRT EVALUATIONS AND SUMMARY RECOMMENDATIONS

Chapters 2 through 6 of this volume focus on the existing knowledge gaps in the degradation modes encountered by the various materials that comprise the reactor pressure vessel. Using Version 2 of the updated Materials Degradation Matrix (MDM) and the Issue Management Tables (IMTs) [1–3], the panelists developed Table 1.3, which lists possible degradation modes for the materials used in BWRs and PWRs, combines those into one RPV table, and simplifies stress corrosion cracking (SCC) and fatigue into single degradation modes. By integrating the knowledge gaps identified in the IMTs, Table 1.4 links with Table 1.3 to describe in Chapters 2 through 6 the key elements of concern for the RPVs. Each of the degradation modes is further broken down into subsets within the chapters and in the Phenomena Identification and Ranking Table (PIRT) process.

The materials include (1) carbon and low alloy steels (C&LAS) base metal and welds, (2) stainless steel base metal and welds and clad, (3) nickel alloy base metal (A600), (4) high chromium, nickel alloy base metal (A690), (5) nickel alloy weld and clad (A82/A182), and (6) high chromium, nickel alloy weld and clad (A52/A152). The degradation modes evaluated include stress corrosion cracking (SCC), fatigue, reduction in fracture properties, and irradiation embrittlement.

Moreover, the IMTs provide detailed information related to RPV subcomponents. Those details have been extracted from the IMTs, rearranged, and summarized in Appendices A (for BWRs) and B (for PWRs). The specifics of the subcomponents provide a detailed resource for the reader to determine a specific location where a mechanism may be important, but generally will not be covered in the individual discussions of the degradation mechanisms.

As noted in Appendix D, the panelists used the PIRT process (Figure 7.1) to prioritize the different materials, subcomponents, degradation phenomena, and mechanisms (Figure 7.2, Tables 7.1 and 7.2, Figure 7.3, and Table 7.3). There are several notable trends observed for PWRs and BWRs. The highest susceptibilities at extended lifetimes for PWRs and BWRs are embrittlement of C&LAS base metal and welds; however, the knowledge of the phenomena and mechanism as well as the confidence in that assessment were ranked from high to very high, indicating that significant progress has been made in understanding embrittlement. However, as addressed in Chapter 6, Neutron Embrittlement, of this report, significant issues and uncertainties remain. Moreover, while there may be mechanistic understanding of the underlying causes, confirmation for extended service and research into mitigation or detection technologies may also be warranted.

Similarly, PWR susceptibility to SCC via intergranular and transgranular (IG/TG) mechanisms of Ni-alloy A600 base metal (used in B&W bottom mounted nozzles and repair pieces) and Ni-alloy A82/A182 welds and base metals [used in DM welds for inlet and outlet nozzles, core flood nozzle (B&W), safety injection nozzles (WEC), bottom mounted nozzles, and repair pieces] were judged to be high. Moreover, the knowledge of the phenomena and mechanism as well as the confidence in that assessment were also ranked very high. Likewise, BWR susceptibility to SCC via IG/TG mechanisms of wrought, forged and HAZ stainless steel and Ni-alloy A82/A182 welds and clad (used in CRD return line nozzle cap, CRD stub tube, CRD housing tube, instrument penetrations, etc.) were ranked high. Additionally, the knowledge of the phenomena and mechanism were ranked as very high and the confidence in that assessment high.

Discussions of these issues are addressed in Chapter 4, Long-Term Integrity of Dissimilar Metal Welds.

The PIRT analysis identified that fatigue for SS welds and clads, Ni-alloy A600 and A690 base metal and welds and clad (A82/182), via low-cycle (LC) environmentally assisted (Env) mechanisms in PWRs were ranked as having very low susceptibilities, low knowledge, and low confidence at extended lifetimes. By contrast, the knowledge ranking for these phenomena were higher for BWRs. The primary uncertainty among the panelists was identified as the fatigue load; the higher the fatigue load, the greater is the susceptibility. Discussions of these issues are addressed in Chapter 5, Environmentally Assisted Fatigue.

The only additional low-susceptibility, low-knowledge, low-confidence issue is SCC due to pitting in PWR, SS upper-shell flange clads. The consensus is that although this is unlikely to be an issue, if crevices exist, the susceptibility might increase to a score of 2. A discussion of SCC in SS welds due to pitting is addressed in Chapter 4, Long-Term Integrity of Dissimilar Metal Welds.

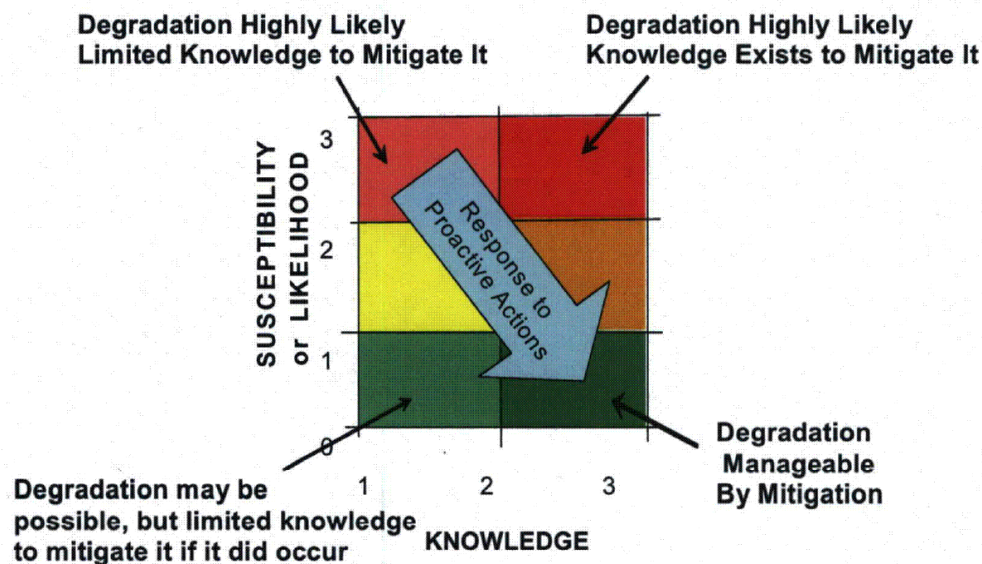


Figure 7.1. PIRT process schematic illustrating the combinations of “damage susceptibility” and “knowledge” scores suggesting various life-management responses [4]. Key to scores: 1, low; 2, medium; 3, high.

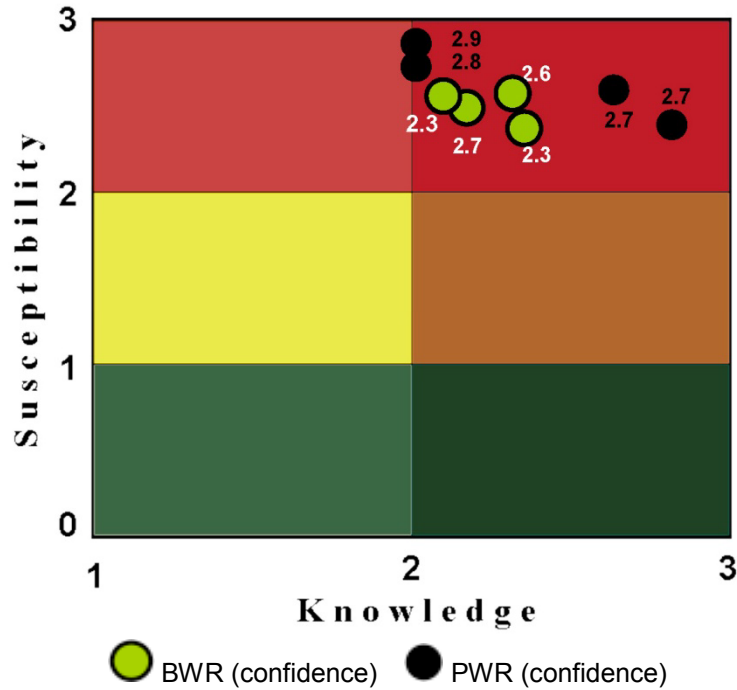


Figure 7.2. Rainbow chart showing sensitivity, high knowledge, and high confidence for PWRs and BWRs.

Table 7.1. PWR: High sensitivity, high knowledge, and high confidence

Material	Phenomena	Sub-Components	Mechanism	S	K	C
C&LAS base metal	Irradiation effects	Nozzle, intermediate, & lower shell courses; inlet and outlet nozzles	Emb.	2.9	2.1	2.9
C&LAS welds and clad	Irradiation effects	Nozzle course welds, inlet and outlet nozzle welds	Emb.	2.8	2.1	2.8
Ni-alloy base (A600)	SCC	Bottom mounted nozzles & repair pieces (B&W)	IG/TG	2.3	2.8	2.7
Ni-alloy W&C (A82/182)	SCC	DM welds for: inlet and outlet nozzles, core flood nozzle (B&W), safety injection nozzle (W), bottom mounted nozzles, repair pieces	IG/TG	2.6	2.6	2.8

Table 7.2. BWR: High sensitivity, high knowledge, and high confidence

Material	Phenomena	Sub-Components	Mechanism	S	K	C
C&LAS base metal	Irradiation effects	All vessel shells, LPCI nozzles, CRD return line, recirculation inlet and outlet nozzles, instrument penetrations	Emb.	2.7	2.4	2.6
C&LAS welds and HAZ	Irradiation effects	Welds of: All vessel shells, LPCI nozzles, CRD return line, recirculation inlet and outlet nozzles, instrument penetrations	Emb.	2.6	2.2	2.7
SS: Wrought, forged, and HAZ	SCC	CRD stub tube, housing tube, flange and cap; SLC housing, in-core housing and flange, instrument penetrations, jet pump riser brace pad and core spray pipe bracket, steam dryer support bracket, feedwater sparger support bracket, surveillance capsule bracket, guide rod bracket	IG/TG	2.4	2.4	2.3
Ni-alloy welds (A82/182)	SCC	CRD return line nozzle cap, CRD stub tube, CRD housing tube, SLC housing, SLC stub tube, in-core housing and flange, instrument penetrations, core spray pipe bracket attachment, shroud support pad, steam dryer support bracket, feedwater sparger support bracket, surveillance capsule holder bracket, guide rod bracket	IG/TG	2.7	2.2	2.2

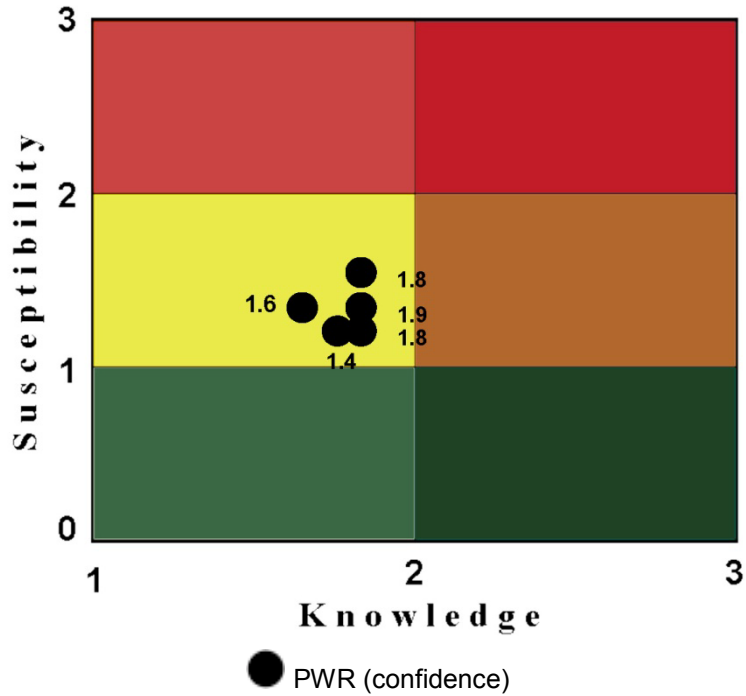


Figure 7.3. Rainbow chart showing low sensitivity, low knowledge, and low confidence for PWRs.

Table 7.3. PWR: Low sensitivity, low knowledge, and low confidence

Material	Phenomena	Sub-Components	Mechanism	S	K	C
SS welds and clad	SCC	Upper shell flange clad	Pitting	1.3	1.7	1.4
SS welds and clad	Fatigue	SS clad on all vessel courses, bottom head, inlet and outlet nozzles	LC-Env.	1.4	1.8	1.9
Ni-alloy base (A600)	Fatigue	Bottom mounted nozzles and repair pieces (B&W)	LC-Env.	1.4	1.6	1.6
Ni-alloy base (A690)	Fatigue	Bottom mounted nozzles and repair pieces (B&W)	LC-Env.	1.6	1.8	1.8
Ni-alloy welds and clad (A82/182)	Fatigue	Attachment weld of core guide lugs, flow baffles (CE), DM welds of: inlet and outlet nozzles, core flood nozzle (B&W), safety injection nozzles (W), bottom mounted nozzles; repair pieces for attachment weld (B&W)	LC-Env.	1.3	1.8	1.8

7.1 REFERENCES*

1. EPRI, *Primary System Corrosion Research Program: EPRI Materials Degradation Matrix, Revision 2*, Technical Report 1020987, Electric Power Research Institute, 2010.
2. EPRI, *BWR Vessel and Internals Project: Boiling Water Reactor Issue Management Tables, BWRVIP-167NP, Revision 2*, Technical Report 1020995, Electric Power Research Institute, 2010.
3. EPRI, *Materials Reliability Program: Pressurized Water Reactor Issue Management Tables, Revision 2*, MRP-205, Technical Report 1021024, Electric Power Research Institute, 2010.
4. NRC, *Expert Panel Report on Proactive Materials Degradation Assessment*, NUREG/CR-6923, U.S. Nuclear Regulatory Commission, February 2007, p. 42.

* Inclusion of references in this report does not necessarily constitute NRC approval or agreement with the referenced information.

8. RECOMMENDATIONS AND CONCLUSIONS

Scoring was completed and compiled for 54 distinct categories of material/degradation issues related to the RPV. There were several notable trends observed for PWRs and BWRs. The highest susceptibilities at extended lifetimes for PWRs and BWRs are embrittlement of carbon and low-alloy steel base metal and welds; however, the knowledge of the phenomena and mechanism as well as the confidence in that assessment were ranked from high to very high, indicating that significant progress has been made in understanding embrittlement. However, as addressed in Chapter 6, which addresses neutron embrittlement, significant issues and uncertainties remain. Moreover, while there may be mechanistic understanding of the underlying causes, confirmation for extended service and research into mitigation or detection technologies may also be warranted. These knowledge gaps and areas of uncertainty are listed below.

8.1 ENVIRONMENTAL EFFECTS ON FRACTURE RESISTANCE

Although degradation of RPV materials due to environmental effects is considered unlikely, hydrogen embrittlement could lead to a reduction of fracture resistance of RPV materials. Based on very limited data, this mechanism should not present a concern for LWRs under normal operating conditions. However, if future relevant test data and extended operating experience indicate that 60 year operation of RPVs could cause hydrogen buildup, then an assessment of hydrogen buildup and the development of subsequent mitigation procedures for 80 year operation may be needed. Based on the current data available, a hydrogen level of 4 ppm and higher in the RPV material could become a contributor to the overall degradation in fracture resistance of the RPV.

8.2 THERMAL EMBRITTLEMENT OF RPV STEELS

It has been observed that the HAZs of higher-temperature low-alloy steel (LAS) components are prone to thermal aging, with the pressurizer experiencing the highest temperature. It typically operates at 343 °C (650 °F) and could undergo a significant shift in HAZ ductile-brittle transition temperature (DBTT) (rivaling the RPV irradiation embrittlement shift). For that reason, the pressurizer, if fabricated from LAS, and portions of the RPV, that operate at high temperature, could be prone to thermal aging and have significant stresses. The RPV components that reach higher temperatures [315 °C (~600 °F)] consist of the RPV flange, the nozzle shell ring, and the outlet nozzles of all plants as well as the vessel heads of some reactors which have head temperatures near the hot leg temperature of about 315 °C (~600 °F). However, many of the RPV heads of the U.S. plants, including the heads in all hot head plants, have been replaced thereby resetting the aging. The nozzle shell ring and outlet nozzles receive a low neutron dose rate exposure, which could synergistically combine with thermal aging, potentially creating greater-than-expected embrittlement. That region, known as the extended beltline, is undergoing pressure-temperature curve evaluation by the Pressurized Water Reactor Owners Group (PWROG); however, thermal aging shift in DBTT is not currently considered in the PWROG evaluation.

Several opportunities to better understand the effects of thermal aging exist. Combustion Engineering pressurizers, fabricated with materials similar to RPV materials and operated at about 343 °C (650 °F), have been retired at Saint Lucie 1 (Fall 2005), Millstone 2 (Fall 2006),

and Fort Calhoun (Fall 2006) and may be available for examination. Because the pressurizer is the reactor coolant system (RCS) pressure boundary component that reaches the highest temperature, any thermal-aging embrittlement seen would provide a leading indicator for the rest of the RCS. Moreover, even without baseline properties, relatively high DBTT, evidence of grain boundary P segregation, and intergranular fracture indicating thermal aging could be determined using the retired pressurizer material. Examination of LAS pressurizer HAZs would provide information on the extent of the long-term embrittlement of a component that has experienced reactor operation. This information could be used to determine if there is a need to address thermal aging embrittlement for operation up to 80 years.

Over the last 20 years, a number of steam generators have been replaced. The bottom heads of Westinghouse designed steam generators were fabricated from SA-508 forgings, the same type as the RPV. Moreover, the same bottom head bowl forging has a cold leg and a hot leg nozzle welded to it. For that reason, retired steam generator bottom bowl nozzle HAZs could be examined with the properties and microstructure of the cold leg side (where no thermal ageing is expected) compared to the hot leg side (where thermal aging is possible). The HAZ of the same material could also be evaluated for evidence of long-term thermal aging.

Within the PWROG research program, a 300,000 h thermal aging exposure of the Arkansas Nuclear One-Unit 1 RPV head is projected to be reached in 2017. Although the aging temperature is relatively low, the material has an exceptionally long aging time and the mechanical properties and microstructure have been well documented, making it a unique candidate for evaluation. The panel recommended that some of these materials be tested to assess any changes in the transition temperature, HAZ microhardness, and microstructure.

8.3 LONG-TERM INTEGRITY OF DISSIMILAR METAL WELDS

Unless data from the initial 40-year operating period and the first license renewal indicate that the SCC factors are insignificant, the following issues need to be considered as part of the evaluation of whether the operating time can be extended to 80 years:

- Effect of long-term thermal aging on the susceptibility of Alloy 82 weld metals to SCC
- Effect of long-term operation on the susceptibility of Alloy 152 and 52 weld metals to SCC
- Effect of alloying elements and the compounds formed during heat treatment on the susceptibility of LASs to SCC under BWR conditions
- Validity of the crack growth data for LAS and in the SCC disposition curves
- Crack behavior at the fusion weld line between Ni alloy weld metal and LAS
- Effect of neutron irradiation on the susceptibility of LAS to SCC

8.4 ENVIRONMENTAL ASSISTED FATIGUE

Fatigue issues for the RPV generally are insignificant and seldom as important as the associated piping connected to the RPV. Fatigue in water environments at regions where cumulative usage factor (CUF) values are projected to be significant at 80 years of operation may require monitoring or assessment. The panel felt that the development of the relationship

between laboratory test data under conditions simulating reactor operating stresses and loading sequences is needed to improve confidence that environmental fatigue does not become a significant factor for long term operation.

8.5 NEUTRON EMBRITTLEMENT

A summary of the extensive recommendations provided by the expert panel is listed below by topic.

- *Flux effects at high neutron fluence recommendations:* Although high-fluence surveillance data may eventually provide a sufficient basis for timely informed decisions regarding extended operation for PWRs expected to reach very high fluences, developing a significant database on high-fluence effects from test reactor (TR) data provides a useful complement to the surveillance transition temperature shift (TTS) data. Currently, the Eason, Odette, Nanstad, and Yamamoto (EONY) model has been incorporated into 10 CFR, Part 50.61a for limited applications. The use of accelerated, higher-flux TR data ultimately requires improved understanding and modeling of flux effects because high-flux irradiation may result in artifacts in TTS that would not be encountered in low-flux (e.g., power reactor) irradiations. Therefore, systematic and objective research on flux effects on TTS at intermediate and high fluence is recommended to resolve uncertainties. Simultaneously, efforts to obtain surveillance specimens from very high fluence irradiations (e.g., the Palisades vessel at a relatively high lead factor, and high-Ni weld specimens from Swedish power reactors) should continue.
- *High-nickel effects and other potential high-fluence embrittlement mechanisms recommendations:* Because LBPs may result in significantly increased embrittlement not predicted by current embrittlement models, additional research is recommended to determine: (1) the conditions leading to the formation of LBP; and, (2) the severity of the corresponding embrittlement. Other contributors to hardening, especially self-interstitial atom cluster dislocation loops, may also be important at high fluence.
- *Thermal annealing and reirradiation recommendations:* To better understand the effects of annealing, material characterization, and modeling, data is needed and includes high dose rate experiments, post-annealing reirradiation, microstructural characterization of reirradiation effects, temper embrittlement of HAZ, and characterization from reirradiated surveillance programs.
- *Attenuation of embrittlement recommendations:* (1) If generic approaches to attenuation are to be used, it is recommended they be improved relative to the approach used in Revision 2 of Regulatory Guide 1.99. Further, assessment of the uncertainties in predicted TTS associated with generic methods is recommended. (2) The issues raised regarding the use of a generic attenuation procedure argue for use of plant-specific approaches to attenuation. Vessel-specific approaches based on computed dpa and dpa rates converted to effective fluence and flux for use in TTS models would not be difficult to implement because the required neutronics calculations are generally available. (3) Assembling a catalogue of experimental studies pertinent to the issue of attenuation, and compiling a corresponding database that can be systematically analyzed using the outlined procedures are recommended as a very high priority.

- *Master Curve fracture toughness recommendations:* The most significant issue impeding more comprehensive use of the Master Curve in RPV embrittlement monitoring and structural integrity analysis is the effect of specimen size on T_0 . In particular, it is important to establish how T_0 values measured using Charpy-sized specimens can be used to reliably predict the transition behavior of much larger structures.
- *Embrittlement beyond the beltline recommendations:* Assuming that the current definition of beltline based on a fluence limit continues to be accepted, the physical extent of the “beltline” implied by this fluence limit will be expanded during operation for up to 80 years to include regions of the RPV where there are nozzle penetrations and shell thickness transitions. This will require: (1) an evaluation of the extended beltline materials that exceed the 1×10^{17} n/cm² fluence and the development of a better understanding of the properties of these relatively under-characterized materials; (2) the inclusion of representative material of the extended beltline in surveillance programs; (3) an assessment of thermal embrittlement in the hot leg nozzle HAZs since there may be a synergistic effect with low flux irradiation; and (4) an assessment of the albedo effect, in which neutrons that pass through the RPV wall reflect off the concrete and stream up through the cavity to the nozzle area. Since the fluence on the outside of the nozzles and RPV can be as high as or higher than the fluence on the inside of the RPV in that region, accurately modeling the fluence in the various areas around the nozzles/extended beltline becomes more important.

APPENDIX A

BWR VESSEL BREAKDOWN FROM IMTs

Reactor Pressure Vessel (RPV) (EPMDA)

**Appendix A
BWR Vessel Breakdown from IMTs**

Degradation Mechanism	Component & ID No.	Material	Conseq. of Failure	Mitigation	Repair/Replace	Gaps
Stress Corrosion Cracking: Intergranular/Transgranular	1.1-1 Top Head and Flange	C&LAS (SA-533, Gr B, Cl 1; SA-508 Cl 2)	A, B	Water Chemistry BWRVIP-190 BWRVIP-225	ASME Sect. XI IWA-4000	B-DM-06 B-DM-07 B-AS-07
	1.1-2 Vessel Flange	C&LAS (SA-336 or SA-508, Cl 2)	A, B	Water Chemistry BWRVIP-190 BWRVIP-225	ASME Sect. XI IWA-4000	B-DM-06 B-DM-07 B-AS-07
	1.1-3 Upper Intermediate (Nozzle), Beltline, and Lower Shells	C&LAS (A-302, Gr B or SA-533, Gr B, Cl 1) SS Clad ⁽¹⁾	A, B, G	Water Chemistry BWRVIP-190 BWRVIP-225 HWC Technology BWRVIP-62 BWRVIP-156 BWRVIP-159 BWRVIP-219	ASME Sect. XI IWA-4000	B-DM-06 B-DM-07 B-DM-08 B-AS-05 B-AS-07 B-AS-11 B-AS-30
	1.1-4 Bottom Head	C&LAS (A-302, Gr B or SA-533, Gr B, Cl 1) SS Clad ⁽¹⁾	A, B, G	Water Chemistry BWRVIP-190 BWRVIP-225 HWC Technology BWRVIP-62 BWRVIP-156 BWRVIP-159 BWRVIP-219	ASME Sect. XI IWA-4000	B-RG-08 B-DM-06 B-DM-07 B-AS-07
	1.2-1 Closure Head Studs, Washers, Nuts	C&LAS (SA-193, Gr B16, or SA-540, Gr B23 or B24)	A	Bolting Integrity EPRI 1018959 EPRI NP-5769 NUREG-1339 NUREG-1801 Reg. Guide 1.65	ASME Sect. XI IWA-4000	B-DM-06

Degradation Mechanism	Component & ID No.	Material	Conseq. of Failure	Mitigation	Repair/Replace	Gaps
	1.2-2 Top of Head Flange Bolts	C&LAS (SA-793)	A	Bolting Integrity EPRI 1018959 EPRI NP-5769 NUREG-1339 NUREG-1801	ASME Sect. XI IWA-4000	B-DM-06
	1.3-1 Top Head Nozzle (Head Spray and Vent)	C&LAS (SA-508, C/2)	A	Water Chemistry BWRVIP-190 BWRVIP-225	ASME Sect. XI IWA-4000	B-DM-06 B-DM-07 B-AS-07
	1.3-2 Main Steam Nozzles and Safe Ends	C&LAS (SA-508, C/2)	A	Water Chemistry BWRVIP-190 BWRVIP-225	ASME Sect. XI IWA-4000	B-DM-06 B-DM-07 B-AS-07
	1.3-3 Feedwater Nozzles	C&LAS (SA-508, C/2)	A	Water Chemistry BWRVIP-190 BWRVIP-225 Oper. Changes GE-NE-523-A71-0594 (Low Flow Controller Oper.)	ASME Sect. XI IWA-4000	B-DM-06 B-DM-07 B-AS-07
	1.3-4 Feedwater Nozzle Safe Ends	C&LAS (SA-508, C/1, CS)	A	Water Chemistry BWRVIP-190 BWRVIP-225 Oper. Changes GE-NE-523-A71-0594 (Low Flow Controller Oper.)	ASME Sect. XI IWA-4000	B-DM-06 B-DM-07

Degradation Mechanism	Component & ID No.	Material	Conseq. of Failure	Mitigation	Repair/Replace	Gaps
	1.3-5 Feedwater Nozzle Safe Ends	Ni-Alloy (Some safe ends – A600 with A82/A182 welds)	A	Water Chemistry BWRVIP-190 BWRVIP-225 HWC Technology BWRVIP-62 BWRVIP-156 BWRVIP-159 BWRVIP-219 Oper. Changes GE-NE-523-A71- 0594 (Low Flow Controller Oper.) Stress Improvement BWRVIP-61 (Weld Overlay, IHSI, MSIP)	ASME Sect. XI IWA-4000 Weld Overlay CC-N-504-2 (Vendor Controlled)	B-DM-03 B-DM-06 B-DM-09 B-DM-10 B-AS-07 B-AS-27
	1.3-6 Core Spray Nozzles	C&LAS (SA-508, Cl 2)	A	Water Chemistry BWRVIP-190 BWRVIP-225	ASME Sect. XI IWA-4000	B-DM-06 B-DM-07 B-AS-07
	1.3-7 Core Spray Nozzle Safe Ends	C&LAS (Carbon Steel)	A	Water Chemistry BWRVIP-190 BWRVIP-225	ASME Sect. XI IWA-4000	B-DM-06 B-DM-07 B-AS-07
	1.3-8 Core Spray Nozzle Safe Ends	SS (incl. SS welds)	A	Water Chemistry BWRVIP-190 BWRVIP-225 (Not mitigated by HWC/NMCA/OLNC) Stress Improvement BWRVIP-61 (Weld Overlay, IHSI, MSIP)	ASME Sect. XI IWA-4000 Weld Overlay CC-N-504-2 (Vendor Controlled)	B-DM-03 B-DM-06 B-DM-09 B-DM-10 B-AS-07 B-AS-27 B-MT-01 B-MT-02

Degradation Mechanism	Component & ID No.	Material	Conseq. of Failure	Mitigation	Repair/Replace	Gaps
	1.3-9 Core Spray Nozzle Safe Ends	Ni-Alloy (A600 with A82/A182 welds)	A	Water Chemistry BWRVIP-190 BWRVIP-225 (Not mitigated by HWC/MMCA/OLNG) Stress Improvement BWRVIP-61 (Weld Overlay, HSI, MSIP)	ASME Sect. XI IWA-4000 Weld Overlay CC-N-504-2 (Vendor Controlled)	B-DM-03 B-DM-06 B-DM-09 B-DM-10 B-AS-07 B-AS-27 B-MT-01
	1.3-10 LPCI Nozzles	C&LAS (SA-508, C/2)	A	Water Chemistry BWRVIP-190 BWRVIP-225	ASME Sect. XI IWA-4000	B-DM-06 B-DM-07 B-AS-05 B-AS-07
	1.3-12 LPCI Nozzle Safe Ends (BWR/5)	Ni-Alloy (A600 with A82/A182 welds)	A	Water Chemistry BWRVIP-190 BWRVIP-225 (Not mitigated by HWC/MMCA/OLNG) Stress Improvement BWRVIP-61 (Weld Overlay, HSI, MSIP)	ASME Sect. XI IWA-4000 Weld Overlay CC-N-504-2 (Vendor Controlled)	B-DM-03 B-DM-06 B-DM-09 B-DM-10 B-AS-07 B-AS-27 B-MT-01
	1.3-13 CRD Return Line Nozzle (Only BWR/2 not capped or flanged)	C&LAS (SA-508, C/2)	A	Water Chemistry BWRVIP-190 BWRVIP-225	ASME Sect. XI IWA-4000	B-DM-06 B-DM-07 B-AS-05 B-AS-07
	1.3-14 CRD Return Line Nozzle Cap (BWR/3-6)	Ni-Alloy (A600 with A82/A182 welds)	A	Water Chemistry BWRVIP-190 BWRVIP-225 (Not mitigated by HWC/MMCA/OLNG)	ASME Sect. XI IWA-4000	B-DM-03 B-DM-06 B-DM-09 B-AS-07 B-AS-27 B-MT-01

Degradation Mechanism	Component & ID No.	Material	Conseq. of Failure	Mitigation	Repair/Replace	Gaps
	1.3-15 Recirculation Inlet and Outlet Nozzles	C&LAS (SA-508, Cl 2)	A, G	Water Chemistry BWRVIP-190 BWRVIP-225	ASME Sect. XI IWA-4000	B-DM-06 B-DM-07 B-AS-05 B-AS-07
	1.3-16 Recirculation inlet and Outlet Nozzle Safe Ends	SS (304, 316, 316L, 316NG & incl. SS welds) Ni-Alloy (A82/A182 welds)	A, G	Water Chemistry BWRVIP-190 BWRVIP-225 HWC Technology BWRVIP-62 BWRVIP-156 BWRVIP-159 BWRVIP-219 Stress Improvement BWRVIP-61 (Weld Overlay, HSI, MSIP)	ASME Sect. XI IWA-4000 Weld Overlay CC-N-504-2 (Vendor Controlled)	B-DM-03 B-DM-06 B-DM-09 B-DM-10 B-AS-07 B-AS-27 B-MT-02
	1.4-1 CRD Stub Tube	Ni-Alloy (A600 with A82/A182 welds)	A, G	Water Chemistry BWRVIP-190 BWRVIP-225 HWC Technology BWRVIP-62 BWRVIP-156 BWRVIP-159 BWRVIP-219	ASME Sect. XI IWA-4000 CC-N-730 EPRI BWRVIP BWRVIP-55-A BWRVIP-58-A BWRVIP- 146NP(R1)	B-DM-03 B-DM-06 B-DM-09 B-AS-07 B-AS-27 B-MT-04 B-MT-05
	1.4-2 CRD Stub Tube	SS (304 typ., furnace sensitized)	A, G	Water Chemistry BWRVIP-190 BWRVIP-225 HWC Technology BWRVIP-62 BWRVIP-156 BWRVIP-159 BWRVIP-219	ASME Sect. XI IWA-4000 CC-N-730 EPRI BWRVIP BWRVIP-55-A BWRVIP-58-A BWRVIP- 146NP(R1)	B-DM-03 B-DM-06 B-DM-09 B-AS-07 B-AS-27 B-MT-02 B-MT-04 B-MT-05

Degradation Mechanism	Component & ID No.	Material	Conseq. of Failure	Mitigation	Repair/Replace	Gaps
	1.4-3 CRD Housing Tube, Flange & Cap	SS (304 typ., 304L, 316L)	A, G	Water Chemistry BWRVIP-190 BWRVIP-225 HWC Technology BWRVIP-62 BWRVIP-156 BWRVIP-159 BWRVIP-219	ASME Sect. XI IWA-4000 CC-N-730 EPRI BWRVIP BWRVIP-55-A BWRVIP-58-A BWRVIP- 146NP(R1)	B-DM-06 B-DM-09 B-MT-02 B-MT-04 B-MT-05
	1.4-4 CRD Housing Tube (<i>Straight-thru design- middle tube</i>)	Ni-Alloy (A600 with A82/A182 welds)	A, G	Water Chemistry BWRVIP-190 BWRVIP-225 HWC Technology BWRVIP-62 BWRVIP-156 BWRVIP-159 BWRVIP-219	ASME Sect. XI IWA-4000 CC-N-730 EPRI BWRVIP BWRVIP-55-A BWRVIP-58-A BWRVIP- 146NP(R1)	B-DM-03 B-DM-06 B-DM-09 B-AS-27 B-MT-04 B-MT-05
	1.4-5 CRD Housing Cap Screws and Nuts	C&LAS	A, G	Bolting Integrity EPRI 1018959 EPRI NP-5769 NUREG-1339 NUREG-1801	ASME Sect. XI IWA-4000 Vendor GE SIL 483R2	None
	1.5-1 SLC Housing	Ni-Alloy (A600 with A82/A182 welds)	A	Water Chemistry BWRVIP-190 BWRVIP-225 HWC Technology BWRVIP-62 BWRVIP-156 BWRVIP-159 BWRVIP-219	ASME Sect. XI IWA-4000 EPRI BWRVIP BWRVIP-53-A	B-DM-03 B-DM-06 B-DM-09 B-AS-27 B-MT-04 B-MT-05

Degradation Mechanism	Component & ID No.	Material	Conseq. of Failure	Mitigation	Repair/Replace	Gaps
	1.5-2 SLC Housing	SS (304)	A	Water Chemistry BWRVIP-190 BWRVIP-225 HWC Technology BWRVIP-62 BWRVIP-156 BWRVIP-159 BWRVIP-219	ASME Sect. XI IWA-4000 EPRI BWRVIP BWRVIP-53-A	B-DM-03 B-DM-06 B-DM-09 B-AS-27 B-MT-02 B-MT-04 B-MT-05
	1.5-3 SLC Nozzle (Full Penetration Weld) (BWR/3-4 B&W, CB&J designs)	C&LAS (SA-508, C/2)	A	Water Chemistry BWRVIP-190 BWRVIP-225	ASME Sect. XI IWA-4000 EPRI BWRVIP BWRVIP-53-A	B-DM-06 B-DM-07
	1.5-4 SLC Housing / Nozzle Safe End	SS (304) Ni-Alloy (A82/A182 welds)	A	Water Chemistry BWRVIP-190 BWRVIP-225 HWC Technology BWRVIP-62 BWRVIP-156 BWRVIP-159 BWRVIP-219	ASME Sect. XI IWA-4000 EPRI BWRVIP BWRVIP-53-A	B-DM-03 B-DM-06 B-DM-09 B-AS-27 B-MT-02 B-MT-04 B-MT-05
	1.5-5 SLC Stub Tube (BWR/6 RDM Vessel Design Only)	Ni-Alloy Weld (A600 with A82/A182 welds)	A	Water Chemistry BWRVIP-190 BWRVIP-225 HWC Technology BWRVIP-62 BWRVIP-156 BWRVIP-159 BWRVIP-219	ASME Sect. XI IWA-4000 EPRI BWRVIP BWRVIP-53-A	B-DM-03 B-DM-06 B-DM-09 B-AS-27 B-MT-04 B-MT-05

Degradation Mechanism	Component & ID No.	Material	Conseq. of Failure	Mitigation	Repair/Replace	Gaps
	1.6-1 In-Core Housing & Flange	SS (304 typ.)	A	Water Chemistry BWRVIP-190 BWRVIP-225 HWC Technology BWRVIP-62 BWRVIP-156 BWRVIP-159 BWRVIP-219	ASME Sect. XI IWA-4000 CC-N-769 EPRI BWRVIP BWRVIP-17 BWRVIP-55-A BWRVIP-214NP	B-DM-06 B-DM-09
	1.6-2 In-Core Housing & Flange	Ni-Alloy Weld (A600 with A82/A182 welds)	A	Water Chemistry BWRVIP-190 BWRVIP-225 HWC Technology BWRVIP-62 BWRVIP-156 BWRVIP-159 BWRVIP-219	ASME Sect. XI IWA-4000 CC-N-769 EPRI BWRVIP BWRVIP-17 BWRVIP-55-A BWRVIP-214NP	B-DM-03 B-DM-06 B-DM-09 B-AS-27 B-MT-04 B-MT-05
	1.7-1 Instrument Penetrations (Water Level and Jet Pump Sensing Lines) (Partial Penetration Welds)	Ni-Alloy Weld (A600 with A82/A182 welds)	A	Water Chemistry BWRVIP-190 BWRVIP-225 HWC Technology BWRVIP-62 BWRVIP-156 BWRVIP-159 BWRVIP-219	ASME Sect. XI IWA-4000 EPRI BWRVIP BWRVIP-57-A	B-DM-03 B-DM-06 B-DM-09 B-AS-27 B-MT-01 B-MT-02 B-MT-04 B-MT-05
	1.7-2 Instrument Penetrations (Water Level and Jet Pump Sensing Lines) (Partial Penetration Welds)	SS (304, 308 / 309 welds)	A	Water Chemistry BWRVIP-190 BWRVIP-225 HWC Technology BWRVIP-62 BWRVIP-156 BWRVIP-159 BWRVIP-219	ASME Sect. XI IWA-4000 EPRI BWRVIP BWRVIP-57-A	B-DM-06 B-DM-09 B-MT-01 B-MT-02

Degradation Mechanism	Component & ID No.	Material	Conseq. of Failure	Mitigation	Repair/Replace	Gaps
	1.7-3 Instrument Penetrations (Water Level and Jet Pump Sensing Lines) (Partial Penetration Welds)	C&LAS (SA-508, Cl 1, SA-541 Cl 1 Mod)	A	Water Chemistry BWRVIP-190 BWRVIP-225	ASME Sect. XI IWA-4000 EPRI BWRVIP BWRVIP-57-A	B-DM-06 B-DM-07 B-AS-05 B-AS-28
	1.8-1 Jet Pump Riser Brace Pad Attachment (BWR/3-6)	SS (300 Series) Ni-Alloy (A600 with A82/A182 welds)	B, C	Water Chemistry BWRVIP-190 BWRVIP-225 HWC Technology BWRVIP-62 BWRVIP-156 BWRVIP-159 BWRVIP-219	ASME Sect. XI IWA-4000 EPRI BWRVIP BWRVIP-52-A	B-DM-03 B-DM-06 B-DM-09 B-AS-27 B-MT-02
	1.8-2 Core Spray Pipe Bracket Attachment (BWR/3-6)	SS (300 Series) Ni-Alloy (A182 welds)	B, C	Water Chemistry BWRVIP-190 BWRVIP-225 (Not mitigated by HWC/MMCA/OLNG)	ASME Sect. XI IWA-4000 EPRI BWRVIP BWRVIP-52-A	B-DM-03 B-DM-06 B-DM-09 B-AS-27 B-MT-01 B-MT-02
	1.8-3 Shroud Support Pad	Ni-Alloy (A82/A182 welds)	B, C, E	Water Chemistry BWRVIP-190 BWRVIP-225 HWC Technology BWRVIP-62 BWRVIP-156 BWRVIP-159 BWRVIP-219	ASME Sect. XI IWA-4000 EPRI BWRVIP BWRVIP-52-A	B-DM-03 B-DM-06 B-DM-09 B-AS-27 B-MT-01 B-MT-02

Degradation Mechanism	Component & ID No.	Material	Conseq. of Failure	Mitigation	Repair/Replace	Gaps
	1.8-4 Steam Dryer Support Bracket	SS (300 Series) Ni-Alloy (A182 welds)	B, C	Water Chemistry BWRVIP-190 BWRVIP-225 (Not mitigated by HWC/MMCA/OLNG)	ASME Sect. XI IWA-4000 EPRI BWRVIP BWRVIP-52-A	B-DM-03 B-DM-06 B-DM-09 B-AS-27 B-MT-02
	1.8-5 Steam Dryer Hold-down Bracket	C&LAS (LAS)	B, C	Water Chemistry BWRVIP-190 BWRVIP-225	ASME Sect. XI IWA-4000 EPRI BWRVIP BWRVIP-52-A	B-DM-06 B-DM-07
	1.8-6 Feedwater Sparger Support Bracket	SS (300 Series) Ni-Alloy (A182 welds)	B, C	Water Chemistry BWRVIP-190 BWRVIP-225 (Not mitigated by HWC/MMCA/OLNG)	ASME Sect. XI IWA-4000 EPRI BWRVIP BWRVIP-52-A	B-DM-03 B-DM-06 B-DM-09 B-AS-27 B-MT-01 B-MT-02
	1.8-7 Surveillance Capsule Holder Bracket	SS (300 Series) Ni-Alloy (A182 welds)	B, C	Water Chemistry BWRVIP-190 BWRVIP-225 HWC Technology BWRVIP-62 BWRVIP-156 BWRVIP-159 BWRVIP-219	ASME Sect. XI IWA-4000 EPRI BWRVIP BWRVIP-52-A	B-DM-03 B-DM-06 B-DM-09 B-AS-27 B-MT-02
	1.8-8 Guide Rod Bracket	SS (300 Series) Ni-Alloy (A182 welds)	B, C	Water Chemistry BWRVIP-190 BWRVIP-225 (Not mitigated by HWC/MMCA/OLNG)	ASME Sect. XI IWA-4000 EPRI BWRVIP BWRVIP-52-A	B-DM-03 B-DM-06 B-DM-09 B-AS-27 B-MT-01 B-MT-02

Degradation Mechanism	Component & ID No.	Material	Conseq. of Failure	Mitigation	Repair/Replace	Gaps
Corrosion & Wear: Wear	1.8-4 Steam Dryer Support Bracket	SS (300 Series) Ni-Alloy (A182 welds)	B, C	Water Chemistry BWRVIP-190 BWRVIP-225 (Not mitigated by HWC/MMCA/OLNG)	ASME Sect. XI IWA-4000 EPRI BWRVIP BWRVIP-52-A	B-DM-03 B-DM-06 B-DM-09 B-AS-27 B-MT-02
	1.8-5 Steam Dryer Hold-down Bracket	C&LAS (LAS)	B, C	Water Chemistry BWRVIP-190 BWRVIP-225	ASME Sect. XI IWA-4000 EPRI BWRVIP BWRVIP-52-A	B-DM-06 B-DM-07
	1.8-6 Feedwater Sparger Support Bracket	SS (300 Series) Ni-Alloy (A182 welds)	B, C	Water Chemistry BWRVIP-190 BWRVIP-225 (Not mitigated by HWC/MMCA/OLNG)	ASME Sect. XI IWA-4000 EPRI BWRVIP BWRVIP-52-A	B-DM-03 B-DM-06 B-DM-09 B-AS-27 B-MT-01 B-MT-02
Corrosion & Wear: Pitting	1.2-1 Closure Head Studs, Washers, Nuts	C&LAS (SA-193, Gr B16, or SA-540, Gr B23 or B24)	A	Bolting Integrity EPRI 1018959 EPRI NP-5769 NUREG-1339 NUREG-1801 Reg. Guide 1.65	ASME Sect. XI IWA-4000	B-DM-06
	1.2-2 Top of Head Flange Bolts	C&LAS (SA-193)	A	Bolting Integrity EPRI 1018959 EPRI NP-5769 NUREG-1339 NUREG-1801	ASME Sect. XI IWA-4000	B-DM-06
	1.4-5 CRD Housing Cap Screws and Nuts	C&LAS	A, G	Bolting Integrity EPRI 1018959 EPRI NP-5769 NUREG-1339 NUREG-1801	ASME Sect. XI IWA-4000 Vendor GE SIL 483R2	None

Degradation Mechanism	Component & ID No.	Material	Conseq. of Failure	Mitigation	Repair/Replace	Gaps
Corrosion & Wear: Flow Accelerated Corrosion	1.3-17 Bottom Drain Nozzles	C&LAS (Carbon Steel)	A, G	Water Chemistry BWRVIP-190 BWRVIP-225	ASME Sect. XI IWA-4000 EPRI BWRVIP BWRVIP-208	B-DM-06 B-DM-07 B-I&E-07 B-RR-06
	1.8-1 Jet Pump Riser Brace Pad Attachment (BWR/3-6)	SS (300 Series) Ni-Alloy (A600 with A82/A182 welds)	B, C	Water Chemistry BWRVIP-190 BWRVIP-225 HWC Technology BWRVIP-62 BWRVIP-156 BWRVIP-159 BWRVIP-219	ASME Sect. XI IWA-4000 EPRI BWRVIP BWRVIP-52-A	B-DM-03 B-DM-06 B-DM-09 B-AS-27 B-MT-02
Fatigue: High-Cycle	1.8-4 Steam Dryer Support Bracket	SS (300 Series) Ni-Alloy (A182 welds)	B, C	Water Chemistry BWRVIP-190 BWRVIP-225 (Not mitigated by HWC/MMCA/OLNG)	ASME Sect. XI IWA-4000 EPRI BWRVIP BWRVIP-52-A	B-DM-03 B-DM-06 B-DM-09 B-AS-27 B-MT-02
	1.8-5 Steam Dryer Hold-down Bracket	C&LAS (LAS)	B, C	Water Chemistry BWRVIP-190 BWRVIP-225	ASME Sect. XI IWA-4000 EPRI BWRVIP BWRVIP-52-A	B-DM-06 B-DM-07
	1.8-6 Feedwater Sparger Support Bracket	SS (300 Series) Ni-Alloy (A182 welds)	B, C	Water Chemistry BWRVIP-190 BWRVIP-225 (Not mitigated by HWC/MMCA/OLNG)	ASME Sect. XI IWA-4000 EPRI BWRVIP BWRVIP-52-A	B-DM-03 B-DM-06 B-DM-09 B-AS-27 B-MT-01 B-MT-02

Degradation Mechanism	Component & ID No.	Material	Conseq. of Failure	Mitigation	Repair/Replace	Gaps
Fatigue: Low-Cycle-Environmental	1.1-1 Top Head and Flange	C&LAS (SA-533, Gr B, Cl 1; SA-508 Cl 2)	A, B	Water Chemistry BWRVIP-190 BWRVIP-225	ASME Sect. XI IWA-4000	B-DM-06 B-DM-07 B-AS-07
	1.1-2 Vessel Flange	C&LAS (SA-336 or SA-508, Cl 2)	A, B	Water Chemistry BWRVIP-190 BWRVIP-225	ASME Sect. XI IWA-4000	B-DM-06 B-DM-07 B-AS-07
	1.1-3 Upper Intermediate (Nozzle), Beltline, and Lower Shells	C&LAS (A-302, Gr B or SA-533, Gr B, Cl 1) SS Clad ^[1]	A, B, G	Water Chemistry BWRVIP-190 BWRVIP-225 HWC Technology BWRVIP-62 BWRVIP-156 BWRVIP-159 BWRVIP-219	ASME Sect. XI IWA-4000	B-DM-06 B-DM-07 B-DM-08 B-AS-05 B-AS-07 B-AS-11 B-AS-30 B-RG-08
	1.1-4 Bottom Head	C&LAS (A-302, Gr B or SA-533, Gr B, Cl 1) SS Clad ^[1]	A, B, G	Water Chemistry BWRVIP-190 BWRVIP-225 HWC Technology BWRVIP-62 BWRVIP-156 BWRVIP-159 BWRVIP-219	ASME Sect. XI IWA-4000	B-DM-06 B-DM-07 B-AS-07
	1.2-1 Closure Head Studs, Washers, Nuts	C&LAS (SA-193, Gr B16, or SA-540, Gr B23 or B24)	A	Bolting Integrity EPRI 1018959 EPRI NP-5769 NUREG-1339 NUREG-1801 Reg. Guide 1.65	ASME Sect. XI IWA-4000	B-DM-06

Degradation Mechanism	Component & ID No.	Material	Conseq. of Failure	Mitigation	Repair/Replace	Gaps
	1.2-2 Top of Head Flange Bolts	C&LAS (SA-193)	A	Bolting Integrity EPRI 1018959 EPRI NP-5769 NUREG-1339 NUREG-1801	ASME Sect. XI IWA-4000	B-DM-06
	1.3-1 Top Head Nozzle (Head Spray and Vent)	C&LAS (SA-508, C12)	A	Water Chemistry BWRVIP-190 BWRVIP-225	ASME Sect. XI IWA-4000	B-DM-06 B-DM-07 B-AS-07
	1.3-3 Feedwater Nozzles	C&LAS (SA-508, C12)	A	Water Chemistry BWRVIP-190 BWRVIP-225 Oper. Changes GE-NE-523-A71- 0594 (Low Flow Controller Oper.)	ASME Sect. XI IWA-4000	B-DM-06 B-DM-07 B-AS-07
	1.3-4 Feedwater Nozzle Safe Ends	C&LAS (SA-508, C1, CS)	A	Water Chemistry BWRVIP-190 BWRVIP-225 Oper. Changes GE-NE-523-A71- 0594 (Low Flow Controller Oper.)	ASME Sect. XI IWA-4000	B-DM-06 B-DM-07

Degradation Mechanism	Component & ID No.	Material	Conseq. of Failure	Mitigation	Repair/Replace	Gaps
	1.3-5 Feedwater Nozzle Safe Ends	Ni-Alloy (Some safe ends – A600 with A82/A182 welds)	A	Water Chemistry BWRVIP-190 BWRVIP-225 HWC Technology BWRVIP-62 BWRVIP-156 BWRVIP-159 BWRVIP-219 Oper. Changes GE-NE-523-A71- 0594 (Low Flow Controller Oper.) Stress Improvement BWRVIP-61 (Weld Overlay, IHSI, MSIP)	ASME Sect. XI IWA-4000 Weld Overlay CC-N-504-2 (Vendor Controlled)	B-DM-03 B-DM-06 B-DM-09 B-DM-10 B-AS-07 B-AS-27
	1.3-6 Core Spray Nozzles	C&LAS (SA-508, Cl 2)	A	Water Chemistry BWRVIP-190 BWRVIP-225	ASME Sect. XI IWA-4000	B-DM-06 B-DM-07 B-AS-07
	1.3-7 Core Spray Nozzle Safe Ends	C&LAS (Carbon Steel)	A	Water Chemistry BWRVIP-190 BWRVIP-225	ASME Sect. XI IWA-4000	B-DM-06 B-DM-07 B-AS-07
	1.3-8 Core Spray Nozzle Safe Ends	SS (incl. SS welds)	A	Water Chemistry BWRVIP-190 BWRVIP-225 (Not mitigated by HWC/NMCA/OLNC) Stress Improvement BWRVIP-61 (Weld Overlay, IHSI, MSIP)	ASME Sect. XI IWA-4000 Weld Overlay CC-N-504-2 (Vendor Controlled)	B-DM-03 B-DM-06 B-DM-09 B-DM-10 B-AS-07 B-AS-27 B-MT-01 B-MT-02

Degradation Mechanism	Component & ID No.	Material	Conseq. of Failure	Mitigation	Repair/Replace	Gaps
	1.3-9 Core Spray Nozzle Safe Ends	Ni-Alloy (A600 with A82/A182 welds)	A	Water Chemistry BWRVIP-190 BWRVIP-225 (Not mitigated by HWC/MMCA/OLNG) Stress Improvement BWRVIP-61 (Weld Overlay, IHSI, MSIP)	ASME Sect. XI IWA-4000 Weld Overlay CC-N-504-2 (Vendor Controlled)	B-DM-03 B-DM-06 B-DM-09 B-DM-10 B-AS-07 B-AS-27 B-MT-01
	1.3-10 LPCI Nozzles	C&LAS (SA-508, C12)	A	Water Chemistry BWRVIP-190 BWRVIP-225	ASME Sect. XI IWA-4000	B-DM-06 B-DM-07 B-AS-05 B-AS-07
	1.3-11 LPCI Nozzle Safe Ends (BWR/5)	C&LAS (Carbon Steel)	A	Water Chemistry BWRVIP-190 BWRVIP-225	ASME Sect. XI IWA-4000	B-DM-06 B-DM-07 B-AS-07
	1.3-12 LPCI Nozzle Safe Ends (BWR/5)	Ni-Alloy (A600 with A82/A182 welds)	A	Water Chemistry BWRVIP-190 BWRVIP-225 (Not mitigated by HWC/MMCA/OLNG) Stress Improvement BWRVIP-61 (Weld Overlay, IHSI, MSIP)	ASME Sect. XI IWA-4000 Weld Overlay CC-N-504-2 (Vendor Controlled)	B-DM-03 B-DM-06 B-DM-09 B-DM-10 B-AS-07 B-AS-27 B-MT-01
	1.3-13 CRD Return Line Nozzle (Only BWR/2 not capped or flanged)	C&LAS (SA-508, C12)	A	Water Chemistry BWRVIP-190 BWRVIP-225	ASME Sect. XI IWA-4000	B-DM-06 B-DM-07 B-AS-05 B-AS-07

Degradation Mechanism	Component & ID No.	Material	Conseq. of Failure	Mitigation	Repair/Replace	Gaps
	1.3-14 CRD Return Line Nozzle Cap (BWR/3-6)	Ni-Alloy (A600 with A82/A182 welds)	A	Water Chemistry BWRVIP-190 BWRVIP-225 (Not mitigated by HWC/MMCA/OLNG)	ASME Sect. XI IWA-4000	B-DM-03 B-DM-06 B-DM-09 B-AS-07 B-AS-27 B-MT-01
	1.3-15 Recirculation Inlet and Outlet Nozzles	C&LAS (SA-508, Cl2)	A, G	Water Chemistry BWRVIP-190 BWRVIP-225	ASME Sect. XI IWA-4000	B-DM-06 B-DM-07 B-AS-05 B-AS-07
	1.3-16 Recirculation inlet and Outlet Nozzle Safe Ends	SS (304, 316, 316L, 316NG & incl. SS welds) Ni-Alloy (A82/A182 welds)	A, G	Water Chemistry BWRVIP-190 BWRVIP-225 HWC Technology BWRVIP-62 BWRVIP-156 BWRVIP-159 BWRVIP-219 Stress Improvement BWRVIP-61 (Weid Overlay, IHSI, MSIP)	ASME Sect. XI IWA-4000 Weid Overlay CC-N-504-2 (Vendor Controlled)	B-DM-03 B-DM-06 B-DM-09 B-DM-10 B-AS-07 B-AS-27 B-MT-02
	1.4-1 CRD Stub Tube	Ni-Alloy (A600 with A82/A182 welds)	A, G	Water Chemistry BWRVIP-190 BWRVIP-225 HWC Technology BWRVIP-62 BWRVIP-156 BWRVIP-159 BWRVIP-219	ASME Sect. XI IWA-4000 CC-N-730 EPRI BWRVIP BWRVIP-55-A BWRVIP-58-A BWRVIP- 146NP(R1)	B-DM-03 B-DM-06 B-DM-09 B-AS-07 B-AS-27 B-MT-04 B-MT-05

Degradation Mechanism	Component & ID No.	Material	Conseq. of Failure	Mitigation	Repair/Replace	Gaps
Reduction in Fracture Properties: Environmental	1.4-2 CRD Stub Tube	SS (304 typ., furnace sensitized)	A, G	Water Chemistry BWRVIP-190 BWRVIP-225	ASME Sect. XI IWA-4000 CC-N-730	B-DM-03 B-DM-06 B-DM-09
	1.4-5 CRD Housing Cap Screws and Nuts	C&LAS	A, G	HWC Technology BWRVIP-62 BWRVIP-156 BWRVIP-159 BWRVIP-219	EPRI BWRVIP BWRVIP-55-A BWRVIP-58-A BWRVIP- 146NP(R1)	B-AS-07 B-AS-27 B-MT-02 B-MT-04 B-MT-05
	1.1-1 Top Head and Flange	C&LAS (SA-533, Gr.B, Cl 1; SA-508 Cl 2)	A, B	Bolting Integrity EPRI 1018959 EPRI NP-5769 NUREG-1339 NUREG-1801	ASME Sect. XI IWA-4000 Vendor GE SIL 483R2	None
	1.1-2 Vessel Flange	C&LAS (SA-336 or SA-508, Cl 2)	A, B	Water Chemistry BWRVIP-190 BWRVIP-225	ASME Sect. XI IWA-4000	B-DM-06 B-DM-07 B-AS-07
	1.3-1 Top Head Nozzle (Head Spray and Vent)	C&LAS (SA-508, Cl 2)	A	Water Chemistry BWRVIP-190 BWRVIP-225	ASME Sect. XI IWA-4000	B-DM-06 B-DM-07 B-AS-07
	1.3-2 Main Steam Nozzles and Safe Ends	C&LAS (SA-508, Cl 2)	A	Water Chemistry BWRVIP-190 BWRVIP-225	ASME Sect. XI IWA-4000	B-DM-06 B-DM-07 B-AS-07

Degradation Mechanism	Component & ID No.	Material	Conseq. of Failure	Mitigation	Repair/Replace	Gaps
	1.3-3 Feedwater Nozzles	C&LAS (SA-508, C12)	A	Water Chemistry BWRVIP-190 BWRVIP-225 Oper. Changes GE-NE-523-A71-0594 (Low Flow Controller Oper.)	ASME Sect. XI IWA-4000	B-DM-06 B-DM-07 B-AS-07
	1.3-4 Feedwater Nozzle Safe Ends	C&LAS (SA-508, C1, CS)	A	Water Chemistry BWRVIP-190 BWRVIP-225 Oper. Changes GE-NE-523-A71-0594 (Low Flow Controller Oper.)	ASME Sect. XI IWA-4000	B-DM-06 B-DM-07
	1.3-5 Feedwater Nozzle Safe Ends	Ni-Alloy (Some safe ends – A600 with A82/A182 welds)	A	Water Chemistry BWRVIP-190 BWRVIP-225 HWC Technology BWRVIP-62 BWRVIP-156 BWRVIP-159 BWRVIP-219 Oper. Changes GE-NE-523-A71-0594 (Low Flow Controller Oper.) Stress Improvement BWRVIP-61 (Weld Overlay, HSI, MSIP)	ASME Sect. XI IWA-4000 Weld Overlay CC-N-504-2 (Vendor Controlled)	B-DM-03 B-DM-06 B-DM-09 B-DM-10 B-AS-07 B-AS-27

Degradation Mechanism	Component & ID No.	Material	Conseq. of Failure	Mitigation	Repair/Replace	Gaps
	1.3-6 Core Spray Nozzles	C&LAS (SA-508, Cl 2)	A	Water Chemistry BWRVIP-190 BWRVIP-225	ASME Sect. XI IWA-4000	B-DM-06 B-DM-07 B-AS-07
	1.3-7 Core Spray Nozzle Safe Ends	C&LAS (Carbon Steel)	A	Water Chemistry BWRVIP-190 BWRVIP-225	ASME Sect. XI IWA-4000	B-DM-06 B-DM-07 B-AS-07
	1.3-8 Core Spray Nozzle Safe Ends	SS (incl. SS welds)	A	Water Chemistry BWRVIP-190 BWRVIP-225 (Not mitigated by HWC/NMCA/OLNC) Stress Improvement BWRVIP-61 (Weld Overlay, HSI, MSIP)	ASME Sect. XI IWA-4000 Weld Overlay CC-N-504-2 (Vendor Controlled)	B-DM-03 B-DM-06 B-DM-09 B-DM-10 B-AS-07 B-AS-27 B-MT-01 B-MT-02
	1.3-9 Core Spray Nozzle Safe Ends	Ni-Alloy (A600 with A82/A182 welds)	A	Water Chemistry BWRVIP-190 BWRVIP-225 (Not mitigated by HWC/NMCA/OLNC) Stress Improvement BWRVIP-61 (Weld Overlay, HSI, MSIP)	ASME Sect. XI IWA-4000 Weld Overlay CC-N-504-2 (Vendor Controlled)	B-DM-03 B-DM-06 B-DM-09 B-DM-10 B-AS-07 B-AS-27 B-MT-01
	1.3-10 LPCI Nozzles	C&LAS (SA-508, Cl 2)	A	Water Chemistry BWRVIP-190 BWRVIP-225	ASME Sect. XI IWA-4000	B-DM-06 B-DM-07 B-AS-05, B-AS-07
	1.3-11 LPCI Nozzle Safe Ends (BWR/5)	C&LAS (Carbon Steel)	A	Water Chemistry BWRVIP-190 BWRVIP-225	ASME Sect. XI IWA-4000	B-DM-06 B-DM-07 B-AS-07

Degradation Mechanism	Component & ID No.	Material	Conseq. of Failure	Mitigation	Repair/Replace	Gaps
	1.3-12 LPCI Nozzle Safe Ends (BWR/5)	Ni-Alloy (A600 with A82/A182 welds)	A	Water Chemistry BWRVIP-190 BWRVIP-225 (Not mitigated by HWC/NMCA/OLNC) Stress Improvement BWRVIP-61 (Weld Overlay, HSI, MSIP)	ASME Sect. XI IWA-4000 Weld Overlay CC-N-504-2 (Vendor Controlled)	B-DM-03 B-DM-06 B-DM-09 B-DM-10 B-AS-07 B-AS-27 B-MT-01
	1.3-14 CRD Return Line Nozzle Cap (BWR/3-6)	Ni-Alloy (A600 with A82/A182 welds)	A	Water Chemistry BWRVIP-190 BWRVIP-225 (Not mitigated by HWC/NMCA/OLNC)	ASME Sect. XI IWA-4000	B-DM-03 B-DM-06 B-DM-09 B-AS-07 B-AS-27 B-MT-01
	1.3-16 Recirculation inlet and Outlet Nozzle Safe Ends	SS (304, 316, 316L, 316NG & incl. SS welds) Ni-Alloy (A82/A182 welds)	A, G	Water Chemistry BWRVIP-190 BWRVIP-225 HWC Technology BWRVIP-62 BWRVIP-156 BWRVIP-159 BWRVIP-219 Stress Improvement BWRVIP-61 (Weld Overlay, HSI, MSIP)	ASME Sect. XI IWA-4000 Weld Overlay CC-N-504-2 (Vendor Controlled)	B-DM-03 B-DM-06 B-DM-09 B-DM-10 B-AS-07 B-AS-27 B-MT-02
	1.3-17 Bottom Drain Nozzles	C&LAS (Carbon Steel)	A, G	Water Chemistry BWRVIP-190 BWRVIP-225	ASME Sect. XI IWA-4000 EPRI BWRVIP BWRVIP-208	B-DM-06 B-DM-07 B-I&E-07 B-RR-06

Degradation Mechanism	Component & ID No.	Material	Conseq. of Failure	Mitigation	Repair/Replace	Gaps
	1.4-1 CRD Stub Tube	Ni-Alloy (A600 with A82/A182 welds)	A, G	Water Chemistry BWRVIP-190 BWRVIP-225	ASME Sect. XI IWA-4000 CC-N-730	B-DM-03 B-DM-06 B-DM-09
	1.4-2 CRD Stub Tube	SS (304 typ., furnace sensitized)	A, G	HWC Technology BWRVIP-62 BWRVIP-156 BWRVIP-159 BWRVIP-219	EPRI BWRVIP BWRVIP-55-A BWRVIP-58-A BWRVIP-146NP(R1)	B-AS-07 B-AS-27 B-MT-04 B-MT-05
	1.4-3 CRD Housing Tube, Flange & Cap	SS (304 typ., 304L, 316L)	A, G	Water Chemistry BWRVIP-190 BWRVIP-225	ASME Sect. XI IWA-4000 CC-N-730	B-DM-06 B-DM-09
	1.4-4 CRD Housing Tube (straight-thru design- middle tube)	Ni-Alloy (A600 with A82/A182 welds)	A, G	HWC Technology BWRVIP-62 BWRVIP-156 BWRVIP-159 BWRVIP-219	EPRI BWRVIP BWRVIP-55-A BWRVIP-58-A BWRVIP-146NP(R1)	B-MT-02 B-MT-04 B-MT-05
				Water Chemistry BWRVIP-190 BWRVIP-225	ASME Sect. XI IWA-4000 CC-N-730	B-DM-03 B-DM-06 B-DM-09
				HWC Technology BWRVIP-62 BWRVIP-156 BWRVIP-159 BWRVIP-219	EPRI BWRVIP BWRVIP-55-A BWRVIP-58-A BWRVIP-146NP(R1)	B-AS-27 B-MT-04 B-MT-05

Degradation Mechanism	Component & ID No.	Material	Conseq. of Failure	Mitigation	Repair/Replace	Gaps
	1.5-1 SLC Housing	Ni-Alloy (A600 with A82/A182 welds)	A	Water Chemistry BWRVIP-190 BWRVIP-225 HWC Technology BWRVIP-62 BWRVIP-156 BWRVIP-159 BWRVIP-219	ASME Sect. XI IWA-4000 EPRI BWRVIP BWRVIP-53-A	B-DM-03 B-DM-06 B-DM-09 B-AS-27 B-MT-04 B-MT-05
	1.5-2 SLC Housing	SS (304)	A	Water Chemistry BWRVIP-190 BWRVIP-225 HWC Technology BWRVIP-62 BWRVIP-156 BWRVIP-159 BWRVIP-219	ASME Sect. XI IWA-4000 EPRI BWRVIP BWRVIP-53-A	B-DM-03 B-DM-06 B-DM-09 B-AS-27 B-MT-02 B-MT-04 B-MT-05
	1.5-3 SLC Nozzle (Full Penetration Weld) (BWR/3-4 B&W, CB&I designs)	C&LAS (SA-508, C/2)	A	Water Chemistry BWRVIP-190 BWRVIP-225	ASME Sect. XI IWA-4000 EPRI BWRVIP BWRVIP-53-A	B-DM-06 B-DM-07
	1.5-4 SLC Housing / Nozzle Safe End	SS (304) Ni-Alloy (A82/A182 welds)	A	Water Chemistry BWRVIP-190 BWRVIP-225 HWC Technology BWRVIP-62 BWRVIP-156 BWRVIP-159 BWRVIP-219	ASME Sect. XI IWA-4000 EPRI BWRVIP BWRVIP-53-A	B-DM-03 B-DM-06 B-DM-09 B-AS-27 B-MT-02 B-MT-04 B-MT-05

Degradation Mechanism	Component & ID No.	Material	Conseq. of Failure	Mitigation	Repair/Replace	Gaps
	1.5-5 SLC Stub Tube (BWR/6 RDM Vessel Design Only)	Ni-Alloy Weld (A600 with A82/A182 welds)	A	Water Chemistry BWRVIP-190 BWRVIP-225 HWC Technology BWRVIP-62 BWRVIP-156 BWRVIP-159 BWRVIP-219	ASME Sect. XI IWA-4000 EPRI BWRVIP BWRVIP-53-A	B-DM-03 B-DM-06 B-DM-09 B-AS-27 B-MT-04 B-MT-05
	1.6-1 In-Core Housing & Flange	SS (304 typ.)	A	Water Chemistry BWRVIP-190 BWRVIP-225 HWC Technology BWRVIP-62 BWRVIP-156 BWRVIP-159 BWRVIP-219	ASME Sect. XI IWA-4000 CC-N-769 EPRI BWRVIP BWRVIP-17 BWRVIP-55-A BWRVIP-214NP	B-DM-06 B-DM-09
	1.6-2 In-Core Housing & Flange	Ni-Alloy Weld (A600 with A82/A182 welds)	A	Water Chemistry BWRVIP-190 BWRVIP-225 HWC Technology BWRVIP-62 BWRVIP-156 BWRVIP-159 BWRVIP-219	ASME Sect. XI IWA-4000 CC-N-769 EPRI BWRVIP BWRVIP-17 BWRVIP-55-A BWRVIP-214NP	B-DM-03 B-DM-06 B-DM-09 B-AS-27 B-MT-04 B-MT-05
	1.7-1 Instrument Penetrations (Water Level and Jet Pump Sensing Lines) (Partial Penetration Welds)	Ni-Alloy Weld (A600 with A82/A182 welds)	A	Water Chemistry BWRVIP-190 BWRVIP-225 HWC Technology BWRVIP-62 BWRVIP-156 BWRVIP-159 BWRVIP-219	ASME Sect. XI IWA-4000 EPRI BWRVIP BWRVIP-57-A	B-DM-03 B-DM-06 B-DM-09 B-AS-27 B-MT-01 B-MT-02 B-MT-04 B-MT-05

Degradation Mechanism	Component & ID No.	Material	Conseq. of Failure	Mitigation	Repair/Replace	Gaps
	1.7-2 Instrument Penetrations (Water Level and Jet Pump Sensing Lines) (Partial Penetration Welds)	SS (304, 308 / 309 welds)	A	Water Chemistry BWRVIP-190 BWRVIP-225 HWC Technology BWRVIP-62 BWRVIP-156 BWRVIP-159 BWRVIP-219	ASME Sect. XI IWA-4000 EPRI BWRVIP BWRVIP-57-A	B-DM-06 B-DM-09 B-MT-01 B-MT-02
	1.7-3 Instrument Penetrations (Water Level and Jet Pump Sensing Lines) (Partial Penetration Welds)	C&LAS (SA-508, Cl 1, SA-541 Cl 1 Mod)	A	Water Chemistry BWRVIP-190 BWRVIP-225	ASME Sect. XI IWA-4000 EPRI BWRVIP BWRVIP-57-A	B-DM-06 B-DM-07 B-AS-05 B-AS-28
	1.8-1 Jet Pump Riser Brace Pad Attachment (BWR/3-6)	SS (300 Series) Ni-Alloy (A600 with A82/A182 welds)	B, C	Water Chemistry BWRVIP-190 BWRVIP-225 HWC Technology BWRVIP-62 BWRVIP-156 BWRVIP-159 BWRVIP-219	ASME Sect. XI IWA-4000 EPRI BWRVIP BWRVIP-52-A	B-DM-03 B-DM-06 B-DM-09 B-AS-27 B-MT-02
	1.8-2 Core Spray Pipe Bracket Attachment (BWR/3-6)	SS (300 Series) Ni-Alloy (A182 welds)	B, C	Water Chemistry BWRVIP-190 BWRVIP-225 (Not mitigated by HWC/NMCA/OLNG)	ASME Sect. XI IWA-4000 EPRI BWRVIP BWRVIP-52-A	B-DM-03 B-DM-06 B-DM-09 B-AS-27 B-MT-01 B-MT-02

Degradation Mechanism	Component & ID No.	Material	Conseq. of Failure	Mitigation	Repair/Replace	Gaps
	1.8-3 Shroud Support Pad	Ni-Alloy (A82/A182 welds)	B, C, E	Water Chemistry BWRVIP-190 BWRVIP-225 HWC Technology BWRVIP-62 BWRVIP-156 BWRVIP-159 BWRVIP-219	ASME Sect. XI IWA-4000 EPRI BWRVIP BWRVIP-52-A	B-DM-03 B-DM-06 B-DM-09 B-AS-27 B-MT-01 B-MT-02
	1.8-4 Steam Dryer Support Bracket	SS (300 Series) Ni-Alloy (A182 welds)	B, C	Water Chemistry BWRVIP-190 BWRVIP-225 (Not mitigated by HWC/NMCA/OLNC)	ASME Sect. XI IWA-4000 EPRI BWRVIP BWRVIP-52-A	B-DM-03 B-DM-06 B-DM-09 B-AS-27 B-MT-02
	1.8-5 Steam Dryer Hold-down Bracket	C&LAS (LAS)	B, C	Water Chemistry BWRVIP-190 BWRVIP-225	ASME Sect. XI IWA-4000 EPRI BWRVIP BWRVIP-52-A	B-DM-06 B-DM-07
	1.8-6 Feedwater Sparger Support Bracket	SS (300 Series) Ni-Alloy (A182 welds)	B, C	Water Chemistry BWRVIP-190 BWRVIP-225 (Not mitigated by HWC/NMCA/OLNC)	ASME Sect. XI IWA-4000 EPRI BWRVIP BWRVIP-52-A	B-DM-03 B-DM-06 B-DM-09 B-AS-27 B-MT-01 B-MT-02

Degradation Mechanism	Component & ID No.	Material	Conseq. of Failure	Mitigation	Repair/Replace	Gaps
Reduction in Fracture Properties: Thermal (Clad), Environmental	1.8-7 Surveillance Capsule Holder Bracket	SS (300 Series) Ni-Alloy (A182 welds)	B, C	Water Chemistry BWRVIP-190 BWRVIP-225 HWC Technology BWRVIP-62 BWRVIP-156 BWRVIP-159 BWRVIP-219	ASME Sect. XI IWA-4000 EPRI BWRVIP BWRVIP-52-A	B-DM-03 B-DM-06 B-DM-09 B-AS-27 B-MT-02
	1.8-8 Guide Rod Bracket	SS (300 Series) Ni-Alloy (A182 welds)	B, C	Water Chemistry BWRVIP-190 BWRVIP-225 (Not mitigated by HWC/NMCA/OLNC)	ASME Sect. XI IWA-4000 EPRI BWRVIP BWRVIP-52-A	B-DM-03 B-DM-06 B-DM-09 B-AS-27 B-MT-01 B-MT-02
	1.1-3 Upper Intermediate (Nozzle), Beltline, and Lower Shells	C&LAS (A-302, Gr B or SA-533, Gr B, Cl 1) SS Clad ^[1]	A, B, G	Water Chemistry BWRVIP-190 BWRVIP-225 HWC Technology BWRVIP-62 BWRVIP-156 BWRVIP-159 BWRVIP-219	ASME Sect. XI IWA-4000	B-DM-06 B-DM-07 B-DM-08 B-AS-05 B-AS-07 B-AS-11 B-AS-30
	1.1-4 Bottom Head	C&LAS (A-302, Gr B or SA-533, Gr B, Cl 1) SS Clad ^[1]	A, B, G	Water Chemistry BWRVIP-190 BWRVIP-225 HWC Technology BWRVIP-62 BWRVIP-156 BWRVIP-159 BWRVIP-219	ASME Sect. XI IWA-4000	B-RG-08 B-DM-06 B-DM-07 B-AS-07

Degradation Mechanism	Component & ID No.	Material	Conseq. of Failure	Mitigation	Repair/Replace	Gaps
Irradiation Effects: Embrittlement	1.3-13 CRD Return Line Nozzle <i>(Only BWR/2 not capped or flanged)</i>	C&LAS <i>(SA-508, C/2)</i>	A	Water Chemistry BWRVIP-190 BWRVIP-225	ASME Sect. XI IWA-4000	B-DM-06 B-DM-07 B-AS-05, B-AS-07
	1.3-15 Recirculation Inlet and Outlet Nozzles	C&LAS <i>(SA-508, C/2)</i>	A, G	Water Chemistry BWRVIP-190 BWRVIP-225	ASME Sect. XI IWA-4000	B-DM-06 B-DM-07 B-AS-05 B-AS-07
	1.1-3 Upper Intermediate (Nozzle), Beltline, and Lower Shells	C&LAS <i>(A-302, Gr B or SA-533, Gr B, Cl 1)</i> SS Clad ^[1]	A, B, G	Water Chemistry BWRVIP-190 BWRVIP-225 HWC Technology BWRVIP-62 BWRVIP-156 BWRVIP-159 BWRVIP-219	ASME Sect. XI IWA-4000	B-DM-06 B-DM-07 B-DM-08 B-AS-05 B-AS-07 B-AS-11 B-AS-30 B-RG-08
	1.3-10 LPCI Nozzles	C&LAS <i>(SA-508, C/2)</i>	A	Water Chemistry BWRVIP-190 BWRVIP-225	ASME Sect. XI IWA-4000	B-DM-06 B-DM-07 B-AS-05 B-AS-07
	1.3-13 CRD Return Line Nozzle <i>(Only BWR/2 not capped or flanged)</i>	C&LAS <i>(SA-508, C/2)</i>	A	Water Chemistry BWRVIP-190 BWRVIP-225	ASME Sect. XI IWA-4000	B-DM-06 B-DM-07 B-AS-05 B-AS-07
	1.3-15 Recirculation Inlet and Outlet Nozzles	C&LAS <i>(SA-508, C/2)</i>	A, G	Water Chemistry BWRVIP-190 BWRVIP-225	ASME Sect. XI IWA-4000	B-DM-06 B-DM-07 B-AS-05 B-AS-07

Degradation Mechanism	Component & ID No.	Material	Conseq. of Failure	Mitigation	Repair/Replace	Gaps
External: Pitting	1.7-3 Instrument Penetrations (Water Level and Jet Pump Sensing Lines) (Partial Penetration Welds)	C&LAS (SA-508, Cl 1, SA-541 Cl 1 Mod)	A	Water Chemistry BWRVIP-190 BWRVIP-225	ASME Sect XI IWA-4000 EPRI BWRVIP BWRVIP-57-A	B-DM-06 B-DM-07 B-AS-05 B-AS-28
	1.1-1 Top Head and Flange	C&LAS (SA-533, Gr B, Cl 1; SA-508 Cl 2)	A, B	Water Chemistry BWRVIP-190 BWRVIP-225	ASME Sect. XI IWA-4000	B-DM-06 B-DM-07 B-AS-07
	1.1-2 Vessel Flange	C&LAS (SA-336 or SA-508, Cl 2)	A, B	Water Chemistry BWRVIP-190 BWRVIP-225	ASME Sect. XI IWA-4000	B-DM-06 B-DM-07 B-AS-07
	1.1-3 Upper Intermediate (Nozzle), Beltline, and Lower Shells	C&LAS (A-302, Gr B or SA-533, Gr B, Cl 1) SS Clad ^[1]	A, B, G	Water Chemistry BWRVIP-190 BWRVIP-225 HWC Technology BWRVIP-62 BWRVIP-156 BWRVIP-159 BWRVIP-219	ASME Sect. XI IWA-4000	B-DM-06 B-DM-07 B-DM-08 B-AS-05 B-AS-07 B-AS-11 B-AS-30 B-RG-08
	1.1-4 Bottom Head	C&LAS (A-302, Gr B or SA-533, Gr B, Cl 1) SS Clad ^[1]	A, B, G	Water Chemistry BWRVIP-190 BWRVIP-225 HWC Technology BWRVIP-62 BWRVIP-156 BWRVIP-159 BWRVIP-219	ASME Sect. XI IWA-4000	B-DM-06 B-DM-07 B-AS-07

Degradation Mechanism	Component & ID No.	Material	Conseq. of Failure	Mitigation	Repair/Replace	Gaps
	1.3-1 Top Head Nozzle (Head Spray and Vent)	C&LAS (SA-508, C12)	A	Water Chemistry BWRVIP-190 BWRVIP-225	ASME Sect. XI IWA-4000	B-DM-06 B-DM-07 B-AS-07
	1.3-2 Main Steam Nozzles and Safe Ends	C&LAS (SA-508, C12)	A	Water Chemistry BWRVIP-190 BWRVIP-225	ASME Sect. XI IWA-4000	B-DM-06 B-DM-07 B-AS-07
	1.3-3 Feedwater Nozzles	C&LAS (SA-508, C12)	A	Water Chemistry BWRVIP-190 BWRVIP-225 Oper. Changes GE-NE-523-A71-0594 (Low Flow Controller Oper.)	ASME Sect. XI IWA-4000	B-DM-06 B-DM-07 B-AS-07
	1.3-4 Feedwater Nozzle Safe Ends	C&LAS (SA-508, C1, CS)	A	Water Chemistry BWRVIP-190 BWRVIP-225 Oper. Changes GE-NE-523-A71-0594 (Low Flow Controller Oper.)	ASME Sect. XI IWA-4000	B-DM-06 B-DM-07

Degradation Mechanism	Component & ID No.	Material	Conseq. of Failure	Mitigation	Repair/Replace	Gaps
	1.3-5 Feedwater Nozzle Safe Ends	Ni-Alloy (Some safe ends – A600 with A82/A182 welds)	A	Water Chemistry BWRVIP-190 BWRVIP-225 HWC Technology BWRVIP-62 BWRVIP-156 BWRVIP-159 BWRVIP-219 Oper. Changes GE-NE-523-A71- 0594 (Low Flow Controller Oper.) Stress Improvement BWRVIP-61 (Weld Overlay, IHSI, MSIP)	ASME Sect. XI IWA-4000 Weld Overlay CC-N-504-2 (Vendor Controlled)	B-DM-03 B-DM-06 B-DM-09 B-DM-10 B-AS-07 B-AS-27
	1.3-6 Core Spray Nozzles	C&LAS (SA-508, Cl 2)	A	Water Chemistry BWRVIP-190 BWRVIP-225	ASME Sect. XI IWA-4000	B-DM-06 B-DM-07 B-AS-07
	1.3-7 Core Spray Nozzle Safe Ends	C&LAS (Carbon Steel)	A	Water Chemistry BWRVIP-190 BWRVIP-225	ASME Sect. XI IWA-4000	B-DM-06 B-DM-07 B-AS-07
	1.3-9 Core Spray Nozzle Safe Ends	Ni-Alloy (A600 with A82/A182 welds)	A	Water Chemistry BWRVIP-190 BWRVIP-225 (Not mitigated by HWC/NMCA/OLNC) Stress Improvement BWRVIP-61 (Weld Overlay, IHSI, MSIP)	ASME Sect. XI IWA-4000 Weld Overlay CC-N-504-2 (Vendor Controlled)	B-DM-03 B-DM-06 B-DM-09 B-DM-10 B-AS-07 B-AS-27 B-MT-01

Degradation Mechanism	Component & ID No.	Material	Conseq. of Failure	Mitigation	Repair/Replace	Gaps
	1.3-10 LPCI Nozzles	C&LAS (SA-508, C/2)	A	Water Chemistry BWRVIP-190 BWRVIP-225	ASME Sect. XI IWA-4000	B-DM-06 B-DM-07 B-AS-05 B-AS-07
	1.3-11 LPCI Nozzle Safe Ends (BWR/5)	C&LAS (Carbon Steel)	A	Water Chemistry BWRVIP-190 BWRVIP-225	ASME Sect. XI IWA-4000	B-DM-06 B-DM-07 B-AS-07
	1.3-12 LPCI Nozzle Safe Ends (BWR/5)	Ni-Alloy (A600 with A82/A182 welds)	A	Water Chemistry BWRVIP-190 BWRVIP-225 (Not mitigated by HWC/NMCA/OLNC) Stress Improvement BWRVIP-61 (Weld Overlay, IHSI, MSIP)	ASME Sect. XI IWA-4000 Weld Overlay CC-N-504-2 (Vendor Controlled)	B-DM-03 B-DM-06 B-DM-09 B-DM-10 B-AS-07 B-AS-27 B-MT-01
	1.3-13 CRD Return Line Nozzle (Only BWR/2 not capped or flanged)	C&LAS (SA-508, C/2)	A	Water Chemistry BWRVIP-190 BWRVIP-225	ASME Sect. XI IWA-4000	B-DM-06 B-DM-07 B-AS-05, B-AS-07
	1.3-14 CRD Return Line Nozzle Cap (BWR/3-6)	Ni-Alloy (A600 with A82/A182 welds)	A	Water Chemistry BWRVIP-190 BWRVIP-225 (Not mitigated by HWC/NMCA/OLNC)	ASME Sect. XI IWA-4000	B-DM-03 B-DM-06 B-DM-09 B-AS-07 B-AS-27
	1.3-15 Recirculation Inlet and Outlet Nozzles	C&LAS (SA-508, C/2)	A, G	Water Chemistry BWRVIP-190 BWRVIP-225	ASME Sect. XI IWA-4000	B-MT-01 B-DM-06 B-DM-07 B-AS-05 B-AS-07

Degradation Mechanism	Component & ID No.	Material	Conseq. of Failure	Mitigation	Repair/Replace	Gaps
	1.3-17 Bottom Drain Nozzles	C&LAS (Carbon Steel)	A, G	Water Chemistry BWRVIP-190 BWRVIP-225	ASME Sect. XI IWA-4000 EPRI BWRVIP BWRVIP-208	B-DM-06 B-DM-07 B-I&E-07 B-RR-06
	1.4-1 CRD Stub Tube	Ni-Alloy (A600 with A82/A182 welds)	A, G	Water Chemistry BWRVIP-190 BWRVIP-225 HWC Technology BWRVIP-62 BWRVIP-156 BWRVIP-159 BWRVIP-219	ASME Sect. XI IWA-4000 CC-N-730 EPRI BWRVIP BWRVIP-55-A BWRVIP-58-A BWRVIP- 146NP(R1)	B-DM-03 B-DM-06 B-DM-09 B-AS-07 B-AS-27 B-MT-04 B-MT-05
	1.4-4 CRD Housing Tube (straight-thru design- middle tube)	Ni-Alloy (A600 with A82/A182 welds)	A, G	Water Chemistry BWRVIP-190 BWRVIP-225 HWC Technology BWRVIP-62 BWRVIP-156 BWRVIP-159 BWRVIP-219	ASME Sect. XI IWA-4000 CC-N-730 EPRI BWRVIP BWRVIP-55-A BWRVIP-58-A BWRVIP- 146NP(R1)	B-DM-03 B-DM-06 B-DM-09 B-AS-27 B-MT-04 B-MT-05
	1.5-1 SLC Housing	Ni-Alloy (A600 with A82/A182 welds)	A	Water Chemistry BWRVIP-190 BWRVIP-225 HWC Technology BWRVIP-62 BWRVIP-156 BWRVIP-159 BWRVIP-219	ASME Sect. XI IWA-4000 EPRI BWRVIP BWRVIP-53-A	B-DM-03 B-DM-06 B-DM-09 B-AS-27 B-MT-04 B-MT-05

Degradation Mechanism	Component & ID No.	Material	Conseq. of Failure	Mitigation	Repair/Replace	Gaps
	1.5-3 SLC Nozzle (Full Penetration Weld) (BWR/3-4 B&W, CB&J designs)	C&LAS (SA-508, Cl 2)	A	Water Chemistry BWRVIP-190 BWRVIP-225	ASME Sect. XI IWA-4000 EPRI BWRVIP BWRVIP-53-A	B-DM-06 B-DM-07
	1.5-5 SLC Stub Tube (BWR/6 RDM Vessel Design Only)	Ni-Alloy Weld (A600 with A82/A182 welds)	A	Water Chemistry BWRVIP-190 BWRVIP-225 HWC Technology BWRVIP-62 BWRVIP-156 BWRVIP-159 BWRVIP-219	ASME Sect. XI IWA-4000 EPRI BWRVIP BWRVIP-53-A	B-DM-03 B-DM-06 B-DM-09 B-AS-27 B-MT-04 B-MT-05
	1.6-2 In-Core Housing & Flange	Ni-Alloy Weld (A600 with A82/A182 welds)	A	Water Chemistry BWRVIP-190 BWRVIP-225 HWC Technology BWRVIP-62 BWRVIP-156 BWRVIP-159 BWRVIP-219	ASME Sect. XI IWA-4000 CC-N-769 EPRI BWRVIP BWRVIP-17 BWRVIP-55-A BWRVIP-214NP	B-DM-03 B-DM-06 B-DM-09 B-AS-27 B-MT-04 B-MT-05
	1.7-1 Instrument Penetrations (Water Level and Jet Pump Sensing Lines) (Partial Penetration Welds)	Ni-Alloy Weld (A600 with A82/A182 welds)	A	Water Chemistry BWRVIP-190 BWRVIP-225 HWC Technology BWRVIP-62 BWRVIP-156 BWRVIP-159 BWRVIP-219	ASME Sect. XI IWA-4000 EPRI BWRVIP BWRVIP-57-A	B-DM-03 B-DM-06 B-DM-09 B-AS-27 B-MT-01 B-MT-02 B-MT-04 B-MT-05

Degradation Mechanism	Component & ID No.	Material	Conseq. of Failure	Mitigation	Repair/Replace	Gaps
External: Intergranular/ Transgranular, Pitting	1.7-3 Instrument Penetrations (Water Level and Jet Pump Sensing Lines) (Partial Penetration Welds)	C&LAS (SA-508, Cl 1, SA-541 Cl 1 Mod)	A	Water Chemistry BWRVIP-190 BWRVIP-225	ASME Sect. XI IWA-4000 EPRI BWRVIP BWRVIP-57-A	B-DM-06 B-DM-07 B-AS-05 B-AS-28
	1.9-1 Support Skirt (Skirt Forging, Cylinder, Flange)	C&LAS (A-302, Gr B or SA-533, Gr B, Cl 1)	B	None	ASME Sect. XI IWA-4000	None
	1.10-1 Stabilizer Bracket	C&LAS	B	None	ASME Sect. XI IWA-4000	None
	1.10-2 Top Head Lifting Lugs	C&LAS	B	None	ASME Sect. XI IWA-4000	None
	1.10-3 Insulation Brackets	C&LAS	None	N/A	ASME Sect. XI IWA-4000	B-AS-20 B-MT-05
	1.3-8 Core Spray Nozzle Safe Ends	SS (incl. SS welds)	A	Water Chemistry BWRVIP-190 BWRVIP-225 (Not mitigated by HWC/MMCA/OLNG) Stress Improvement BWRVIP-61 (Weld Overlay, HSI, MSIP)	ASME Sect. XI IWA-4000 Weld Overlay CC-N-504-2 (Vendor Controlled)	B-DM-03 B-DM-06 B-DM-09 B-DM-10 B-AS-07 B-AS-27 B-MT-01 B-MT-02

Degradation Mechanism	Component & ID No.	Material	Conseq. of Failure	Mitigation	Repair/Replace	Gaps
	1.3-16 Recirculation inlet and Outlet Nozzle Safe Ends	SS (304, 316, 316L, 316NG & incl. SS welds) Ni-Alloy (A82/A182 welds)	A, G	Water Chemistry BWRVIP-190 BWRVIP-225 HWC Technology BWRVIP-62 BWRVIP-156 BWRVIP-159 BWRVIP-219 Stress Improvement BWRVIP-61 (Weld Overlay, IHSI, MSIP)	ASME Sect. XI IWA-4000 Weld Overlay CC-N-504-2 (Vendor Controlled)	B-DM-03 B-DM-06 B-DM-09 B-DM-10 B-AS-07 B-AS-27 B-MT-02
	1.4-2 CRD Stub Tube	SS (304 typ., furnace sensitized)	A, G	Water Chemistry BWRVIP-190 BWRVIP-225 HWC Technology BWRVIP-62 BWRVIP-156 BWRVIP-159 BWRVIP-219	ASME Sect. XI IWA-4000 CC-N-730 EPRI BWRVIP BWRVIP-55-A BWRVIP-58-A BWRVIP- 146NP(R1)	B-DM-03 B-DM-06 B-DM-09 B-AS-07 B-AS-27 B-MT-02 B-MT-04 B-MT-05
	1.4-3 CRD Housing Tube, Flange & Cap	SS (304 typ., 304L, 316L)	A, G	Water Chemistry BWRVIP-190 BWRVIP-225 HWC Technology BWRVIP-62 BWRVIP-156 BWRVIP-159 BWRVIP-219	ASME Sect. XI IWA-4000 CC-N-730 EPRI BWRVIP BWRVIP-55-A BWRVIP-58-A BWRVIP- 146NP(R1)	B-DM-06 B-DM-09 B-MT-02 B-MT-04 B-MT-05

Degradation Mechanism	Component & ID No.	Material	Conseq. of Failure	Mitigation	Repair/Replace	Gaps
1. [Degradation of cladding is only significant as related to potential crack propagation into the LAS base metal. Clad degradation may be possibly influenced by neutron effects.]	1.5-2 SLC Housing	SS (304)	A	Water Chemistry BWRVIP-190 BWRVIP-225 HWC Technology BWRVIP-62 BWRVIP-156 BWRVIP-159 BWRVIP-219	ASME Sect. XI IWA-4000 EPRI BWRVIP BWRVIP-53-A	B-DM-03 B-DM-06 B-DM-09 B-AS-27 B-MT-02 B-MT-04 B-MT-05
	1.5-4 SLC Housing / Nozzle Safe End	SS (304) Ni-Alloy (A82/A182 welds)	A	Water Chemistry BWRVIP-190 BWRVIP-225 HWC Technology BWRVIP-62 BWRVIP-156 BWRVIP-159 BWRVIP-219	ASME Sect. XI IWA-4000 EPRI BWRVIP BWRVIP-53-A	B-DM-03 B-DM-06 B-DM-09 B-AS-27 B-MT-02 B-MT-04 B-MT-05
	1.6-1 In-Core Housing & Flange	SS (304 typ.)	A	Water Chemistry BWRVIP-190 BWRVIP-225 HWC Technology BWRVIP-62 BWRVIP-156 BWRVIP-159 BWRVIP-219	ASME Sect. XI IWA-4000 CC-N-769 EPRI BWRVIP BWRVIP-17 BWRVIP-55-A BWRVIP-214NP	B-DM-06 B-DM-09
	1.7-2 Instrument Penetrations (Water Level and Jet Pump Sensing Lines) (Partial Penetration Welds)	SS (304, 308 / 309 welds)	A	Water Chemistry BWRVIP-190 BWRVIP-225 HWC Technology BWRVIP-62 BWRVIP-156 BWRVIP-159 BWRVIP-219	ASME Sect. XI IWA-4000 EPRI BWRVIP BWRVIP-57-A	B-DM-06 B-DM-09 B-MT-01 B-MT-02

APPENDIX B

PWR VESSEL BREAKDOWN FROM IMTs

**Appendix B
PWR Vessel Breakdown from IMTs**

Degradation Mechanism	Component & ID No.	Material	Conseq. of Failure	Mitigation	Repair/Replace	Gaps
Corrosion & Wear: Pitting, Wear	1.1-1 Upper Shell Flange (Vessel Flange)	LAS-SS Clad (SA-336 or A/SA-508, Cl 2 or 3)	A, B, E, F, G	Water Chemistry – Primary EPRI 1014986	ASME Sect. XI IWA-4000	P-DM-09 P-DM-10 P-AS-01 P-AS-02 P-AS-27
	1.7-1 Closure Studs, Nuts, and Washers	LAS (A/SA-540, Cl 2 or 3, Gr B23 or B24)	None	Not Applicable	Not Applicable	Not assigned when no conseq. of failure exists.
Corrosion & Wear: Wear	1.4-1 Bottom Mounted Instrument Guide Tubes (trimble interface)	SS (F304 or F316)	B, E, G	Water Chemistry – Primary EPRI 1014986	ASME Sect. XI IWA-4000	P-DM-09 P-DM-13 P-AS-02 P-AS-09
	1.5-4 Core Guide Lugs	Ni-Alloy (A600 SB-166 or SB- 167 UNS N06600)	None	Not Applicable	Not Applicable	Not assigned when no conseq. of failure exists.
Fatigue: High-Cycle, Low-Cycle- Environmental	1.5-4 Core Guide Lugs	Ni-Alloy (A600 SB-166 or SB- 167 UNS N06600)	None	Not Applicable	Not Applicable	Not assigned when no conseq. of failure exists.
	1.5-5 Attachment Weld – Core Guide Lugs	Weld-Ni-Alloy (A82/A132/A182)	None	Not Applicable	Not Applicable	Not assigned when no conseq. of failure exists.

Degradation Mechanism	Component & ID No.	Material	Conseq. of Failure	Mitigation	Repair/Replace	Gaps
	1.5-6 Flow Baffles (CE)	Ni-Alloy & Welds (A600 SB-168 UNS N06600)	None	Not Applicable	Not Applicable	Not assigned when no conseq. of failure exists.
Fatigue: Low-Cycle- Environmental	1.1-1 Upper Shell Flange (Vessel Flange)	LAS-SS Clad (SA-336 or A/SA-508, Cl 2 or 3)	A, B, E, F, G	Water Chemistry – Primary EPRI 1014986	ASME Sect. XI IWA-4000	P-DM-09 P-DM-10 P-AS-01 P-AS-02 P-AS-27
	1.1-2 Upper Shell Course (Nozzle Course)	LAS-SS Clad (Forging: SA-336 or A/SA-508, CL 2 or 3) (Plate: SA-302 Gr B, SA-533 Gr B Cl 1)	A, B, E, F, G	Water Chemistry – Primary EPRI 1014986	ASME Sect. XI IWA-4000	P-DM-09 P-DM-10 P-AS-01 P-AS-02 P-AS-27 P-AS-28
	1.1-3 Intermediate Shell Course	LAS-SS Clad (Forging: SA-336 or A/SA-508, Cl 2 or 3) (Plate: SA-302 Gr B, SA-533 Gr B Cl 1)	A, B, C, E, F, G	Water Chemistry – Primary EPRI 1014986	ASME Sect. XI IWA-4000	P-DM-09 P-DM-10 P-AS-01 P-AS-02 P-AS-04 P-AS-05 P-AS-06 P-AS-27 P-AS-37

Degradation Mechanism	Component & ID No.	Material	Conseq. of Failure	Mitigation	Repair/Replace	Gaps
	1.1-4 Lower Shell Course	LAS-SS Clad (Forging: SA-336 or A/SA-508, Cl 2 or 3) (Plate: SA-302 Gr B, SA-533 Gr B Cl 1)	A, B, C, E, F, G	Water Chemistry – Primary EPRI 1014986	ASME Sect. XI IWA-4000	P-DM-09 P-DM-10 P-AS-01 P-AS-02 P-AS-04 P-AS-05 P-AS-06 P-AS-27 P-AS-37
	1.1-5 Transition Forging (B&W Only)	LAS-SS Clad (A508 Cl 2)	A, B, C, E, F, G	Water Chemistry – Primary EPRI 1014986	ASME Sect. XI IWA-4000	P-DM-09 P-DM-10 P-AS-01 P-AS-02 P-AS-27
	1.1-6 Bottom Head Transition Course	LAS-SS Clad (Forging: A508 Cl 2) (Plate: SA-302 Gr B, SA-533 Gr B Cl 1)	A, B, C, E, F, G	Water Chemistry – Primary EPRI 1014986	ASME Sect. XI IWA-4000	P-DM-09 P-DM-10 P-AS-01 P-AS-02 P-AS-27
	1.1-7 Bottom Head	LAS-SS Clad (SA-302 Gr B, SA- 533 Gr B Cl 1)	A, B, C, E, F, G	Water Chemistry – Primary EPRI 1014986	ASME Sect. XI IWA-4000	P-DM-09 P-DM-10 P-AS-01 P-AS-02
	1.2-1 Inlet Nozzles	LAS-SS Clad (SA-336 or A/SA-508 Cl 2 or 3)	A, B, E, F, G	Water Chemistry – Primary EPRI 1014986	ASME Sect. XI IWA-4000	P-DM-09 P-DM-10 P-AS-01 P-AS-02 P-AS-28

Degradation Mechanism	Component & ID No.	Material	Conseq. of Failure	Mitigation	Repair/Replace	Gaps
	1.2-2 Outlet Nozzles	LAS-SS Clad (SA-336 or A/SA-508 Cl 2 or 3)	B, E, G	Water Chemistry – Primary EPRI 1014986	ASME Sect. XI IWA-4000	P-DM-09 P-DM-10 P-AS-01 P-AS-02 P-AS-28
	1.2-3 Safe Ends – Inlet and Outlet Nozzles	SS & Welds (SA-182 Gr F304 or F316)	Inlet: A, B, E, F, G Outlet: B, E, G	Water Chemistry – Primary EPRI 1014986	ASME Sect. XI IWA-4000	P-DM-09 P-DM-13 P-AS-02 P-AS-09
	1.2-4 DM Welds – Inlet and Outlet Nozzles	Weld-Ni-Alloy (A82/A182)	Inlet: A, B, E, F, G Outlet: B, E, G	Water Chemistry – Primary EPRI 1014986 EPRI 1013420 (Zn Application) MRP-213 (H ₂ Optimization) Stress Improvement MRP-126 MRP-121 MS/P Peening (Laser or Mechanical)	ASME Sect. XI IWA-4000 Weld Overlay CC-N-740-2 MRP-169R1 MRP-208 Material Mod. Weld Excavation Weld Inlay SCRIP (MRP-194)	P-DM-09 P-DM-14 P-AS-02 P-AS-11 P-MT-01 P-MT-09 P-RG-09 P-RR-04
	1.2-5 Core Flood Nozzle (CFN) (B&W)	LAS-SS Clad (A 508 Cl 2)	A, B, E, F, G	Water Chemistry – Primary EPRI 1014986	ASME Sect. XI IWA-4000	P-DM-09 P-DM-10 P-AS-01 P-AS-02
	1.2-6 Safe Ends – Core Flood Nozzle (B&W)	SS & Welds (SA-336 Cl F8M) (SS Weld Buildup)	A, B, E, F, G	Water Chemistry – Primary EPRI 1014986	ASME Sect. XI IWA-4000	P-DM-09 P-DM-13 P-AS-02 P-AS-09

Degradation Mechanism	Component & ID No.	Material	Conseq. of Failure	Mitigation	Repair/Replace	Gaps
	1.2-7 DM Welds – Core Flood Nozzle (B&W)	Weld-Ni-Alloy (A82/A182)	A, B, E, F, G	Water Chemistry – Primary EPRI 1014986 EPRI 1013420 (Zn Application) MRP-213 (H ₂ Optimization) Stress Improvement MRP-126 MRP-121 MS/IP Peening (Laser or Mechanical)	ASME Sect. XI IWA-4000 Weld Overlay CC-N-740-2 MRP-169R1 MRP-208 Material Mod. Weld Excavation Weld Inlay SCrP (MRP-194)	P-DM-09 P-DM-14 P-AS-02 P-AS-11 P-MT-01 P-MT-09 P-RG-09 P-RR-04
	1.2-8 Safety Injection (SI) Nozzles (Westinghouse)	LAS (SA-336 or SA-508 C/2 or 3)	A, B, E, F, G	Water Chemistry – Primary EPRI 1014986	ASME Sect. XI IWA-4000	P-DM-09 P-DM-10 P-AS-01 P-AS-02
	1.2-9 Safe Ends – SI Nozzles (Westinghouse)	SS & Welds (SA-182 Gr F304 or F316)	A, B, E, F, G	Water Chemistry – Primary EPRI 1014986	ASME Sect. XI IWA-4000	P-DM-09 P-DM-13 P-AS-02 P-AS-09
	1.2-10 DM Welds – SI Nozzles (Westinghouse)	Weld- Ni-Alloy (A82/A182)	A, B, E, F, G	Water Chemistry – Primary EPRI 1014986 EPRI 1013420 (Zn Application) MRP-213 (H ₂ Optimization) Stress Improvement MRP-126 MRP-121 MS/IP Peening (Laser or Mechanical)	ASME Sect. XI IWA-4000 Weld Overlay CC-N-740-2 MRP-169R1 MRP-208 Material Mod. Weld Excavation Weld Inlay SCrP (MRP-194)	P-DM-09 P-DM-14 P-AS-02 P-AS-11 P-MT-01 P-MT-09 P-RG-09 P-RR-04

Degradation Mechanism	Component & ID No.	Material	Conseq. of Failure	Mitigation	Repair/Replace	Gaps
	1.3-1 Bottom Mounted Nozzles	Ni-Alloy (A600 SB-166 or SB-167 UNS N06600)	B, E, G	Water Chemistry – Primary EPRI 1014986 EPRI 1013420 (Zn Application) MRP-213 (H ₂ Optimization)	ASME Sect. XI IWA-4000 MNSA (vendor controlled)	P-DM-09 P-AS-02 P-AS-11 P-MT-01 P-MT-02 P-MT-09 P-I&E-02
	1.3-2 DM Welds – Bottom Mounted Nozzles	Weld-Ni-Alloy (A82/A182)	B, E, G	Water Chemistry – Primary EPRI 1014986 EPRI 1013420 (Zn Application) MRP-213 (H ₂ Optimization)	ASME Sect. XI IWA-4000 MNSA (vendor controlled)	P-DM-09 P-AS-02 P-AS-11 P-MT-01 P-MT-02 P-MT-09 P-I&E-02 P-I&E-03
	1.3-3 Safe Ends – Bottom Mounted Nozzles (IMI Nozzles)	SS & Welds (SA-182 Gr F304 or F316)	B, E, G	Water Chemistry – Primary EPRI 1014986	ASME Sect. XI IWA-4000	P-DM-09 P-DM-13 P-AS-02 P-AS-09
	1.3-4 Repair Pieces – Bottom Mounted Nozzles (IMI Nozzles) (B&W)	Ni-Alloy (A600 SB-166 or SB-167 UNS N06600)	G	Water Chemistry – Primary EPRI 1014986 EPRI 1013420 (Zn Application) MRP-213 (H ₂ Optimization)	ASME Sect. XI IWA-4000	P-DM-09 P-AS-02 P-AS-11 P-MT-01 P-MT-02 P-MT-09

Degradation Mechanism	Component & ID No.	Material	Conseq. of Failure	Mitigation	Repair/Replace	Gaps
	1.3-5 Repair Pieces – Attachment Weld (B&W)	Weld-Ni-Alloy (A82/A182)	G	Water Chemistry – Primary EPRI 1014986 EPRI 1013420 (Zn Application) MRP-213 (H ₂ Optimization)	ASME Sect. XI IWA-4000	P-DM-09 P-AS-02 P-AS-11 P-MT-01 P-MT-02 P-MT-09
	1.4-1 Bottom Mounted Instrument Guide Tubes	SS (F304 or F316)	B, E, G	Water Chemistry – Primary EPRI 1014986	ASME Sect. XI IWA-4000	P-DM-09 P-DM-13
	1.4-2 Seal Table	SS (Type 316)	B, E, G	Water Chemistry – Primary EPRI 1014986	ASME Sect. XI IWA-4000	P-AS-02 P-AS-09
	1.4-3 Seal Table Fitting	SS (Type 316)	B, E	Water Chemistry – Primary EPRI 1014986	ASME Sect. XI IWA-4000	P-DM-09 P-DM-13
	1.5-1 CFN Flow Restrictor (B&W Only)	SS & Welds (SA-376 Gr TP304 or SA-182 Gr F304)	B, E, F, G	Water Chemistry – Primary EPRI 1014986	None	P-AS-02 P-AS-09
	1.5-2 Flow Stabilizers (Turning Vanes) (B&W)	SS (A 240 Type 304)	None	Not Applicable	Not Applicable	P-DM-09 P-DM-13 P-AS-02 P-AS-09
						Not assigned when no conseq. of failure exists.

Degradation Mechanism	Component & ID No.	Material	Conseq. of Failure	Mitigation	Repair/Replace	Gaps
	1.5-3 Attachment Welds – Flow Stabilizers (Turning Vanes) (B&W)	Weld-Ni-Alloy (A82/A182)	None	Not Applicable	Not Applicable	Not assigned when no conseq. of failure exists.
	1.5-7 Core Stop Lugs (CE)	Ni-Alloy	None	Not Applicable	Not Applicable	Not assigned when no conseq. of failure exists.
	1.5-8 Attachment Weld – Core Stop Lugs (CE)	Weld-Ni-Alloy	None	Not Applicable	Not Applicable	Not assigned when no conseq. of failure exists.
	1.6-1 Support Skirt & Flange (B&W)	CS (SA-516 Gr 70)	None	Not Applicable	Not Applicable	Not assigned when no conseq. of failure exists.
	1.6-2 Anchor Bolts and Nuts – Support Skirt & Flange (B&W)	LAS (A 490)	None	Not Applicable	Not Applicable	Not assigned when no conseq. of failure exists.
	1.6-3 Dowel (Shear) Pins – Support Skirt (B&W)	LAS (A 490)	None	Not Applicable	Not Applicable	Not assigned when no conseq. of failure exists.

Degradation Mechanism	Component & ID No.	Material	Conseq. of Failure	Mitigation	Repair/Replace	Gaps
Reduction in Fracture Properties: Thermal, Environmental	1.6-4 External Support Brackets (Westinghouse)	LAS (SA-212 Gr B, SA-516 Gr 70 or SA-533 Gr B, Cl 1)	None	Not Applicable	Not Applicable	Not assigned when no conseq. of failure exists.
	1.7-1 Closure Studs, Nuts, and Washers	LAS (A/SA-540, Cl 2 or 3, Gr B23 or B24)	None	Not Applicable	Not Applicable	Not assigned when no conseq. of failure exists.
	1.1-1 Upper Shell Flange (Vessel Flange)	LAS-SS Clad (SA-336 or A/SA-508, Cl 2 or 3)	A, B, E, F, G	Water Chemistry - Primary EPRI 1014986	ASME Sect. XI IWA-4000	P-DM-09 P-DM-10 P-AS-01, P-AS-02, P-AS-27
	1.1-2 Upper Shell Course (Nozzle Course)	LAS-SS Clad (Forging: SA-336 or A/SA-508, CL 2 or 3) (Plate: SA-302 Gr B, SA-533 Gr B Cl 1)	A, B, E, F, G	Water Chemistry - Primary EPRI 1014986	ASME Sect. XI IWA-4000	P-DM-09 P-DM-10 P-AS-01 P-AS-02 P-AS-27 P-AS-28
	1.1-3 Intermediate Shell Course	LAS-SS Clad (Forging: SA-336 or A/SA-508, Cl 2 or 3) (Plate: SA-302 Gr B, SA-533 Gr B Cl 1)	A, B, C, E, F, G	Water Chemistry - Primary EPRI 1014986	ASME Sect. XI IWA-4000	P-DM-09 P-DM-10 P-AS-01 P-AS-02 P-AS-04 P-AS-05 P-AS-06 P-AS-27 P-AS-37

Degradation Mechanism	Component & ID No.	Material	Conseq. of Failure	Mitigation	Repair/Replace	Gaps
	1.1-4 Lower Shell Course	LAS-SS Clad (Forging: SA-336 or A/SA-508, Cl 2 or 3) (Plate: SA-302 Gr B, SA-533 Gr B Cl 1)	A, B, C, E, F, G	Water Chemistry – Primary EPRI 1014986	ASME Sect. XI IWA-4000	P-DM-09 P-DM-10 P-AS-01 P-AS-02 P-AS-04 P-AS-05 P-AS-06 P-AS-27 P-AS-37
	1.1-5 Transition Forging (B&W Only)	LAS-SS Clad (A508 Cl 2)	A, B, C, E, F, G	Water Chemistry – Primary EPRI 1014986	ASME Sect. XI IWA-4000	P-DM-09 P-DM-10 P-AS-01 P-AS-02 P-AS-27
	1.1-6 Bottom Head Transition Course	LAS-SS Clad (Forging: A508 Cl 2) (Plate: SA-302 Gr B, SA-533 Gr B Cl 1)	A, B, C, E, F, G	Water Chemistry – Primary EPRI 1014986	ASME Sect. XI IWA-4000	P-DM-09 P-DM-10 P-AS-01 P-AS-02 P-AS-27
	1.1-7 Bottom Head	LAS-SS Clad (SA-302 Gr B, SA- 533 Gr B Cl 1)	A, B, C, E, F, G	Water Chemistry – Primary EPRI 1014986	ASME Sect. XI IWA-4000	P-DM-09 P-DM-10 P-AS-01 P-AS-02
	1.2-1 Inlet Nozzles	LAS-SS Clad (SA-336 or A/SA-508 Cl 2 or 3)	A, B, E, F, G	Water Chemistry – Primary EPRI 1014986	ASME Sect. XI IWA-4000	P-DM-09 P-DM-10 P-AS-01 P-AS-02 P-AS-28

Degradation Mechanism	Component & ID No.	Material	Conseq. of Failure	Mitigation	Repair/Replace	Gaps
Reduction in Fracture Properties: Environmental	1.2-2 Outlet Nozzles	LAS-SS Clad (SA-336 or A/SA-508 Cl 2 or 3)	B, E, G	Water Chemistry – Primary EPRI 1014986	ASME Sect. XI IWA-4000	P-DM-09 P-DM-10 P-AS-01 P-AS-02 P-AS-28
	1.2-5 Core Flood Nozzle (CFN) (B&W)	LAS-SS Clad (A 508 Cl 2)	A, B, E, F, G	Water Chemistry – Primary EPRI 1014986	ASME Sect. XI IWA-4000	P-DM-09 P-DM-10 P-AS-01 P-AS-02
	1.2-8 Safety Injection (SI) Nozzles (Westinghouse)	LAS (SA-336 or SA-508 Cl 2 or 3)	A, B, E, F, G	Water Chemistry – Primary EPRI 1014986	ASME Sect. XI IWA-4000	P-DM-09 P-DM-10 P-AS-01 P-AS-02
	1.2-3 Safe Ends – Inlet and Outlet Nozzles	SS & Welds (SA-182 Gr F304 or F316)	Inlet: A, B, E, F, G Outlet: B, E, G	Water Chemistry – Primary EPRI 1014986	ASME Sect. XI IWA-4000	P-DM-09 P-DM-13 P-AS-02 P-AS-09
	1.2-4 DM Welds – Inlet and Outlet Nozzles	Weld-Ni-Alloy (A82/A182)	Inlet: A, B, E, F, G Outlet: B, E, G	Water Chemistry – Primary EPRI 1014986 EPRI 1013420 (Zn Application) MRP-213 (H ₂ Optimization) Stress Improvement MRP-126 MRP-121 MS/IP Peening (Laser or Mechanical)	ASME Sect. XI IWA-4000 Weld Overlay CC-N-740-2 MRP-169R1 MRP-208 Material Mod. Weld Excavation Weld Inlay SCrP (MRP-194)	P-DM-09 P-DM-14 P-AS-02 P-AS-11 P-MT-01 P-MT-09 P-RG-09 P-RR-04

Degradation Mechanism	Component & ID No.	Material	Conseq. of Failure	Mitigation	Repair/Replace	Gaps
	1.2-6 Safe Ends – Core Flood Nozzle (B&W)	SS & Welds (SA-336 Cl F8M) (SS Weld Buildup)	A, B, E, F, G	Water Chemistry – Primary EPRI 1014986	ASME Sect. XI IWA-4000	P-DM-09 P-DM-13 P-AS-02 P-AS-09
	1.2-7 DM Welds – Core Flood Nozzle (B&W)	Weld-Ni-Alloy (A82/A182)	A, B, E, F, G	Water Chemistry – Primary EPRI 1014986 EPRI 1013420 (Zn Application) MRP-213 (H ₂ Optimization) Stress Improvement MRP-126 MRP-121 MS/IP Peening (Laser or Mechanical)	ASME Sect. XI IWA-4000 Weld Overlay CC-N-740-2 MRP-169R1 MRP-208 Material Mod. Weld Excavation Weld Inlay SCrP (MRP-194)	P-DM-09 P-DM-14 P-AS-02 P-AS-11 P-MT-01 P-MT-09 P-RG-09 P-RR-04
	1.2-9 Safe Ends – SI Nozzles (Westinghouse)	SS & Welds (SA-182 Gr F304 or F316)	A, B, E, F, G	Water Chemistry – Primary EPRI 1014986	ASME Sect. XI IWA-4000	P-DM-09 P-DM-13 P-AS-02 P-AS-09
	1.2-10 DM Welds – SI Nozzles (Westinghouse)	Weld- Ni-Alloy (A82/A182)	A, B, E, F, G	Water Chemistry – Primary EPRI 1014986 EPRI 1013420 (Zn Application) MRP-213 (H ₂ Optimization) Stress Improvement MRP-126 MRP-121 MS/IP Peening (Laser or Mechanical)	ASME Sect. XI IWA-4000 Weld Overlay CC-N-740-2 MRP-169R1 MRP-208 Material Mod. Weld Excavation Weld Inlay SCrP (MRP-194)	P-DM-09 P-DM-14 P-AS-02 P-AS-11 P-MT-01 P-MT-09 P-RG-09 P-RR-04

Degradation Mechanism	Component & ID No.	Material	Conseq. of Failure	Mitigation	Repair/Replace	Gaps
	1.3-1 Bottom Mounted Nozzles	Ni-Alloy (A600 SB-166 or SB-167 UNS N06600)	B, E, G	Water Chemistry – Primary EPRI 1014986 EPRI 1013420 (Zn Application) MRP-213 (H ₂ Optimization)	ASME Sect. XI IWA-4000 MNSA (vendor controlled)	P-DM-09 P-AS-02 P-AS-11 P-MT-01 P-MT-02 P-MT-09 P-I&E-02
	1.3-2 DM Welds – Bottom Mounted Nozzles	Weld-Ni-Alloy (A82/A182)	B, E, G	Water Chemistry – Primary EPRI 1014986 EPRI 1013420 (Zn Application) MRP-213 (H ₂ Optimization)	ASME Sect. XI IWA-4000 MNSA (vendor controlled)	P-DM-09 P-AS-02 P-AS-11 P-MT-01 P-MT-02 P-MT-09 P-I&E-02 P-I&E-03
	1.3-3 Safe Ends – Bottom Mounted Nozzles (IMI Nozzles)	SS & Welds (SA-182 Gr F304 or F316)	B, E, G	Water Chemistry – Primary EPRI 1014986	ASME Sect. XI IWA-4000	P-DM-09 P-DM-13 P-AS-02 P-AS-09
	1.3-4 Repair Pieces – Bottom Mounted Nozzles (IMI Nozzles) (B&W)	Ni-Alloy (A600 SB-166 or SB-167 UNS N06600)	G	Water Chemistry – Primary EPRI 1014986 EPRI 1013420 (Zn Application) MRP-213 (H ₂ Optimization)	ASME Sect. XI IWA-4000	P-DM-09 P-AS-02 P-AS-11 P-MT-01 P-MT-02 P-MT-09

Degradation Mechanism	Component & ID No.	Material	Conseq. of Failure	Mitigation	Repair/Replace	Gaps
	1.3-5 Repair Pieces – Attachment Weld (B&W)	Weld-Ni-Alloy (A82/A182)	G	Water Chemistry – Primary EPRI 1014986 EPRI 1013420 (Zn Application) MRP-213 (H ₂ Optimization)	ASME Sect. XI IWA-4000	P-DM-09 P-AS-02 P-AS-11 P-MT-01 P-MT-02 P-MT-09
	1.4-1 Bottom Mounted Instrument Guide Tubes	SS (F304 or F316)	B, E, G	Water Chemistry – Primary EPRI 1014986	ASME Sect. XI IWA-4000	P-DM-09 P-DM-13
	1.4-2 Seal Table	SS (Type 316)	B, E, G	Water Chemistry – Primary EPRI 1014986	ASME Sect. XI IWA-4000	P-AS-02 P-AS-09
	1.4-3 Seal Table Fitting	SS (Type 316)	B, E	Water Chemistry – Primary EPRI 1014986	ASME Sect. XI IWA-4000	P-DM-09 P-DM-13
	1.5-1 CFN Flow Restrictor (B&W Only)	SS & Welds (SA-376 Gr TP304 or SA-182 Gr F304)	B, E, F, G	Water Chemistry – Primary EPRI 1014986	None	P-AS-02 P-AS-09
	1.5-2 Flow Stabilizers (Turning Vanes) (B&W)	SS (A 240 Type 304)	None	Not Applicable	Not Applicable	P-DM-09 P-DM-13 P-AS-02 P-AS-09 Not assigned when no conseq. of failure exists.

Degradation Mechanism	Component & ID No.	Material	Conseq. of Failure	Mitigation	Repair/Replace	Gaps
	1.5-3 Attachment Welds – Flow Stabilizers (Turning Vanes) (B&W)	Weld-Ni-Alloy (A82/A182)	None	Not Applicable	Not Applicable	Not assigned when no conseq. of failure exists.
	1.5-4 Core Guide Lugs	Ni-Alloy (A600 SB-166 or SB-167 UNS N06600)	None	Not Applicable	Not Applicable	Not assigned when no conseq. of failure exists.
	1.5-5 Attachment Weld – Core Guide Lugs	Weld-Ni-Alloy (A82/A132/A182)	None	Not Applicable	Not Applicable	Not assigned when no conseq. of failure exists.
	1.5-6 Flow Baffles (CE)	Ni-Alloy & Welds (A600 SB-168 UNS N06600)	None	Not Applicable	Not Applicable	Not assigned when no conseq. of failure exists.
	1.5-7 Core Stop Lugs (CE)	Ni-Alloy	None	Not Applicable	Not Applicable	Not assigned when no conseq. of failure exists.
	1.5-8 Attachment Weld – Core Stop Lugs (CE)	Weld-Ni-Alloy	None	Not Applicable	Not Applicable	Not assigned when no conseq. of failure exists.

Degradation Mechanism	Component & ID No.	Material	Conseq. of Failure	Mitigation	Repair/Replace	Gaps
Reduction in Fracture Properties: Thermal	1.7-1 Closure Studs, Nuts, and Washers	LAS (A/SA-540, Cl 2 or 3, Gr B23 or B24)	None	Not Applicable	Not Applicable	Not assigned when no conseq. of failure exists.
	External: Wastage, Pitting	LAS-SS Clad (SA-336 or A/SA-508, Cl 2 or 3)	A, B, E, F, G	Water Chemistry - Primary EPRI 1014986	ASME Sect. XI IWA-4000	P-DM-09 P-DM-10 P-AS-01 P-AS-02 P-AS-27
Reduction in Fracture Properties: Thermal	1.1-1 Upper Shell Flange (Vessel Flange)	LAS-SS Clad (Forging: SA-336 or A/SA-508, CL 2 or 3) (Plate: SA-302 Gr B, SA-533 Gr B Cl 1)	A, B, E, F, G	Water Chemistry - Primary EPRI 1014986	ASME Sect. XI IWA-4000	P-DM-09 P-DM-10 P-AS-01 P-AS-02 P-AS-27 P-AS-28
	1.1-2 Upper Shell Course (Nozzle Course)	LAS-SS Clad (Forging: SA-336 or A/SA-508, CL 2 or 3) (Plate: SA-302 Gr B, SA-533 Gr B Cl 1)	A, B, E, F, G	Water Chemistry - Primary EPRI 1014986	ASME Sect. XI IWA-4000	P-DM-09 P-DM-10 P-AS-01 P-AS-02 P-AS-27 P-AS-28
Reduction in Fracture Properties: Thermal	1.1-3 Intermediate Shell Course	LAS-SS Clad (Forging: SA-336 or A/SA-508, Cl 2 or 3) (Plate: SA-302 Gr B, SA-533 Gr B Cl 1)	A, B, C, E, F, G	Water Chemistry - Primary EPRI 1014986	ASME Sect. XI IWA-4000	P-DM-09 P-DM-10 P-AS-01 P-AS-02 P-AS-04 P-AS-05 P-AS-06 P-AS-27 P-AS-37

Degradation Mechanism	Component & ID No.	Material	Conseq. of Failure	Mitigation	Repair/Replace	Gaps
	1.1-4 Lower Shell Course	LAS-SS Clad (Forging: SA-336 or A/SA-508, Cl 2 or 3) (Plate: SA-302 Gr B, SA-533 Gr B Cl 1)	A, B, C, E, F, G	Water Chemistry – Primary EPRI 1014986	ASME Sect. XI IWA-4000	P-DM-09 P-DM-10 P-AS-01 P-AS-02 P-AS-04 P-AS-05 P-AS-06 P-AS-27 P-AS-37
	1.1-5 Transition Forging (B&W Only)	LAS-SS Clad (A508 Cl 2)	A, B, C, E, F, G	Water Chemistry – Primary EPRI 1014986	ASME Sect. XI IWA-4000	P-DM-09 P-DM-10 P-AS-01 P-AS-02 P-AS-27
	1.1-6 Bottom Head Transition Course	LAS-SS Clad (Forging: A508 Cl 2) (Plate: SA-302 Gr B, SA-533 Gr B Cl 1)	A, B, C, E, F, G	Water Chemistry – Primary EPRI 1014986	ASME Sect. XI IWA-4000	P-DM-09 P-DM-10 P-AS-01 P-AS-02 P-AS-27
	1.1-7 Bottom Head	LAS-SS Clad (SA-302 Gr B, SA- 533 Gr B Cl 1)	A, B, C, E, F, G	Water Chemistry – Primary EPRI 1014986	ASME Sect. XI IWA-4000	P-DM-09 P-DM-10 P-AS-01 P-AS-02
	1.2-1 Inlet Nozzles	LAS-SS Clad (SA-336 or A/SA-508 Cl 2 or 3)	A, B, E, F, G	Water Chemistry – Primary EPRI 1014986	ASME Sect. XI IWA-4000	P-DM-09 P-DM-10 P-AS-01 P-AS-02 P-AS-28

Degradation Mechanism	Component & ID No.	Material	Conseq. of Failure	Mitigation	Repair/Replace	Gaps
	1.2-2 Outlet Nozzles	LAS-SS Clad (SA-336 or A/SA-508 Cl 2 or 3)	B, E, G	Water Chemistry – Primary EPRI 1014986	ASME Sect. XI IWA-4000	P-DM-09 P-DM-10 P-AS-01 P-AS-02 P-AS-28
	1.2-5 Core Flood Nozzle (CFN) (B&W)	LAS-SS Clad (A 508 Cl 2)	A, B, E, F, G	Water Chemistry – Primary EPRI 1014986	ASME Sect. XI IWA-4000	P-DM-09 P-DM-10 P-AS-01 P-AS-02
	1.2-8 Safety Injection (SI) Nozzles (Westinghouse)	LAS (SA-336 or SA-508 Cl 2 or 3)	A, B, E, F, G	Water Chemistry – Primary EPRI 1014986	ASME Sect. XI IWA-4000	P-DM-09 P-DM-10 P-AS-01 P-AS-02
	1.6-1 Support Skirt & Flange (B&W)	CS (SA-516 Gr 70)	None	Not Applicable	Not Applicable	Not assigned when no conseq. of failure exists.
	1.6-2 Anchor Bolts and Nuts – Support Skirt & Flange (B&W)	LAS (A 490)	None	Not Applicable	Not Applicable	Not assigned when no conseq. of failure exists.
	1.6-3 Dowel (Shear) Pins – Support Skirt (B&W)	LAS (A 490)	None	Not Applicable	Not Applicable	Not assigned when no conseq. of failure exists.

Degradation Mechanism	Component & ID No.	Material	Conseq. of Failure	Mitigation	Repair/Replace	Gaps
External: Pitting	1.6-4 External Support Brackets (Westinghouse)	LAS (SA-212 Gr B, SA-516 Gr 70 or SA-533 Gr B, Cl 1)	None	Not Applicable	Not Applicable	Not assigned when no conseq. of failure exists.
	1.2-3 Safe Ends – Inlet and Outlet Nozzles	SS & Welds (SA-182 Gr F304 or F316)	Inlet: A, B, E, F, G Outlet: B, E, G	Water Chemistry – Primary EPRI 1014986	ASME Sect. XI IWA-4000	P-DM-09 P-DM-13 P-AS-02 P-AS-09
	1.2-6 Safe Ends – Core Flood Nozzle (B&W)	SS & Welds (SA-336 Cl F8M) (SS Weld Buildup)	A, B, E, F, G	Water Chemistry – Primary EPRI 1014986	ASME Sect. XI IWA-4000	P-DM-09 P-DM-13 P-AS-02 P-AS-09
	1.2-9 Safe Ends – SI Nozzles (Westinghouse)	SS & Welds (SA-182 Gr F304 or F316)	A, B, E, F, G	Water Chemistry – Primary EPRI 1014986	ASME Sect. XI IWA-4000	P-DM-09 P-DM-13 P-AS-02 P-AS-09
	1.3-1 Bottom Mounted Nozzles	NI-Alloy (A600 SB-166 or SB-167 UNS N06600)	B, E, G	Water Chemistry – Primary EPRI 1014986 EPRI 1013420 (Zn Application) MRP-213 (H ₂ Optimization)	ASME Sect. XI IWA-4000 MNSA (vendor controlled)	P-DM-09 P-AS-02 P-AS-11 P-MT-01 P-MT-02 P-MT-09 P-I&E-02
	1.3-3 Safe Ends – Bottom Mounted Nozzles (IMI)	SS & Welds (SA-182 Gr F304 or F316)	B, E, G	Water Chemistry – Primary EPRI 1014986	ASME Sect. XI IWA-4000	P-DM-09 P-DM-13 P-AS-02 P-AS-09

Degradation Mechanism	Component & ID No.	Material	Conseq. of Failure	Mitigation	Repair/Replace	Gaps
External: Stress Corrosion Cracking, Pitting	1.3-4 Repair Pieces – Bottom Mounted Nozzles (IMI Nozzles) (B&W)	Ni-Alloy (A600 SB-166 or SB- 167 UNS N06600)	G	Water Chemistry – Primary EPRI 1014986 EPRI 1013420 (Zn Application) MRP-213 (H ₂ Optimization)	ASME Sect. XI IWA-4000	P-DM-09 P-AS-02 P-AS-11 P-MT-01 P-MT-02 P-MT-09
	1.4-1 Bottom Mounted Instrument Guide Tubes	SS (F304 or F316)	B, E, G	Water Chemistry – Primary EPRI 1014986	ASME Sect. XI IWA-4000	P-DM-09 P-DM-13 P-AS-02 P-AS-09
	1.4-2 Seal Table	SS (Type 316)	B, E, G	Water Chemistry – Primary EPRI 1014986	ASME Sect. XI IWA-4000	P-DM-09 P-DM-13 P-AS-02 P-AS-09
	1.4-3 Seal Table Fitting	SS (Type 316)	B, E	Water Chemistry – Primary EPRI 1014986	ASME Sect. XI IWA-4000	P-DM-09 P-DM-13 P-AS-02 P-AS-09
	1.2-4 DM Welds – Inlet and Outlet Nozzles	Weld-Ni-Alloy (A82/A182)	Inlet: A, B, E, F, G Outlet: B, E, G	Water Chemistry – Primary EPRI 1014986 EPRI 1013420 (Zn Application) MRP-213 (H ₂ Optimization) Stress Improvement MRP-126 MRP-121 MS/IP Peening (Laser or Mechanical)	ASME Sect. XI IWA-4000 Weld Overlay CC-N-740-2 MRP-169R1 MRP-208 Material Mod. Weld Excavation Weld Inlay SCrP (MRP-194)	P-DM-09 P-DM-14 P-AS-02 P-AS-11 P-MT-01 P-MT-09 P-RG-09 P-RR-04

Degradation Mechanism	Component & ID No.	Material	Conseq. of Failure	Mitigation	Repair/Replace	Gaps
	1.2-7 DM Welds – Core Flood Nozzle (B&W)	Weld-Ni-Alloy (A82/A182)	A, B, E, F, G	Water Chemistry – Primary EPRI 1014986 EPRI 1013420 <i>(Zn Application)</i> MRP-213 <i>(H₂ Optimization)</i> Stress Improvement MRP-126 MRP-121 MS/IP Peening <i>(Laser or Mechanical)</i>	ASME Sect. XI IWA-4000 Weld Overlay CC-N-740-2 MRP-169R1 MRP-208 Material Mod. Weld Excavation Weld Inlay SCrP (MRP-194)	P-DM-09 P-DM-14 P-AS-02 P-AS-11 P-MT-01 P-MT-09 P-RG-09 P-RR-04
	1.2-10 DM Welds – SI Nozzles (Westinghouse)	Weld- Ni-Alloy (A82/A182)	A, B, E, F, G	Water Chemistry – Primary EPRI 1014986 EPRI 1013420 <i>(Zn Application)</i> MRP-213 <i>(H₂ Optimization)</i> Stress Improvement MRP-126 MRP-121 MS/IP Peening <i>(Laser or Mechanical)</i>	ASME Sect. XI IWA-4000 Weld Overlay CC-N-740-2 MRP-169R1 MRP-208 Material Mod. Weld Excavation Weld Inlay SCrP (MRP-194)	P-DM-09 P-DM-14 P-AS-02 P-AS-11 P-MT-01 P-MT-09 P-RG-09 P-RR-04
	1.3-2 DM Welds – Bottom Mounted Nozzles	Weld-Ni-Alloy (A82/A182)	B, E, G	Water Chemistry – Primary EPRI 1014986 EPRI 1013420 <i>(Zn Application)</i> MRP-213 <i>(H₂ Optimization)</i>	ASME Sect. XI IWA-4000 MNSA <i>(vendor controlled)</i>	P-DM-09 P-AS-02 P-AS-11 P-MT-01 P-MT-02 P-MT-09 P-I&E-02 P-I&E-03

Degradation Mechanism	Component & ID No.	Material	Conseq. of Failure	Mitigation	Repair/Replace	Gaps
Irradiation Effects: Embrittlement	1.3-5 Repair Pieces – Attachment Weld (B&W)	Weld-Ni-Alloy (A82/A182)	G	Water Chemistry – Primary EPRI 1014986 EPRI 1013420 (Zn Application) MRP-213 (H ₂ Optimization)	ASME Sect. XI IWA-4000	P-DM-09 P-AS-02 P-AS-11 P-MT-01 P-MT-02 P-MT-09
	1.1-2 Upper Shell Course (Nozzle Course)	LAS-SS Clad (Forging: SA-336 or A/SA-508, CL 2 or 3) (Plate: SA-302 Gr B, SA-533 Gr B Cl 1)	A, B, E, F, G	Water Chemistry – Primary EPRI 1014986	ASME Sect. XI IWA-4000	P-DM-09 P-DM-10 P-AS-01 P-AS-02 P-AS-27 P-AS-28
	1.1-3 Intermediate Shell Course	LAS-SS Clad (Forging: SA-336 or A/SA-508, Cl 2 or 3) (Plate: SA-302 Gr B, SA-533 Gr B Cl 1)	A, B, C, E, F, G	Water Chemistry – Primary EPRI 1014986	ASME Sect. XI IWA-4000	P-DM-09 P-DM-10 P-AS-01 P-AS-02 P-AS-04 P-AS-05 P-AS-06 P-AS-27 P-AS-37
	1.1-4 Lower Shell Course	LAS-SS Clad (Forging: SA-336 or A/SA-508, Cl 2 or 3) (Plate: SA-302 Gr B, SA-533 Gr B Cl 1)	A, B, C, E, F, G	Water Chemistry – Primary EPRI 1014986	ASME Sect. XI IWA-4000	P-DM-09 P-DM-10 P-AS-01 P-AS-02 P-AS-04 P-AS-05 P-AS-06 P-AS-27 P-AS-37

Degradation Mechanism	Component & ID No.	Material	Conseq. of Failure	Mitigation	Repair/Replace	Gaps
Stress Corrosion Cracking: Intergranular/Transgranular	1.2-1 Inlet Nozzles	LAS-SS Clad (SA-336 or A/SA-508 Cl 2 or 3)	A, B, E, F, G	Water Chemistry – Primary EPRI 1014986	ASME Sect. XI IWA-4000	P-DM-09 P-DM-10 P-AS-01 P-AS-02 P-AS-28
	1.2-2 Outlet Nozzles	LAS-SS Clad (SA-336 or A/SA-508 Cl 2 or 3)	B, E, G	Water Chemistry – Primary EPRI 1014986	ASME Sect. XI IWA-4000	P-DM-09 P-DM-10 P-AS-01 P-AS-02 P-AS-28
	1.2-3 Safe Ends – Inlet and Outlet Nozzles	SS & Welds (SA-782 Gr F304 or F316)	Inlet: A, B, E, F, G Outlet: B, E, G	Water Chemistry – Primary EPRI 1014986	ASME Sect. XI IWA-4000	P-DM-09 P-DM-13 P-AS-02 P-AS-09
	1.2-4 DM Welds – Inlet and Outlet Nozzles	Weld-Ni-Alloy (A82/A182)	Inlet: A, B, E, F, G Outlet: B, E, G	Water Chemistry – Primary EPRI 1014986 (Zn Application) MRP-213 (H ₂ Optimization) Stress Improvement MRP-126 MRP-121 MSIP Peening (Laser or Mechanical)	ASME Sect. XI IWA-4000 Weld Overlay CC-N-740-2 MRP-169R1 MRP-208 Material Mod. Weld Excavation Weld Inlay SCrP (MRP-194)	P-DM-09 P-DM-14 P-AS-02 P-AS-11 P-MT-01 P-MT-09 P-RG-09 P-RR-04
	1.2-6 Safe Ends – Core Flood Nozzle (B&W)	SS & Welds (SA-336 Cl F8M) (SS Weld Buildup)	A, B, E, F, G	Water Chemistry – Primary EPRI 1014986	ASME Sect. XI IWA-4000	P-DM-09 P-DM-13 P-AS-02 P-AS-09

Degradation Mechanism	Component & ID No.	Material	Conseq. of Failure	Mitigation	Repair/Replace	Gaps
	1.2-7 DM Welds – Core Flood Nozzle (B&W)	Weld-Ni-Alloy (A82/A182)	A, B, E, F, G	Water Chemistry – Primary EPRI 1014986 EPRI 1013420 (Zn Application) MRP-213 (H ₂ Optimization) Stress Improvement MRP-126 MRP-121 MS/IP Peening (Laser or Mechanical)	ASME Sect. XI IWA-4000 Weld Overlay CC-N-740-2 MRP-169R1 MRP-208 Material Mod. Weld Excavation Weld Inlay SCrP (MRP-194)	P-DM-09 P-DM-14 P-AS-02 P-AS-11 P-MT-01 P-MT-09 P-RG-09 P-RR-04
	1.2-9 Safe Ends – SI Nozzles (Westinghouse)	SS & Welds (SA-182 Gr F304 or F316)	A, B, E, F, G	Water Chemistry – Primary EPRI 1014986	ASME Sect. XI IWA-4000	P-DM-09 P-DM-13 P-AS-02 P-AS-09
	1.2-10 DM Welds – SI Nozzles (Westinghouse)	Weld- Ni-Alloy (A82/A182)	A, B, E, F, G	Water Chemistry – Primary EPRI 1014986 EPRI 1013420 (Zn Application) MRP-213 (H ₂ Optimization) Stress Improvement MRP-126 MRP-121 MS/IP Peening (Laser or Mechanical)	ASME Sect. XI IWA-4000 Weld Overlay CC-N-740-2 MRP-169R1 MRP-208 Material Mod. Weld Excavation Weld Inlay SCrP (MRP-194)	P-DM-09 P-DM-14 P-AS-02 P-AS-11 P-MT-01 P-MT-09 P-RG-09 P-RR-04

Degradation Mechanism	Component & ID No.	Material	Conseq. of Failure	Mitigation	Repair/Replace	Gaps
	1.3-1 Bottom Mounted Nozzles	Ni-Alloy (A600 SB-166 or SB-167 UNS N06600)	B, E, G	Water Chemistry – Primary EPRI 1014986 EPRI 1013420 (Zn Application) MRP-213 (H ₂ Optimization)	ASME Sect. XI IWA-4000 MNSA (vendor controlled)	P-DM-09 P-AS-02 P-AS-11 P-MT-01 P-MT-02 P-MT-09 P-I&E-02
	1.3-2 DM Welds – Bottom Mounted Nozzles	Weld-Ni-Alloy (A82/A182)	B, E, G	Water Chemistry – Primary EPRI 1014986 EPRI 1013420 (Zn Application) MRP-213 (H ₂ Optimization)	ASME Sect. XI IWA-4000 MNSA (vendor controlled)	P-DM-09 P-AS-02 P-AS-11 P-MT-01 P-MT-02 P-MT-09 P-I&E-02 P-I&E-03
	1.3-3 Safe Ends – Bottom Mounted Nozzles (IMI Nozzles)	SS & Welds (SA-182 Gr F304 or F316)	B, E, G	Water Chemistry – Primary EPRI 1014986	ASME Sect. XI IWA-4000	P-DM-09 P-DM-13 P-AS-02 P-AS-09
	1.3-4 Repair Pieces – Bottom Mounted Nozzles (IMI Nozzles) (B&W)	Ni-Alloy (A600 SB-166 or SB-167 UNS N06600)	G	Water Chemistry – Primary EPRI 1014986 EPRI 1013420 (Zn Application) MRP-213 (H ₂ Optimization)	ASME Sect. XI IWA-4000	P-DM-09 P-AS-02 P-AS-11 P-MT-01 P-MT-02 P-MT-09

Degradation Mechanism	Component & ID No.	Material	Conseq. of Failure	Mitigation	Repair/Replace	Gaps
	1.3-5 Repair Pieces – Attachment Weld (B&W)	Weld-Ni-Alloy (A82/A182)	G	Water Chemistry – Primary EPRI 1014986 EPRI 1013420 (Zn Application) MRP-213 (H ₂ Optimization)	ASME Sect. XI IWA-4000	P-DM-09 P-AS-02 P-AS-11 P-MT-01 P-MT-02 P-MT-09
	1.4-1 Bottom Mounted Instrument Guide Tubes	SS (F304 or F316)	B, E, G	Water Chemistry – Primary EPRI 1014986	ASME Sect. XI IWA-4000	P-DM-09 P-DM-13
	1.4-2 Seal Table	SS (Type 316)	B, E, G	Water Chemistry – Primary EPRI 1014986	ASME Sect. XI IWA-4000	P-AS-02 P-AS-09
	1.4-3 Seal Table Fitting	SS (Type 316)	B, E	Water Chemistry – Primary EPRI 1014986	ASME Sect. XI IWA-4000	P-DM-09 P-DM-13
	1.5-1 CFN Flow Restrictor (B&W Only)	SS & Welds (SA-376 Gr TP304 or SA-182 Gr F304)	B, E, F, G	Water Chemistry – Primary EPRI 1014986	None	P-AS-02 P-AS-09
	1.5-2 Flow Stabilizers (Turning Vanes) (B&W)	SS (A 240 Type 304)	None	Not Applicable	Not Applicable	P-DM-09 P-DM-13 P-AS-02 P-AS-09 Not assigned when no conseq. of failure exists.

Degradation Mechanism	Component & ID No.	Material	Conseq. of Failure	Mitigation	Repair/Replace	Gaps
	1.5-3 Attachment Welds – Flow Stabilizers (Turning Vanes) (B&W)	Weld-Ni-Alloy (A82/A182)	None	Not Applicable	Not Applicable	Not assigned when no conseq. of failure exists.
	1.5-4 Core Guide Lugs	Ni-Alloy (A600 SB-166 or SB-167 UNS N06600)	None	Not Applicable	Not Applicable	Not assigned when no conseq. of failure exists.
	1.5-5 Attachment Weld – Core Guide Lugs	Weld-Ni-Alloy (A82/A132/A182)	None	Not Applicable	Not Applicable	Not assigned when no conseq. of failure exists.
	1.5-6 Flow Baffles (CE)	Ni-Alloy & Welds (A600 SB-168 UNS N06600)	None	Not Applicable	Not Applicable	Not assigned when no conseq. of failure exists.
	1.5-7 Core Stop Lugs (CE)	Ni-Alloy	None	Not Applicable	Not Applicable	Not assigned when no conseq. of failure exists.
	1.5-8 Attachment Weld – Core Stop Lugs (CE)	Weld-Ni-Alloy	None	Not Applicable	Not Applicable	Not assigned when no conseq. of failure exists.

Degradation Mechanism	Component & ID No.	Material	Conseq. of Failure	Mitigation	Repair/Replace	Gaps
	1.7-1 Closure Studs, Nuts, and Washers	LAS (A/SA-540, C/2 or 3 Gr B23 or B24)	None	Not Applicable	Not Applicable	Not assigned when no conseq. of failure exists.

APPENDIX C

DISPLACEMENTS PER ATOM AND PHYSICAL DEFECTS

Appendix C

Displacements Per Atom and Physical Defects

High-energy neutron interactions with atomic nuclei create a spectrum of energetic primary recoil atoms (PRAs) with energies up to several tens of thousands of electron volts. The PRAs produce displacement cascades in the form of a branching series of atomic collisions until the energies of the final generation of recoiling atoms fall below that needed to displace atoms from their crystal lattice sites. The defects created in the cascade are in the form of single vacancies and small clusters of vacancies and self-interstitial atoms (SIAs). SIA defects are two atoms sharing one crystal lattice site. The accepted dose unit of primary damage is displacements per atom (dpa). The dpa value is computed as follows.

1. Determine the number and energy (T) distributions of PRAs by neutronic codes and cross sections for each neutron energy.
2. Subtract the kinetic energy that is imparted to (bled off by) electrons, but that does not cause damage in metals, from the total PRA energy, thus leaving the kinetic damage energy [$T_{\text{dam}}(T)$] in the atomic recoils.
3. Determine the total average damage energy per atom $\langle T_{\text{dam}} \rangle$ deposited by a spectrum of neutrons by integration or summation for all PRAs with energies greater than a threshold energy for creating displacements (40 eV).

Note: $\langle T_{\text{dam}} \rangle$ is not sensitive to the choice of displacement threshold energy (E_d). The computed $\langle T_{\text{dam}} \rangle$ (eV/atom) is a classical unit of radiation dose, entirely equivalent to a gray (J/kg) for ionizing gamma radiation. The number of dpa is simply $\text{dpa} = 0.8 \langle T_{\text{dam}} \rangle / 2E_d$. However, since E_d is a constant, dpa are simply a different unit of the same deposited dose as $\langle T_{\text{dam}} \rangle$. From these considerations it is obvious that threshold energy neutron fluence units are not appropriate for attenuation assessments. For example, using a criterion of $E > 1$ MeV would implicitly discount 10 keV PRAs created by 0.5 MeV neutrons while fully counting 10 keV PRAs created by 1 MeV neutrons.

It is possible to use molecular dynamics codes to compute more direct measures of radiation damage defect production such as surviving vacancies and interstitial or defect clusters created in displacement cascades. However, given the complex multiscale-multiphysics nature of radiation effects in RPV steels, it is easy to conclude that it is likely that there is no single unique physical measure of damage. Thus the dpa is the best available practical measure of damage dose.

APPENDIX D

PIRT TABLES BY MATERIAL, PHENOMENA, AND MECHANISM

Reactor Type: PIRT-BWR adj.

Material: C & LAS: Base Metal

Phenomena: Corrosion

Sub-Component: Bottom drain nozzles.

Mechanism	Panelist	Susceptibility	Confidence	Knowledge	Rational
FAC	1	1	3	3	FAC in BHD is plausible if plants operated a very long time on moderate HWC. However, plants now use NMCA so the concern is not applicable. Also examinations of the location has shown wall-thinning to be less than what models predict.
	2	1	1	2	
	3	1	2	2	
	4	1	2	3	Elbow below drain, looking at radiographs. No issues found so far.
	5	1	1	1	
	6	1	1	1	More information needed
	7	1	3	3	Issue not significant specifically for long-term operation.
	8	1	2	2	Is being studied. Not only important to EL.
	9	1	1	3	There is generally good knowledge about FAC locations and issues and this hasn't tended to be a problem in primary pressure boundary system. However, if proper flow conditions exist, this could be an issue. Since I'm not familiar with the specific flow conditions, I decreased my confidence to reflect this.

Average: **1.00** **1.78** **2.22**

Std. Dev.: **0.00** **0.83** **0.83**

Reactor Type: PIRT-BWR adj.

Material: C & LAS: Base Metal

Phenomena: Fatigue

Sub-Component: Steam dryer hold-down bracket.

Mechanism	Panelist	Susceptibility	Confidence	Knowledge	Rational
HC	1	1	3	3	
	2	1	2	2	
	3	1	2	3	
	4	2	1	1	There are vibration issues in the steam dryers
	5	2	2	2	
	6	2	2	2	Some evidence
	7	1	2	3	Loading conditions insufficient for high cycle fatigue.
	8	1	2	3	Not highly loaded thus HCF not likely an important issue .
	9	2	2	2	steam dryer fatigue has been an issue for certain plant designs after undergoing a power uprate. This is not a general concern and not really an LTO concern since if it's an issue, degradation occurs quickly.
Average:		1.44	2.00	2.33	
Std. Dev.:		0.53	0.50	0.71	

Reactor Type: PIRT-BWR adj.

Material: C & LAS: Base Metal

Phenomena: Fatigue

Sub-Component: Top head and flange, vessel flange, all vessel shells, bottom head, closure head studs, washers, and nuts; top of head flange bolts, top head nozzle, main steam nozzles, feedwater nozzles, core spray nozzles, LPCI nozzles, CRD return line nozzle, recirculation inlet and outlet nozzles, CRD housing cap screws and nuts.

Mechanism	Panelist	Susceptibility	Confidence	Knowledge	Rational
LC-Env.	1	1	3	3	early life HC fatigue occurred in feedwater nozzle inner radius locations - corrected by altering low flow feedwater controls. CRDRL nozzle/cap sees no flow
	2	2	2	3	
	3	2	1	2	
	4	1	2	2	In ISI program.
	5	2	3	3	
	6	2	3	3	Some experience but relatively good information available
	7	2	1	2	Loading conditions may be sufficient for low cycle fatigue in some of sub-components.
	8	2	1	2	LCF may affect some components.
	9	2	2	1	I scored this the same as the PWR for generally the same reasons. Note that there are different material susceptibilities as a function of oxygen content which could be important for any materials not protected from the environment by cladding, but component loading is still more important for fatigue.

Average: **1.78** **2.00** **2.33**

Std. Dev.: **0.44** **0.87** **0.71**

Reactor Type: PIRT-BWR adj.

Material: C & LAS: Base Metal

Phenomena: Irradiation Effects

Sub-Component: All vessel shells, LPCI nozzles, CRD return line, recirculation inlet and outlet nozzles, instrument penetrations.

Mechanism	Panelist	Susceptibility	Confidence	Knowledge	Rational
Emb.	1	2	3	3	ranking is based on RPV shell. The nozzles listed are ex-vessel (except for instrument pens.) and see little fluence
	2	3	2	2	
	3	3	3	3	
	4	3	3	2	Dose rate effects need more study.
	5	2	2	2	
	6	2	2	2	Flux effects are still not well understood
	7	3	3	3	Although fluence is relatively low, relatively low temperature and low flux can cause sufficient embrittlement of some materials and sub-components for LTO.
	8	3	3	3	In spite of low fluence, low flux and temperature may result in some embrittlement during EL.
	9	3	2	2	While this is less an issue for the BWRs than the PWRs, it may still be an important issue for some plants in P-T space out to 80 years and there is still a relative lack of knowledge on flux effects.

Average: **2.67** **2.56** **2.44**

Std. Dev.: **0.50** **0.53** **0.53**

Reactor Type: PIRT-BWR adj.

Material: C & LAS: Base Metal

Phenomena: Red. In Fract. Properties

Sub-Component: Top head and flange, vessel flange, top head nozzle, main steam nozzles, feedwater nozzles, core spray nozzles, LPCI nozzles, bottom drain nozzles, SLC nozzle, instrument penetrations, steam dryer hold-down bracket.

Mechanism	Panelist	Susceptibility	Confidence	Knowledge	Rational
Env.	1	2	3	3	
	2	2	2	2	
	3	1	3	2	
	4	1	3	2	No anticipated changes
	5	2	1	1	
	6	1	2	2	More information needed
	7	1	3	3	Operating temperature too low to cause significant loss of fracture toughness.
	8	1	3	2	Temperature too low for major fracture toughness reduction.
	9	1	2	2	scored the same as for PWR materials
Average:		1.33	2.44	2.11	
Std. Dev.:		0.50	0.73	0.60	

Reactor Type: PIRT-BWR adj.

Material: C & LAS: Base Metal

Phenomena: SCC

Sub-Component: Top head and flange, vessel flange, all vessel shells, bottom head, closure head studs, washers, and nuts; top of head flange bolts, top head nozzle, main steam nozzles, feedwater nozzles, core spray nozzles, LPCI nozzles, CRD return line nozzle, recirculation inlet and outlet nozzles, CRD housing cap screws and nuts, SLC nozzle, instrument penetrations, steam dryer holdown bracket.

Mechanism	Panelist	Susceptibility	Confidence	Knowledge	Rational	
IG/TC	1	1	3	3		
	2	2	2	2		
	3	2	2	2		
	4	1	1	1	Can be susceptible with high yield strength.	
	5	2	3	3		
	6	2	3	3	Known issue, but manageable	
	7	2	2	2	Materials in temperature range not highly sensitive to SCC, but needs investigation for LTO.	
	8	2	2	2	Alloy not particularly vulnerable to SCC, but should confirm for extended life (EL).	
	9	1	2	2	Don't expect to see SCC in C&LAS and OPE has been good with respect to that. There is potential for SCC due to outside environment or inside environment for many of these components and I'm not sure if both are being considered. Inside environment is more likely to result in SCC even though susceptibility to either environment is still expected to be low.	
Average:				1.67	2.22	2.22
Std. Dev.:				0.50	0.67	0.67

Reactor Type: PIRT-BWR adj.

Material: C & LAS: Welds & HAZ

Phenomena: Corrosion

Sub-Component: Welds of bottom drain nozzles

Mechanism	Panelist	Susceptibility	Confidence	Knowledge	Rational
FAC	1	1	3	3	FAC in BHDL is plausible if plants operated a very long time on moderate HWC. However, plants now use NMCA so the concern is not applicable. Also examinations of the location has shown wall-thinning to be less than what models predict.
	2	1	1	2	
	3	1	3	3	
	4	1	2	3	Elbow below drain, looking at radiographs. No issues found so far.
	5	1	1	1	
	6	1	1	1	More information needed
	7	1	3	3	Issue not significant specifically for long-term operation.
	8	1	3	3	Is being studied. Not only important to EL.
	9	1	1	3	scored the same for base materials

Average: 1.00 2.00 2.44

Std. Dev.: 0.00 1.00 0.88

Reactor Type: PIRT-BWR adj.

Material: C & LAS: Welds & HAZ

Phenomena: Fatigue

Sub-Component: Weld of steam dryer hold-down bracket.

Mechanism	Panelist	Susceptibility	Confidence	Knowledge	Rational
HC	1	1	3	3	
	2	1	2	3	
	3	1	3	3	
	4	2	2	2	Some cracking observed; wear and vibration seen. Covered by ISI program.
	5	1	1	1	
	6	2	2	2	Some evidence
	7	1	3	3	Issue not significant specifically for long-term operation.
	8	1	3	3	Is being studied. Not only important to EL.
	9	2	2	2	scored the same for base materials

D-8

Average: **1.33** **2.33** **2.44**

Std. Dev.: **0.50** **0.71** **0.73**

Reactor Type: PIRT-BWR adj.

Material: C & LAS: Welds & HAZ

Phenomena: Fatigue

Sub-Component: Welds of: Top head and flange, vessel flange, all vessel shells, bottom head, closure head studs, washers, and nuts; top of head flange bolts, top head nozzle, main steam nozzles, feedwater nozzles, core spray nozzles, LPCI nozzles, CRD return line nozzle, recirculation inlet and outlet nozzles, CRD housing cap screws and nuts.

Mechanism	Panelist	Susceptibility	Confidence	Knowledge	Rational
LC-Env.	1	1	3	3	early life HC fatigue occurred in feedwater nozzle inner radius locations - corrected by altering low flow feedwater controls. CRDRL nozzle/cap sees no flow
	2	2	3	2	
	3	2	2	2	
	4	1	2	2	In ISI program.
	5	1	2	2	
	6	2	3	3	Some experience but relatively good information available
	7	2	2	2	Loading conditions may be sufficient for low cycle fatigue in some sub-components.
	8	2	2	2	LCF may affect some components.
	9	2	2	1	scored the same as for base materials; weld more likely to have flaws however

Average: **1.67** **2.33** **2.11**

Std. Dev.: **0.50** **0.50** **0.60**

Reactor Type: PIRT-BWR adj.

Material: C & LAS: Welds & HAZ

Phenomena: Irradiation Effects

Sub-Component: Welds of: All vessel shells, LPCI nozzles, CRD return line, recirculation inlet and outlet nozzles, instrument penetrations.

Mechanism	Panelist	Susceptibility	Confidence	Knowledge	Rational
Emb.	1	2	3	3	ranking is based on RPV shell. The nozzles listed are ex-vessel (except for instrument pens.) and see little fluence
	2	2	3	2	
	3	3	3	2	
	4	3	3	2	Dose rate effects need more study.
	5	2	2	2	
	6	2	2	2	Flux effects are still not well understood
	7	3	3	3	Although fluence is relatively low, relatively low temperature and low flux can cause sufficient embrittlement of some materials and sub-components for LTO.
	8	3	3	2	In spite of low fluence. low flux and temperature may result in some embrittlement during EL.
	9	3	2	2	scored the same as for base materials; weld more likely to have flaws however
Average:	2.56	2.67	2.22		
Std. Dev.:	0.53	0.50	0.44		

Reactor Type: PIRT-BWR adj.

Material: C & LAS: Welds & HAZ

Phenomena: Red. In Fract. Properties

Sub-Component: Same as Reduction in Fracture Properties of C & LAS steels, but welds of those components.

Mechanism	Panelist	Susceptibility	Confidence	Knowledge	Rational
Env.	1	2	3	3	
	2	2	2	1	
	3	1	3	3	
	4	1	3	2	No anticipated changes
	5	2	1	1	
	6	1	2	2	More information needed
	7	1	3	3	Operating temperature too low to cause significant loss of fracture toughness.
	8	1	3	3	Temperature too low for major fracture toughness reduction. .
	9	1	2	2	scored the same for base materials

Average: **1.33** **2.44** **2.22**

Std. Dev.: **0.50** **0.73** **0.83**

Reactor Type: PIRT-BWR adj.

Material: C & LAS: Welds & HAZ

Phenomena: SCC

Sub-Component: Same as SCC of C & LAS base metal, but welds of those components.

Mechanism	Panelist	Susceptibility	Confidence	Knowledge	Rational
IG/TG	1	1	3	3	
	2	2	2	3	
	3	2	2	2	
	4	1	3	1	Can be susceptible with high yield strength.
	5	2	2	1	
	6	2	3	3	Known issue, but manageable
	7	2	2	2	Materials in temperature range not highly sensitive to SCC, but needs investigation for LTO.
	8	2	2	2	Alloy not particularly vulnerable to SCC, at these temperatures but should confirm for EL.
	9	1	2	2	scored the same as for base materials; weld more likely to have flaws however
Average:	1.67	2.33	2.11		
Std. Dev.:	0.50	0.50	0.78		

Reactor Type: PIRT-BWR adj.

Material: SS: Wrought, Forged, & HAZ

Phenomena: Fatigue

Sub-Component: CRD stub tube.

Mechanism	Panelist	Susceptibility	Confidence	Knowledge	Rational
LC-Env.	1	1	3	3	
	2	2	2	2	
	3	2	1	2	
	4	2	2	2	More prone to SCC.
	5	2	3	3	
	6	1	3	3	Better understood
	7	2	1	2	Loading conditions may be sufficient for low cycle fatigue in some sub-components.
	8	2	1	2	LCF may occur during EL
	9	1	2	2	Same score as PWR BMIs for largely the same reasons. i.e., scored this low because I don't expect significant fatigue loads in this region. If significant fatigue loads exist, susceptibility increases to a 2 or 3. I also decreased confidence to reflect this lack of knowledge.
Average:		1.67	2.00	2.33	
Std. Dev.:		0.50	0.87	0.50	

Reactor Type: PIRT-BWR adj.

Material: SS: Wrought, Forged, & HAZ

Phenomena: Fatigue

Sub-Component: Jet pump riser brace pad attachment, steam dryer support bracket, feedwater sparger support bracket.

Mechanism	Panelist	Susceptibility	Confidence	Knowledge	Rational
HC	1	2	3	2	Only location seeing appreciable fatigue duty is the jet pump riser brace.
	2	1	3	2	
	3	1	3	3	
	4	3	2	2	Some fatigue cracking observed on riser brace leaf and jet pump. Subject to monitor through ISI or BWRVIP programs.
	5	1	1	1	
	6	1	1	1	Not well established
	7	1	3	3	Issue not significant specifically for long-term operation.
	8	1	3	3	Is being studied. Not only important to EL.
	9	2	2	2	I rated this a 2 for same reasons as above. This can be a problem in some plants due to design and operation conditions, but HCF is not really an LTO issue.
Average:		1.44	2.33	2.11	
Std. Dev.:		0.73	0.87	0.78	

Reactor Type: PIRT-BWR adj.

Material: SS: Wrought, Forged, & HAZ

Phenomena: Red. In Fract. Properties

Sub-Component: CRD stub tube, CRD housing tube, flange, and cap, SLC housing, in-core housing & flange, instrument penetrations. Jet pump riser brace pad attachment, core spray pipe bracket, steam dryer and feedwater sparger support brackets, surveillance capsule bracket, guide rod bracket.

Mechanism Env.	Panelist	Susceptibility	Confidence	Knowledge	Rational
	1	1	3	3	Most of these are not likely to see appreciable fluence, even for 80 years. The locations most impacted are JP riser brace pad and surveillance capsule bracket. IASCC and loss of toughness in core shroud. More information needed Issue not significant specifically for long-term operation. Is being studied. Not only important to EL. don't expect this to be an issue - not enough fluence for IE concerns, only slight concern would be long-term thermal stability of austenitic SSs (as with PWRs), but lesser for BWRs due to lower temp.
	2	1	2	2	
	3	1	3	3	
	4	2	2	2	
	5	1	1	1	
	6	1	2	2	
	7	1	3	3	
	8	1	3	3	
	9	1	2	2	

Average: **1.11** **2.33** **2.33**

Std. Dev.: **0.33** **0.71** **0.71**

Reactor Type: PIRT-BWR adj.

Material: SS: Wrought, Forged, & HAZ

Phenomena: SCC

Sub-Component: CRD stub tube, housing tube, flange & cap; SLC housing, in-core housing and flange, instrument penetrations, jet pump riser brace pad and core spray pipe bracket, steam dryer support bracket, feedwater sparger support bracket, surveillance capsule bracket, guide rod bracket.

Mechanism	Panelist	Susceptibility	Confidence	Knowledge	Rational
IG/TG	1	2	3	3	This listing is difficult to rank. Some locations are more susceptible than others and some are mitigated by HWC/NIMCA. Only stub tube cracking to date has been in thermally sensitized materials. Also this ranking is for the HAZ - base metal is much lower susceptibility. Currently monitoring many cracks. Stub tube. Known issue, but manageable Materials in temperature range are sensitive to SCC, especially for LTO. Temperature make alloys sensitive to SCC during EL IGSCC of higher carbon materials is well known and lots of OPE. These SS could have cracking issues in the HAZ (if they haven't experienced them already). Less susceptible SSs will have less of an issue. Therefore, I gave this a 2 on average. It's a 3 for susceptible materials and a 1 for less susceptible materials but the category doesn't distinguish.
	2	2	2	3	
	3	3	2	2	
	4	3	2	2	
	5	2	3	3	
	6	2	3	3	
	7	3	2	2	
	8	3	2	2	
	9	2	2	2	
Average:	2.44	2.33	2.44		
Std. Dev.:	0.53	0.50	0.53		

Reactor Type: PIRT-BWR adj.

Material: SS: Welds & Clad

Phenomena: Fatigue

Sub-Component: All vessel shells.

Mechanism	Panelist	Susceptibility	Confidence	Knowledge	Rational
LC-Env.	1	1	3	3	
	2	1	2	2	
	3	1	2	2	
	4				
	5	1	3	3	
	6	1	3	3	Solved analytically
	7	1	2	2	Loading conditions insufficient even for low cycle fatigue.
	8	1	2	2	Loading too low for low cycle fatigue.
	9	1	2	2	really don't expect fatigue loading of the vessel shells to be an issue given the expected low primary loads.

Average: **1.00** **2.38** **2.38**

Std. Dev.: **0.00** **0.52** **0.52**

Reactor Type: PIRT-BWR adj.

Material: SS: Welds & Clad

Phenomena: Irradiation Effects

Sub-Component: All vessel shells.

Mechanism	Panelist	Susceptibility	Confidence	Knowledge	Rational
Emb.	1	2	3	3	clad is not credited for structural integrity
	2	1	3	2	
	3	1	3	3	
	4	2	2	2	Possible embrittlement of under clad HAZ in beltline and adjacent materials.
	5	1	1	1	
	6	1	2	2	Effects generally known, bt integration lacking
	7	1	3	3	Fluence too low for SS clad to experience significant embrittlement.
	8	1	3	3	SS clad embrittlement not significant at low fluence.
	9	1	2	2	don't expect the fluence to be high enough in cladding to lead to fracture reduction, even at 80 years. Would need dpa > 0.5 before this would be a concern.

Average: **1.22** **2.44** **2.33**

Std. Dev.: **0.44** **0.73** **0.71**

Reactor Type: PIRT-BWR adj.

Material: SS: Welds & Clad

Phenomena: Red. In Fract. Properties

Sub-Component: All vessel shells, bottom head.

Mechanism Th.	Panelist	Susceptibility	Confidence	Knowledge	Rational
	1	1	3	2	
	2	2	2	2	
	3	1	2	2	
	4	1	2	2	Lower temperature than PWR.
	5	2	2	2	
	6	1	3	3	Not a significant issue
	7	1	3	3	Issue not significant specifically for long-term operation.
	8	1	2	2	Temperature make alloys sensitive to SCC during EL
	9	1	2	2	same scoring and rationale as above for wrought material
Average:		1.22	2.33	2.22	
Std. Dev.:		0.44	0.50	0.44	

Reactor Type: PIRT-BWR adj.

Material: SS: Welds & Clad

Phenomena: Red. In Fract. Properties

Sub-Component: Instrument penetrations.

Mechanism	Panelist	Susceptibility	Confidence	Knowledge	Rational
Env.	1	1	3	2	
	2	1	2	2	
	3	1	3	3	
	4	2	2	2	More prone to SCC.
	5	1	1	1	
	6	1	2	2	More information needed
	7	1	3	3	Issue not significant specifically for long-term operation.
	8	1	3	3	Is being studied. Not only important to EL.
	9	1	2	2	same scoring and rationale as above for wrought material

Average: **1.11** **2.33** **2.22**

Std. Dev.: **0.33** **0.71** **0.67**

Reactor Type: PIRT-BWR adj.

Material: SS: Welds & Clad

Phenomena: SCC

Sub-Component: Same as SCC of SS wrought, forged, and HAZ, but welds of those components.

Mechanism	Panelist	Susceptibility	Confidence	Knowledge	Rational
IG/TG	1	1	3	3	
	2	1	3	2	
	3	3	2	2	
	4	3	3	3	Many observations. Need to monitor and mitigate.
	5	1	3	3	
	6	1	3	3	Not a significant issue
	7	2	2	2	Materials in temperature range are sensitive to SCC, especially for LTO.
	8	3	2	2	Temperature make alloys sensitive to SCC during EL
	9	2	2	2	same score as for wrought materials but greater likelihood of flaws
Average:	1.89	2.56	2.44		
Std. Dev.:	0.93	0.53	0.53		

Reactor Type: PIRT-BWR adj.
Material: Ni-Alloy: Wrought (A600)
Phenomena: Fatigue

Sub-Component: CRD Return Line Nozzle Cap, CRD stub tube.

Mechanism	Panelist	Susceptibility	Confidence	Knowledge	Rational
LC-Env.	1	1	3	3	CRDRL cap sees no flow
	2	1	2	2	
	3	2	1	2	
	4	2	2	2	More prone to SCC. Return line monitored by ISI.
	5	1	2	2	
	6	1	2	2	Probably a non-issue
	7	2	1	2	Loading conditions may be sufficient for low cycle fatigue in some sub-components.
	8	2	1	2	LCF may occur during EL.
	9	1	2	2	scored same as for PWR BMIs for the same reasons

Average: **1.44** **1.78** **2.11**
 Std. Dev.: **0.53** **0.67** **0.33**

Reactor Type: PIRT-BWR adj.

Material: Ni-Alloy: Wrought (A600)

Phenomena: Red. In Fract. Properties

Sub-Component: CRD return line nozzle cap, CRD stub tube, CRD housing tube, SLC housing, SLC stub tube, In-core housing & flange, instrument penetrations, jet pump riser brace pad attachment

Mechanism	Panelist	Susceptibility	Confidence	Knowledge	Rational
Env.	1	1	3	3	
	2	1	2	2	
	3	1	2	2	
	4	1	2	2	Not expected.
	5	1	1	1	
	6	1	2	2	More information needed
	7	1	3	3	Issue not significant specifically for long-term operation.
	8	1	2	2	Is being studied. Not only important to EL.
	9	2	2	2	scored same as for PWR BMIs for the same reasons

Average: **1.11** **2.11** **2.11**

Std. Dev.: **0.33** **0.60** **0.60**

Reactor Type: PIRT-BWR adj.

Material: Ni-Alloy: Wrought (A600)

Phenomena: SCC

Sub-Component: CRD return line nozzle cap, CRD stub tube, CRD housing tube, SLC housing, SLC stub tube, in-core housing & flange, instrument penetrations, jet pump riser brace pad attachment.

Mechanism	Panelist	Susceptibility	Confidence	Knowledge	Rational
IG/TG	1	1	3	3	Alloy 600 has performed well in the BWR environment. To date the only cracks have been in craviced locations such as access hole covers. Also curious about inclusion of internal materials - it is being ranked by the piping / materials group.
	2	2	2	2	
	3	3	2	2	
	4	3	3	3	Included in ISI or BWRVIP inspections.
	5	2	3	3	
	6	2	3	3	Evidence, but data available
	7	2	1	1	Insufficient information.
	8	3	2	2	Susceptible but information lacking
	9	2	1	1	While the BWR OPE has generally been good, given the susceptibility of PWR there may be some areas (and at longer operating times that may be susceptible). Susceptibility will increase with H2 concentration and temperature. Some of these components (depending on location) may see HWC and some may see more oxygenated conditions. Components under HWC will be more susceptible.
Average:				2.22	2.22
Std. Dev.:				0.67	0.83

Reactor Type: PIRT-BWR adj.

Material: Ni-Alloy: Welds & Clad (A82/182)

Phenomena: Fatigue

Sub-Component: CRD Return Line Nozzle Cap, CRD stub tube.

Mechanism	Panelist	Susceptibility	Confidence	Knowledge	Rational
LC-Env.	1	1	3	3	CRDRL cap sees no flow
	2	1	2	2	
	3	2	1	2	
	4	2	2	2	More prone to SCC. Return line monitored by ISI.
	5	1	2	2	
	6	1	2	2	Probably a non-issue
	7	2	1	2	Loading conditions may be sufficient for low cycle fatigue in some sub-components.
	8	2	1	2	LCF may occur during EL
	9	1	2	2	scored same as base metal for the same reasons (also same as PWR). Not sure if return line sees higher loading.

Average: **1.44** **1.78** **2.11**

Std. Dev.: **0.53** **0.67** **0.33**

Reactor Type: PIRT-BWR adj.

Material: Ni-Alloy: Welds & Clad (A82/182)

Phenomena: Red. In Fract. Properties

Sub-Component: CRD return line nozzle cap, CRD stub tube, CRD housing tube, SLC housing, SLC stub tube, In-core housing & flange, instrument penetrations, jet pump riser brace pad attachment, core spray pipe bracket attachment, shroud support pad, steam dryer support bracket, feedwater sparger support bracket, guide rod bracket.

Mechanism Env.	Panelist	Susceptibility	Confidence	Knowledge	Rational	
	1	1	3	3	Most of these are not likely to see appreciable fluence, even for 80 years. The locations most impacted are JP riser brace pad and surveillance capsule bracket.	
	2	2	2	2		
	3	1	3	3		
	4	1	2	2		Not expected.
	5	2	1	1		
	6	1	2	2		More information needed
	7	1	3	3		Issue not significant specifically for long-term operation.
	9	2	2	2		scored same as base metal for the same reasons (also same as PWR).
Average:						1.38 2.25 2.25
Std. Dev.:					0.52 0.71 0.71	

Reactor Type: PIRT-BWR adj.

Material: Ni-Alloy: Welds & Clad (A82/182)

Phenomena: SCC

Sub-Component: CRD return line nozzle cap, CRD stub tube, CRD housing tube, SLC housing, SLC stub tube, in-core housing & flange, instrument penetrations, core spray pipe bracket attachment, shroud support pad, steam dryer support bracket, feedwater sparger support bracket, surveillance capsule holder bracket, guide rod bracket.

Mechanism	Panelist	Susceptibility	Confidence	Knowledge	Rational
IG/TG	1	2	3	3	
	2	3	2	2	
	3	3	2	2	
	4	3	3	3	Monitoring shroud support leg welds with some indications.
	5	3	3	3	
	6	3	3	3	Known issue, but can be managed
	7	2	1	1	Insufficient information.
	8	3	2	2	Susceptible but information. Lacking
	9	2	1	1	same scores for the same rationale as for base material/HAZs.

Average: **2.67** **2.22** **2.22**

Std. Dev.: **0.50** **0.83** **0.83**

Reactor Type: PIRT-PWR adj.

Material: C & LAS: Base Metal

Phenomena: Fatigue

Sub-Component: Upper shell flange, all shell courses, transition forging (B&W), bottom head, inlet&outlet nozzles, safety injection nozzles, core flood nozzle (B&W), safety injection nozzles.

Mechanism	Panelist	Susceptibility	Confidence	Knowledge	Rational
LC-Env.	1	1	3	2	There may be specific locations with high fatigue duty, but the generic susceptibility is low
	2	1	3	2	
	3	2	1	2	
	4	1	3	2	Loads are low; believe that CJUF is low with no environmental exposure expected normally
	5	1	3	3	
	6	1	3	3	Generally solvable by analysis
	7	2	1	1	Loading conditions may be sufficient for low cycle fatigue in some sub-components.
	8	2	2	2	LCF may affect some components.
	9	2	2	1	I don't think that this is a general problem, but fatigue may be an issue for some specific plants out to 80 years, especially if environmental effects are considered. I lowered the knowledge somewhat because we still don't have good tools to predict fatigue in structures based on laboratory data.

Average: **1.44** **2.33** **2.00**

Std. Dev.: **0.53** **0.87** **0.71**

Reactor Type: PIRT-PWR adj.

Material: C & LAS: Base Metal

Phenomena: Irradiation Effects

Sub-Component: Nozzle, intermediate, & lower shell courses; inlet and outlet nozzles.

Mechanism	Panelist	Susceptibility	Confidence	Knowledge	Rational
Emb.	1	2	3	3	
	2	3	3	2	
	3	3	3	2	
	4	3	3	2	Beitline and nozzles are susceptible; we have lots of data, but little data at high fluence and our prediction equations could be better.
	5	3	3	2	
	6	3	2	2	High fluence daa needed
	7	3	3	2	Some materials are very sensitive to irradiation and there are insufficient data regarding high fluence effects for LTO, including nozzles.
	8	3	3	2	An opn issue for EL that must be addressed at high fluence and low flux in sensitive alloys.
	9	3	3	2	radiation embrittlement will certainly be important especially for base metal near the beitline welds. Embrittlement of nozzles may also be an issue for some plants based on their location (i.e., dose) and nozzle geometry (i.e., stress concentration factor).

Average: **2.89** **2.89** **2.11**

Std. Dev.: **0.33** **0.33** **0.33**

Reactor Type: PIRT-PWR adj.
Material: C & LAS: Base Metal
Phenomena: Red. In Fract. Properties
Sub-Component: Entire vessel

Mechanism	Panelist	Susceptibility	Confidence	Knowledge	Rational
Env.	1	1	2	2	
	2	2	2	2	
	3	1	3	2	
	4	1	2	2	Not exposed to the environment
	5	2	1	1	
	6	1	2	2	More information needed
	7	1	3	2	Operating temperature too low to cause significant loss of fracture toughness.
	8	1	3	2	Temperature too low for major fracture toughness reduction.
	9	1	2	2	reduction due to environmental effects should be minimal with or without assuming a cladding breach.

Average: **1.22** **2.22** **1.89**

Std. Dev.: **0.44** **0.67** **0.33**

Th.	Panelist	Susceptibility	Confidence	Knowledge	Rational
Th.	1	1	2	2	
	2	1	2	2	
	3	2	2	3	
	4	1	2	2	Higher temperature components (head, outlet nozzles) could be susceptible, but there is little data.
	5	1	1	1	
	6	1	2	2	More information needed
	7	2	2	2	Insufficient data exist for LTO.
	8	2	2	2	Insufficient data for EL.
	9	1	2	2	Expect materials to be thermally stable for operating temperatures out to 80 years.

Reactor Type: PIRT-PWR adj.

Material: C & LAS: Base Metal

Phenomena: Red. In Fract. Properties

Average:	1.33	1.89	2.00
Std. Dev.:	0.50	0.33	0.50

Reactor Type: PIRT-PWR adj.

Material: C & LAS: Base Metal

Phenomena: SCC

Sub-Component: Closure Studs, Nuts, and Washers

Mechanism	Panelist	Susceptibility	Confidence	Knowledge	Rational
IG/TG	1	1	3	3	
	2	1	3	2	
	3	2	1	2	
	4	1	3	2	Can be susceptible with high yield strength. No expected changes to susceptibility with age. Covered by inspection program.
	5	1	3	2	
	6	1	3	2	Some evidence but replaceable
	7	2	1	2	Materials in temperature range not highly sensitive to SCC, but needs investigation for LTO.
	8	2	1	2	Alloy not particularly vulnerable to SCC, but should confirm for extended life (EL).
	9	1	3	2	likelihood to SCC due to either containment environment on outside or possibility of leaking coolant to create a wetted crevice environment should be low.

Average: **1.33** **2.33** **2.11**

Std. Dev.: **0.50** **1.00** **0.33**

Reactor Type: PIRT-PWR adj.

Material: C & LAS: Welds

Phenomena: Fatigue

Sub-Component: Upper shell flange, all shell courses, transition forging (B&W), bottom head, inlet&outlet nozzles, safety injection nozzles, core flood nozzle (B&W), safety injection nozzles.

Mechanism	Panelist	Susceptibility	Confidence	Knowledge	Rational
LC-Env.	1	1	3	2	There may be specific locations with high fatigue duty, but the generic susceptibility is low
	2	1	3	2	
	3	2	1	1	Loads are low; believe that CJUF is low with no environmental exposure expected normally
	4	1	3	2	
	5	1	3	3	
	6	1	3	3	Generally solvable by analysis
	7	2	1	1	Loading conditions may be sufficient for low cycle fatigue in some sub-components.
	8	2	1	1	LCF may affect some components.
	9	2	2	1	Don't expect differences in properties from base metal. However, greater likelihood of defects increases likelihood somewhat

Average: **1.44** **2.22** **1.78**

Std. Dev.: **0.53** **0.97** **0.83**

Reactor Type: PIRT-PWR adj.

Material: C & LAS: Welds

Phenomena: Irradiation Effects

Sub-Component: Nozzle course welds, inlet and outlet nozzle welds.

Mechanism	Panelist	Susceptibility	Confidence	Knowledge	Rational
Emb.	1	2	3	3	
	2	3	3	2	
	3	3	3	2	
	4	2	2	2	Ranking is for listed components (nozzle region). If the bellline welds are included, then ranking would be 3 3. Bellline and nozzles are susceptible; we have lots of data, but little data at high fluence and our prediction equations could be better.
	5	3	3	2	
	6	3	2	2	High fluence daa needed
	7	3	3	2	Some materials are very sensitive to irradiation and there are insufficient data regarding high fluence effects for LTO, including nozzles.
	8	3	3	2	An opn issue for EL that must be addressed at high fluence and low flux in sensitive alloys.
	9	3	3	2	Don't expect differences in properties from base metal. However, greater likelihood of defects increases likelihood somewhat

Average: **2.78** **2.78** **2.11**
 Std. Dev.: **0.44** **0.44** **0.33**

Reactor Type: PIRT-PWR adj.
Material: C & LAS: Welds
Phenomena: Red. In Fract. Properties
Sub-Component: Entire RPV

Mechanism	Panelist	Susceptibility	Confidence	Knowledge	Rational
Env.	1	1	2	2	
	2	2	2	2	
	3	1	3	2	
	4	1	2	2	Not exposed to the environment
	5	2	1	1	
	6	1	2	2	More information needed
	7	1	3	2	Operating temperature too low to cause significant loss of fracture toughness.
	8	1	3	2	Temperature too low for major fracture toughness reduction.
	9	1	2	2	Don't expect differences from base metal

Average: **1.22** **2.22** **1.89**
 Std. Dev.: **0.44** **0.67** **0.33**

Th.	1	2	2	2	2
	2	2	2	2	
	2	2	2	3	
	2	2	2	2	Referring to weld HAZ: Higher temperature components (head, outlet nozzle HAZs) could be susceptible, but there is little data.
	1	1	1	1	
	1	2	2	2	More information needed
	2	2	2	2	Insufficient data exist for LTO.
	2	2	2	2	Insufficient data for EL.
	1	2	2	2	Don't expect differences from base metal

Reactor Type: PIRT-PWR adj.

Material: C & LAS: Welds

Phenomena: Red. In Fract. Properties

Average:	1.67	1.89	2.00
Std. Dev.:	0.50	0.33	0.50

Reactor Type: PIRT-PWR adj.

Material: C & LAS: Welds

Phenomena: SCC

Sub-Component: Closure studs, Nuts, and Washers.

Mechanism	Panelist	Susceptibility	Confidence	Knowledge	Rational
IG/TG	1				
	2	1	3	2	unclear to me why these components are being ranked with weld metal
	3	2	1	2	
	4	1	3	2	I know of no welds in these components
	5	1	3	2	
	6	1	3	3	Welds generally not involved
	7	2	1	2	Materials in temperature range not highly sensitive to SCC, but needs investigation for LTO.
	8	2	1	2	Alloys not particularly vulnerable to SCC, at these temperatures but should confirm for EL.
	9	0	3	3	I scored this a zero because there shouldn't be any welds on these components. If welds, same score as for base materials.

Average: **1.25** **2.25** **2.25** **2.25**

Std. Dev.: **0.71** **1.04** **1.04** **0.46**

Reactor Type: PIRT-PWR adj.

Material: SS; Welds & Clad

Phenomena: Fatigue

Sub-Component: SS clad on all vessel courses, bottom head, inlet & outlet nozzles.

Mechanism	Panelist	Susceptibility	Confidence	Knowledge	Rational
LC-Env.	1	1	3	3	
	2	1	2	2	
	3	2	1	1	
	4	1	2	2	Not load bearing; low CUF. Possible FIV in core guide lugs; Failures at Cook not yet known
	5	1	2	2	
	6	1	3	3	Fatigue generally not an issue
	7	2	1	1	Loading conditions may be sufficient for low cycle fatigue in some sub-components.
	8	2	1	1	LCF may affect these components.
	9	2	2	1	while I gave the same general score as for C&LAS steels, I think fatigue is more likely in clad due to thermal fatigue at cladding interface and interaction with environment/fluid (i.e. highest loads at the surface).

Average: **1.44** **1.89** **1.78**

Std. Dev.: **0.53** **0.78** **0.83**

Reactor Type: PIRT-PWR adj.

Material: SS: Welds & Clad

Phenomena: Irradiation Effects

Sub-Component: Clad on nozzle courses, inlet and outlet nozzles.

Mechanism	Panelist	Susceptibility	Confidence	Knowledge	Rational
Emb.	1	1	2	2	
	2	1	2	2	Currently included in aging mgmt.
	3	1	3	3	
	4	1	2	2	Possible embrittlement of under clad HAZ in bellline and adjacent materials.
	5	1	1	1	
	6	1	2	2	Effects generally known, but integration is lacking
	7	1	3	3	Issue not significant specifically for long-term operation.
	8	1	3	3	Is being studied. Not only important to EL.
	9	2	2	2	cladding embrittlement is not nearly as important as C&LAS. However, there is data that shows that significant toughness reduction can occur by 0.5 - 1 dpa. This may be an issue at some plants if this fluence level is reached by 80 years.
Average:		1.11	2.22	2.22	
Std. Dev.:		0.33	0.67	0.67	

Reactor Type: PIRT-PWR adj.

Material: SS: Welds & Clad

Phenomena: Red. In Fract. Properties

Sub-Component: Bottom mounted instrument guide tubes, seal table and fitting, [core flood nozzle flow restrictor, flow stabilizers] (B&W).

Mechanism	Panelist	Susceptibility	Confidence	Knowledge	Rational
Env.	1	2	2	2	
	2	2	1	2	Currently included in aging mgmt.
	3	1	3	3	
	4	2	1	1	
	5	2	1	1	
	6	1	1	1	Not enough data/information
	7	1	3	3	Issue not significant specifically for long-term operation.
	8	1	3	3	Is being studied. Not only important to EL.
	9	1	2	2	don't expect any differences from C&LAS effects
Average:		1.44	1.89	2.00	
Std. Dev.:		0.53	0.93	0.87	

Reactor Type: PIRT-PWR adj.

Material: SS: Welds & Clad

Phenomena: Red. In Fract. Properties

Sub-Component: SS clad on all vessel courses, bottom head, inlet & outlet nozzles, core flood nozzle (B&W).

Mechanism Th.	Panelist	Susceptibility	Confidence	Knowledge	Rational
	1	1	2	2	
	2	2	1	2	Currently included in aging mgmt.
	3	1	3	3	
	4	1	2	2	Possible embrittlement of under clad HAZ in heads and outlet nozzles.
	5	2	1	2	
	6	1	1	1	Not enough data/information
	7	1	3	3	Issue not significant specifically for long-term operation.
	8	1	3	3	Is being studied. Not only important to EL.
	9	2	1	1	While these materials are austenitic, and are generally expected to retain properties for many years, I increased susceptibility somewhat to cover possible embrittlement out to 80 years. I don't know how much we really know about this.

Average: **1.33** **1.89** **2.11**

Std. Dev.: **0.50** **0.93** **0.78**

Reactor Type: PIRT-PWR adj.

Material: SS: Welds & Clad

Phenomena: SCC Corrosion

Sub-Component: Upper shell flange clad.

Mechanism	Panelist	Susceptibility	Confidence	Knowledge	Rational
Pitting	1	1	3	3	
	2	1	1	2	
	3	2	1	1	
	4	1	2	2	Pitting in clad has not been observed.
	5	1	1	1	
	6	1	2	2	Not familiar with pitting issue
	7	2	1	1	Insufficient data exist for LTO.
	8	2	1	1	Insufficient data for EL.
	9	1	1	2	while I don't think this will be an issue in general, I'm somewhat uncertain as to the likelihood of crevices due to the specifics of the design. If crevices exist, then my susceptibility would increase to a 2.
Average:	1.33	1.44	1.67		
Std. Dev.:	0.50	0.73	0.71		

Reactor Type: PIRT-PWR adj.

Material: Ni-Alloy: Base Metal (A600)

Phenomena: Fatigue

Sub-Component: Bottom mounted nozzles and repair pieces (B&W).

Mechanism	Panelist	Susceptibility	Confidence	Knowledge	Rational
LC-Env.	1	1	2	2	
	2	1	2	2	
	3	2	1	1	
	4	2	1	1	
	5	1	2	2	
	6	1	2	2	More an SCC issue
	7	2	1	1	Loading conditions may be sufficient for low cycle fatigue in some sub-components.
	8	2	1	1	LCF may affect these components.
	9	1	2	2	Scored this low because I don't expect significant fatigue loads in this region. If significant fatigue loads exist, susceptibility increases to a 2 or 3. I also decreased confidence to reflect this lack of knowledge.

Average: **1.44** **1.56** **1.56**

Std. Dev.: **0.53** **0.53** **0.53**

Reactor Type: PIRT-PWR adj.

Material: Ni-Alloy: Base Metal (A600)

Phenomena: Red. In Fract. Properties

Sub-Component: Bottom mounted nozzles and repair pieces (B&W).

Mechanism	Panelist	Susceptibility	Confidence	Knowledge	Rational
Env.	1	1	3	3	
	2	1	1	2	Currently included in aging mgmt.
	3	1	3	3	
	4	2	1	2	Possible low temperature reduction in fracture toughness
	5	1	1	1	
	6	1	2	2	More information needed
	7	1	3	3	Issue not significant specifically for long-term operation.
	8	1	3	3	Is being studied. Not only important to EL.
	9	2	2	2	these materials have generally good fracture resistance to environmental except at lower temperatures (100 - 200F) likely due to hydrogen uptake.

Average: **1.22** **2.11** **2.33**

Std. Dev.: **0.44** **0.93** **0.71**

Reactor Type: PIRT-PWR adj.

Material: Ni-Alloy: Base Metal (A600)

Phenomena: SCC

Sub-Component: Bottom mounted nozzles & repair pieces (B&W).

Mechanism	Panelist	Susceptibility	Confidence	Knowledge	Rational
IG/ITG	1	2	3	3	
	2	2	3	3	Currently included in aging mgmt.
	3	3	2	3	
	4	3	3	2	Being addressed through current inspection and mitigation activities
	5	2	3	3	
	6	2	3	3	Some evidence but data available
	7	1	3	3	Issue not significant specifically for long-term operation.
	8	3	2	3	Is being studied. Not only important to EL.
	9	3	3	2	this is a known issue now with at least 2 examples of plant OE. While a lower temperature than the upper head, this will continue to be an issue out to 80 years. Note, I'm also considering HAZ as part of base material

Average: **2.33** **2.78** **2.78**

Std. Dev.: **0.71** **0.44** **0.44**

Reactor Type: PIRT-PWR adj.

Material: Ni-Alloy: Base Metal (A690)

Phenomena: Fatigue

Sub-Component: Bottom mounted nozzles & repair pieces (B&W).

Mechanism	Panelist	Susceptibility	Confidence	Knowledge	Rational
LC-Env.	1	2	3	3	
	2	2	2	2	
	3	2	1	1	
	4	1	2	2	
	5	1	2	2	
	6	1	2	2	More an SCC issue
	7	2	1	1	Loading conditions may be sufficient for low cycle fatigue in some sub-components.
	8	2	1	1	LCF may affect these components.
	9	1	2	2	expect no difference from A600 performance
Average:	1.56	1.78	1.78	1.78	
Std. Dev.:	0.53	0.67	0.67	0.67	

Reactor Type: PIRT-PWR adj.

Material: Ni-Alloy: Base Metal (A690)

Phenomena: Red. In Fract. Properties

Sub-Component: Bottom mounted nozzles & repair pieces (B&W).

Mechanism	Panelist	Susceptibility	Confidence	Knowledge	Rational
Env.	1	1	3	3	
	2	1	2	1	Currently included in aging mgmt.
	3	1	3	3	
	4	1	1	2	Possible low temperature reduction in fracture toughness
	5	1	1	1	
	6	1	2	2	More information needed
	7	1	3	3	Issue not significant specifically for long-term operation.
	8	1	3	3	Is being studied. Not only important to EL.
	9	2	2	1	low temperature fracture may be a concern for these alloys; however, they have not been studied as extensively as have A600.

Average: **1.11** **2.22** **2.11**

Std. Dev.: **0.33** **0.83** **0.93**

Reactor Type: PIRT-PWR adj.

Material: Ni-Alloy: Base Metal (A690)

Phenomena: SCC

Sub-Component: Bottom mounted nozzles & repair pieces (B&W).

Mechanism	Panelist	Susceptibility	Confidence	Knowledge	Rational
IG/TC	1	1	3	3	
	2	1	3	3	
	3	2	1	1	
	4	1	2	2	Fair amount of data; Some conditions (high cold work) show significant crack growth rate.
	5	1	3	3	
	6	1	3	3	Much better than A600
	7	2	1	1	Insufficient data for LTO.
	8	2	1	1	Insufficient data for EL.
	9	2	2	2	While A690 is much less susceptible than A600; high cold work in A690 can result in similar susceptibility. If CW is avoided during fabrication, would expect good performance; note I'm also considering HAZ as part of this.

Average: **1.44** **2.11** **2.11**

Std. Dev.: **0.53** **0.93** **0.93**

Reactor Type: PIRT-PWR adj.

Material: Ni-Alloy: Welds & Clad (A82/182)

Phenomena: Fatigue

Sub-Component: Attachment weld of core guide lugs, flow baffles (CE), DM welds of inlet and outlet nozzles, core flood nozzle (B&W), safety injection nozzles (W), bottom mounted nozzles; repair pieces for attachment weld (B&W).

Mechanism	Panelist	Susceptibility	Confidence	Knowledge	Rational	
LC-Env.	1	1	3	3	There may be specific locations with high fatigue duty, but the generic susceptibility is low	
	2	1	2	2		
	3	2	1	1		
	4	1	2	2		Data is available.
	5	1	2	2		
	6	1	2	2		SCC-fatigue interaction
	7	2	1	1		Loading conditions may be sufficient for low cycle fatigue in some sub-components.
	8	2	1	1		LCF may affect some components.
	9	1	2	2		I've scored this the same for susceptibility as base material, but I'm not sure if any of these locations see higher fatigue loads. Higher fatigue loads would increase susceptibility

Average: **1.33** **1.78** **1.78**

Std. Dev.: **0.50** **0.67** **0.67**

Reactor Type: PIRT-PWR adj.

Material: Ni-Alloy: Welds & Clad (A82/182)

Phenomena: Red. In Fract. Properties

Sub-Component: DM welds for: core flood nozzle (B&W), safety injection nozzles (W), bottom mounted nozzles; repair pieces for attachment weld (B&W).

Mechanism	Panelist	Susceptibility	Confidence	Knowledge	Rational
Env.	1	1	2	3	
	2	2	3	2	Currently included in aging mgmt.
	3	1	3	3	
	4	2	1	1	Possible low temperature reduction in fracture toughness
	5	2	3	3	
	6	1	2	2	More information needed
	7	1	3	3	Issue not significant specifically for long-term operation.
	8	1	3	3	Is being studied. Not only important to EL.
	9	2	2	2	Again, expect similar performance to base material

Average: **1.44** **2.44** **2.44**

Std. Dev.: **0.53** **0.73** **0.73**

Reactor Type: PIRT-PWR adj.

Material: Ni-Alloy: Welds & Clad (A82/182)

Phenomena: SCC

Sub-Component: DM welds for: inlet and outlet nozzles, core flood nozzle (B&W), safety injection nozzle (W), bottom mounted nozzles, repair pieces.

Mechanism	Panelist	Susceptibility	Confidence	Knowledge	Rational
IG/TC	1	2	3	3	
	2	2	3	3	
	3	3	2	2	
	4	3	3	2	Well known to be highly susceptible. Extent of problem at lower cold leg temperature uncertain.
	5	3	3	3	
	6	3	3	3	Known issue with data and experience
	7	1	3	3	Issue not significant specifically for long-term operation.
	8	3	2	2	Is being studied. Not only important to EL.
	9	3	3	2	welds are typically more susceptible than base material. Again, have lots of OE w.r.t. A82/A182 PWSCC.

Average: **2.56** **2.78** **2.56**

Std. Dev.: **0.73** **0.44** **0.53**

Reactor Type: PIRT-PWR adj.

Material: Ni-Alloy: Welds & Clad (A52/152)

Phenomena: Fatigue

Sub-Component: Attachment weld of core guide lugs, flow baffles (CE), DM welds of inlet and outlet nozzles, core flood nozzle (B&W), safety injection nozzles (W), bottom mounted nozzles, repair pieces for attachment weld (B&W).

Mechanism	Panelist	Susceptibility	Confidence	Knowledge	Rational	
LC-Env.	1	1	3	3	There may be specific locations with high fatigue duty, but the generic susceptibility is low	
	2	1	2	2		
	3	2	1	1		
	4	1	2	2		
	5	1	2	2		
	6	1	2	2		Need more data
	7	2	1	1		Loading conditions may be sufficient for low cycle fatigue in some sub-components.
	8	2	1	1		LCF may affect some components.
	9	1	2	2		I've scored this the same for susceptibility as base material, but I'm not sure if any of these locations see higher fatigue loads. Higher fatigue loads would increase susceptibility

Average: **1.33** **1.78** **1.78** **1.78**

Std. Dev.: **0.50** **0.67** **0.67** **0.67**

Reactor Type: PIRT-PWR adj.

Material: Ni-Alloy: Welds & Clad (A52/152)

Phenomena: Red. In Fract. Properties

Sub-Component: DM welds for: core flood nozzle (B&W), safety injection nozzles (W), bottom mounted nozzles; repair pieces for attachment weld (B&W).

Mechanism	Panelist	Susceptibility	Confidence	Knowledge	Rational
Env.	1	1	2	2	
	2	1	2	3	Currently included in aging mgmt.
	3	1	3	3	
	4	1	1	2	Possible low temperature reduction in fracture toughness
	5	1	2	3	
	6	1	2	2	More information needed
	7	1	3	3	Issue not significant specifically for long-term operation.
	8	1	3	3	Is being studied. Not only important to EL.
	9	2	2	1	Again, expect similar performance to base material

Average: **1.11** **2.22** **2.44**

Std. Dev.: **0.33** **0.67** **0.73**

Reactor Type: PIRT-PWR adj.

Material: Ni-Alloy: Welds & Clad (A52/152)

Phenomena: SCC

Sub-Component: DM welds for: inlet and outlet nozzles, core flood nozzle (B&W), safety injection nozzle (W), bottom mounted nozzles, repair pieces.

Mechanism	Panelist	Susceptibility	Confidence	Knowledge	Rational
IG/TG	1	1	3	3	
	2	1	2	2	Currently included in aging mgmt.
	3	2	1	1	
	4	1	2	2	Fair amount of data; Some conditions (high cold work) show significant crack growth rate.
	5	1	2	2	
	6	1	2	2	Much better than A82/182
	7	1	3	3	Issue not significant specifically for long-term operation.
	8	2	1	1	Is being studied. Not only important to EL.
	9	1	2	2	The susceptibility of the welds has been demonstrated to be excellent in the lab. There are some instances of higher susceptibility (still much lower than 600, A82/182, and bad 690) that are still being investigated.

Average: **1.22** **2.00** **2.00** **2.00**

Std. Dev.: **0.44** **0.71** **0.71** **0.71**

BIBLIOGRAPHIC DATA SHEET

(See instructions on the reverse)

1. REPORT NUMBER
(Assigned by NRC, Add Vol., Supp., Rev.,
and Addendum Numbers, if any.)

NUREG/CR-7153,
Volumes 1 - 5

2. TITLE AND SUBTITLE

Expanded Materials Degradation Assessment (EMDA)

3. DATE REPORT PUBLISHED

MONTH

YEAR

October

2014

4. FIN OR GRANT NUMBER

5. AUTHOR(S)

J. Busby, ORNL

6. TYPE OF REPORT

Technical

7. PERIOD COVERED (Inclusive Dates)

8. PERFORMING ORGANIZATION - NAME AND ADDRESS (If NRC, provide Division, Office or Region, U. S. Nuclear Regulatory Commission, and mailing address; if contractor, provide name and mailing address.)

Oak Ridge National Laboratory
Reactor and Nuclear Systems Division
PO Box 2008
Oak Ridge, TN 37831

9. SPONSORING ORGANIZATION - NAME AND ADDRESS (If NRC, type "Same as above", if contractor, provide NRC Division, Office or Region, U. S. Nuclear Regulatory Commission, and mailing address.)

Office of Nuclear Regulatory Research
Division of Engineering
U.S. Nuclear Regulatory Commission
Washington, DC 20555

10. SUPPLEMENTARY NOTES

11. ABSTRACT (200 words or less)

Most nuclear power plants in the United States are currently licensed for up to 60 years of operation. The nuclear industry is assessing the feasibility of operation for up to 80 years. The U.S. Nuclear Regulatory Commission (NRC) and U.S. Department of Energy (DOE) co-sponsored the Expanded Materials Degradation Assessment (EMDA) to identify information gaps and research priorities for aging related degradation of reactor components for up to 80 years. Expert panels were convened to examine four main component groups using the phenomena identification and ranking technique: reactor core internals and piping systems, the reactor pressure vessel, concrete and civil structures, and electrical cables. Panelists included participants from NRC, DOE national laboratories, industry, academia, and international organizations. The EMDA reports include a ranking of degradation scenarios according to the probability of occurrence and level of knowledge, along with a summary of the current state of knowledge for each component group.

12. KEY WORDS/DESCRIPTORS (List words or phrases that will assist researchers in locating the report.)

Light water reactors
Long term operation
Corrosion
Aging

13. AVAILABILITY STATEMENT

unlimited

14. SECURITY CLASSIFICATION

(This Page)

unclassified

(This Report)

unclassified

15. NUMBER OF PAGES

16. PRICE



Federal Recycling Program



**UNITED STATES
NUCLEAR REGULATORY COMMISSION**
WASHINGTON, DC 20555-0001

OFFICIAL BUSINESS



NUREG/CR-7153, Vol. 3

Aging of Reactor Pressure Vessels

October 2014